Mădălina Victoria Natu Tavares

Drug loading strategies and processing of polymer blends for intraocular controlled drug release application

A Thesis submitted for the degree of
Doctor in Chemical Engineering

2011

Universidade de Coimbra

Abstract

In 2010 there were 60.5 million people with glaucoma worldwide and this number is expected to increase to 79.6 million by 2020. In most glaucoma patients medical therapy consists of topical eyedrops. However, administration and compliance are often problematic. Surgical and laser treatment for glaucoma is traumatic for the patients, involving high costs and might require repetition of the procedure.

Therefore the aim of the present work was the development of drug-eluting biodegradable implants designed to provide a localized and long-term (6 months to 2 years) sustained release of the drug that can be used in the treatment of glaucoma. The implant should degrade within the site of implantation, eliminating the need for further surgery. The implant should be introduced in the ophthalmologist office, under local anaesthesia, with high implications in patient recovery and costs. By delivering controlled amounts of drug the implant would be pharmacologically efficient and increase patient compliance.

Several polymer processing and drug loading techniques were used in order to prepare controlled drug delivery systems (CDDS) for intraocular application. The chosen materials were poly(ε-caprolactone), PCL, because of its slow degradation, which makes it useful for long term delivery and poly(oxyethylene-b-oxypropylene-b-oxyethylene), Lu, because of its release modulation capacity. Moreover, they are both commercially available, inexpensive and well characterised polymers. Three drugs were incorporated: timolol maleate, acetazolamide and dorzolamide hydrochloride. They are all agents that can decrease intraocular pressure (IOP) in open-angle glaucoma. Two types of devices were prepared: monolithic (sponges, fibers, disks) and hybrid (disks), using supercritical solvent impregnation (SSI), electrospinning, melt compression and solvent casting.

PCL blends were successfully impregnated with timolol maleate using a SSI technique. SSI efficiency results suggested that the best impregnating conditions were obtained when a cosolvent was used and when specific drug-polymer interactions occurred as a consequence of different chemical structures due to polymer blending. Pressure can be either a favourable factor, when there was enough drug affinity for the polymers, or an unfavourable factor, when weaker bonding was

involved. Drug loading, heterogeneous/homogeneous dispersion of drug inside the matrix, hydrophilicity and crystallinity all influenced the drug release. The in vitro release results suggested that a sustained drug release rate can be obtained by changing the SSI operational conditions and by modulating the composition of blends, as a mean to control crystallinity, hydrophilicity and drug affinity for the polymer matrix.

Bicomponent fibers of PCL and Lu were obtained by electrospinning. Acetazolamide and timolol maleate were loaded in the fibers in different concentrations (below and above the drug solubility limit in polymer) in order to determine the effect of drug solubility in polymer, drug state, drug loading and fiber composition on fiber morphology, drug distribution and drug release kinetics. High loadings fibers (with drug in crystalline form) showed higher burst and faster release than low drug content fibers, indicating that the release was more sustained when the drug was encapsulated inside the fibers in an amorphous form. Moreover, timolol maleate was released faster than acetazolamide, indicating that drug solubility in polymer influences the partition of drug between polymer and elution medium, while fiber composition also controlled drug release. At low loadings total release was not achieved, suggesting that drug remained trapped in the fibers. The modelling of release data implied a three stage release mechanism: a dissolution stage, a desorption and subsequent diffusion through water filled pores, followed by polymer degradation control.

Dorzolamide loaded disks (hybrid device) were prepared by solvent-casting of PCL/Lu and subsequent coating with PCL solution. By blending, crystallinity, water uptake and mass loss were modified relative to the pure polymers. Burst was diminished by coating the disks with a PCL shell. All samples presented burst release except PCL-coated samples that showed controlled release during 18 days. For PCL-coated samples, barrier-control of diffusion coupled with partition control from the core slowed down the release, while for 50/50 Lu/PCL-coated samples, the enhancement in porosity of the core diminished partition-control of drug release. Non-linear regression analysis suggested that a degradation model fully described the release curve considering a triphasic release mechanism: the instantaneous diffusion (burst), diffusion and polymer degradation stages. MTT test indicated that the materials were not cytotoxic for corneal endothelial cells. A good *in vitro–in vivo* correlation was obtained, with similar amounts of drug released *in vitro* and *in vivo*. The decrease in IOP was similar to that obtained by dorzolamide eyedrop instillation.

Implantable monolithic disks for glaucoma treatment were prepared by blending PCL, Lu and dorzolamide. Their *in vivo* performance was assessed by their capacity

to decrease IOP in normotensive and hypertensive eyes. Drug mapping showed that release was complete from blend disks and the low molecular weight (MW) PCL after 1 month *in vivo*. The high MW PCL showed non-cumulative release rates above the therapeutic level during 3 months *in vitro*. *In vivo*, the fibrous capsule formation around the implant controlled the drug release, working as a barrier membrane. Histologic analysis showed normal foreign body reaction response to the implants. In hypertensive eyes, the most sustained decrease was shown by the high MW PCL. The blending offers the possibility to manipulate the release rate and the amount of released drug in order to prepare devices tailored to the patients needs.

The long term degradation of all the prepared constructs (films, fibers, sponges and disks) was studied. The influence on degradation rate of several factors (construct type, crystallinity, MW, drug presence, blending) was assessed through water uptake, mass loss, crystallinity and MW evaluation. The degradation rate was higher for blends than for PCL and it was similar between different types of blends. The low MW disks had a degradation rate that was lower by one order of magnitude than high MW constructs. Porosity was shown to be a very important factor because at initial stage (or initial porosity), it will enhance water uptake and degradation, while at a later stage (or developed porosity), it will decrease degradation rate because of diminished autocatalytic effects. High initial porosity produced an acceleration of degradation for sponges, fibers and films when compared to disks, while developed porosity reduced degradation for drug-loaded disks when compared to disks without drug. Modelling of the experimental data suggested that the contribution of surface effects was as significant as autocatalytic effects in overall bulk degradation.

This work has revealed some insights into possible polymer processing and drug loading techniques for the preparation of CDDS for intraocular delivery. It also presented some results regarding the preliminary pre-clinical evaluation of PCL-based implants. *In vivo*, the drug-eluting implants were able to reduce IOP in an animal model of glaucoma. Nevertheless, another extremely important issue has to be addressed: patient compliance. Patience compliance is of extreme importance especially in the therapy of chronic diseases because patients have to keep up constantly with their pharmacological regimen. The superiority of CDDS relative to conventional therapy has to be proven in long term compliance studies because this is one of the main reasons of developing CDDS therapy in the first place.

Resumo

Em 2010 existiam cerca de 60,5 milhões de pessoas com glaucoma no mundo, devendo este número aumentar para 79,6 milhões em 2020. Na maioria dos pacientes com glaucoma o tratamento médico consiste na aplicação de colírios tópicos. No entanto a administração e a adesão do paciente ao tratamento são muitas vezes problemáticas. No caso do glaucoma a cirurgia e o tratamento a laser são frequentemente traumáticos para os pacientes. Além disso, estes tratamentos envolvem custos elevados e podem exigir a repetição do procedimento.

O objectivo do presente trabalho foi desenvolver implantes biodegradáveis destinados a fornecer uma libertação controlada e localizada de fármaco a longo prazo (6 meses a 2 anos) e que possam ser usados no tratamento do glaucoma. O implante deve-se degradar dentro do local de implantação, eliminando a necessidade de uma nova cirurgia. O implante pode ser colocado no consultório do oftalmologista, sob anestesia local, o que favorece a recuperação do paciente. Ao libertar quantidades controladas de fármacos o implante é farmacologicamente eficiente, aumentando assim a adesão do paciente à terapia.

Este trabalho descreve várias técnicas de processamento de polímeros e de imobilização de fármacos que podem ser utilizados para a preparação de sistemas de libertação controlada de fármacos (SLCF) para aplicação intraocular. Os materiais escolhidos foram a poli(ε-caprolactona), PCL devido à sua lenta degradação, o que a torna útil para a libertação de longa duração e o poli(oxietileno-b-oxipropileno-b-oxietileno), Lu, devido à sua capacidade de modulação da libertação. Além disso, ambos os polímeros estão disponíveis comercialmente, são baratos e estão bem caracterizados. Três fármacos foram incorporados: maleato de timolol, acetazolamida e cloridrato de dorzolamida. São todos agentes que podem diminuir a pressão intra-ocular (PIO) em pacientes com glaucoma de ângulo aberto. Dois tipos de dispositivos foram preparados: monolítico (esponjas, fibras e discos) e híbrido (discos), usando técnicas de impregnação com solvente supercrítico (ISS), de "electrospinning", de compressão e de evaporação de solvente.

As misturas de PCL foram impregnadas com maleato de timolol usando uma técnica ISS. Os resultados de eficiência da impregnação indicaram que as melhores

condições de impregnação foram obtidas quando um co-solvente foi usado e quando ocorreu um aumento das interações polímero-fármaco devido à mistura de polímeros. A pressão pode ser um factor favorável, quando existe suficiente afinidade entre o fármaco e os polímeros, ou um factor desfavorável quando as interações são mais fracas. A percentagem de impregnação, a distribuição de fármaco dentro de matriz polímerica, a cristalinidade e a hidrofilicidade influenciaram a libertação de fármaco. Os resultados de libertação in vitro sugerem que a libertação controlada de fármacos pode ser obtida através da variação das condições operacionais de SSI, através da composição das misturas, como um meio para controlar a cristalinidade, hidrofilicidade e afinidade do fármaco para a matriz polimérica.

Fibras bicomponentes de PCL e Lu foram obtidas por "electrospinning". Acetazolamida e maleato de timolol foram imobilizados nas fibras em diferentes concentrações (abaixo e acima do limite de solubilidade do fármaco no polímero), a fim de determinar o efeito da solubilidade do fármaco no polímero, o estado de agregação do fármaco, a oclusão do fármaco e a composição das fibras na distribuição de fármaco, na cinética de libertação e na morfologia das fibras. As fibras contendo maior quantidade de fármaco (com fármaco na forma cristalina) apresentaram maior "burst" e libertação mais rápida do que as fibras contendo menor quantidade de fármaco, indicando que a libertação foi mais constante quando o fármaco foi encapsulado dentro das fibras na forma amorfa. Além disso, o maleato de timolol foi libertado mais rapidamente do que a acetazolamida, indicando que a solubilidade no polímero influencia a partição do fármaco entre o polímero e o meio de eluição, enquanto que a composição das fibras também controlou a libertação. Em fibras contendo baixa quantidade de fármacos, não se obteve a libertação total, sugerindo que o fármaco permaneceu imobilizado nas fibras. A modelação dos dados de libertação indica um mecanismo de libertação com três fases: a fase de dissolução, uma de dessorção e difusão, seguida de controle por degradação de polímeros.

Discos carregados com dorzolamida (dispositivo híbrido) foram preparados por "solvent-casting" de PCL/Lu e por revestimento posterior com uma solução de PCL. As misturas apresentaram propriedades diferentes (em termos de cristalinidade, de absorção de água e de perda de massa) em relação aos polímeros puros. Todas as amostras apresentaram libertação "burst", excepto as amostras de PCL-revestidas, as quais apresentaram libertação controlada durante 18 dias. Para as amostras de revestidas com PCL, o controlo por difusão na barreira e por partição desacelerou a libertação, enquanto que para as amostras 50/50 PCL/Lu-revestido, o aumento da porosidade do núcleo diminuiu o controlo de partição de liberação de fármaco. Um modelo de degradação da curva de libertação, sugeriu que há que considerar

um mecanismo de libertação trifásico: a difusão instantânea ("burst"), a difusão e a degradação de polímero. O teste de MTT mostrou que os materiais não são citotóxicos para células endoteliais da córnea. Obteve-se uma boa correlação *in vitro–in vivo*, observando-se quantidades similares de fármaco libertado *in vitro* e *in vivo*. A diminuição da PIO foi similar à obtida por aplicação de um colírio de dorzolamida.

Discos monolíticos implantáveis foram preparados através da mistura de PCL, Lu e dorzolamida. O desempenho in vivo foi avaliado através a capacidade de diminuir a PIO em olhos normotensos e hipertensos. O mapeamento do fármaco mostrou que a libertação foi completa nas misturas e no polímero de baixo peso molecular (PM) PCL após um mês *in vivo*. O polímero de alto PM apresentou taxas de libertação não-cumulativa acima do nível terapêutico, durante três meses *in vitro*. Verificou-se a formação de uma cápsula fibrosa em redor do implante que controlou a libertação da fármaco, funcionando como uma membrana de barreira. A análise histológica sugeriu que havia uma resposta normal de reacção de corpo estranho aos implantes. Nos olhos hipertensos, a queda mais sustentada de PIO foi demonstrada pelo polímero de alto PM. A mistura oferece a possibilidade de manipular a taxa de libertação e a quantidade de fármaco libertado a fim de preparar dispositivos adaptados às necessidades dos pacientes.

Estudou-se também a degradação a longo prazo de todas as amostras preparadas (filmes, fibras, esponjas e discos). A influência na taxa de degradação de vários factores (morfologia, cristalinidade, presença de fármaco, PM, composição) foi avaliada através de estudos de absorção de água, de perda de massa, de evolução da cristalinidade e de PM. A taxa de degradação foi maior para as misturas do que para os sistemas só de PCL e foi similar para os diferentes tipos de misturas. Os discos de baixo PM tiveram uma taxa de degradação uma ordem de grandeza menor do que os discos de alto PM. Verificou-se que a porosidade é um factor muito importante, visto que na fase inicial houve um aumento de absorção de água e de degradação, enquanto que numa fase posterior (ou porosidade desenvolvida), houve uma diminuiçaõ da taxa de degradação devido à diminuição de efeitos autocatalíticos. A alta porosidade inicial produziu uma aceleração da degradação de esponjas, fibras e filmes, quando comparada aos discos, enquanto que a porosidade desenvolvida reduziu a degradação dos discos com fármaco, quando comparada com discos sem fármaco. A modelação dos dados experimentais sugere que a contribuição dos efeitos de superfície era tão importante quanto os efeitos autocatalíticos na degradação em massa.

Este trabalho descreveu várias técnicas de processamento de polímeros e de imobilização de fármacos para a preparação de SLCF para aplicação intraocular.

Sugeriu também alguns resultados sobre a avaliação pré-clínica de implantes à base de PCL. *In vivo*, os implantes foram capazes de reduzir a PIO num modelo animal de glaucoma. No entanto, há que realçar uma outra questão muito importante que deve ser abordada: a adesão do paciente. A adesão do paciente é de extrema importância, especialmente no tratamento de doenças crónicas, pois os pacientes têm de manter constantemente o seu regime medicamentoso. A superioridade da SLCF em relação à terapia convencional, tem de ser comprovada em estudos a longo prazo porque o aumento da adesão do paciente foi uma das principais razões do desenvolvimento de terapias SLCF.

Rezumat

Existau 60,5 milioane de oameni cu glaucom în 2010 la nivel mondial şi acest număr este de aşteptat să crească la 79,6 milioane până în 2020. La pacienţii cu glaucom, tratamentul medical convenţional constă în administrarea de picături. Din păcate, administrarea şi aderenţa la tratament sunt adesea problematice. Tratamentul chirurgical sau cu laser pentru glaucom este adesea traumatizant pentru pacienţi, implicând costuri ridicate şi de cele mai multe ori, repetarea procedurii.

Scopul prezentei lucrări a fost dezvoltarea de sisteme de eliberare controlată de medicamente, biodegradabile, concepute pentru a oferi eliberare localizată, pe termen lung (de la 6 luni la 2 ani) şi care pot fi utilizate în tratamentul glaucomului. Implantul se degradează la locul de implantare, eliminând necesitatea de chirurgie pentru extragere. Implantul poate fi introdus în cabinetul oftalmologistului, sub anestezie locala, cu implicatii mari în recuperarea pacienţilor şi a costului procedurii. Prin eliberarea controlată de medicament, implantul are o eficienţă farmacologică sporită şi creşte aderenţa la tratament.

Diverse tehnici de încorporare de medicamente şi de procesare de polimeri au fost utilizate pentru a obţine sisteme de eliberare controlată de medicamente (SECM) pentru aplicaţii intraoculare. Materialele alese au fost poli(ε-caprolactonă), PCL, din cauza degradării sale lente, fiind astfel utilă pentru eliberarea pe termen lung şi poli(oxietilenă-b-oxipropilenă-b-oxietilenă), Lu, din cauza capacităţii de reglare a eliberării. În plus, ambii polimeri sunt disponibili în comerţ, ieftini şi bine caracterizaţi. Trei medicamente au fost încorporate: maleat de timolol, acetazolamidă şi clorhidrat de dorzolamidă. Aceştia sunt rpincipii active care pot scădea tensiunea intraoculară (TIO) în glaucom cu unghi deschis. Trei tipuri de dispozitive au fost obţinute: de tip matrice (bureţi, fibre, discuri) şi de tip hibrid (discuri), folosind impregnarea cu solvent supercritic (ISS), "electrospinning", formarea prin compresie şi formarea prin întindere-suflare.

Sisteme pe bază de PCL au fost cu succes impregnate cu maleat de timolol, folosind o tehnică ISS. Rezultatele privind eficienţa încorporării de medicament au sugerat că cele mai bune condiţii de impregnare s-au obţinut atunci când

un cosolvent a fost folosit şi atunci când interacţiuni specifice între medicament şi polimer au apărut din cauza modificării caracterului chimic datorită formării amestecurilor de polimeri. Presiunea poate fi un factor favorabil, atunci când există afinitate între medicament şi polimer, sau un factor nefavorabil când interacţiunile sunt mai slabe. Gradul de încorporare, distribuţia medicamentului în matrice, caracterul hidrofilic, gradul de cristalinitate, toate influenţează eliberarea controlată a medicamentului. Rezultatele testelor de eliberare in vitro au sugerat că o viteză de eliberare susţinută poate fi obţinută prin optimizarea condiţiilor de tehnicii SSI şi prin relarea compoziţiei amestecurilor de polimeri, ca un mijloc de a controla cristalinitatea, caracterul hidrofilic şi afinitatea între medicament şi matricea polimerică.

Fibre bicomponente de PCL şi Lu au fost obţinute prin "electrospinning". Acetazolamida şi maleatul de timolol au fost încorporate în fibre în concentraţii diferite (sub limita şi peste limita de solubilitate a medicamentului în polimer), pentru a determina efectul solubilitaţii, starea de agregare a medicamentului, a gradului de încorporare şi a compoziţiei asupra morfologiei, distribuţiei de medicament şi a cineticii de eliberare. Fibrele cu grad de încărcare ridicat de medicament (cu medicament în stare cristalină) au eliberat medicamentul mai repede decât fibrele cu grad de încărcare scăzut, fapt ce sugerează că eliberarea este mai susţinută atunci când medicamentul este încorporat în interiorul fibrelor, în stare amorfă. În plus, maleatul de timolol a fost eliberat mai repede decat acetazolamida, indicând faptul că solubilitatea medicamentului în polimer influenţează fenomenul de partiţie a medicamentului între matricea polimerică şi mediul de eluţie, în timp ce compoziţia fibrelor influenţează, de asemenea, eliberarea medicamentului. La grad de încărcare scăzut, eliberarea totală a medicamentului nu a fost realizată, sugerând că o parte din medicament a rămas imobilizată în fibre. Modelarea datelor de eliberare a indicat un mecanism de eliberare în trei etape: etapa "burst", etapa controlată de desorbţie şi de difuzie, ultima etapă fiind controlată de viteza de degradare a polimerului.

Discuri cu dorzolamidă (dispozitiv hibrid) au fost obţinute prin formare de filme PCL/Lu şi acoperirea ulterioară cu soluţie PCL. Prin amestecare, cristalinitatea, capacitatea de gonflare şi eroziunea au fost modificate în raport cu polimerii puri. Efectul "burst" a fost diminuat prin aplicarea membranei de PCL. Toate probele au prezentat etapa "burst", cu excepţia probelor PCL cu membrană, care au produs eliberare controlată timp de 18 de zile. Pentru probele PCL cu membrană, eliberarea a fost controlată de difuzia prin membrană şi de partiţia medicamentului, în timp ce pentru probele 50/50 Lu/PCL cu membrană, porozitatea ridicată a rezervorului a diminuat controlul eliberării prin difuzie şi partiţie. Un model de

degradare a polimerului a descris pe deplin cinetica de eliberare, considerând un mecanism trifazic: difuzie instantanee ("burst"), difuzie şi degradarea polimerului. Testul MTT a indicat faptul că materialele nu au fost citotoxice pentru celule endoteliale prevalate din cornee de iepure. S-a obţinut o corelare bună *in vitro–in vivo*. Dispozitivele au produs o scădere a TIO similară cu cea obţinută prin aplicare de picături cu dorzolamidă.

Discuri implantabile de tip matrice au fost preparate prin amestecare de PCL, Lu şi dorzolamidă. Performanţă *in vivo* a fost evaluată prin capacitatea de a reduce TIO în ochi normotensivi şi hipertensivi. Testele de distribuţie a medicamentului au arătat că eliberarea a fost completă din discuri de amestec şi din polimerul cu masa moleculară (MM) joasă , PCL10, dupa 1 lună *in vivo*. Polimerul cu MM ridicată, PCL40 a prezentat viteze de eliberare peste nivelul terapeutic timp de 3 luni *in vitro*. *In vivo*, formarea capsulei fibroase în jurul implantului a controlat eliberarea de medicament, într-o manieră similară cu membrana-barieră dintr-un sistem de tip rezervor. Analiza histologică a arătat răspuns normal la corp străin. În ochi hipertensivi, scăderea TIO cea mai susţinută a fost obţinută de polimerul cu MM ridicată, PCL40. Amestecare oferă posibilitatea de a manipula viteza de eliberare şi cantitatea de medicament eliberată pentru a pregăti dispozitive adaptate la nevoile pacienţilor.

Degradarea pe termen lung a tuturor probelor (filme, fibre, bureţi şi discuri) a fost studiată. Influenţa asupra vitezei de degradare a mai multor factori (tipul probei, cristalinitatea, MM, încorporare de medicament, compoziţia amestecului) a fost evaluată prin teste de gonflare, eroziune, evoluţie de cristalinitate şi MM. Viteza de degradare a fost mai mare pentru amestecuri decât pentru PCL şi a fost similară între diferite tipuri de amestecuri. Discurile cu MM joasă au avut o viteză de degradare cu un ordin de mărime mai mic decât discurile cu MM ridicată. Porozitatea s-a dovedit a fi un factor foarte important, deoarece, în etapa iniţială va produce creşterea capacităţii de gonflare şi în consecinţă degradarea, în timp ce într-o etapă ulterioară, va reduce viteza de degradare din cauza diminuării efectelor autocatalitice. Porozitatea ridicată iniţială a produs o accelerare a degradării pentru bureţi, fibre şi filme în comparaţie cu discurile, în timp ce porozitate "produsă" a redus degradarea pentru discuri cu medicament în comparaţie cu discuri fără medicament. Modelarea datelor experimentale a sugerat că prevalenţa efectelor de suprafaţă a fost la fel de importantă ca efectele autocatalitice pentru degradarea în masă.

Acest studiu a descris diverse metode de procesare de polimeri şi tehnici de încorporare de medicamente pentru a obţine SECM pentru aplicaţii intraoculare. Au fost prezentate, de asemenea, rezultate cu privire la evaluarea precilinică a

implanturilor bazate pe PCL. *In vivo*, implanturile au redus TIO într-un model animal de glaucom. Cu toate acestea, un alt aspect extrem de important trebuie să fie abordat: evaluarea aderenţei pacientului la tratament. Aderenţa la tratament este extrem de importantă în special în tratamentul bolilor cronice, deoarece pacienţii trebuie să respecte tratamentul medicamentos prescris. Superioritatea SECM în comparaţie cu terapia convenţională trebuie să fie dovedită în studii de aderenţă la tratament pe termen lung, deoarece acesta a fost unul dintre motivele principale de dezvoltare a terapiei SECM.

Acknowledgements

I would like to thank FCT for providing financial support during my PhD project research period.

I would like to thank my supervisors, prof. Helena and prof. Hermínio for giving me the opportunity to work during my PhD project in their research groups. Their scientific advice is gratefully acknowledged.

I would like to thank prof. Carlos Ribeiro and prof. Manuel Gaspar for all their help regarding the in vivo experimentation.

Aş vrea să le mulţumesc părinţilor mei şi Inei pentru că m-au sprijinit tot timpul şi mi-au uşurat dorul de casă.

I would also like to thank Miguel for all his support. You are my friend, my family, my partner.

List of Publications

This thesis consists of an overview of the following publications:

- I – M.V. Natu, M.H. Gil, H.C. de Sousa (2008) Supercritical solvent impregnation of poly(ε-caprolactone)/poly(oxyethylene-b-oxypropylene-b-oxyethylene) and poly(ε-caprolactone)/poly(ethylene-vinyl acetate) blends for controlled release applications. The Journal of Supercritical Fluids, 47, 93–102, DOI:10.1016/j.supflu.2008.05.006;

- II – M.V. Natu, H.C. de Sousa, M.H. Gil (2010) Effects of drug solubility, state and loading on controlled release in bicomponent electrospun fibers. International Journal of Pharmaceutics, 397, 50–58, DOI:10.1016/j.ijpharm.2010.06.045;

- III – M.V. Natu, H.C. de Sousa, M.H. Gil (2011) Electrospun Drug-Eluting Fibers for Biomedical Applications. In Active Implants and Scaffolds for Tissue Regeneration, Studies in Mechanobiology, Tissue Engineering and Biomaterials, vol.8, Springer, ISBN 978-3-642-18064-4, DOI:10.1007/8415_2010_56, in press;

- IV – M.V. Natu, M.N. Gaspar, C.A. Fontes Ribeiro, I.J. Correia, D. Silva, H.C. de Sousa, M.H. Gil (2011) A poly(ε-caprolactone) device for sustained release of an anti-glaucoma drug. Biomedical Materials, 6, 025003, DOI:10.1088/1748-6041/6/2/025003;

- V – M.V. Natu, M.N. Gaspar, C.A. Fontes Ribeiro, A.M. Cabrita, H.C. de Sousa, M.H. Gil In vitro and in vivo evaluation of an intraocular implant for glaucoma treatment. European Journal of Pharmaceutics and Biopharmaceutics, submitted;

- VI – M.V. Natu, H.C. de Sousa, M.H. Gil Long term degradation of poly(ε-caprolactone) constructs obtained through different polymer processing techniques (supercritical fluid technology, electrospinning, melt-compression and solvent casting). Polymer Degradation and Stability, submitted.

Outline

The current Thesis is a result of the Ph.D. research project (funded by FCT, reference: SFRH/BD/30198/2006) with the title *Drug loading strategies and processing of polymer blends for intraocular controlled drug release application.* The Thesis is divided in eight Chapters.

In Chapter 1, an introduction to the main subject that is covered in the Thesis is given. In this Chapter, an overview of glaucoma, its manifestation and current treatment is given. Problems with current drug delivery routes to the eye and benefits and drawbacks of controlled drug delivery systems (CDDS) for ophthalmologic diseases are also presented. A very brief introduction on supercritical fluids (SCF) technology and electrospinning is given in order to understand the versatility of these techniques for the preparation and drug loading of CDDS.

Chapter 2 presents the results of the study on the supercritical solvent impregnation of timolol maleate in poly(ε-caprolactone)-based blends. SCF-assisted impregnation enables the production of drug-eluting implants because both drug loading and porous polymer morphology is achieved in one step. This very porous morphology allows further processing of the drug loaded matrix in order to obtain implants with various dimensions and shapes. The effects of pressure, cosolvent and blend composition on drug loading and release kinetics were evaluated.

Electrospinning of polymer and drug solutions was used in order to fabricate fiber CDDS. Due to easy drug entrapment, high surface area, morphology control and biomimetic characteristics, fibers can perform as CDDS. The effect of electrospinning processing on crystallinity, hydrophilicity and degradation of bicomponent fibers as well as the effect of drug solubility in polymer, drug state, drug loading and fiber composition on morphology, drug distribution and release kinetics are described in Chapter 3.

Chapter 4 presents the preparation of an implantable device for dorzolamide delivery by solvent casting. Dip-coating was used as a strategy to decrease/eliminate burst release. Preliminary in vivo results in normal tension rabbit eyes were also reported.

Chapter 5 describes the preparation of drug-eluting implants by melt compression so that high drug loading per implant mass is achieved. Results concerning the in vivo performance (in terms of the effect on intraocular pressure) in an animal model of glaucoma are also presented. Differences between in vitro and in vivo drug release, offering insights into the mechanisms of drug release are considered.

Chapter 6 presents the results of long-term degradation tests for the various constructs (films, fibers, sponges and disks) that were obtained during this research project. The influence on degradation rate of several factors (construct type, crystallinity, molecular weight (MW), drug presence, blending) was assessed through water uptake, mass loss, crystallinity and MW evaluation.

A general discussion of all obtained results and final conclusions are presented in Chapter 7.

Acronyms

CDDS controlled drug delivery system

IOP intraocular pressure

CAI carbonic anhydrase inhibitors

ACh acetylcholine

RGC retinal ganglion cells

TM trabecular meshwork

AH aqueous humor

SCF supercritical fluids

NTP normal temperature and pressure

scCO$_2$ supercritical carbon dioxide

SSI supercritical solvent impregnation

PCL poly(ε-caprolactone)

Lu Lutrol F 127

Lw Luwax EVA 3

PBS phosphate buffer saline

DSC differential scanning calorimetry

PVAc poly(vinylacetate)

SEM scanning electron microscopy

UV ultraviolet

EPMA electron probe microanalysis

MTT 3-[4,5-dimethyl-thiazol-2-yl]-2,5-diphenyltetrazolium bromide

DMA dynamic mechanical analysis

TGA thermogravimetric analysis

XRD X-ray diffraction

MW molecular weight

SEC size exclusion chromatography

Contents

List of Figures

List of Tables

Chapter 1

Introduction

1.1 Controlled drug delivery systems

A controlled drug delivery system (CDDS) is "a formulation or a device that enables the introduction of a therapeutic substance in the body and improves its efficacy and safety by controlling the rate, time, and place of release of drugs in the body". The release consists of the administration of the drug, the release of the drug by the CDDS and the subsequent transport of the drug to the site of action. The CDDS can be a drug formulation or a device (such as biosensors, microfluidics, microchips, pumps and conduits) used to deliver the drug. Drugs can be introduced in the body by systemic delivery (which includes oral, colorectal, parenteral, transdermal, transmucosal, nasal, pulmonary, cardiovascular, central nervous system and intraosseous routes) or local delivery, which is targeted to various organs (Jain [2008]).

With standard drug delivery systems, the concentration of the drug reaches a maximum level and then decreases rapidly to a low value. Thus, a new dose has to be administered frequently. Sometimes, the obtained drug concentration can be higher than the required therapeutic dose and can even be higher than the toxic level. Standard delivery systems produce a pharmacologic profile that gives rise to the alternation of doses that produce either over-dosage or lack of efficiency. CDDS eliminate the variation in drug concentration, producing a more efficient pharmacologic profile. With a CDDS, a drug is delivered in a predetermined, predictable and reproducible manner. Thus, the drug concentration will be adjusted so that it is below the toxic level and above the optimal therapeutic level. The objective of a CDDS is to maintain a prolonged constant drug level in a carefully controlled concentration range. The principle of action of a CDDS with respect to standard drug delivery systems is shown in Fig 1.1.

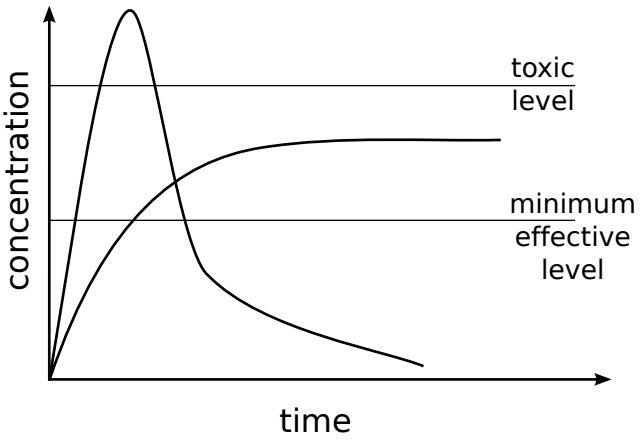

Figure 1.1: Comparison between CDDS and traditional delivery

A CDDS presents several advantages when compared to traditional delivery (Jain [2008], Tiwari and Rajabi-Siahboomi [2008]):

- clinical advantages
  - extend the duration of drug action
  - improvement of drug safety and efficacy
  - lower dosing frequency
  - lower drug toxicity (local/systemic)
  - chronopharmacological benefits
  - lower fluctuations in drug blood/tissue level
  - lower total drug usage when compared with conventional therapy
  - improved patient compliance
- commercial/industrial advantages
  - economical to the health care system and the patient
  - lower cost of drug development
  - product life-cycle extension
  - product differentiation
  - market expansion
  - innovative/technological leadership

Potential limitations of CDDS technology include (Jain [2008], Tiwari and Rajabi-Siahboomi [2008]):

- delay in onset of drug action
- burst risk
- difficulty in dose adjustment in some cases
- higher cost when compared with conventional therapy
- not suitable for all drugs
- lower patient acceptance
- more difficult administration when compared with conventional therapy

The control of drug release from CDDS can be achieved by several mechanisms (shown schematically in Fig. 1.2): diffusion, dissolution, swelling, osmosis, degradation (enzymatic/chemical) and external (magnetic, ultrasound) or self-regulation (Heller [1996]). Release mechanisms will be discussed with more detail in section 1.5.3.

Drug release can be controlled by diffusion through the polymer matrix (in the case of matrix system) or through the polymer membrane (in the case of reservoir systems). Solvent diffusion into the system can also control the drug release. In this case, either swelling or osmosis control the release phenomenon. The drug is immobilized in a insoluble polymer matrix (usually hydrogels) that swells when in contact with the solvent. The solvent will diffuse in the polymer matrix, induce matrix swelling and trigger the diffusion of the solvated drug molecules from the matrix. In osmotic systems, the drug is contained in a polymer reservoir (a semi-permeable membrane) that allows water diffusion through the membrane, but not drug diffusion. The membrane has a small orifice that will allow drug diffusion when hydrostatic pressure in the system is modified. Other mechanisms include the release due to polymer degradation and/or polymer dissolution. The disintegration of the polymer matrix (either by physical or chemical mechanisms) will trigger the release of the incorporated drug. In self-regulated or externally regulated systems, certain stimuli regulate the drug release (such as temperature, pH, ultrasound, electromagnetic fields). The self-regulated systems adjust the drug concentration and the kinetic profile to the physiological needs. Thus, these systems try to imitate biofeedback mechanisms.

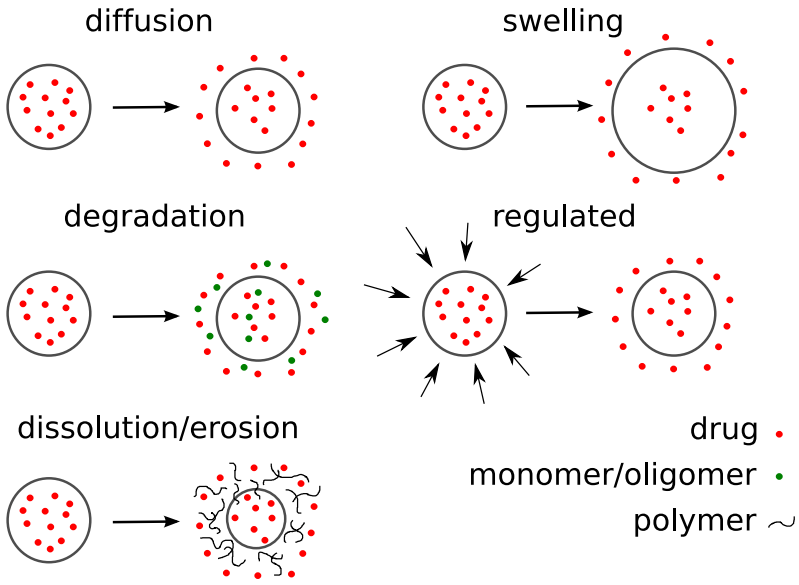

Figure 1.2: Drug release mechanisms

1.2 Drug delivery to the eye

The routes for ocular delivery include non-invasive methods such as topical and systemic administration (oral ingestion or parenteral injection). Topical administration of drugs (in the form of solutions, suspensions and ointments) is usually preferred over other types of drug administration due to ease of application, rapid onset of drug action and good patient acceptance (Amo and Urtti [2008], Kaur and Kanwar [2002]). The local instillation of drugs can achieve therapeutic concentrations in the anterior segment (cornea, anterior chamber, iris, crystalline lens, and ciliary body), but less effectively to the posterior segment (vitreous humor, retinal pigmented epithelium, retina and choroid) (Hughes et al. [2005]). Several ocular diseases, such as inflammation, dry eye and glaucoma, can be treated by topical application (Felt et al. [2002]).

Systemic administration can be used as an adjunct therapy when diseases do not respond as desired to topical medication or in acute episodes of disease manifestation (Gupta et al. [2008]). It is also more effective to treat diseases of the posterior segment of the eye with systemic medication than with eyedrops (Amo and Urtti [2008]). With systemic delivery, drug transport is achieved through the blood-ocular barriers. Two main sites of the blood-ocular barrier exist in the eye: the blood-aqueous barrier (transport through the cilliary body) and the blood-retinal barrier (transport through the retina) (Velez and Whitcup [1999]). Some posterior segment diseases treated by systemic administration include diabetic retinopathy and endophthalmitis (Hughes et al. [2005]).

Invasive methods of delivery can also be used, applied either to the intraocular segments (injections in the intracameral, suprachoroidal, intravitreal, subretinal regions and intracameral or intravitreal surgery), or to the periocular (subconjunctival and sub-Tenon injections) and scleral segments (intrascleral, episcleral, subconjunctival surgery) (Amo and Urtti [2008]). A schematic representation of the different segments of the eye is shown in Fig. 1.3. The periocular route is often employed to treat severe infections of the anterior portion of the eye or to administer drugs as an adjunctive treatment to glaucoma filtering surgery. The intracameral injection may be used in intraocular antibiotic therapy in case of severe infections of the eye. Injections within the posterior chamber can be used after cataract surgery to prevent complications. Intravitreal injection of drugs represents a direct way of attaining effective drug concentrations in the vitreous cavity. Intracapsular administration route allows the treatment of diseases affecting the capsular bag such as posterior capsular opacification, a frequent complication of cataract surgery. Subretinal injections allow drug delivery directly to the retina, or more precisely to the retinal pigment epithelium cells. Thus, diseases such as glaucoma filtering surgery failure, proliferative vitreoretinopathy, cytomegalovirus retinitis, endophthalmitis, posterior uveitis, posterior capsule opacification and retinal degenerative diseases can be treated by intraocular injections (Urtti [2006], Felt et al. [2002], Bourges et al. [2006]).

However, all the above mentioned drug delivery routes present several disadvantages. Drug solution drainage, lachrymation lead to drug loss into the systemic circulation and reduce the bioavailability of the topically applied drugs. Thus, topical therapy is based on frequent instillations, inducing poor patient compliance and ocular and/or systemic toxicity. Through the systemic route most of the drugs do not cross the blood-ocular barriers and the systemic exposure may cause unwanted side effects. With periocular and intraocular administration, bolus dosage and frequent delivery may be required to ensure therapeutic levels over an extended period of time. Frequent injections may not be practical for chronic diseases that sometimes require multiple weekly administrations over months or years. In addition, multiple intraocular injections can lead to complications, such as vitreous haemorrhage, retinal detachment, and endophthalmitis (Velez and Whitcup [1999], Amo and Urtti [2008]).

To overcome these problems, research efforts focused in the development of CDDS. Improved topical formulations, such as hydrogels, particulates and inserts with higher precorneal residence time are already used in clinical practice or under development. Though some of these systems provide an increase in drug bioavailability, they present poor performance in the treatment of posterior segment

pathologies or in the treatment of chronic diseases that require continuous drug administration. Intraocular CDDS, capable of local delivery and extended drug release for long periods of time, have been investigated (Felt et al. [2002]). These CDDS will be described in the following sections.

1.2.1 Topical controlled drug delivery systems

Currently, in order to improve drug bioavalability, formulations of ocular drugs for topical delivery are being developed. The challenge consists in increasing bioavailability from less than 1-3% to at least 15-20%. Research is aimed at increasing drug absorption in the ocular tissues either by maximizing corneal drug penetration or by minimizing corneal drug loss (Kaur and Kanwar [2002]).

One possibility to improve drug residence time on the cornea and decrease drug drainage rate is to increase solution viscosity. Polymeric hydrogels, used in ophthalmology, are generally classified in two distinct groups: preformed gels (they are administered to the eye as viscous preparations and do not undergo a liquid-gel transition) and in situ-forming gels (they are applied as solutions/suspensions and undergo a sol-gel transition in response to factors like pH, temperature or ion concentration). In situ-forming gels facilitate the administration, since they are applied in liquid form. pH-responsive polymers (pseudolatexes, cellulose acetate phthalate latex or carbomer) become viscous gels after instillation due to modification of the pH. The existence of ionizable groups on the macromolecule, which can react at a specific pH with the electrolytes of the lachrymal fluid or with mucin from the tear film ensures adhesive properties (Ludwig [2005]). Temperature-sensitive polymers (such as poloxamers, cellulose derivatives and xyloglucans), are liquid at room temperature and undergo gelation at body temperature. Unfortunately, these formulations present a major disadvantage: the risk of gelling before use due to improper packing or storage conditions (Nanjawade et al. [2007]). Polymers that undergo gelling in the presence of cations from tears include gellan gum, carrageenans and alginates. The gelling is caused by the crosslinking of the charged polysaccharide by mono/divalent ions. Timoptic®, a gellan gum based CDDS formulation used in glaucoma treatment is available on the market (Nanjawade et al. [2007]).

Another strategy to increase drug bioavailability is to promote binding between polymers and mucus (present on the surface of the cornea). Mucoadhesive polymers can be entrapped and/or bound in the mucus layer of the tear film or retained in the conjunctival sac, thus withstanding drainage. Such polymers usually have ionizable groups capable of hydrogen bonding or electrostatic interactions with mucin, while thiolated polymers are capable of forming covalent bonds with mucin.

Such systems increase the contact time between the drug and the cornea and allow a lower instillation frequency compared with the eyedrops, but they might produce irritation, blurred vision and sticky eyelids (Ludwig [2005]).

Colloidal suspensions of particulate drug carriers were developed in order to combine sustained release action with the ease of application of eyedrops. Such polymers include polyacrylates, poly(ε-caprolactone), poly(D,L-lactic acid), poly(D,L-lactide-co-glycolide), hyaluronan, chitosan, polysaccharides, albumin and lipids. Upon instillation, the particles are retained in the cul-de-sac, where the drug can be slowly released. However, the commercial development of these products remains limited due to stability issues after sterilization, long manufacturing process and only slight improvement of the pharmacological performance (Felt et al. [2002]). Piloplex®is a colloidal CDDS, in which pilocarpine is ionically bound to poly(methyl methacrylate-co-acrylic acid) nanoparticles used in glaucoma treatment (Ludwig [2005]). The main advantages of nanoparticles relative to microparticles is given by their smaller size which allows transport through the blood-retinal barrier in the eye, making them useful in the treatment of diseases affecting the posterior segment. Moreover, the smaller size might decrease the uncomfortable feeling of foreign body sensation upon instillation of microparticle formulations (Nagarwal et al. [2009]).

Liposomes and niosomes are vesicular systems in which the drug is encapsulated in lipid structures. They can entrap both hydrophilic and hydrophobic drugs in aqueous solutions and due to surface charge interaction with corneal surface, they can increase ocular absorption for drugs with low partition coefficient, low solubility or high molecular weight. Despite these advantages, liposomes present short shelf life, low loadings and sterilization problems. Niosomes are also lipid bilayered structures made of non-ionic surfactant polymers. They have all the advantages of liposomes, but present higher stability (Kaur et al. [2004]).

Ophthalmic inserts are solid or semi-solid preparations and are usually introduced in the lower fornix. They present several advantages such as accurate dosing, increase in drug bioavailability, absence of preservatives and increased shelf life. Ophthalmic inserts are generally classified according to their solubility. Soluble inserts are made of erodible polymers (such as collagen, crosslinked gelatin derivatives, polyesters, poly(vinyl alcohol) and cellulose derivatives), which do not need to be removed from the eye in the end of therapy. Insoluble inserts can be of reservoir or matrix type. The reservoir systems can release drug either by diffusion or by an osmotic process. The matrix type is mainly represented by therapeutic contact lenses. The main advantage of this system is the simultaneous vision correction and drug release. However, the main problem associated with contact lenses is the

difficult control of incorporated drug amount. Inserts are a promising alternative to classical formulations. However, only a few of these formulations have been commercialized. This can be attributed to difficult placement, discomfort (possible movement around the eye, vision impairment), inadvertent loss, and lower patient acceptance (Felt et al. [2002]).

1.2.2 Intraocular controlled drug delivery systems

Intraocular controlled drug release can be achieved by two means: injectable solutions (semi-solid formulations and particulates) or implantable devices with various geometries (see table 1.1) that can be either implanted through surgery or injected.

Intraocular CDDS were developed in order to overcome some of the limitations of topical and systemic routes of administration for ophthalmic drugs. These implants can be placed in various sites to deliver drug to the eye (Fig. 1.3). The purpose of the implant is to provide local, sustained controlled drug release from the polymeric carrier. Local delivery of drugs to the eye using intraocular implants offers several advantages over systemic therapy. Higher intraocular drug levels can be achieved with local delivery when compared to systemic or topical therapy because no drug is lost in the transport through the blood-ocular barriers. Intraocular implants also provide control over the drug release rate, maintaining it in the therapeutic window of the drug, avoiding thus the exposure to toxic doses (bolus effect). This is particularly useful because most of the ocular drugs have important side-effects. Moreover, sustained release of drugs over long periods of time allows less frequent dosing than with conventional delivery or eliminate the need of self-medication, when patient compliance is of concern. Finally, these devices contain lower amounts of drug for similar treatment periods than traditional formulations, which is especially important from the economic/commercial point of view (Yasukawa et al. [2005], Amo and Urtti [2008]).

Another strategy for intraocular delivery is to encapsulate the drug in a liquid/semi-solid formulation, that can be delivered by injection to the eye. Semi-solid formulations (viscous polymers, sol-gel formulations) and particulates (micro/nanospheres, micro/nanocapsules, liposomes, micelles) can be administered as intravitreal injection, a less invasive procedure than the surgical implantation. They provide sustained drug delivery for weeks or months, allowing less frequent injections than with conventional injectable drug solutions (Moshfeghi and Peyman [2005], Amo and Urtti [2008]).

However, there are some disadvantages associated to CDDS implant/injections therapy. Drugs that are used during a short time scale may produce toxicity, when

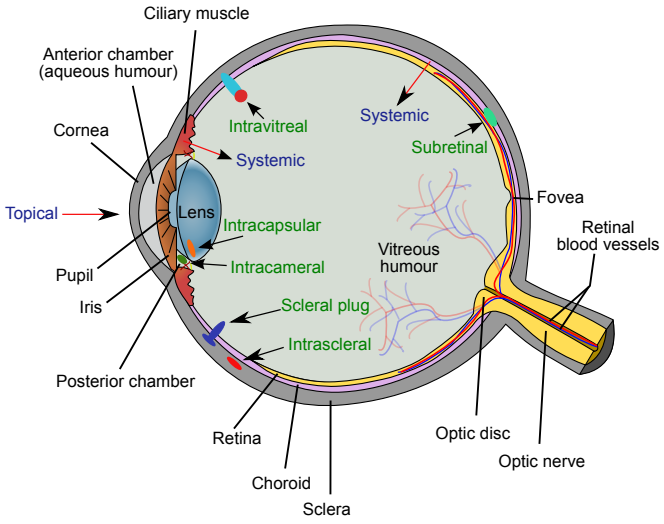

Figure 1.3: Various intraocular implantation sites (adapted from Weiner [2008])

employed in long term therapy. The surgical placement or removal of intravitreal implants can cause adverse effects due to the invasiveness of the procedure (such as inflammation and infection) or due to the placement of the implant in the eye (such as vitreous haemorrhage and retinal detachment). Biodegradable implants may not require a surgery for their removal, which is an important advantage against non-biodegradable implants. The intravitreal injections of the particulate systems may cause vitreal clouding (Amo and Urtti [2008], Velez and Whitcup [1999]). As mentioned in section 1.2, intravitreal route is only one of the available delivery routes. Subconjunctival implantation/injection represents another route for the delivery of drugs, especially to the anterior segment of the eye. When compared with intravitreal procedures, this approach is less invasive (thus, it can be done in the ophthalmologist office, under local anaesthesia, which is more economic and less traumatic for the patient) and does not produce some of the adverse effects associated with intravireal delivery such as vitreous haemorrhage and retinal detachment (Hosoya et al. [2005]).

The ocular implants can be classified with respect to their degradability into non-biodegradable and biodegradable devices. Non-biodegradable implants can provide more accurate control of drug release and longer release periods than the biodegradable implants. However, they require an additional surgery for implant removal (Amo and Urtti [2008]). Implants can also be classified according to the mechanism of drug release into: monolithic-type, which is composed of a homogeneous/heterogeneous mixture of drugs and polymers, the binding-type, in which the drug is chemically or physically bound to the polymer, and the

reservoir-type, in which drugs are enclosed within a polymer shell (Yasukawa et al. [2005]).

Various polymers, in terms of degradability and hydrophilic/hydrophobic character, were used for manufacturing intraocular implants. Biodegradable polymers are cleaved into mono/oligomeric soluble form in the body through enzymatic or non-enzymatic reactions, while non-biodegradable polymers are not degraded/eroded in the body. Biodegradable polymers belong to the classes of polyesters, poly-orthoesters, polyanhydrides, polyhydroxyalkanoates. Non-biodegradable polymers that were used for intraocular CDDS include cellulose derivatives, silicone, acrylates, poly(vinyl alcohol) and poly(vinyl acetate). Hydrophilic polymers include albumin, gelatin, collagen, chitosan, starch, dextran, fibrin, and hyaluronic acid. They form a hydrogel when crosslinked and drugs/biomolecules can be loaded through entrapment in the polymer network (in which case they are monolithic-type) or through covalent bonding or polyion complexation (the binding-type) (Yasukawa et al. [2005]).

The procedures for making implants involve powder compression, heat press, melt compression, moulding, extrusion, and preparation as films. The choice of the technique and selection of the technique parameters will be dictated by the type of polymer to be processed, the type of drug to be loaded and the properties of the final drug/polymer mixture. Polymer films can be produced by melt-pressing or solvent-casting. Solvent-casting might involve using organic solvents in order to dissolve the polymer, which might be problematic for loading biomolecules. Moulding and extrusion are temperature aided processes in which the polymers are heated/melted and then compacted/compressed into the final shape. Therefore, these procedures might be inadequate for drugs that are thermolabile. Nevertheless, extrusion methods allow for large-scale manufacture of implants and result in homogeneous dispersion of the drug within the polymer matrix. Cold processes are available for the loading of thermolabile drugs such as powder compression (by means of a tablet press) or freeze-drying followed by cold compression. Hydrogels are also suitable to deliver thermolabile drugs/biomolecules due to the mildness of the preparation procedure (solvent casting or crosslinking are usually performed in aqueous solutions, close to or at room temperature and under strict pH control) (Breitenbach [2002], Choonara et al. [2007], Donello and Yang [2007], Yasukawa et al. [2005]). For reservoir-type implants, the core of the implant can be prepared using one of the already-mentioned techniques followed by deposition of the polymer shell through coating processes such as spray coating, dip coating or melt coating (Wong et al. [1999]).

In the monolithic-type implant, the drug is dissolved/dispersed in the polymer

matrix and the drug release takes place either by diffusion, by polymer degradation or by a combination of the two. When non-biodegradable polymers are used, drug release occurs only by diffusion through the polymer matrix. In the case of biodegradable polymer, we should distinguish between surface degrading and bulk degrading polymers. In the first case, polymer degradation is as fast as drug diffusion and release kinetics is usually of zero-type, while bulk degrading polymers (where polymer degradation is much slower than drug diffusion) usually present a $t^{0.5}$ kinetics, characteristic to diffusion-controlled systems (Yasukawa et al. [2005], Heller [1996]). In the reservoir system, the drug is surrounded by the polymer shell which controls the drug release by diffusion across the shell (Fialho et al. [2003]). A more detailed discussion on release mechanisms is presented in section 1.5.3.

Table 1.1: Examples of implantable ocular CDDS

Polymer	Drug	Construct	Application	Implantation site	Drug release	In vivo	Ref.
PCL	dexamethasone	disk	ME	intravitreal	55 weeks	rabbit	Silva-Cunha et al. [2009]
PCL	triamcinolone acetonide	filament	AMD, DR	subretinal	30 days	rabbit	Beeley et al. [2005]
PLGA	dexamethasone	filament	ME	intravitreal	90 days	on the market	Ozurdex
PLGA	cyclosporin A	pellet	CGR, PI	intracameral	3 months	rabbit	Theng et al. [2003]
PLGA	tacrolimus	scleral plug	Uv	intravitreal	35 days	rabbit	Sakurai et al. [2003]
PLGA	ganciclovir	donut tablet	CMVR	intravitreal	120 days	no	Choonara et al. [2007]
PLGA	5-fluorouridine, triamcinolone, tissue plasminogen activator	cylinder	PVR	intravitreal	30 days	no	Zhou et al. [1998]
PLA	ganciclovir	scleral plug	CMVR	intravitreal	24 weeks	rabbit	Yasukawa et al. [2000]

Table 1.1 – Continued

Polymer	Drug	Construct	Application	Implantation site	Drug release	In vivo	Ref.
PLA	triamcinolone acetonide	one side coated disk	Uv, DME, PVR	intrascleral	12 weeks	rabbit	Kim et al. [2008]
PLA	betamethasone phosphate	disk	Uv, DR, PVR	intrascleral	60 days	rabbit	Okabe et al. [2003a]
PMM	triamcinolone acetonide	disk	Uv, PVR	subconjuctival	56 days	rabbit	Felt-Baeyens et al. [2006]
Gel	basic fibroblast growth	hydrogel sheet	CNV	intracorneal	21 days	rabbit	Yang et al. [2000]
PLA, PGA, PLGA, PCL, PHA, Chi	vasodilator	rod, wafer, particle	glaucoma, RD, PVR	intravitreal	6 months	clinical trials	Donello and Yang [2007]
PVA, PVAc, PCL, PGA, PLA, PA	rapamycin, ascomycin	reservoir	DE	intrascleral	no	no	Peyman [2006]
PLA, PDLA, PCL, PGA, PA, Chi, polypeptides	growth factors, apoptosis inhibitors	fiber	glaucoma	on the optic nerve	no	no	Nelson et al. [2000]
biodegradable polymer	antiglaucoma drug	reservoir tube	glaucoma	suprachoroidal	no	no	Gifford et al. [2007]

Table 1.1 – Continued

Polymer	Drug	Construct	Application	Implantation site	Drug release	In vivo	Ref.
PTFE, FEP, PLA, PGA, Si	antiglaucoma drug	reservoir cylinder	glaucoma	subconjuctival, intrascleral, intravitreal, suprachoroidal	80 weeks	no	Wong et al. [1999]
Si, PU, parylene	antiglaucoma drug	punctal plug	glaucoma	lacrimal punctum	100 days	clinical trials	Butuner [2009]
Si, PVA	fluocinolone acetonide	pellet and suture stub	Uv, DME	intravitreal	30 months	on the market	Jaffe et al. [2000]
PVA, PEVA	ganciclovir	pellet and suture stub	CMVR	intravitreal	8 months	on the market	Amo and Urtti [2008]
PVA, PEVA	betamethasone	disk	Uv, DR, PVR	intrascleral	30 days	rabbit	Okabe et al. [2003b]
PA, PS, Si	retinal pigment epithelium cells	anchored capsule	RP, AMD	intravitreal	6 months	phase II	Neurotech
PA, PEVA	triamcinolone acetonide	helical coil	DME, AMD	intravitreal	6 months	phase I	I-vation

Table 1.1 – Continued

Polymer	Drug	Construct	Application	Implantation site	Drug release	In vivo	Ref.
non-biodegradable polymer	fluocinolone acetonide	filament	Uv	intravitreal	36 months	phase III	Bethke [2006]

Abbreviations: PLA, poly(lactic acid); PGA, poly(glycolic acid); PLGA, poly-(lactic-co-glycolic acid); PCL, poly(ε-caprolactone); PA, poly(anhydrides); PU, poly(urethane); PMM, poly(methylidene malonate); Gel, gelatin; Chi, chitosan; PTFE, poly(tetrafluroethylene); Si, silicone; FEP, poly(fluorinated ethylene-propylene); PVA, poly(vinyl alcohol); PVAc, poly(vinyl acetate); PEVA, poly(ethylene-co-vinyl acetate); PA, polyacrylates; PS, polysulfone; ME, macular edema; AMD, age-related macular degeneration; DR, diabetic retinopathy; PI, post-operative inflammation; CGR, corneal graft rejection; Uv, uveitis; CMVR, cytomegalovirus retinitis; PVR, proliferative vitreoretinopathy; DME, diabetic macular edema; CNV, corneal neovascularization; RD, retinal damage; DE, dry eye; RP, retinitis pigmentosa.

1.3 Glaucoma

Glaucoma is one of the leading causes of blindness in the developed world. There were 60.5 million people with glaucoma in 2010, increasing to 79.6 million by 2020 (Quigley and Broman [2006]). The annual direct treatment cost for late-stage glaucoma ranges from 429 to 523 euro for each patient (Poulsen et al. [2005]), producing high load on the health system. A high IOP, progressive optic neuropathy, visual impairment or blindness are common characteristics of this condition (Yudcovitch [2010]). The condition can be classified according to a structural or to a etiological basis. Glaucoma is classified into closed angle glaucoma or open angle glaucoma, based on the appearance of the angle of the anterior chamber. Based on etiology, in primary glaucoma, no specific cause can be identified, and in secondary glaucoma, optic neuropathy appears due to some other ocular disease, such as inflammation or trauma (Titcomb [1999]).

1.3.1 Glaucoma damage theories

There are several theories that explain the relationship between elevated IOP and glaucoma damage. Direct mechanical damage, ischemia, and apoptosis are the most widely accepted theories. In the mechanical damage theory, IOP directly damages the optic nerve by compression, which interferes with flow and cellular function, producing the death of optic nerve fibers. According to ischemic theory, increased IOP causes optic nerve fiber death by interfering with circulation of blood to and from the optic nerve head. Apoptosis theory states that cells die when their lifespan has been reached or when they have become damaged beyond repair. Glaucomatous damage may result from a combination of these mechanisms or by another mechanism. Moreover, different mechanisms may be involved in different types of glaucoma. Acute angle closure glaucoma might be caused mainly by mechanical damage of the optic nerve. On the other hand, normal tension glaucoma might involve ischemic-based damage as indicated by the greater frequency of haemorrhages associated with this type of glaucoma. Regardless of the mechanism, current treatments have one primary goal: IOP decrease. Although researchers are exploring new ways to slow down damage, such as neuroprotection and neuroregeneration, the main treatment goal remains reducing IOP (Yudcovitch [2010]).

1.3.2 IOP reduction as target in glaucoma treatment

Clinical trials designed to assess the efficacy of glaucoma treatment have focused on the role of lowering IOP in the prevention of optic field loss and optic nerve damage. These studies demonstrated that lowering IOP can reduce the damage caused by glaucoma. In order to reduce this damage, IOP should be lowered by different percentages, considering risk factors for each patient. A reduction of 20% is desired for patients with risk factors such as ethnicity, vascular compromise, a reduction of 30% for early glaucoma patients, that present field loss, while 40 to 50% reduction in IOP is essential for patients with moderate to severe glaucoma, that show both field loss and optic nerve damage. However, these reduction percentages do not take into account individual variability and, as such, target pressures reductions may deviate from these general IOP reduction percentages (Yudcovitch [2010]).

1.3.3 Physiology of aqueous production and outflow

IOP is normally maintained by three mechanisms: aqueous fluid production rate, outflow channel resistance and episcleral veins pressure level. Aqueous fluid is produced by active secretion from the ciliary body, using the enzyme carbonic anhydrase and provides about 80% of the aqueous production. Passive secretion via ultra-filtration and diffusion from the ciliary body accounts for the other 20%. Most of aqueous outflow involves the transport across the trabecular meshwork in the anterior chamber of the eye. Aqueous enters the trabecular meshwork after flowing through the pupil from the posterior chamber. From the trabecular meshwork, aqueous flows through Schlemm's canal and drains into a venous plexus, from where it exits the eye through the episcleral veins. Another portion of aqueous outflow involves the uveoscleral pathway. Following this pathway, aqueous passes in the anterior chamber and is transported across the ciliary muscle into the supraciliary and suprachoroidal spaces and exits the eye via the sclera (Yudcovitch [2010]).

1.3.4 Pharmaceutical treatment of glaucoma

IOP reduction can be achieved either by reducing aqueous humor production and/or by increasing aqueous outflow (Felt et al. [2002]). The first approach is attained by using beta-blockers, alpha-2 agonists, and carbonic anhydrase inhibitors, whereas the second approach is accomplished with the use of prostaglandin analogs and cholinergics, while sympathomimetics act by both suppressing aqueous production and increasing its outflow (Pang and Clark [2008]).

- Beta-blockers (timolol, betaxolol, carteolol, levobunolol, metipranolol)

  The ciliary epithelium contains beta-receptors which facilitate aqueous production in the eye, when stimulated. Beta-blocking drugs are able to reduce aqueous production by blocking beta-receptors. A typical IOP decrease with topical beta-blocker instillation ranges from 10 to 25%. Beta-blockers are additive in effect with other glaucoma drugs. An approximately 30% reduction in IOP can be obtained with systemic beta-blockers (atenolol, metoprolol, nadolol). Systemic side-effects include bronchial constriction/asthma, chronic obstructive pulmonary disease, bradycardia, congestive heart failure, and diabetes or hyperlipidemia (Yudcovitch [2010]).

- Prostaglandins (bimatoprost, latanoprost, travoprost, unoprostone)

  Prostaglandin derivatives are very potent drugs for lowering IOP. The mechanism of IOP reduction involves increasing uveoscleral outflow by enlarging the intercellular spaces on the ciliary body. The IOP reduction is typically between 30 and 35%. Prostaglandins have various side-effects such as hypertrichosis (eyelash lengthening and thickening), subtle hyperpigmentation of the iris, possible re-activation of herpes simplex virus in previously infected individuals, conjunctivitis, iritis (Yudcovitch [2010]).

- Carbonic anhydrase inhibitors, (brinzolamide, dorzolamide)

  CAI inhibit the carbonic anhydrase in the ciliary epithelium and reduce the production of bicarbonate ion, which limits sodium and fluid transport across the ciliary epithelium, and decreases aqueous production. Topical treatment results in a 15 to 20% decrease in IOP. Topical CAI are useful IOP-lowering compounds, have minimal systemic side effects and their action is not influenced by the circadian rhythm. Topical CAI are not usually used as a first-line medication because they are less efficient when compared to other glaucoma drugs. They are indicated in adjunctive therapy when the primary treatment (that consists of beta-blockers or prostaglandins) does not control IOP adequately. Oral CAI (acetazolamide, methazolamide) are used to treat acute angle closure glaucoma or other causes of extremely elevated IOP because the present several side-effects (Pang and Clark [2008]).

- Alpha-2 agonists or selective sympathomimetics (apraclonidine and brimonidine)

  They stimulate alpha-2 receptors in the ciliary epithelium and cause both a decrease in aqueous production and an increase in uveoscleral outflow. Brimonidine reduces IOP approximately by 25 to 30%. Tachyphylaxis (reduced

medication effect) can develop with brimonidine use, but with lower frequency of development than with apraclonidine, which makes the former more useful for long-term treatment. Brimonidine also tends to produce fewer ocular allergic reactions. It is additive with beta-blockers and CAI in lowering IOP. Possible side-effects include ocular hyperemia, burning/stinging, blur, foreign body sensation, and allergic reactions. Potential side-effects of apraclonidine include eyelid retraction, mydriasis, conjunctival blanching, and/or ocular allergy. Patients who have severe cardiovascular disease, low blood pressure, or bradycardia should not take apraclonidine (Yudcovitch [2010]).

- Adrenergic agonists or non-selective sympathomimetics (epinephrine)

  Epinephrine was the first sympathomimetic drug to be used in the treatment of primary open angle glaucoma. The primary mechanism of epinephrine action involves facilitating the uveoscleral outflow, and usually results in a 15 to 20% decrease in IOP. It is no longer a commonly used glaucoma medication because newer, more effective, and safer drugs are available. It is contraindicated for patients with hypertension, heart or vascular disease, and those who have had cataract surgery (Titcomb [1999]).

- Cholinergic agonists (carbachol, echothiophate iodide, physostigmine, pilocarpine)

  They work by directly stimulating acetylcholine (ACh) receptors, present on the ciliary muscles of the ciliary body. When stimulated, the ACh receptors produce muscle contraction, enlarging the trabecular meshwork spaces, thus increasing aqueous outflow. Pilocarpine is used in acute angle closure glaucoma, when immediate action is required. It produces usaully a 20% reduction in IOP. Over time, tachyphylaxis can occur and this will require higher concentrations of pilocarpine to maintain IOP reduction. Several ocular and systemic side-effects can occur with pilocarpine such as ciliary muscle spasm, retinal detachment and miosis, which reduces both the amount of light entering the eye and the field of vision. Pilocarpine is contraindicated in patients under 40 years of age, patients with cataracts, patients with inflammatory or vascular glaucoma, and patients with a history or risk of retinal detachments (Titcomb [1999]).

- Hyperosmotics (glycerol, isosorbide, mannitol, urea)

  They are indicated in the treatment of acute angle closure glaucoma or other causes of highly elevated IOP (with pressures over 40 mmHg). Hyperosmotics cause increased blood serum osmolarity, extracting water from ocular tissues

into the bloodstream. By increasing the osmotic gradient between plasma and the eye, shrinkage of the vitreous occurs, reducing ocular volume and lowering IOP. Hyperosmotics are either administered orally or by intra-venous injection. Glycerol can cause hyperglycemia and should not be used with diabetic patients. Isosorbide is not metabolized into sugar and it is safe to use with diabetics. Mannitol can cause diuresis, headaches, chills, and chest pain. Urea has numerous systemic side-effects and is rarely used. All hyperosmotics cause nausea and vomiting as a common side-effect (Titcomb [1999]).

- Alcohol and marijuana

  They can temporarily lower IOP, although with minimal and temporary effect when compared to more effective drugs. Intoxication, central nervous system depression, vomiting, nausea, and addiction are a few of the side-effects of alcohol use. D-tetrahydrocannabinol is one of the active components in marijuana and can be prescribed for treatment of chronic pain and IOP reduction. Inhaled marijuana smoke will lower IOP only slightly and temporarily. The most promising formulation involve a topical ocular drop, which is still under development. However, systemic side-effects (and legislation) currently contraindicate the widespread use of cannabinoids in glaucoma treatment.

1.3.5 Neuroprotection, gene therapy, neuroregeneration

Pharmaceutical treatment of glaucoma involves the protection of the optic nerve indirectly through lowering of the IOP. Neuroprotection therapy uses pharmaceutical agents that slow down or prevent death of retinal ganglion cells (RGC), which form the optic nerve, and maintain their normal function. An important advantage of this strategy is that it allows treatment of a disease whose etiology is unknown or varies between patients (Weinreb and Levin [1999], Mozaffarieh and Flammer [2007]). Gene therapy works by targeting specific tissues (such as trabecular meshwork, ciliary epithelium, ciliary muscle or RGC) in order to correct aqueous production and outflow and prevent RGC death. Studies designed to determine whether gene therapy can be applied to glaucomatous damage in the trabecular meshwork and the optic nerve are currently underway (Borras et al. [2002]). Neuroregeneration and repopulation with RGC involves directed axon growth and manipulation of stem and progenitor cells towards transformation into retinal cells. Optic nerve regeneration strategies involve peripheral nerve grafts, differentiation of stem or precursor cells into RGC and integration of transplanted cells into the retina or promotion of axon regrowth (Dahlmann-Noor et al. [2010], Levin [2005]).

1.3.6 Laser and surgical treatments for glaucoma

Alternative therapies for glaucoma include laser and surgical treatments. These are indicated in cases of poor IOP control by medication, or for patients that can not be prescribed glaucoma drugs because of adverse reactions, or in cases of advanced glaucoma that requires additional treatment to the pharmaceutical. However, medications are required after surgical treatment to maintain IOP control, but the dosages and types of medications might differ after surgery.

The purpose of surgical treatment is to either mechanically open a channel for aqueous outflow between the anterior chamber and the subscleral or subconjunctival spaces (as in trabeculectomy, sclerostomy, valve or tube implantation), or to partially destroy the cells involved in aqueous humor production (cyclocryodestruction). Laser treatment consists of directing a laser beam to the trabecular meshwork or iris so that openings are created. it can also be applied to destroy the cilliary processes and significantly decrease aqueous humor production. Advantages of laser treatment when compared to surgery include less risk of bleeding and/or infection, less dependence on patient compliance required to control IOP following laser surgery and less diurnal variation in IOP following laser treatment. The most commonly used laser treatments for glaucoma include trabeculoplasty (treatment of the trabecular meshwork), peripheral iridotomy (treatment of the iris) and cyclophotocoagulation (treatment of the ciliary processes). Laser treatment can reduce IOP by 20 to 30 %, although a new treatment might be required within 5 years for 50% of the patients (Titcomb [1999]).

1.3.7 Animal models of glaucoma

The development of animal models for glaucoma are essential in providing understanding of the mechanisms of aqueous humor production and outflow as well as homeostasis control of IOP. A model of glaucoma is useful for studying the effects of elevated IOP in the eye and for developing new treatment strategies. Since high IOP is a major risk factor in glaucoma, one common approach consists in increasing IOP to a level that preferentially kills RGC without damaging the retina and other ocular structures (Levkovitch-Verbin [2004], Vecino [2008]). A good animal model should reproduce human disease as closely as possible, be reproducible, easy to induce, with few tissue damage and side effects (such as pro-inflammatory reactions) and should have a low cost, so that enough animals can be used to obtain statistically significant results. Besides these characteristics, a glaucoma model should present a sustained chronic increase in IOP, allow frequent

IOP measurements and permit assessment of retinal neuronal damage (Rudzinski and Saragovi [2005]).

Spontaneous glaucoma models have been described in different animal species (rabbits, dogs, monkeys, mice). These animal models are suitable for studying the causes of the disease. Unfortunately, animals with spontaneous glaucoma are difficult to obtain and even more difficult to obtain in a similar stage of the pathology (with the exception of genetically engineered animals). Therefore, experimental models of induced glaucoma had to be developed (Vecino [2008]).

There are several animal species that can be used as suitable models for glaucoma. Primates are a clear choice due to the close phylogeny and homology with humans. However, primates are very expensive, difficult to handle, require special housing facilities and highly experienced teams (Levkovitch-Verbin [2004]). Consequently, rodent models of glaucoma were developed because these animals are inexpensive, easy to house and handle, and produce fewer ethical issues (Vecino [2008]). There is high similarity between rodents and human genomes, which allows them to be used in studies of human optic nerve disease. Moreover, their eyes and optic nerves are easily accessible. And, in the case of rabbits, the comparable size of the eyes to those of humans and the extensive information available about rabbit ocular biochemistry and physiology makes it more appropriate for the testing of new drug delivery systems (Diepold et al. [1989]). In addition, rodents have a much shorter life span than humans and this allows the study of diseases that take decades to develop in humans (Levkovitch-Verbin [2004]). However, their eyes also present a number of differences such as the absence of the macula and the fovea.

Chronic increase in IOP can be achieved mainly by three mechanisms: blocking the trabecular network (pre-trabecular mechanism), reducing aqueous humor outflow (trabecular mechanism) and blocking the limbal plexus (post-trabecular mechanism). In the first case, the introduction of viscous substances at the TM, blocks normal AH outflow and consequently raises IOP, while in the other two cases, the decrease in AH outflow is produced by modifying the TM and post-trabecular anatomy, respectively (Rudzinski and Saragovi [2005]).

Blockage of AH drainage at the level of the TM can be achieved by injection into the anterior chamber of ghost red blood cells, latex microspheres or other viscoelastic substances such as hyaluronate (Urcola et al. [2006], Diepold et al. [1989]). A single injection of hyaluronate maintains elevated levels of IOP for 8 days, while an injection performed once a week induces a sustained and significant hypertension that lasts all along the duration of the study (50 % increase, during 10 weeks) (Moreno et al. [2005]). Feasibility and reproducibility are the main advantages of this experimental model. However, it also presents several disadvantages such as

transient IOP increase (viscoelastic substances are cleared rapidly from the eye) and spikes in IOP (very high IOP values can produce retinal ischemia). Thus, to maintain high IOP weekly injections are necessary (Rudzinski and Saragovi [2005]).

Reduction of AH outflow in the TM can be produced by laser photocoagulation. The treated eyes develop sustained, high IOP with decreased outflow and optic nerve cupping like in human glaucoma. This is a simple, reliable and reproducible method to produce experimental glaucoma. Treatment is very fast (approximately 3 min per eye), which allows many animals to be treated in 1 day. The laser burns close the intertrabecular spaces and light microscopic examination shows only loss of RGC and their nerve fibres (Levkovitch-Verbin [2004]). Nevertheless, this method presents some disadvantages, such as the need for specialized equipment, multiple laser treatments needed in order to maintain high IOP values for several months and anterior chamber complications (hyphema and corneal opacities) (Rudzinski and Saragovi [2005]).

Cortisteroid induced ocular hypertension is another way to simulate glaucoma in which topically applied or subconjunctivally injected steroids cause a gradual increase in IOP, within 2 weeks from the beginning of treatment. Accumulation of cellular debris at the TM decreases AH outflow. This is a very simple model, that was extensively used in the past, but it presents some drawbacks: not all rodents are responsive to the treatment and secondary effects such as cataracts can be produced (Diepold et al. [1989], Rudzinski and Saragovi [2005]).

Drainage form the limbal plexus can be interrupted by injection or cauterization of the episcleral veins. Injections of hypertonic saline solutions in the episcleral veins increases the outflow resistance. This technique is less invasive than laser TM photocoagulation and has less anterior chamber complications. However, repeated injections are needed to maintain chronic high IOP and it was shown to produce high inter-animal variability in IOP. Cauterization of episcleral veins is easy to perform and causes long-term, high increase in IOP. This model has advantages over other in vivo models because it does not require sophisticated equipment, with rare complications of surgery. Moreover, inter-animal variability of IOP is lower than with episcleral saline injections (Rudzinski and Saragovi [2005]).

1.3.8 Concluding remarks

Glaucoma is a complex condition, whose etiology is still not yet fully understood. Thus, it is very difficult to design agents that can act upon optic nerve damage, the real cause of vision loss. Glaucoma can not be cured, so the treatment involving IOP reduction in order to preserve vision is “at best a race with the patient’s life

expectancy". Hopefully, in the future, glaucoma cure will be possible (Titcomb [1999]).

1.4 Supercritical fluids solvent impregnation

Supercritical fluids (SCF) technology is a versatile process that allows the synthesis and the processing of high performance materials, including biomaterials. Industrial products obtained with SCF technology include powder coatings, polymers, polymer additives and pigments. SCF processing can produce special morphologies and properties in materials due to the interactions in the supercritical environment, where different types of interactions from the the traditional organic solvent/water medium can occur (Kazarian [2004]).

A substance is in its supercritical state when its pressure and temperature are higher than its critical pressure and critical temperature, respectively. Some properties of a SCF are intermediate to those of liquids and gases. The density is higher than that of a gas, while the diffusivity is higher than that of a liquid. Due to these properties, a SCF can be a good solvent for some compounds/materials. Moreover, some applications of SCF processing were developed due to the non-interaction with certain materials (see Fig. 1.4) (Knox [2005]). Solvents are frequently chosen according to the temperatures and pressures corresponding to the supercritical region where processing is desired. However, other factors such as toxicity, cost and environmental issues are important as well. For pharmaceutical applications, supercritical carbon dioxide ($scCO_2$) is an ideal processing medium. It is chemically inert and has relatively low critical temperature and pressure (304 K and 7.4 MPa, respectively), which allows processing of thermolabile and/or biologically-active compounds. Furthermore, carbon dioxide is non-toxic, relatively inexpensive, recyclable, and environmentally-friendly (Subramaniam et al. [1997]).

1.4.1 CDDS preparation in supercritical medium

The impregnation of polymers with drugs/biomolecules using $scCO_2$ technology (supercritical solvent impregnation, SSI) is a suitable process for CDDS preparation because there is no residual solvent present in the processed materials, unless a cosolvent is used. $ScCO_2$ is a gas at ambient conditions and even in the case of solvent contamination, $scCO_2$ is not toxic. Organic solvent contamination is undesirable for materials with biomedical application. The traditional methods of drug loading involve the use of water or organic solvents as carriers for the drug into the polymer matrix (Domingo et al. [2002]). Moreover, using SCF technology, low

temperatures can be used for processing, impurities (such as residual monomers) can be extracted and process parameters such as pressure and temperature can be easily manipulated in order to obtain improved polymer properties and specific drug deposition and release (Kazarian [2004]).

Impregnation of a polymer matrix by a drug dissolved in a SCF is a supercritical adsorption or absorption process (depending on whether the polymer goes below glass transition temperature), governed by three phenomena (see Fig. 1.5): the drug solubility in SCF, that controls the amount of drug that can be carried by the SCF, the polymer swelling that determines the ease of impregnation and the adsorption isotherms and/or partition coefficients of the drug in the polymer phase, that will determine the amount of drug that can be loaded in the matrix (Kikic and Vecchione [2003]). As such, the impregnation process is feasible when the solute is soluble in the SCF, the polymer is swollen by the supercritical solution and the partition coefficient is favourable enough to allow the matrix to be charged with enough solute. A characteristic feature of SSI process, that makes it suitable for the preparation of CDDS are the low competition between the solvent and the solute for the substrate adsorption sites, since, at supercritical conditions, the solute will be transported and adsorbed preferentially. The gas-like viscosity and diffusivity of SCF allows rapid penetration and drug deposition into the polymer and compensates the relatively low solvent strength of $scCO_2$ (Domingo et al. [2002]).

Impregnation processes can be classified with regard to solute solubility in SCF and affinity for polymer into processes in which the deposition takes place due to the good solubility in the SCF (in this case, even a solute that has low affinity for the polymer matrix can be impregnated) or processes in which loading occurs due to a high affinity of the solute for the polymer matrix. In the first case, the polymer matrix is subjected to the SCF-solute medium; when the cell is depressurized, the SCF leaves the polymer matrix, leaving the solute trapped inside the polymer matrix. In the second case, a different mechanism applies to the impregnation of compounds with low solubility in SCF. In such cases, the high affinity of these solutes for certain polymer matrices can result in the preferential partitioning of a solute in favour of polymer over SCF (Kikic and Vecchione [2003]). The partitioning mechanism has an advantage over the deposition mechanism because it does not result in solute recrystallization and produce materials with homogeneous drug distribution (Kazarian [2004]).

SCF processes can also be classified with respect to the solute modification inside the polymer matrix into processes in which the solutes are not modified such as the impregnation of drugs and dyes, and processes in which the solutes undergo

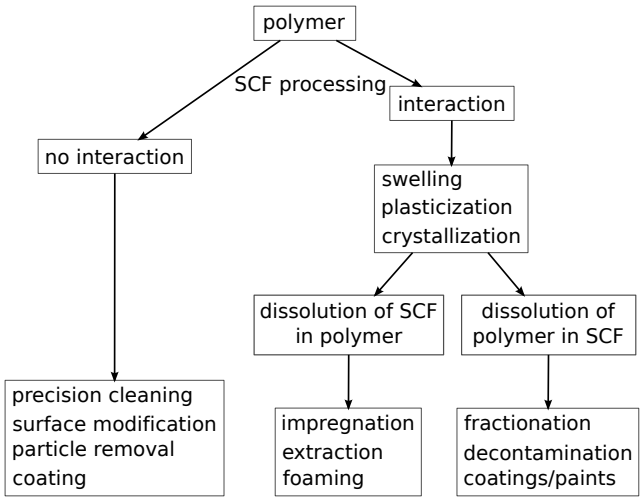

Figure 1.4: SCF processing effect on polymers and applications (adapted from Shieh et al. [1996b])

modification such as the impregnation of monomers and initiators for polymer blends preparation or the impregnation of organometallic complexes (Kikic and Vecchione [2003]).

1.4.2 SCF effect on polymers

Several effects of the SCF upon the polymer can be considered: polymer dissolution in SCF, polymer swelling (or the dissolution of the SCF in the polymer) and polymer plasticization. SCF can swell and plasticize glassy and rubbery polymers, reducing the glass transition temperature. Moreover, SCF can interact with crystalline polymers and reduce the melting temperature. The swelling and plasticizing effects are important for many polymer processing operations: viscosity reduction for polymer extrusion and blending, drug diffusion enhancement for impregnation and extraction, enhancement of monomer diffusion for polymer synthesis, foaming of polymers, and changes in polymer morphology due to induced crystallization (Kikic and Vecchione [2003], Kazarian [2000]).

The swelling/plasticization of polymers is characterized by increased segmental and chain mobility, allowing easier polymer processing and faster solute diffusion. The plasticizing effect of $scCO_2$ is the result of the ability of $scCO_2$ molecules to interact with polymer containing basic functional groups (such as carbonyl and phenyl). It has been shown that such interactions between $scCO_2$ and polymer functional groups reduce chain-chain interactions and increase the mobility of polymer segments (Kazarian [2000]). Swelling is a very important step in the

SSI process: the greater the swelling, the faster the diffusion of the solute. The solubility of carbon dioxide in many polymers is as high as that of typical organic solvents, ranging from 10% to more than 30% by weight. As already mentioned, the high diffusivity of $scCO_2$ in polymers allows an efficient impregnation process (Guney and Akgerman [2002]). It is possible to change the extent of polymer swelling by changing the density of the SCF. In this way, diffusion of solute within the SCF-swollen polymer matrix and the amount of solute incorporated in the polymer can be controlled.

In amorphous polymers, SCF interactions with the polymers are much more pronounced, while in crystalline polymers, SCF swelling and plasticization are lower in extent. Moreover, due to plasticization, SCF processing may induce crystallization in amorphous polymers or increase crystallinity in semi-crystalline polymers. As such, SCF treatment will generally be more suitable for crystalline materials than amorphous materials in precision cleaning, surface modification/coating or particle removal applications. On the other hand, amorphous materials are more suitable for applications such as polymer foaming, SSI, extraction, polymer crystallization or formation of microcellular structures (Shieh et al. [1996b,a]).

1.4.3 Cosolvents

While $scCO_2$ is a good solvent for many non-polar (and some polar) molecules with low molecular weights, it is a poor solvent for most polymers and other polar molecules. A common approach is to include a small amount of a cosolvent to increase the solubility of the solute. The cosolvent will be a substance that has a greater affinity for the solute than does carbon dioxide (Knox [2005]). The presence of the cosolvent in the SCF mixture will increase the complexity of the system and the interactions between components. Specific interactions (see Fig. 1.5) cause the formation of clusters with molecules of solute, solvent and cosolvent, and thus the region around the solute molecule is enriched with cosolvent. This local composition can be several times greater than that of the bulk composition (Sauceau et al. [2004]). Thus, the effect of cosolvent on SSI is due both to different solvent power of the mobile phase (and solute solubility) and also to a change in drug partition in the polymer phase. The cosolvent may affect the polymer phase through the adsorption of the cosolvent in the polymer phase that may alter its chemical nature, thus affecting the partition of the solute. Moreover, polymer swelling can be different in the presence of the cosolvent when compared with pure SCF (Kazarian et al. [1998]).

Cosolvent effect on the solubility enhancement of solid solutes in SCF was investigated through the choice of cosolvents of different polarity/functionality

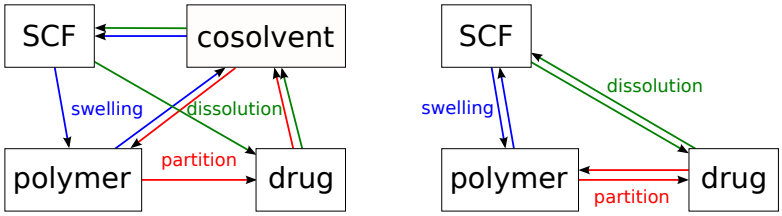

Figure 1.5: SCF medium interactions (adapted from Kikic and Vecchione [2003])

and in different concentration. Solvent self-association and Lewis character are important because they will diminish or enhance the interactions between the functional groups of the cosolvent and the solute or the polymer (Kazarian et al. [1998], Sauceau et al. [2004]). As already discussed, solubility enhancement in the presence of cosolvent is due to the interactions between the solute and cosolvent. Thus, it is expected that the largest cosolvent effect on polar solute is from the polar cosolvent, while for the non-polar solute the largest cosolvent effect comes from the non-polar solvent (Li et al. [2003]).

The interactions between the cosolvent and the solute, and thus the cosolvent effect (in terms of solubility enhancement) can also be manipulated by SSI pressure. The importance of the cosolvent effect decreases with increasing pressure because at very high pressures, the local concentration of the cosolvent approaches the bulk concentration. While the local concentration decreases, the bulk concentration of cosolvent (and thus solubility) always increases with increasing pressure, due to an increase in density. Thus, it has been observed that, at low cosolvent concentration, the cosolvent effect depends predominantly on the bulk concentration of cosolvent around the solute, and as the cosolvent concentration is increased, the effect of local concentration enhancement becomes significant. This result show the importance of specific interactions between the cosolvents and the solute in comparison with density effect (Sauceau et al. [2004]).

With respect to the other manifestation of the cosolvent effect, it was observed that the partition coefficient of the cosolvent between the SCF and the polymer phase decreases rapidly with an increase in SCF density near critical region and flattens at higher density in the supercritical region (the density effect). This may be due to increased solvent power of SCF and consequntly an increase of cosolvent solubility in SCF at first, followed by weakening of interaction between the cosolvent and the polymer due to higher polymer swelling. Such intermolecular interactions are very important in the partitioning process. The preponderance of the two effects can vary according to the system. Although, the bulk concentration of cosolvent (and consequently cosolvent-solute interactions) increases at higher

pressure, cosolvent interactions with the polymer (and consequently partitioning) decreases due to higher polymer swelling (Sauceau et al. [2004]).

In conclusion, careful selection of cosolvents could improve SCF processing, particularly for solutes with extremely limited solubility in pure SCF. As discussed above, it is expected that a multicomponent SCF mixture can be highly selective for particular solutes due to specific interactions.

1.4.4 Drug release from SCF impregnated matrices

The good performance of a CDDS is dependent on drug distribution in the matrix as well as on the physical state of the drug. In general, crystallization of drugs in a polymer matrix can result in unpredictable dissolution rates (López-Periago et al. [2009]). With SSI it is possible to obtain amorphous drug dispersions even at relatively high loadings, due to the poor solvent properties of SCF for most drugs and the high drug partition in the polymer phase. With traditional methods, crystallization of the drug can occur in the solvent-rich areas (that are good solvents for the drug) of the polymer matrix during the solvent evaporation process (Wang et al. [2002]).

One problem with SSI is the surface precipitation of the drug that results from the characteristics of the impregnation process. During the depressurization procedure, the drug dissolved in the SCF will precipitate from the solution on the polymer surface. The depressurization stage is of critical importance with respect to this issue. If the depressurization is fast, then the polymer will be very porous and will result in a heterogeneous drug distribution, with higher concentrations close to the surface, resulting in burst effect. If the depressurization is slow, the initial polymer morphology will be preserved and present homogeneous drug distribution (Guney and Akgerman [2002]).

The release profiles typically present a biphasic release pattern: a diffusional period of rapid release of drug precipitated on the surface of the polymer rather than being impregnated within the polymer matrix (usually within the first day), followed by a swelling/diffusional phase of linear release of the drug that has been impregnated within the polymer matrix, that occurs before the dissolution/degradation of the polymers, if biodegradable (Braga et al. [2008], Natu et al. [2008]).

The pharmacological activity of a drug can be determined by the release kinetics in terms of released drug mass and release drug rate. Several phenomena that can influence SSI (Fig. 1.6) have to be considered when parameters that can control drug loading and drug release from SCF impregnated matrices are studied:

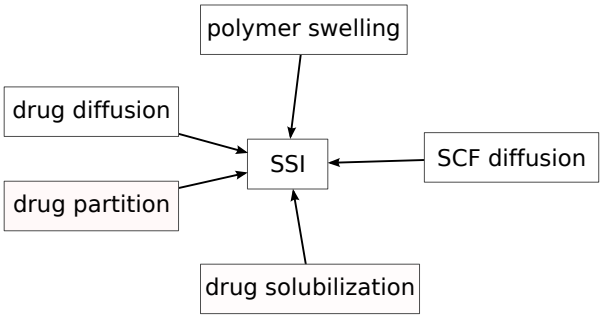

Figure 1.6: Simultaneous phenomena involved in SSI

- Pressure and temperature

  One major advantage of SCF technology is the possibility to adjust solvent power by simply changing the pressure or temperature of the system. The solvent power increases with pressure at constant temperature because density rises with increasing pressure. The intermolecular distance between molecules decreases and consequently the interaction between the solute and the solvent increase, leading to higher solubility (Duarte et al. [2004]). Nevertheless, selecting the best process parameters is not straight forward and an increase in pressure does not necessarily lead to better impregnation. When drug has good solubility in SCF and/or low affinity for the polymer, lower pressures and densities favour impregnation (Duarte et al. [2007]). At higher densities, the interactions between the solute and the SCF increase and are detrimental to the interactions between the solute and the polymeric matrix, thus leading to lower impregnation yields (Braga et al. [2008]).

  The effect of the temperature on the solute solubility depends on the pressure range. Under a certain range of pressure, the solubility decreases when the temperature increases and above a certain pressure, the solubility increases when the temperature increases (retrosolubility phenomenon) (Belhadj-Ahmed et al. [2009]). Usually, the higher the temperature, the higher the solute concentration in the SCF. Additionally, higher temperatures will increase polymer swelling, creating more free volume within the polymer matrix which enhances solute diffusion (Bush et al. [2007]).

- Operation type (batch or continuous process), contact time and SCF flow rate

  The SSI can be carried out either in batch or continuous mode. The determination of the best operating conditions requires a knowledge of phase

equilibria and drug solubility in a SCF (Duarte et al. [2004]). When selecting a contact time in the batch mode, one has to consider the equilibrium solute solubility in SCF at the process pressure and temperature. In a continuous operation, the flow rate of SCF has to be carefully selected so that it ensures good mass transfer and allows the solute concentration in the fluid phase approach the equilibrium value, otherwise it will lead to poorer impregnation than in batch mode Duarte et al. [2007]. In dynamic mode, the solute concentration in SCF phase can be significantly lower than the solute solubility (in static mode), when the equilibrium is not reached for the operating conditions (Belhadj-Ahmed et al. [2009]).

Usually, an increase in contact time will produce a better impregnation yield due to increased solute concentration and enhanced polymer swelling, allowing increased diffusion of drug into the polymer and ensuring solute impregnation in the polymer bulk. Nevertheless, a higher contact time can lead to heterogeneous drug distribution and solute crystallization on polymer surface (Wang et al. [2002]). Concerning the effect of flow rate, the solute concentration increases when the flow rate increases. For a range of flow rate, the solute concentration will stabilize and above a certain value (threshold) of flow rate it will decrease. After the threshold value of flow rate, the higher the flow rate, the smaller the dissolved amount of solute in SCF due to an increase of the dilution effect (Belhadj-Ahmed et al. [2009]).

- Sample geometry and dimensions

The geometry and the dimensions of the samples used in SSI process can have a significant effect on the amount of the impregnated drug and the drug distribution. Under similar experimental conditions, impregnation was more efficient for polymer beads than for polymer rods. The effect of dimensions was demonstrated by the rod samples where drug loading decreased significantly with increasing rod diameter. The cross-section analysis of the rods indicated that polymer swelling was not complete during the selected processing time for the rods with higher diameter. Moreover, the rods presented gradient drug deposition, with higher amounts of drug at the surface that subsequently caused burst release (Argemí et al. [2008]). This suggests that SCF diffusion in the polymer is of extreme importance for the success of the impregnation. When selecting a sample geometry, one has to consider the SCF sorption and diffusion kinetics in the polymer and allow sufficient contact time for the impregnation of bigger/thicker samples (Duarte et al. [2006]). If shorter

processing times are desired, then smaller/thinner samples, such as films, should be used.

- Polymer swelling

  The chemistry of the polymer is very important in SSI because it will determine SCF sorption and diffusion in the polymer, as already mentioned. For the preparation of CCDS, polymer-SCF interactions are extremely important for the diffusion of drugs inside the polymer matrix. If the polymer does not interact with the SCF, then there is no possibility to load the drug in the polymeric matrix. As such, a polymer that contains certain functional groups (like carbonyl) will interact with the SCF and swell, allowing more drug to diffuse inside the polymer and higher amounts of drug to be impregnated (Braga et al. [2008]).

  Amorphous polymers are easily processed with SCF, while crystalline polymers are not, since the SCF sorption occurs mainly in the amorphous regions. This allows easy drug impregnation in the core and throughout the amorphous polymer. For semi-crystalline polymers, the induced crystallization in the amorphous fractions prevents the dispersion of the drug in the matrix, leading to heterogeneous drug loading, mainly at the surface López-Periago et al. [2008]. A heterogeneous medium might be responsible for heterogeneous impregnation of glassy polymers, where glassy and rubbery parts coexist within the polymer, each inducing different uptakes of solute. This effect is more significant at shorter processing times (Diankov et al. [2007]), that does not allow complete SCF diffusion in the polymer. Moreover, the presence of the drug in polymeric matrix might accelerate the SCF diffusion-front propagation (Uzer et al. [2006]).

  Sorption diffusion coefficients are relatively insensitive to pressure or temperature. The desorption diffusion coefficients (determined at ambient conditions) are higher than sorption diffusion coefficients. The plasticizing effect of the SCF might be responsible for this result. Even though sorption takes place under supercritical conditions and desorption proceeds at ambient conditions, the release of carbon dioxide from the polymeric matrix during desorption is faster, due to the higher chain mobility of the plasticized polymer (Duarte et al. [2006]). This might be particularly useful to consider when selecting a depressurization rate in order to ensure maximum drug loading and homogeneous deposition.

- Drug solubility in SCF (or SCF and cosolvent) and drug concentration

  Solutes with good solubility in SCF will be easily impregnated in a polymer, although with a heterogeneous distribution (Kikic and Vecchione [2003]). The solute loading depends on the solute concentration in the fluid phase: there is an increase in the amount of impregnated drug with an increase in solute concentration (that ranged from 10 to 100% of the solubility value). It was suggested that, rather than adsorption, partition of the solute between the fluid phase and the swelled polymer network could explain the behaviour (Diankov et al. [2007]).

  As already discussed, a cosolvent can enhance the solute solubility in SCF by several orders of magnitude due to the interaction with the solute molecules. Moreover, the cosolvent can also modify the interactions between the high pressure phase (that contains the drug) and the polymeric matrix, by improving the compatibility, swelling and plasticizing power of this phase with the polymer (Braga et al. [2008]).

- Drug chemistry (drug solubility, compatibility in polymer)

  Drug chemistry will determine drug-polymer interactions and allow the impregnation of drugs that have low solubility in SCF, but high affinity for the polymer. Thus, smaller amounts of drug (with high partition in polymer) are required to achieve similar loadings with traditional methods, even if SCF is a poorer solvent for the drug than organic solvents. Usually, there is an increase in drug loading with an increase of drug solubility in polymer (which estimates drug-polymer compatibility) (Liu et al. [2005]). Such interactions allow the incorporation of drug in amorphous form because they prevent drug self-association and crystallization even at higher loadings (López-Periago et al. [2009]). The affinity based method of CDDS preparation is especially suitable for molecular dispersions of drugs with low water solubility, since dissolution is improved for drugs in amorphous state (Kazarian and Martirosyan [2002]). When drug is not compatible with the polymer, SSI will lead to drug crystallization on polymer surface even if care is taken against drug precipitation during depressurization (Wang et al. [2002]).

1.4.5 Concluding remarks

SCF technology can be used for loading of drugs in polymers. The most attractive aspects of this technology are the easy manipulation of several parameters (such as pressure, temperature, cosolvent choice) in order to control drug loading,

drug distribution and polymeric material properties (such as morphology and crystallinity), with great effect on the performance of the CDDS. SSI is particularly useful for the production of drug-eluting implants because in only one step both drug loading and a foam-like polymer structure is achieved. This very porous morphology allows further processing (by cold compression, for example) of the drug loaded matrix in order to obtain implants with various dimensions and shapes.

1.5 Electrospun fibers as controlled drug delivery systems

This section was published as a book chapter in *Active Implants and Scaffolds for Tissue Regeneration*, part of the series *Studies of Mechanobiology, Tissue Engineering and Biomaterials* (Springer).

Electrospinning is a method of producing fibers with diameters ranging from micrometer to nanometer scale by accelerating a jet of charged polymer solution/melt in an electric field. Recently, this technology has been expanding due to the simplicity of the process and the various materials that can be used. Fibers can be produced from either natural or synthetic polymers. Such fibers have diverse applications including filtration, catalysis, textiles, composite materials, biomedicine (wound dressings, drug delivery, tissue engineering, cosmetics), sensors, electronic devices, liquid crystals, photovoltaic cells and much more (Fridrikh et al. [2003], Huang et al. [2003]).

Usually, the experimental set-up consists of a high voltage power supply connecting an electrode with needle-like geometry (through which the polymer solution is ejected) to the collector electrode. The polymer solution is pumped at the desired flow rate using a syringe pump. A diagram presenting the most common electrospinning set-up is shown in Fig. 1.7.

Recent works suggest that the most important mechanism of electrospinning is a rapidly whipping/bending fluid jet (Hohman et al. [2001]). The jet instability is produced by the competition between surface tension and charge repulsion, in which the destabilizing effect of charge repulsion is responsible for the stretching of the fluid jet and simultaneous decrease in the jet diameter. Surface tension has a stabilizing effect leading to the cessation of stretching and attaining a limiting terminal jet diameter. The process can be decomposed into five components: fluid charging, formation of the cone-jet, thinning of the steady jet, onset and growth of jet instabilities and fiber collection (Rutledge and Fridrikh [2007]). Several process parameters (voltage, nozzle to collector distance, polymer flow rate, spinning

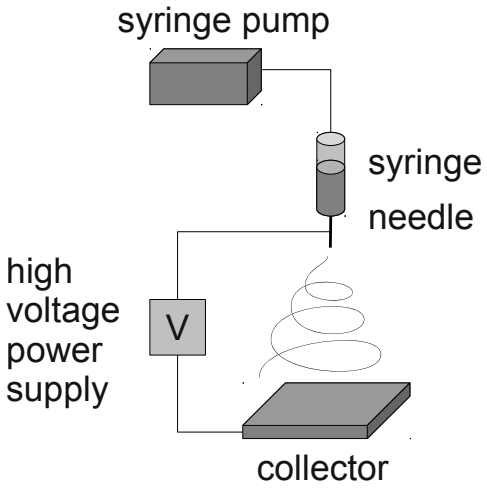

Figure 1.7: Basic electrospining set-up

environment) and solution parameters (concentration-viscosity, conductivity, surface tension, solvent volatility) can be manipulated in order to obtain the desired properties of the fibers such as fiber diameter and morphology. Moreover, the fibers can be collected with a multitude of collectors producing fiber mats that contain either aligned or unoriented fibers (McClure et al. [2009]).

Electrospun fibers have been shown to function as drug delivery systems because of high surface area (which enhances mass transfer), similar topography and porosity to the extracellular matrix making them ideal candidates as active implants/scaffolds. The easy control of the macrostructure (oriented or arranged randomly, fiber mat porosity) and the microstructure (individual fiber porosity) will determine both the bulk physico-chemical properties and the biological response to the implant/scaffold. Variuos drugs ranging from low molecular agents to proteins and even cells (López-Rubio et al. [2009]) can be easily encapsulated inside or on the surface of the fibers depending on the application. Some disadvantages include drug loading that is limited by the drug solubility in the electrospining solution or burst effect due to surface deposited drug.

CDDS can be classified according to different criteria (Heller [1996], Cussler [1997]). The most common one is to classify with respect to the rate control mechanism. These classifications may also be applied to drug-containing polymeric fibers:

- Drug diffusion controlled systems

  Diffusion can take place either through the bulk polymer as in bicomponent mixed fibers or through a barrier as in core-shell fibers

- Solvent diffusion controlled systems

  Drug release is determined by the rate of polymer swelling

- Chemically controlled systems

  Either polymer erosion or enzymatic/hydrolytic polymer degradation control the drug release rate

- Regulated systems

  The application of a magnetic field or another external stimulus can trigger the release (as in composite fibers containing magnetic particles)

The active ingredient can be loaded either during electrospinning or during post-processing of the electrospun fibers. In the former case, the drug is either co-dissolved with the polymers in the electrospinning solution or the drug is loaded in particles that will be co-electrospun with the polymers (Qi et al. [2006], Liang et al. [2005], Wang et al. [2010]). The later case includes various modalities of drug loading: fiber soaking in the drug solution, drug impregnation using supercritical fluids technology (Ayodeji et al. [2007]), loading in previously molecular imprinted fibers (Chronakis et al. [2006b,a]), functionalization of the fiber surface through grafting copolymerization (Ma et al. [2006]) and subsequent drug/protein binding (Casper et al. [2007, 2005]).

By electrospinning, the drug is usually entrapped as solid particles inside or on the surface of the fibers. According to the type of solid-solid or polymer-drug mixture, the drug loaded fibers can be classified as:

- Solid solutions

  The drug is dissolved at molecular level in the polymer

- Solid dispersions

  The drug is distributed in the polymer as either crystalline or amorphous aggregates

- Phase-separated systems or reservoir systems

  The drug is contained inside the core of the fiber or encapsulated in particles, that are surrounded by a polymer shell (as in core-shell constructs or composite fibers, see section 1.5.1)

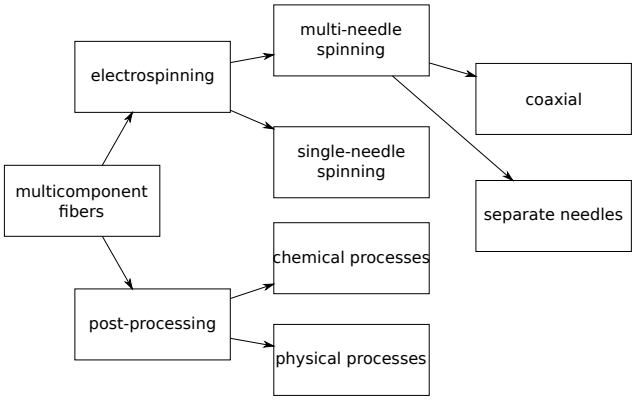

Figure 1.8: Preparation methods for multicomponent fibers

1.5.1 Multicomponent fibers

Multicomponent fibers have attracted special attention because new properties can be obtained through the combination of different materials. Synthetic polymers with good processability and good mechanical properties can be mixed with natural hydrophilic polymers producing an increase in cellular attachment and biocompatibility (McClure et al. [2009]). Unfortunately, sometimes the solvent that is used to dissolve both polymers can damage the structure of the natural polymer or phase separation can worsen the mechanical properties. One possible solution is to incorporate function-regulating biomolecules in synthetic polymers to increase bioactivity (Casper et al. [2005]) or to modify the structure of the polymer before electrospinning (Skotak et al. [2008]).

Multicomponent fibers can be obtained mainly by two techniques (Sawicka and Gouma [2006], Liang et al. [2007]) as shown in Fig. 1.8: electrospinning of polymers solution in a single-needle configuration (if a mixture of polymers is co-dissolved in the electrospinning solution) or a multi-needle configuration (in which the polymer solutions are separated in parallel or concentric syringes) and post-treatment of the electrospun fibers (which can include either coating with other inorganic/polymer layers (Casper et al. [2007], Lee et al. [2009]), grafting (Ma et al. [2006]), crosslinking (Lee et al. [2007]), chemical vapour deposition (Zeng et al. [2005a]) or functionalization with other (bio)polymers (Casper et al. [2005]).

In addition to the combination of physico-chemical properties that arise from using various components, there can be obtained a variety of fiber morphologies as presented in Fig. 1.9 such as core-shell fibers, micro/nanotubes, interpenetrating phase morphologies (matrix dispersed or co-continuous fibers) Bogntizki et al. [2001], Wei et al. [2006], nanoscale morphologies (spheres, rods, micelles, lamellae, vesicle tubules, and cylinders) obtained by self-assembly of block copolymers (Kalra et al. [2006]), multilayers (either with different composition or different fiber diameter)

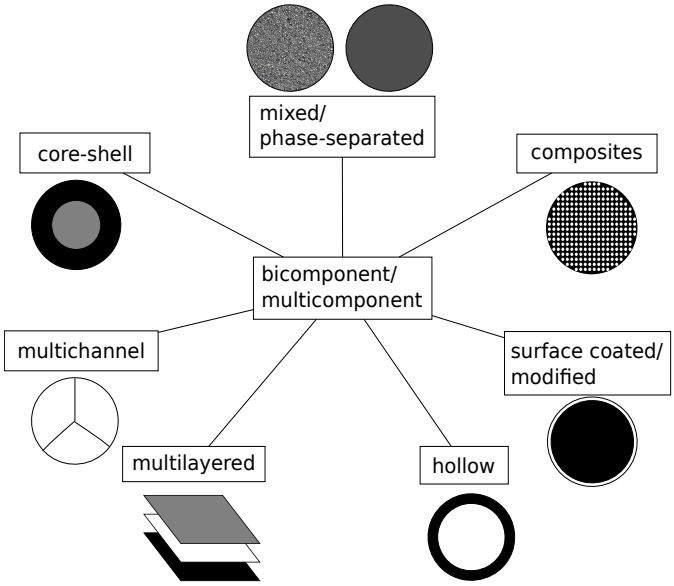

Figure 1.9: Various fiber constructs types

(Vaz et al. [2005], Pham et al. [2006]). Moreover, the fiber morphology can be further controlled after electrospinning by selective removal of one component using thermal treatment or dissolution (Hong et al. [2008], You et al. [2006]).

Many of the fiber constructs are supposed to work as implants/tissue scaffolds besides functioning as drug delivery devices. Good mechanical properties are required in order to preserve the structural integrity of the implant. Crosslinking (Sisson et al. [2009]), thermal interfiber bonding (accomplished near the melting temperature of the electrospun polymer and impregnated with a hydrogel that maintains the structure of the scaffold against shrinkage) in order to improve biomechanical properties (Lee et al. [2008]) or continuous alignment of electrospun fiber yarn obtained by self-bundling electrospinning and further treated by drawing and annealing to improve tensile strength (Wang et al. [2008]) are just some of the available post-processing techniques.

1.5.2 Release control of drug loaded fibers

Fibers can be easily loaded with drug in a similar fashion as multicomponent fibers (section 1.5.1), the drug being an extra component. By blend electrospinnning, the drug or drug vehicle (such as microspheres (Qi et al. [2006]), nanoparticles (Liang et al. [2005], Wang et al. [2010])) is mixed or phase-separated with the polymer phase and by coaxial electrospinnning, the drug is contained either in the core or in the shell. The advantage of encapsulating the drug in the core or in a vehicle is that usually burst release is minimized/avoided since the drug has longer diffusional paths (Wang et al. [2010]) and the protection of active agents

(such as proteins) that are sensitive to organic solvents can be achieved. Moreover, it does not require good interaction between the polymer and drug, but it must show sufficient interfacial compatibility in order to prevent delamination (Tiwari et al. [2010]). In contrast, for the cases of drugs loaded by blend electrospinning, poor interaction between the drug and polymer affect the drug distribution in the polymer matrix and consequently the release behavior (Chew et al. [2005], Zeng et al. [2005b]). Incorporation of bioactive agents that are usually water soluble and can not be dissolved in the same solvent as the polymer (usually organic solvents) can be performed by emulsion electrospining (Chew et al. [2005], Xu et al. [2005]).

Various post-treatment modalities exist in order to further control the fiber drug release. These can be grouped in two main categories: physical and chemical. The first category includes functionalization of electrospun fibers with biomolecules using coating (Casper et al. [2007]), subcritical carbon dioxide impregnation of electrospun fibers with which it is possible to load drugs and obtain more sustained release profiles in comparison to loading through soaking in drug solution (Ayodeji et al. [2007]). The second category consists of coating electrospun fiber by chemical vapour deposition in order to prolong the release and avoid burst effect (Zeng et al. [2005a]), molecular imprinting of fibers (either by loading the template molecule (Chronakis et al. [2006b]) or by loading molecularly imprinted particles (Chronakis et al. [2006a]) inside the fibers during electrospinning) that can selectively rebind the target molecule (biological receptor molecule) and produce targeted drug delivery.

Drug delivery systems are intended to deliver well controlled amounts of drug between the minimum effective level and the toxic level during a predetermined time interval (Heller [1996]). Control of burst effect is essential either to avoid toxicity or to ensure immediate action at the targeted location (as in the case of antibiotics (Kim et al. [2004])). These are the reasons why the factors that affect the release rate should be considered when designing a new fiber drug delivery system:

- Fiber construct geometry (fiber mats or multilayers) and thickness

  The drug deposited in single layers is released faster than from multilayers either because the drug layers are intercalated with non-drug layers that function as barrier to drug release (Okuda et al. [2010]) or because the inner layers are not equally exposed to the release medium (Ranganath and Wang [2008])

- Fiber diameter and porosity

  A thinner or more porous fiber implies a bigger surface and consequently accelerates the release (Cui et al. [2006]). However, thicker, but more porous

fibers release drug faster than thinner, less porous fibers (Buschle-Diller et al. [2007])

- Fiber composition

  The choice of a degradable polymer will allow release control through a hydrolytic (Ranganath and Wang [2008]) or enzymatic mechanism (Zeng et al. [2005b]). Besides, blending various components leads to modulating release capacity (Buschle-Diller et al. [2007]) either by improving fiber wetting properties (using hydrophilic polymers (Nie et al. [2008], Maretschek et al. [2008])) or aiding incorporation of drug. In this case, it is possible to avoid burst effect by blending polymers with amphiphilic copolymers which can be compatible with both the drug and the initial incompatible polymer (Kim et al. [2004])

- Fiber crystallinity

  Initial polymer crystallinity influences the drug release (it blocks the release of the drug from the crystalline domains due to limited water uptake). When the release of drug from the amorphous domains or from the fiber surface is finished, no more drug is released (Kenawy et al. [2002]). Moreover, there is an increase in crystallinity during drug release (the drug works as a plasticizer, the polymer chains gain more mobilility and as it is leached out, they crystallize), which decreases the release of residual drug (Xu et al. [2006])

- Fiber mat swelling

  Water uptake by fibers or by the (macro)pores created between fibers will speed up drug release (Buschle-Diller and Xie [2009]) as the dissolution of drug molecules is the initial step in the release process (Chien [1992])

- Drug loading

  Higher loadings will produce faster release (Cui et al. [2006], Xu et al. [2006], Buschle-Diller and Xie [2009], Luong-Van et al. [2006], Zamani et al. [2010]); on one hand, at high loadings, there is more surface segregated drug that dissolves fast and on the other hand, there is an increase in porosity during drug elution proportional to the initial amount of drug (Xu et al. [2006], Cui et al. [2006])

- Drug state

  In general, drug release was shown to be more sustained, when drug is incorporated in amorphous state (Zamani et al. [2010], Xie and Wang [2006]),

than when drug is loaded in crystalline state Thakur et al. [2008]. Moreover, it was shown that, even when the drug is in amorphous state, the drug release was faster from the solid solution than from the amorphous dispersion (Yu et al. [2009])

- Drug molecular weight

  Drugs with smaller volumes will be released faster since they diffuse faster through the aqueous pores created by the water uptake in the fiber (Buschle-Diller et al. [2007], Taepaiboon et al. [2006])

- Drug solubility in the release medium

  Usually, the higher drug solubility, the faster the release (Buschle-Diller et al. [2007])

- Drug-polymer-solvent interaction

  Solubility and compatibility of drugs with the polymer and/or the electrospinning solvent is essential since it ensures proper drug incorporation inside the fibers and not on the fiber surface (Chew et al. [2005], Buschle-Diller and Xie [2009], Zeng et al. [2005b]). Phase separation between the drug and polymer will produce amorphous or crystalline drug at the fiber surface leading to faster release (Verreck et al. [2003b]). Moreover, the interaction between drug and the polymer can block the crystallization of the drug in the fibers, if so desired (Yu et al. [2009]) and can even determine sustained release of drugs that are present in crystalline state because of hydrogen bonding to the polymer (Taepaiboon et al. [2006])

However, in order to predict the outcome of a drug from fibers, it is important to consider the interaction among the various factors in such a complex system. We have already discussed how the drug state controls drug release. However, sometimes high drug loadings are needed for long term applications. Usually, at high loads, the drug will crystallize and/or phase-separate from the polymer and form conglomerates that will produce a heterogeneous distribution of the drug inside the fibers (Chew et al. [2005], Huang et al. [2006]) or deposition on the fiber surface (Verreck et al. [2003b]). Thus, in long term release applications where high amounts of loaded drug are required, a compromise must be found between loading and release rate that change in contrary directions. Careful consideration should also be paid when selecting best pair of polymer and drug, although some applications require material properties that may not match in terms of compatibility the drugs used in the treatment of the targeted diseases.

1.5.3 Release modeling in fiber CDDS

As summarized in Table 1.2, a multitude of drug/biomolecules loaded fibers have already been produced. They have been produced either from polymers (synthetic and natural) or inorganic compounds. Most of the release mechanisms were attributed to drug diffusion (as it is the case for most non-biodegradable, non-erodible polymers), solvent diffusion (as in the case of natural polymers that are usually hydrophilic (Sikareepaisan et al. [2008])), polymer erosion (as in the case of erodible (bio)polymers (Yu et al. [2009], Taepaiboon et al. [2006])), polymer degradation (as for hydrolytic or enzymatic degradable polymers) or external triggers (like a magnetic field). In the release system governed by drug diffusion, one has to consider two cases, one in which the diffusion takes place through the bulk of polymer (bulk diffusion) or through a membrane/layer (barrier diffusion, similar to the reservoir devices as in the case of core-shell fibers, composite fibers or multilayered constructs). There are cases in which several mass transport mechanisms superpose. However, in most cases, there is only one that is the "rate-limiting" step. For example, in the case in which diffusion is coupled with chemical reaction (in most cases, hydrolysis), if diffusion is faster than the chemical reaction, then mass transfer is controlled by the polymer degradation (Tzafriri [2000]) and when diffusion is not much faster than reaction, then diffusion and degradation superpose (Ranganath and Wang [2008]). In some systems, the release process is composed of sequential stages, with each stage being controlled by a different phenomenon. For example, in the first stage you can have the drug release controlled by the polymer erosion and subsequent diffusion, followed by polymer degradation control stage (Kim et al. [2007]).

Related to core-shell fibers, we can consider two controlling phenomena: diffusion through the polymer shell (barrier diffusion) or partition of the drug from the core to the shell. The diffusion through the shell polymer should not be too slow, otherwise this diffusion will be rate-limiting step. In this instance, the system behaves as monolith fibers and not core-shell fibers (reservoir system). Shell porosity must also be carefully controlled since the drug from the core will be released through water-filled channels rather than through the barrier/shell polymer (Tiwari et al. [2010]). Composite fibers that contain drug vehicles such as microspheres and nanoparticles (see section 1.5.2) are also a type of reservoir system (double barrier system) in which the drug molecules have to diffuse through longer pathways: the polymer comprising the vehicle and the "shell" polymer (Wang et al. [2010]).

Drug diffusion (more precisely solid state diffusion) was mentioned earlier as one of the most common mechanisms of drug release. There are models that consider diffusion of solutes in polymers insignificant in comparison with diffusion

in water-filled spaces in between polymer chains, so they assume that water uptake and subsequent solubilization of the drug is an important step in the release process and it is the solvated molecule that is actually diffusing (Perale et al. [2009]). This is the assumption behind biphasic diffusion that includes an initial diffusion phase through the polymer (either amorphous or semi-crystalline) and a second diffusion phase through water-filled pores formed in the fiber due to polymer swelling/chain rearrangement or polymer recrystallization (Verreck et al. [2003b], Zong et al. [2003]).

The power law equation, which was developed considering that the main mechanism for drug release is drug diffusion through the polymer or solvent diffusion inside the polymer that produces polymer relaxation/chain rearrangement (Eq.1.1) is the most widely used equation in works concerning drug release:

$$\frac{\mathrm{m_t}}{\mathrm{m_{tot}}} = \mathrm{a_0} + \mathrm{k\,t^n} \tag{1.1}$$

where m_t/m_{tot} is the fractional release of the drug at time t, a_0 is a constant, representing the percentage of burst release, k is the kinetic constant and n is the release exponent, indicating the mechanism of drug release (which can either be Fickian drug diffusion or polymer relaxation and an intermediate case combining the two (Peppas and Brannon-Peppas [1994])).

Other models consider different phenomena that control the release such as desorption due to the fact that under the assumption of diffusion control, 100 % release of the drug is expected, but this was not verified experimentally. In the desorption model, the release is not controlled by diffusion, but by the desorption of the drug from fiber pores or from the fiber surface. Thus, only the drug on the fiber and pore surfaces can be released, whereas the drug from the bulk can only be released when the polymer starts to degrade. These assumptions are similar to the theory of mobile agent, that can be released by diffusion and the immobilized agent, that can be released through degradation (Tzafriri [2000]).

The Eq.1.2 is based on a pore model, in which the effective drug diffusion coefficient, D_{eff} is considered and not the actual diffusion coefficient in water, D (with $D_{eff}/D \ll 1$) because desorption from the pore is the rate limiting step and not drug diffusion in water, which is relatively fast.

$$\frac{\mathrm{m_t}}{\mathrm{m_{tot}}} = \alpha \left[1 - \exp\left(-\frac{\pi^2}{8}\frac{\mathrm{t}}{\tau_\mathrm{r}}\right)\right] \tag{1.2}$$

where the porosity factor $\alpha = m_{s0}/(m_{s0} + m_{b0}) < 1$, with $\mathrm{m_{s0}}$ and $\mathrm{m_{b0}}$ being the initial amount of drug at the fiber surface and the initial amount of drug in the fiber bulk, respectively; m_t is the drug amount released at time t, while the total

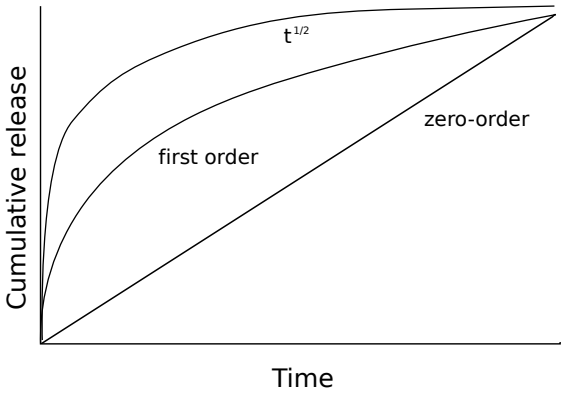

Figure 1.10: Types of release kinetics

initial amount of drug in the fiber is $m_{tot} = m_{s0} + m_{b0}$ and τ_r is the characteristic time of the release process (Srikar et al. [2008]).

Various release kinetics exist and the most desirable one is the zero-order kinetics in which the drug is released at constant rate, independent of time (see Fig. 1.10). Usually, zero-order kinetics is achieved for reservoir systems such as core-shell fibers or composite fibers in which the drug is properly encapsulated in the core of the fiber or in other vehicles (micro/nanoparticles). Burst stage in this kind of system is diminished (or non-existent) because there is no drug deposited on the surface of the fibers. As the controlling release phenomena is drug partition from one phase to another and not diffusion, there is no decrease in release rate over time as expected in a diffusion-controlled system (the release rate depends on the concentration gradient and on the length of diffusion path; as release proceeds, the concentration gradient decreases and the diffusion length increases and both contribute to slowing down the release rate).

Other strategies to attain zero-order release include polymer degradation controlled release (either accompanied by erosion or not) because then drug is released due to polymer chain cleavage (Zeng et al. [2005b], Ranganath and Wang [2008]). The drug is released either because the diffusion paths are shortened as degradation takes place (surface degradation) or because porosity is increased due to the leaching of degradation products (bulk degradation) (Heller [1996]). Another strategy to obtain constant release rate is the use of multilayered constructs (Okuda et al. [2010]), in which sequential electrospinning is used to obtain drug loaded layers surrounded by barrier layers.

Burst effect can be determined by fiber porosity (Tiwari et al. [2010]), poor drug solublity in electrospinning solvent (Buschle-Diller and Xie [2009]), poor drug solubility in polymer (Zeng et al. [2005b]), high drug solubility in release medium (Buschle-Diller et al. [2007]), heterogeneous drug distribution (Chew et al.

[2005]) or surface segregated drug (Kenawy et al. [2002]). Most of the times, the polymer and drug selection depend on the properties of the implantation site that need to be matched by the fiber mat and the targeted disease. Thus, the burst stage can only be controlled in unicomponent/monolith fibers by manipulating the process parameters and not by the material choice. Ensuring a homogeneous drug distribution (Luong-Van et al. [2006]) (usually by encapsulating drug in amorphous state (Zamani et al. [2010], Xu et al. [2006])), low drug loadings (Zamani et al. [2010]), or coating the drug loaded fibers (Casper et al. [2007]) are some simple techniques to diminish burst if so desired.

Table 1.2: Examples of fiber CDDS

Polymer	Drug loading (%, w/w)	Construct	Rel. mechanism	Rel. kinetics	Studied rel. time	Reference
PCL	heparin (0.05, 0.5)	unicomponent	bulk diffusion	$t^{0.5}$	14 days	Luong-Van et al. [2006]
PCL	metronidazole benzoate (5, 10, 15)	unicomponent	bulk diffusion	$\sim t^{0.5}$	20 days	Zamani et al. [2010]
PCL, PLA	tetracycline (2), chlorotetracycline hydrochloride (2), amphotericin B (1)	unicomponent, bicomponent	bulk diffusion	na	1.5 hours	Buschle-Diller et al. [2007]
PCL-co-EEP	NGF (0.0123), FITC-BSA (4.08)	unicomponent	bulk diffusion	$\sim t^{0.5}$	90 days	Chew et al. [2005]
PEG-b-PLLA	BCNU (5, 10, 20)	unicomponent	bulk diffusion	t^0.5	70 hours	Xu et al. [2006]
PLGA	paclitaxel (9.1)	unicomponent	bulk diffusion, hydrolytic degradation	t^0	80 days	Ranganath and Wang [2008]
PDLLA	tetracycline (2), chlorotetracycline (2)	unicomponent	bulk diffusion, polymer swelling	$\sim t^{0.5}$	50 hours	Buschle-Diller and Xie [2009]
PDLLA	paracetanol (2, 5, 8)	unicomponent	bulk diffusion, hydrolytic degradation	na	350 hours	Cui et al. [2006]

Table 1.2 – Continued

Polymer	Drug loading (%, w/w)	Construct	Rel. mechanism	Rel. kinetics	Studied rel. time	Reference
PLLA	paclitaxel (15), doxorubicin hydrochloride (1.6), doxorubicin base (1.6)	unicomponent	bulk diffusion, enzymatic degradation	t^0	4 hours	Zeng et al. [2005b]
PLLA	lidocaine hydrochloride (40, 80), mupirocin (3.75, 7.5)	unicomponent	bulk diffusion	na	72 hours	Thakur et al. [2008]
PLLA	rifampin (15, 25, 50), paclitaxel (na), doxorubicin hydrochloride (na)	unicomponent, bicomponent	enzymatic degradation	t^0	7 hours	Zeng et al. [2003]
PLA-POE-PLA	paracetamol (2)	unicomponent	bulk diffusion, pH responsive degradation	na	144 hours	Qi et al. [2008]
PLGA	paclitaxel (9.2, 9.9)	unicomponent	bulk diffusion, hydrolytic degradation	$t^{0.5}$	60 days	Xie and Wang [2006]
PLGA, PEG-b-PLA	cefoxitin sodium (1, 5)	unicomponent	bulk diffusion	na	150 hours	Kim et al. [2004]
PU	itraconazole (10, 40), ketanserin (10)	unicomponent	biphasic diffusion	$t^{0.5}$	20 hours	Verreck et al. [2003b]

Table 1.2 – Continued

Polymer	Drug loading (%, w/w)	Construct	Rel. mechanism	Rel. kinetics	Studied rel. time	Reference
PVA	sodium salicylate (10, 20), diclofenac sodium (10, 20), naproxen (10, 20), indomethacin (10, 20)	unicomponent	bulk diffusion, polymer erosion		24 hours	Taepaiboon et al. [2006]
PVP	ibuprofen (20, 33.3)	unicomponent	polymer erosion	na	180 seconds	Yu et al. [2009]
CA	vitamin A (0.5), vitamin E (5)	unicomponent	bulk diffusion	$t^{0.5}$	24 hours	Taepaiboon et al. [2007]
CA	curcumin (5, 10, 15, 20)	unicomponent	bulk diffusion	$t^{0.5}$	50 hours	Suwantong et al. [2007]
HPMC	itraconazole (20, 40)	unicomponent	bulk diffusion	na	3.4 hours	Verreck et al. [2003a]
gelatin	Centella asiatica extract (5, 10, 20, 30)	unicomponent	bulk diffusion, polymer erosion	na	7 days	Sikareepaisan et al. [2008]
PDLLA/HA	RhBMP-2 (0.00015-0.00016)	bicomponent	bulk diffusion, hydrolytic degradation	na	60 days	Nie et al. [2008]
PCL, Res	ketoprofen ($\sim$ 5)	bicomponent	bulk diffusion	na	360 hours	Kenawy et al. [2009]

Table 1.2 – Continued

Polymer	Drug loading (%, w/w)	Construct	Rel. mechanism	Rel. kinetics	Studied rel. time	Reference
PLLA/PEI, PLLA/PLL	Cytochrome C (na)	bicomponent	diffusion	na	29 days	Maretschek et al. [2008]
PLA, PEVA	tetracycline hydrochloride (5, 25)	bicomponent	bulk diffusion	na	120 hours	Kenawy et al. [2002]
PCL, PEO, PLLA, PLGA	lysozyme (na)	bicomponent	bulk diffusion, polymer erosion	na	300 hours	Kim et al. [2007]
PCL, PEG	BSA (1.96, 3.12, 5.56), lysozyme (na)	core-shell	barrier diffusion	na	27 days	Jiang et al. [2005]
PCL	resveratrol (4, 6, 8, 10), gentamycin sulfate (10, 20, 30, 40)	core-shell	enzymatic degradation	$\sim t^0$	180 hours	Huang et al. [2006]
PLA-co-CL	TPPS (1), ChroB (1)	multilayers	bulk diffusion, barrier diffusion	sigmoidal	7 hours	Okuda et al. [2010]
PCL, LDH	diclofenac sodium (0.49, 1.47, 2.45, 4.9)	composite	ionic exchange	$t^{0.5}$	250 days	Tammaro et al. [2009]
PLLA, Ca-alginate	BSA microsphere (na)	composite	barrier diffusion	na	120 hours	Qi et al. [2006]

Table 1.2 – Continued

Polymer	Drug loading (%, w/w)	Construct	Rel. mechanism	Rel. kinetics	Studied rel. time	Reference
PLGA, PLA-PEG-PLA	DNA nanoparticle (na)	composite	hydrolytic degradation, solvent diffusion	na	7 days	Liang et al. [2005]
PLGA/PEDOT	dexamethasone (na)	hollow fibers	external trigger	pulsed	1300 hours	Abidian et al. [2006]

Abbreviations: PDLLA, poly(D,L-lactide); PEG, poly(ethylene glycol); PLLA, poly(L-lactic acid); PDLLA-co-GA, poly-(D,L-lactide-co-glycolide); PLA-POE-PLA, poly(D,L-lactic acid) poly(orthoester) triblock copolymer; PLA-PEG-PLA, poly(lactic acid) poly(ethylene glycol) triblock copolymer; PEG-b-PLLA, pol(etylene glycol) poly(L-lactic acid) diblock copolymer; HPMC, hydroxypropylmethylcellulose; PVP, poly(vinylpyrrolidone); PCL, poly(ε-caprolactone); Res, Tecophilic Resin HP-60D-60; PEI, Poly(ethylene imine); PLL, Poly(L-lysin); PEVA, poly(ethylene-co-vinyl acetate); PLA-co-CL, poly(L-lactide-co-ε-caprolactone); PEO, poly(ethylene oxide); PEDOT, poly(3,4-ethylenedioxythiophene); PU, polyurethane; HA, hydroxylapatite; LDH, Mg-Al hydrotalcite clay; SPI, soy protein isolate; CA, cellulose acetate; BSA, bovine serum albumin; FITC-BSA, fluorescein isothiocyanate conjugate bovine; NGF, recombinant human β-nerve growth factor; BCNU, 1,3-bis(2-chloroethyl)-1-nitrosourea; RhBMP-2, recombinant human bone morphogenetic protein-2; TPPS, 5,10,15,20-tetraphenyl-21H,23H-porphinetetrasulfonic acid disulfuric acid; ChroB, 2,6-dichloro-4′-hydroxy-3′,3″-dimethylfuchsone-5′,5″-dicarboxylic acid disodium salt); AITC, allyl isothiocyanate.

1.5.4 Concluding remarks

Electrospinning is a simple and versatile method to produce fibers using charged polymer solutions. As CDDS, electrospun fibers are an excellent choice because of easy drug entrapment, high surface area, morphology control and biomimetic characteristics. Various drugs and biomolecules can be easily encapsulated inside or on fiber surface either during electrospinning or through post-processing of the fibers. Multicomponent fibers have attracted special attention because new properties and morphologies can be easily obtained through the combination of different polymers. Several factors that affect the drug release such as construct geometry and thickness, diameter and porosity, composition, crystallinity, swelling capacity, drug loading, drug state, drug molecular weight, drug solubility in the release medium, drug-polymer-electrospinning solvent interactions can be easily manipulated in order to prepare a CDDS with the desired properties. For ocular delivery, a fiber CDDS provides higher structural flexibility, more suitable for use in a soft tissue environment, such as the ocular structures. Moreover, faster integration at the implantation site (as evidenced by thin fibrous capsule formation (Kashanian et al. [2010]) is expected due to the biomimetic features.

Bibliography

M.R. Abidian, D.-H. Kim, and D.C. Martin. Conducting-polymer nanotubes for controlled drug release. *Adv. Mater.*, 18:405–409, 2006. [DOI:10.1002/adma.200501726].

E.M. Del Amo and A. Urtti. Current and future ophthalmic drug delivery systems. A shift to the posterior segment. *Drug Discov. Today*, 13:135–143, 2008. [DOI:10.1016/j.drudis.2007.11.002].

A. Argemí, A. López-Periago, C. Domingo, and J. Saurina. Spectroscopic and chromatographic characterization of triflusal delivery systems prepared by using supercritical impregnation technologies. *J. Pharm. Biomed. Anal.*, 46:456 – 462, 2008. [DOI:10.1016/j.jpba.2007.11.005].

O. Ayodeji, E. Graham, D. Kniss, J. Lannutti, and D. Tomasko. Carbon dioxide impregnation of electrospun polycaprolactone fibers. *J. Supercrit. Fluid*, 41:173 – 178, 2007. [DOI:10.1016/j.supflu.2006.09.011].

N.R. Beeley, J.V. Rossi, P.A. Mello-Filho, M.I. Mahmoud, G.Y. Fujii, E. de Juan, and S.E. Varner. Fabrication, implantation, elution, and retrieval of a steroid-

loaded polycaprolactone subretinal implant. *J. Biomed. Mater. Res. A*, 73: 437–444, 2005. [DOI:10.1002/jbm.a.30294].

F. Belhadj-Ahmed, E. Badens, P. Llewellyn, R. Denoyel, and G. Charbit. Impregnation of vitamin E acetate on silica mesoporous phases using supercritical carbon dioxide. *J. Supercrit. Fluids*, 51:278 – 286, 2009. [DOI:10.1016/j.supflu.2009.07.012].

W. Bethke. Present and future retinal implants. `http://www.revophth.com/index.asp?page=1_990.htm`, 2006.

M. Bogntizki, T. Frese, M. Steinhart, A. Greiner, and J.H. Wendorff. Preparation of fibers with nanoscaled morphologies: Electrospinning of polymer blends. *Polym. Eng. Sci.*, 41:982–989, 2001. [DOI:10.1002/pen.10799].

T. Borras, C.R. Brandt, R. Nickells, and R. Ritch. Gene therapy for glaucoma: treating a multifaceted, chronic disease. *Invest. Ophthalmol. Vis. Sci.*, 43:2513–2518, 2002. [PubMed:12147578].

J.L. Bourges, C. Bloquel, A. Thomas, F. Froussart, A. Bochot, F. Azan, R. Gurny, D. BenEzra, and F. Behar-Cohen. Intraocular implants for extended drug delivery: therapeutic applications. *Adv. Drug Deliv. Rev.*, 58:1182–1202, 2006. [DOI:10.1016/j.addr.2006.07.026].

M.E.M. Braga, M.T. Vaz Pato, H.S.R. Costa Silva, E.I. Ferreira, M.H. Gil, C.M.M. Duarte, and H.C. de Sousa. Supercritical solvent impregnation of ophthalmic drugs on chitosan derivatives. *J. Supercrit. Fluid*, 44:245–257, 2008. [DOI:10.1016/j.supflu.2007.10.002].

J. Breitenbach. Melt extrusion: from process to drug delivery technology. *Eur. J. Pharm. Biopharm.*, 54:107–117, 2002. [PubMed:12191680].

G. Buschle-Diller and Z. Xie. Electrospun poly(D,L-lactide) fibers for drug delivery: The influence of cosolvent and the mechanism of drug release. *J. Appl. Polym. Sci.*, 115:1–8, 2009. [DOI:10.1002/app.31026].

G. Buschle-Diller, J. Cooper, Z. Xie, Y. Wu, J. Waldrup, and X. Ren. Release of antibiotics from electrospun bicomponent fibers. *Cellulose*, 14:553–562, 2007. [DOI:10.1007/s10570-007-9183-3].

J.R. Bush, A. Akgerman, and K.R. Hall. Synthesis of controlled release device with supercritical CO_2 and co-solvent. *J. Supercrit. Fluids*, 41:311 – 316, 2007. [DOI:10.1016/j.supflu.2006.09.008].

Z. Butuner. Sustained release delivery of active agents to treat glaucoma and ocular hypertension, 2009. US0280158A1.

C.L. Casper, N. Yamaguchi, K.L. Kiick, and J.F. Rabolt. Functionalizing electrospun fibers with biologically relevant macromolecules. *Biomacromolecules*, 6: 1998–2007, 2005. [DOI:10.1021/bm050007e].

C.L. Casper, W. Yang, M.C. Farach-Carson, and J.F. Rabolt. Coating electrospun collagen and gelatin fibers with perlecan domain I for increased growth factor binding. *Biomacromolecules*, 8:1116–1123, 2007. [DOI:10.1021/bm061003s].

S.Y. Chew, J. Wen, E.K. Yim, and K W. Leong. Sustained release of proteins from electrospun biodegradable fibers. *Biomacromolecules*, 6:2017–2024, 2005. [DOI:10.1021/bm0501149].

Y.W. Chien. *Novel drug delivery systems*, chapter Fundamentals of Rate-Controlled Drug Delivery, pages 43–137. Informa Healthcare, 1992.

Y.E. Choonara, V. Pillay, T. Carmichael, and M.P. Danckwerts. Studies on a novel doughnut-shaped minitablet for intraocular drug delivery. *AAPS PharmSciTech*, 8:E118, 2007. [DOI:10.1208/pt0804118].

I.S. Chronakis, A. Jakob, B. Hagstrom, and L. Ye. Encapsulation and selective recognition of molecularly imprinted theophylline and 17-beta-estradiol nanoparticles within electrospun polymer nanofibers. *Langmuir*, 22:8960–8965, 2006a. [DOI:10.1021/la0613880].

I.S. Chronakis, B. Milosevic, A. Frenot, and L. Ye. Generation of molecular recognition sites in electrospun polymer nanofibers via molecular imprinting. *Macromolecules*, 39:357–361, 2006b. [DOI:10.1021/ma052091w].

W. Cui, X. Li, X. Zhu, G. Yu, S. Zhou, and J. Weng. Investigation of drug release and matrix degradation of electrospun poly(D,L-lactide) fibers with paracetanol inoculation. *Biomacromolecules*, 7:1623–1629, 2006. [DOI:10.1021/bm060057z].

E. L. Cussler. *Diffusion: mass transfer in fluid systems*, chapter Controlled Release and Related Phenomena, pages 467–478. Cambridge University Press, 1997.

A.H. Dahlmann-Noor, S. Vijay, G.A. Limb, and P.T. Khaw. Strategies for optic nerve rescue and regeneration in glaucoma and other optic neuropathies. *Drug Discov. Today*, 15:287–299, 2010. [DOI:10.1016/j.drudis.2010.02.007].

S. Diankov, D. Barth, A. Vega-Gonzalez, I. Pentchev, and P. Subra-Paternault. Impregnation isotherms of hydroxybenzoic acid on PMMA in supercritical carbon dioxide. *J. Supercrit. Fluids*, 41:164 – 172, 2007. [DOI:10.1016/j.supflu.2006.08.008].

R. Diepold, J. Kreuter, J. Himber, R. Gurny, V.H. Lee, J.R. Robinson, M.F. Saettone, and O.E. Schnaudigel. Comparison of different models for the testing of pilocarpine eyedrops using conventional eyedrops and a novel depot formulation (nanoparticles). *Graefes Arch. Clin. Exp. Ophthalmol.*, 227:188–193, 1989. [PubMed:2721988].

C. Domingo, J. Garcia-Carmona, M.A. Fanovich, and J. Saurina. Study of adsorption processes of model drugs at supercritical conditions using partial least squares regression. *Anal. Chim. Acta*, 452:311 – 319, 2002. [DOI:10.1016/S0003-2670(01)01469-6].

J.E. Donello and R. Yang. Vasoactive agent intraocular implant, 2007. US0260203A1.

A.R.C. Duarte, P. Coimbra, H. C. de Sousa, and C.M.M. Duarte. Solubility of flurbiprofen in supercritical carbon dioxide. *J. Chem. Eng. Data*, 49:449–452, 2004. [DOI:10.1021/je034099b].

A.R.C. Duarte, C. Martins, P. Coimbra, M.H.M. Gil, H.C. de Sousa, and C.M.M. Duarte. Sorption and diffusion of dense carbon dioxide in a biocompatible polymer. *J. Supercrit. Fluid*, 38:392 – 398, 2006. [DOI:10.1016/j.supflu.2005.12.002].

A.R.C. Duarte, A.L. Simplicio, A. Vega-González, P. Subra-Paternault, P. Coimbra, M.H. Gil, H.C. de Sousa, and C.M.M. Duarte. Supercritical fluid impregnation of a biocompatible polymer for ophthalmic drug delivery. *J. Supercrit. Fluids*, 42:373–377, 2007. [DOI:10.1016/j.supflu.2007.01.007].

O. Felt, S. Einmahl, P. Furrer, V. Baeyens, and R. Gurny. *Polymeric Biomaterials*, chapter Polymeric Systems for Ophthalmic Drug Delivery, pages 1–45. Marcel Dekker, 2002.

O. Felt-Baeyens, S. Eperon, P. Mora, D. Limal, S. Sagodira, P. Breton, B. Simonazzi, L. Bossy-Nobs, Y. Guex-Crosier, and R. Gurny. Biodegradable scleral implants as new triamcinolone acetonide delivery systems. *Int. J. Pharm.*, 322:6–12, 2006. [DOI:10.1016/j.ijpharm.2006.05.053].

S.L. Fialho, M.G.B. Rego, J.A. Cardillo, R.C. Siqueira, R. Jorge, and A.S. Cunha Júnior. Implantes biodegradáveis destinados à administração intra-ocular. *Arq. Bras. Oftalmol.*, 66:891–896, 2003. [DOI:10.1590/S0004-27492003000700029].

S.V. Fridrikh, J.H. Yu, M.P. Brenner, and G.C. Rutledge. Controlling the fiber diameter during electrospinning. *Phys. Rev. Lett.*, 90:144502, 2003. [PubMed:12731920].

H.S. Gifford, A. MacFarlane, and C. Reich. Drug delivery treatment device, 2007. US0233037A1.

O. Guney and A. Akgerman. Synthesis of controlled-release products in supercritical medium. *AIChE J.*, 48:856 – 866, 2002. [DOI:10.1002/aic.690480419].

S.K. Gupta, D.G. Niranjan, S.S. Agrawal, S. Srivastava, and R. Saxena. Recent advances in pharmacotherapy of glaucoma. *Indian J. Pharmacol.*, 40:197–208, 2008. [DOI:10.4103/0253-7613.44151].

J. Heller. *Biomaterials Science. An Introduction to Materials in Medicine*, chapter Drug Delivery Systems, pages 346–356. Academic Press, 1996.

M.M. Hohman, M. Shin, G. Rutledge, and M.P. Brenner. Electrospinning and electrically forced jets. I. stability theory. *Phys. Fluids*, 13:2201 – 2221, 2001. [DOI:10.1063/1.1383791].

C.K. Hong, K.S. Yang, S.H. Oh, J.-H. Ahn, B.-H. Cho, and C. Nah. Effect of blend composition on the morphology development of electrospun fibres based on PAN/PMMA blends. *Polym. Int.*, 57:1357–1362(6), 2008. [DOI:10.1002/pi.2481].

K. Hosoya, V.H. Lee, and K.J. Kim. Roles of the conjunctiva in ocular drug delivery: a review of conjunctival transport mechanisms and their regulation. *Eur. J. Pharm. Biopharm.*, 60:227–240, 2005. [DOI:10.1016/j.ejpb.2004.12.007].

Z.-M. Huang, Y.-Z. Zhang, M. Kotaki, and S. Ramakrishna. A review on polymer nanofibers by electrospinning and their applications in nanocomposites. *Comp. Sci. Tech.*, 63:2223 – 2253, 2003. [DOI:10.1016/S0266-3538(03)00178-7].

Z.M. Huang, C.L. He, A. Yang, Y. Zhang, X.J. Han, J. Yin, and Q. Wu. Encapsulating drugs in biodegradable ultrafine fibers through co-axial electrospinning. *J. Biomed. Mater. Res. A*, 77:169–179, 2006. [DOI:10.1002/jbm.a.30564].

P.M. Hughes, O. Olejnik, J.E. Chang-Lin, and C.G. Wilson. Topical and systemic drug delivery to the posterior segments. *Adv. Drug Deliv. Rev.*, 57:2010–2032, 2005. [DOI:10.1016/j.addr.2005.09.004].

I-vation. I-vation intravitreal implant, SurModics. http://www.surmodics.com/clinical-ophthalmology.html, 2009.

G.J. Jaffe, C.H. Yang, H. Guo, J.P. Denny, C. Lima, and P. Ashton. Safety and pharmacokinetics of an intraocular fluocinolone acetonide sustained delivery device. *Invest. Ophthalmol. Vis. Sci.*, 41:3569–3575, 2000. [PubMed:11006254].

K.K. Jain. *Drug Delivery Systems*, chapter Drug Delivery Systems – An Overview, pages 1–50. Humana Press, 2008.

H. Jiang, Y. Hu, Y. Li, P. Zhao, K. Zhu, and W. Chen. A facile technique to prepare biodegradable coaxial electrospun nanofibers for controlled release of bioactive agents. *J. Control. Release*, 108:237–243, 2005. [DOI:10.1016/j.jconrel.2005.08.006].

V. Kalra, P.A. Kakad, S. Mendez, T. Ivannikov, M. Kamperman, and Y.L. Joo. Self-assembled structures in electrospun poly(styrene-block-isoprene) fibers. *Macromolecules*, 39:5453–5457, 2006. [DOI:10.1021/ma052643a].

S. Kashanian, F. Harding, Y. Irani, S. Klebe, K. Marshall, A. Loni, L. Canham, D. Fan, K.A. Williams, N.H. Voelcker, and J.L. Coffer. Evaluation of mesoporous silicon/polycaprolactone composites as ophthalmic implants. *Acta Biomater.*, 6: 3566–3572, 2010. [DOI:10.1016/j.actbio.2010.03.031].

I.P. Kaur and M. Kanwar. Ocular preparations: the formulation approach. *Drug Dev. Ind. Pharm.*, 28:473–493, 2002. [DOI:10.1081/DDC-120003445].

I.P. Kaur, A. Garg, A.K. Singla, and D. Aggarwal. Vesicular systems in ocular drug delivery: an overview. *Int. J. Pharm.*, 269:1–14, 2004. [PubMed:14698571].

S. G. Kazarian. Polymer processing with supercritical fluids. *Polym. Sci. Ser. C*, pages 78–101, 2000.

S.G. Kazarian. *Supercritical fluid technology for drug product development*, chapter Supercritical Fluid Impregnation of Polymers for Drug Delivery, pages 343–365. Marcel-Dekker, 2004.

S.G. Kazarian and G.G. Martirosyan. Spectroscopy of polymer/drug formulations processed with supercritical fluids: in situ ATR-IR and Raman study of impregnation of ibuprofen into PVP. *Int. J. Pharm.*, 232:81–90, 2002. [PubMed:11790492].

S.G. Kazarian, M.F. Vincent, B.L. West, and C.A. Eckert. Partitioning of solutes and cosolvents between supercritical CO2 and polymer phases. *J. Supercrit. Fluids*, 13:107–112, 1998. [DOI:10.1016/S0896-8446(98)00041-2].

E.-R. Kenawy, G.L. Bowlin, K. Mansfield, J. Layman, D.G. Simpson, E H. Sanders, and G.E. Wnek. Release of tetracycline hydrochloride from electrospun poly(ethylene-co-vinylacetate), poly(lactic acid), and a blend. *J. Control. Release*, 81:57–64, 2002. [PubMed:11992678].

E.-R. Kenawy, F.I. Abdel-Hay, M.H. El-Newehy, and G.E. Wnek. Processing of polymer nanofibers through electrospinning as drug delivery systems. *Mater. Chem. Phys.*, 113:296 – 302, 2009. [DOI:10.1016/j.matchemphys.2008.07.081].

I. Kikic and F. Vecchione. Supercritical impregnation of polymers. *Curr. Opin. Solid St. M.*, 7:399–405, 2003. [DOI:10.1016/j.cossms.2003.09.001].

K. Kim, Y. K. Luu, C. Chang, D. Fang, B. S. Hsiao, B. Chu, and M. Hadjiargyrou. Incorporation and controlled release of a hydrophilic antibiotic using poly(lactide-co-glycolide)-based electrospun nanofibrous scaffolds. *J. Control. Release*, 98: 47–56, 2004. [DOI:10.1016/j.jconrel.2004.04.009].

T.G. Kim, D.S. Lee, and T.G. Park. Controlled protein release from electrospun biodegradable fiber mesh composed of poly(ε-caprolactone) and poly(ethylene oxide). *Int. J. Pharm.*, 338:276–283, 2007. [DOI:10.1016/j.ijpharm.2007.01.040].

Y.M. Kim, J.O. Lim, H.K. Kim, S.Y. Kim, and J.P. Shin. A novel design of one-side coated biodegradable intrascleral implant for the sustained release of triamcinolone acetonide. *Eur. J. Pharm. Biopharm.*, 70:179–186, 2008. [DOI:10.1016/j.ejpb.2008.04.023].

D.E. Knox. Solubilities in supercritical fluids. *Pure Appl. Chem.*, 77:513 – 530, 2005. [DOI:10.1351/pac200577030513].

J.A. Lee, K.C. Krogman, M. Ma, R.M. Hill, P.T. Hammond, and G.C. Rutledge. Highly reactive multilayer-assembled TiO2 coating on electrospun polymer nanofibers. *Adv. Mater.*, 21:1252–1256, 2009. [DOI:10.1002/adma.200802458].

S.J. Lee, J.J. Yoo, G.J. Lim, A. Atala, and J. Stitzel. In vitro evaluation of electrospun nanofiber scaffolds for vascular graft application. *J. Biomed. Mater. Res. A*, 83:999–1008, 2007. [DOI:10.1002/jbm.a.31287].

S.J Lee, S.H. Oh, J. Liu, S. Soker, A. Atala, and J.J. Yoo. The use of thermal treatments to enhance the mechanical properties of electrospun poly(epsilon-caprolactone) scaffolds. *Biomaterials*, 29:1422–1430, 2008. [DOI:10.1016/j.biomaterials.2007.11.024].

L.A. Levin. Neuroprotection and regeneration in glaucoma. *Ophthalmol. Clin. North. Am.*, 18:585–596, 2005. [DOI:10.1016/j.ohc.2005.07.001].

H. Levkovitch-Verbin. Animal models of optic nerve diseases. *Eye*, 18:1066–1074, 2004. [DOI:10.1038/sj.eye.6701576].

Q. Li, Z. Zhang, C. Zhong , Y. Liu, and Q. Zhou. Solubility of solid solutes in supercritical carbon dioxide with and without cosolvents. *Fluid Phase Equilib.*, 207:183–192, 2003.

D. Liang, Y.K. Luu, K. Kim, B.S. Hsiao, M. Hadjiargyrou, and B. Chu. In vitro non-viral gene delivery with nanofibrous scaffolds. *Nucleic Acids Res.*, 33:e170, 2005. [DOI:10.1093/nar/gni171].

D. Liang, B.S. Hsiao, and B. Chu. Functional electrospun nanofibrous scaffolds for biomedical applications. *Adv. Drug Deliv. Rev.*, 59:1392–1412, 2007. [DOI:10.1016/j.addr.2007.04.021].

H. Liu, N. Finn, and M. Z. Yates. Encapsulation and sustained release of a model drug, indomethacin, using CO2-based microencapsulation. *Langmuir*, 21:379–385, 2005. [DOI:10.1021/la047934b].

A. López-Periago, A. Vega, P. Subra, A. Argemí, J. Saurina, C. García-González, and C. Domingo. Supercritical CO2 processing of polymers for the production of materials with applications in tissue engineering and drug delivery. *J. Mater. Sci.*, 43:1939–1947, 2008. [DOI:10.1007/s10853-008-2461-0].

A. López-Periago, A. Argemí, J.M. Andanson, V. Fernández, C.A. García-González, S.G. Kazarian, J. Saurina, and C. Domingo. Impregnation of a biocompatible polymer aided by supercritical CO2: Evaluation of drug stability and drug-matrix interactions. *J. Supercrit. Fluids*, 48:56 – 63, 2009. [DOI:10.1016/j.supflu.2008.09.015].

A. López-Rubio, E. Sanchez, Y. Sanz, and J.M. Lagaron. Encapsulation of living bifidobacteria in ultrathin PVOH electrospun fibers. *Biomacromolecules*, 10: 2823–2829, 2009. [DOI:10.1021/bm900660b].

A. Ludwig. The use of mucoadhesive polymers in ocular drug delivery. *Adv. Drug Deliv. Rev.*, 57:1595–1639, 2005. [DOI:10.1016/j.addr.2005.07.005].

E. Luong-Van, L. Grandahl, K.N. Chua, K.W. Leong, V. Nurcombe, and S.M. Cool. Controlled release of heparin from poly(ε-caprolactone) electrospun fibers. *Biomaterials*, 27:2042–2050, 2006. [DOI:10.1016/j.biomaterials.2005.10.028].

Z. Ma, M. Kotaki, and S. Ramakrishna. Surface modified nonwoven polysulphone (psu) fiber mesh by electrospinning: A novel affinity membrane. *J. Membr. Sci.*, 272:179 – 187, 2006. [DOI:10.1016/j.memsci.2005.07.038].

S. Maretschek, A. Greiner, and T. Kissel. Electrospun biodegradable nanofiber nonwovens for controlled release of proteins. *J. Control. Release*, 127:180–187, 2008. [DOI:10.1016/j.jconrel.2008.01.011].

M.J. McClure, S.A. Sell, C.E. Ayres, D.G. Simpson, and G.L. Bowlin. Electrospinning-aligned and random polydioxanone-polycaprolactone-silk fibroin-blended scaffolds: geometry for a vascular matrix. *Biomed. Mater.*, 4:055010, 2009. [DOI:10.1088/1748-6041/4/5/055010].

M.C. Moreno, H.J. Marcos, J. Oscar Croxatto, P.H. Sande, J. Campanelli, C.O. Jaliffa, J. Benozzi, and R. E. Rosenstein. A new experimental model of glaucoma in rats through intracameral injections of hyaluronic acid. *Exp. Eye Res.*, 81: 71–80, 2005. [DOI:10.1016/j.exer.2005.01.008].

A.A. Moshfeghi and G.A. Peyman. Micro- and nanoparticulates. *Adv. Drug Deliv. Rev.*, 57:2047–2052, 2005. [DOI:10.1016/j.addr.2005.09.006].

M. Mozaffarieh and J. Flammer. Is there more to glaucoma treatment than lowering IOP? *Surv. Ophthalmol.*, 52 Suppl 2:174–179, 2007. [DOI:10.1016/j.survophthal.2007.08.013].

R.C. Nagarwal, S. Kant, P.N. Singh, P. Maiti, and J.K. Pandit. Polymeric nanoparticulate system: a potential approach for ocular drug delivery. *J. Con. Rel.*, 136: 2–13, 2009. [DOI:10.1016/j.jconrel.2008.12.018].

B.K. Nanjawade, F.V. Manvi, and A.S. Manjappa. In situ-forming hydrogels for sustained ophthalmic drug delivery. *J. Con. Rel.*, 122:119–134, 2007. [DOI:10.1016/j.jconrel.2007.07.009].

M.V. Natu, M.H. Gil, and H.C. de Sousa. Supercritical solvent impregnation of poly(ε-caprolactone)/poly(oxyethylene-b-oxypropylene-b-oxyethylene) and poly(ε-caprolactone)/poly(ethylene-vinyl acetate) blends for controlled release applications. *J. Supercrit. Fluids*, 47:93–102, 2008. [DOI:10.1016/j.supflu.2008.05.006].

K.D. Nelson, A.A. Romero-Sanchez, G.M. Smith, N. Alikacem, D. Radulescu, P. Waggoner, and Z. Hu. Drug releasing biodegradable fiber implant, 2000. US6596296.

Neurotech. Encapsulated Cell Technology, Neurotech. http://www.neurotechusa.com/ect/about_encapsulated_cell_technology.asp, 2008.

H. Nie, B.W. Soh, Y.C. Fu, and C.H. Wang. Three-dimensional fibrous PLGA/HAp composite scaffold for BMP-2 delivery. *Biotechnol. Bioeng.*, 99:223–234, 2008. [DOI:10.1002/bit.21517].

J. Okabe, H. Kimura, N. Kunou, K. Okabe, A. Kato, and Y. Ogura. Biodegradable intrascleral implant for sustained intraocular delivery of betamethasone phosphate. *Invest. Ophthalmol. Vis. Sci.*, 44:740–744, 2003a. [PubMed:12556407].

K. Okabe, H. Kimura, J. Okabe, A. Kato, N. Kunou, and Y. Ogura. Intraocular tissue distribution of betamethasone after intrascleral administration using a non-biodegradable sustained drug delivery device. *Invest. Ophthalmol. Vis. Sci.*, 44:2702–2707, 2003b. [PubMed:12766076].

T. Okuda, K. Tominaga, and S. Kidoaki. Time-programmed dual release formulation by multilayered drug-loaded nanofiber meshes. *J. Control. Release*, 143:258–264, 2010. [DOI:10.1016/j.jconrel.2009.12.029].

Ozurdex. OZURDEX (dexamethasone intravitreal implant) 0.7mg. http://www.allergan.com/products/eye_care/ozurdex.htm, 2010.

I.-H. Pang and A.F. Clark. *Ocular Therapeutics*, chapter IOP as a Target – Inflow and Outflow Pathways, pages 45–67. Elsevier, 2008.

N.A. Peppas and L. Brannon-Peppas. Water diffusion and sorption in amorphous macromolecular systems and foods. *J. Food Eng.*, 22:189–210, 1994. [DOI:10.1016/0260-8774(94)90030-2].

G. Perale, P. Arosio, D. Moscatelli, V. Barri, M. Muller, S. Maccagnan, and M. Masi. A new model of resorbable device degradation and drug release: transient 1-dimension diffusional model. *J. Control. Release*, 136:196–205, 2009. [DOI:10.1016/j.jconrel.2009.02.014].

G. Peyman. Treatment of ocular disease, 2006. US0263429A1.

Q.P. Pham, U. Sharma, and A.G. Mikos. Electrospun poly(ε-caprolactone) microfiber and multilayer nanofiber/microfiber scaffolds: characterization of scaffolds and measurement of cellular infiltration. *Biomacromolecules*, 7:2796–2805, 2006. [DOI:10.1021/bm060680j].

P.B. Poulsen, P. Buchholz, J.G. Walt, T.L. Christensen, and J. Thygesen. Cost analysis of glaucoma-related-blindness in Europe. *Int. Congr. Ser.*, 1282:262 – 266, 2005. [DOI:10.1016/j.ics.2005.05.091].

H. Qi, P. Hu, J. Xu, and A. Wang. Encapsulation of drug reservoirs in fibers by emulsion electrospinning: morphology characterization and preliminary release assessment. *Biomacromolecules*, 7:2327–2330, 2006. [DOI:10.1021/bm060264z].

M. Qi, X. Li, Y. Yang, and S. Zhou. Electrospun fibers of acid-labile biodegradable polymers containing ortho ester groups for controlled release of paracetamol. *Eur. J. Pharm. Biopharm.*, 70:445–452, 2008. [DOI:10.1016/j.ejpb.2008.05.003].

H.A. Quigley and A. T. Broman. The number of people with glaucoma worldwide in 2010 and 2020. *Br. J. Ophthalmol.*, 90:262–267, 2006. [DOI:10.1136/bjo.2005.081224].

S.H. Ranganath and C.H. Wang. Biodegradable microfiber implants delivering paclitaxel for post-surgical chemotherapy against malignant glioma. *Biomaterials*, 29:2996–3003, 2008. [DOI:10.1016/j.biomaterials.2008.04.002].

M. Rudzinski and H.U. Saragovi. Glaucoma: Validated and facile in vivo experimental models of a chronic neurodegenerative disease for drug development. *Curr. Med. Chem. - Central Nervous System Agents*, 5:43–49, 2005. [DOI:10.2174/1568015053202796].

G.C. Rutledge and S.V. Fridrikh. Formation of fibers by electrospinning. *Adv. Drug Deliv. Rev.*, 59:1384–1391, 2007. [DOI:10.1016/j.addr.2007.04.020].

E. Sakurai, M. Nozaki, K. Okabe, N. Kunou, H. Kimura, and Y. Ogura. Scleral plug of biodegradable polymers containing tacrolimus (FK506) for experimental uveitis. *Invest. Ophthalmol. Vis. Sci.*, 44:4845–4852, 2003. [PubMed:14578407].

M. Sauceau, J.-J. Letourneau, B. Freiss, D. Richon, and J. Fages. Solubility of eflucimibe in supercritical carbon dioxide with or without a co-solvent. *J. Supercrit. Fluids*, 31:133 – 140, 2004. [DOI:10.1016/j.supflu.2003.11.004].

K. Sawicka and P. Gouma. Electrospun composite nanofibers for functional applications. *J. Nanopart. Res.*, 8:769–781, 2006. [DOI:10.1007/s11051-005-9026-9].

Y.-T. Shieh, J.-H. Su, G. Manivannan, P.H.C. Lee, S.P. Sawan, and W. Dale Spall. Interaction of supercritical carbon dioxide with polymers. II. Amorphous polymers. *J. Appl. Polym. Sci.*, 59:707 – 717, 1996a. [DOI:10.1002/(SICI)1097-4628(19960124)59:4¡707::AID-APP16¿3.0.CO;2-M].

Y.-T. Shieh, J.-H. Su, G. Manivannan, P.H.C. Lee, S.P. Sawan, and W. Dale Spall. Interaction of supercritical carbon dioxide with polymers. I. Crystalline polymers. *J. Appl. Polym. Sci.*, 59:695 – 705, 1996b. [DOI:10.1002/(SICI)1097-4628(19960124)59:4¡695::AID-APP15¿3.0.CO;2-P].

P. Sikareepaisan, A.Suksamrarn, and P. Supaphol. Electrospun gelatin fiber mats containing a herbal- *centella asiatica*- extract and release characteristic of asiaticoside. *Nanotechnology*, 19:015102, 2008. [DOI:10.1088/0957-4484/19/01/015102].

A. Silva-Cunha, S.L. Fialho, M.C. Naud, and F. Behar-Cohen. Poly-ε-caprolactone intravitreous devices: an in vivo study. *Invest. Ophthalmol. Vis. Sci.*, 50:2312–2318, 2009. [DOI:10.1167/iovs.08-2969].

K. Sisson, C. Zhang, M.C. Farach-Carson, D.B. Chase, and J.F. Rabolt. Evaluation of Cross-Linking Methods for Electrospun Gelatin on Cell Growth and Viability. *Biomacromolecules*, 2009. [DOI:10.1021/bm900036s].

M. Skotak, A.P. Leonov, G. Larsen, S. Noriega, and A. Subramanian. Biocompatible and biodegradable ultrafine fibrillar scaffold materials for tissue engineering by facile grafting of L-lactide onto chitosan. *Biomacromolecules*, 9:1902–1908, 2008. [DOI:10.1021/bm800158c].

R. Srikar, A. L. Yarin, C.M. Megaridis, A.V. Bazilevsky, and E. Kelley. Desorption-limited mechanism of release from polymer nanofibers. *Langmuir*, 24:965–974, 2008. [DOI:10.1021/la702449k].

B. Subramaniam, R.A. Rajewski, and K. Snavely. Pharmaceutical processing with supercritical carbon dioxide. *J. Pharm. Sci.*, 86:885–890, 1997. [DOI:10.1021/js9700661].

O. Suwantong, P. Opanasopit, U. Ruktanonchai, and P. Supaphol. Electrospun cellulose acetate fiber mats containing curcumin and release characteristic of the herbal substance. *Polymer*, 48:7546 – 7557, 2007. [DOI:10.1088/0957-4484/17/9/041].

P. Taepaiboon, U. Rungsardthong, and P. Supaphol. Drug-loaded electrospun mats of poly(vinyl alcohol) fibres and their release characteristics of four model drugs. *Nanotechnology*, 17:2317, 2006. [DOI:10.1016/j.polymer.2007.11.019].

P. Taepaiboon, U. Rungsardthong, and P. Supaphol. Vitamin-loaded electrospun cellulose acetate nanofiber mats as transdermal and dermal therapeutic agents of vitamin A acid and vitamin E. *Eur. J. Pharm. Biopharm.*, 67:387–397, 2007. [DOI:10.1016/j.ejpb.2007.03.018].

L. Tammaro, G. Russo, and V. Vittoria. Encapsulation of diclofenac molecules into poly(ε-caprolactone) electrospun fibers for delivery protection. *J. Nanomater.*, 2009, 2009. [DOI:10.1155/2009/238206].

R.A. Thakur, C.A. Florek, J. Kohn, and B.B. Michniak. Electrospun nanofibrous polymeric scaffold with targeted drug release profiles for potential application as wound dressing. *Int. J. Pharm.*, 364:87–93, 2008. [DOI:10.1016/j.ijpharm.2008.07.033].

J.T. Theng, S.E. Ti, L. Zhou, K.W. Lam, S.P. Chee, D. Tan, and S.E. Ti. Pharmacokinetic and toxicity study of an intraocular cyclosporine DDS in the anterior segment of rabbit eyes. *Invest. Ophthalmol. Vis. Sci.*, 44:4895–4899, 2003. [PubMed:14578414].

L.C. Titcomb. Treatment of glaucoma: part 1. *Pharm. J.*, 263:324–329, 1999. URL `http://www.pharmj.com/editorial/19990828/education/glaucoma.html`.

S.B. Tiwari and A.R. Rajabi-Siahboomi. *Drug Delivery Systems*, chapter Extended-Release Oral Drug Delivery Technologies: Monolithic Matrix Systems, pages 217–243. Humana Press, 2008.

S.K. Tiwari, R. Tzezana, E. Zussman, and S.S. Venkatraman. Optimizing partition-controlled drug release from electrospun core-shell fibers. *Int. J. Pharm.*, 392: 209–217, 2010. [DOI:10.1016/j.ijpharm.2010.03.021].

A. R. Tzafriri. Mathematical modeling of diffusion-mediated release from bulk degrading matrices. *J. Control. Release*, 63:69–79, 2000. [PubMed:10640581].

J.H. Urcola, M. Hernandez, and E. Vecino. Three experimental glaucoma models in rats: comparison of the effects of intraocular pressure elevation on retinal ganglion cell size and death. *Exp. Eye Res.*, 83:429–437, 2006. [DOI:10.1016/j.exer.2006.01.025].

A. Urtti. Challenges and obstacles of ocular pharmacokinetics and drug delivery. *Adv. Drug Deliv. Rev.*, 58:1131–1135, 2006. [DOI:10.1016/j.addr.2006.07.027].

S. Uzer, U. Akman, and O. Hortaçsu. Polymer swelling and impregnation using supercritical CO2: A model-component study towards producing controlled-release drugs. *J. Supercrit. Fluids*, 38:119 – 128, 2006. [DOI:10.1016/j.supflu.2005.11.005].

C.M. Vaz, S. van Tuijl, C.V. Bouten, and F.P. Baaijens. Design of scaffolds for blood vessel tissue engineering using a multi-layering electrospinning technique. *Acta Biomater.*, 1:575–582, 2005. [DOI:10.1016/j.actbio.2005.06.006].

E. Vecino. Animal models in the study of the glaucoma: past, present and future. *Arch. Soc. Esp. Oftalmol.*, 83:517–519, 2008. [PubMed:18803121].

G. Velez and S.M. Whitcup. New developments in sustained release drug delivery for the treatment of intraocular disease. *Br. J. Ophthalmol.*, 83:1225–1229, 1999. [PubMed Central:PMC1722856].

G. Verreck, I. Chun, J. Peeters, J. Rosenblatt, and M.E. Brewster. Preparation and characterization of nanofibers containing amorphous drug dispersions generated by electrostatic spinning. *Pharm. Res.*, 20:810–817, 2003a. [PubMed:12751639].

G. Verreck, I. Chun, J. Rosenblatt, J. Peeters, A.V. Dijck, J. Mensch, M. Noppe, and M.E. Brewster. Incorporation of drugs in an amorphous state into electrospun nanofibers composed of a water-insoluble, nonbiodegradable polymer. *J. Control. Release*, 92:349–360, 2003b. [PubMed:14568415].

X. Wang, K. Zhang, M. Zhu, B.S. Hsiao, and B. Chu. Enhanced mechanical performance of self-bundled electrospun fiber yarns via post-treatments. *Macromol. Rapid Commun.*, 29:826–831, 2008. [DOI:10.1002/marc.200700873].

Y. Wang, C. Yang, and D. Tomasko. Confocal microscopy analysis of supercritical fluid impregnation of polypropylene. *Ind. Eng. Chem. Res.*, 41:1780–1786, 2002. [DOI:10.1021/ie010575k].

Y. Wang, B. Wang, W. Qiao, and T. Yin. A novel controlled release drug delivery system for multiple drugs based on electrospun nanofibers containing nanoparticles. *J. Pharm. Sci.*, 2010. [DOI:10.1002/jps.22189].

M. Wei, B. Kang, C. Sung, and J. Mead. Core-sheath structure in electrospun nanofibers from polymer blends. *Macromol. Mater. Eng.*, 291:1307–1314, 2006. [DOI:10.1002/mame.200600284].

A.L. Weiner. *Ocular Therapeutics*, chapter Drug Delivery Systems in Ophthalmic Applications, pages 7–43. Elsevier, 2008.

R.N. Weinreb and L.A. Levin. Is neuroprotection a viable therapy for glaucoma? *Arch. Ophthalmol.*, 117:1540–1544, 1999. [PubMed:10565524].

V.G. Wong, M.W.L. Hu, and Jr.D.E. Berger. Controlled-release biocompatible ocular drug delivery implant devices and methods, 1999. US6331313.

J. Xie and C.H. Wang. Electrospun micro- and nanofibers for sustained delivery of paclitaxel to treat C6 glioma in vitro. *Pharm. Res.*, 23:1817–1826, 2006. [DOI:10.1007/s11095-006-9036-z].

X. Xu, L. Yang, X. Xu, X. Wang, X. Chen, Q. Liang, J. Zeng, and X. Jing. Ultrafine medicated fibers electrospun from W/O emulsions. *J. Control. Release*, 108:33 – 42, 2005. [DOI:10.1016/j.jconrel.2005.07.021].

X. Xu, X. Chen, X. Xu, T. Lu, X. Wang, L. Yang, and X. Jing. BCNU-loaded PEG-PLLA ultrafine fibers and their in vitro antitumor activity against Glioma C6 cells. *J. Control. Release*, 114:307–316, 2006. [DOI:10.1016/j.jconrel.2006.05.031].

C.F. Yang, T. Yasukawa, H. Kimura, H. Miyamoto, Y. Honda, Y. Tabata, Y. Ikada, and Y. Ogura. Experimental corneal neovascularization by basic fibroblast growth factor incorporated into gelatin hydrogel. *Ophthalmic Res.*, 32:19–24, 2000. [PubMed:10657751].

T. Yasukawa, H. Kimura, N. Kunou, H. Miyamoto, Y. Honda, Y. Ogura, and Y. Ikada. Biodegradable scleral implant for intravitreal controlled release of ganciclovir. *Graefes Arch. Clin. Exp. Ophthalmol.*, 238:186–190, 2000. [PubMed:10766290].

T. Yasukawa, Y. Ogura, E. Sakurai, Y. Tabata, and H. Kimura. Intraocular sustained drug delivery using implantable polymeric devices. *Adv. Drug Deliv. Rev.*, 57:2033–2046, 2005. [DOI:10.1016/j.addr.2005.09.005].

Y. You, J.H. Youk, S.W. Lee, B.-M. Min, S.J. Lee, and W.H. Park. Preparation of porous ultrafine pga fibers via selective dissolution of electrospun PGA/PLA blend fibers. *Mater. Let.*, 60:757 – 760, 2006. [DOI:10.1016/j.matlet.2005.10.007].

D.-G. Yu, X.-X. Shen, C. Branford-White, K. White, L.-M. Zhu, and S.W.A. Bligh. Oral fast-dissolving drug delivery membranes prepared from electrospun polyvinylpyrrolidone ultrafine fibers. *Nanotechnology*, 20:055104, 2009. [DOI:10.1088/0957-4484/20/5/055104].

L. Yudcovitch. Pharmaceutical, Laser and Surgical Treatments for Glaucoma: An Update. `http://www.pacificu.edu/optometry/ce/courses/15166/pharglapg1.cfm#Introduction`, 2010.

M. Zamani, M. Morshed, J. Varshosaz, and M. Jannesari. Controlled release of metronidazole benzoate from poly(ε-caprolactone) electrospun nanofibers for periodontal diseases. *Eur. J. Pharm. Biopharm.*, 75:179–185, 2010. [DOI:10.1016/j.ejpb.2010.02.002].

J. Zeng, X. Xu, X. Chen, Q. Liang, X. Bian, L. Yang, and X. Jing. Biodegradable electrospun fibers for drug delivery. *J. Control. Release*, 92:227–231, 2003. [PubMed:14568403].

J. Zeng, A. Aigner, F. Czubayko, T. Kissel, J.H. Wendorff, and A. Greiner. Poly(vinyl alcohol) nanofibers by electrospinning as a protein delivery system and the retardation of enzyme release by additional polymer coatings. *Biomacromolecules*, 6:1484–1488, 2005a. [DOI:10.1021/bm0492576].

J. Zeng, L. Yang, Q. Liang, X. Zhang, H. Guan, X. Xu, X. Chen, and X. Jing. Influence of the drug compatibility with polymer solution on the release kinetics of electrospun fiber formulation. *J. Control. Release*, 105:43–51, 2005b. [DOI:10.1016/j.jconrel.2005.02.024].

T. Zhou, H. Lewis, R.E. Foster, and S.P. Schwendeman. Development of a multiple-drug delivery implant for intraocular management of proliferative vitreoretinopathy. *J. Con. Rel.*, 55:281–295, 1998. [PubMed:9795083].

X. Zong, S. Ran, K.S. Kim, D. Fang, B.S. Hsiao, and B. Chu. Structure and morphology changes during in vitro degradation of electrospun poly(glycolide-co-lactide) nanofiber membrane. *Biomacromolecules*, 4:416–423, 2003. [DOI:10.1021/bm025717o].

Chapter 2

Supercritical solvent impregnation of polymer matrices for controlled release applications

The text that comprises this Chapter was published in the journal *The Journal of Supercritical Fluids* (2008), volume 47, pages 93–102.

Abstract

Poly(ε-caprolactone) blends were successfully impregnated with timolol maleate, an anti-glaucoma drug, using a supercritical solvent impregnation (SSI) technique. Supercritical fluid impregnation efficiency results suggested that the best impregnating conditions were obtained when a cosolvent was used and when specific drug-polymer interactions occurred as a consequence of different chemical structures due to polymer blending. Pressure can be either a favourable factor, when there is enough drug affinity for the polymers, or an unfavourable factor when weaker bonding is involved. In order to determine the relative hydrophilicity/hydrophobicity of the blends, contact angle analysis was performed, while crystallinity determination was also useful to understand the obtained release profiles. Drug loading, heterogeneous/homogeneous dispersion of drug inside the matrix, hydrophilicity, crystallinity, all seem to influence the obtained drug release rates. The "in vitro" release results suggested that a sustained drug release rate can be obtained by changing the SSI operational conditions and by modulating the composition of blends, as a mean to control crystallinity, hydrophilicity and drug affinity for the polymer matrix. After a first day burst release, all samples showed a sustained release profile (1.2-4 μg/ml/day, corresponding to a mass of 3-10 μg/day) which is between the therapeutic and toxic levels of timolol maleate, during a period

of 1 month. These drug-loaded polymeric matrices can be a feasible alternative treatment modality for the conventional repeated daily administration of eye drops.

2.1 Introduction

The two main causes of blindness in adult population are age related macular degeneration and primary open angle glaucoma, two diseases that affect the posterior segment of the eye (Kocur and Resnikoff [2002]). Glaucoma is frequently asymptomatic at the time of diagnosis, but it can result in progressive visual field loss and and, in extreme cases, eventual blindness. Timolol maleate (a beta blocker) is considered as the "golden standard" against which other glaucoma medications are compared in terms of efficacy, side effects and cost. Although topically administered timolol maleate is frequently recommended as first-line therapy, some systemic side effects of this drug may limit its use. For example, timolol maleate and other topically applied beta blockers have been associated to asthma exacerbation, worsening congestive heart failure, heart block and, rarely, to sudden death (Lewis et al. [1999]).

Low drug bioavailability and systemic toxicity are usually caused by the relative impermeability of the cornea, by tear dynamics and blinking and by nasolacrimal drug drainage. In the case of eye drops medications, only around 5 % of the applied drug actually penetrates through cornea (Urtti [2006]). The drug that is not absorbed by the cornea will reach the bloodstream through the nasolacrimal duct causing some of the above mentioned systemic side effects. To avoid low drug bioavailability, topical eye formulations normally require high drug concentrations and frequent dosing treatments which also may increase systemic side effects risks. To overcome these issues, several efforts have been made in order to improve the ocular delivery and bioavailability of topically applied ocular drugs and to reduce their adverse effects. The most common approach is by developing ophthalmic polymeric-based controlled drug delivery systems (CDDS) such as bioadhesives and in situ forming hydrogels, colloidal systems, ocular inserts and implantable devices (Ding [1998], Bourlais et al. [1998], Ludwig [2005], Bourges et al. [2006], Yasukawa et al. [2004]).

Polymeric-based CDDS can be prepared in numerous different ways. Dispersing a drug, or therapeutic agent, in biocompatible and/or biodegradable polymeric matrices encompasses the majority of all research in this field and there are several well-known methods to incorporate and disperse drugs into polymeric matrices. However and in most cases, these conventional methods present several disadvantages, like the potential use of toxic organic solvents (specially for water

insoluble drugs), drug/solvent dissolution and compatibility issues, undesired drug reactions, drug photochemical and thermal degradation, low incorporation yields and heterogeneous drug dispersion.

Drugs may also be impregnated and dispersed in polymeric matrices by dissolving them in compressed high volatile fluids (like carbon dioxide) at temperatures and pressures near or above their critical temperatures and pressures, and contacting the resulting mixture with the polymeric matrices to be infused. In these conditions, the compressed fluid can act also as a swelling and plasticizer agent for polymers, dilating the matrices and helping drug diffusion into them. This recent technique, known as Supercritical Solvent Impregnation (SSI), already proved its advantages for the development of drug impregnated polymeric materials which can be used as CDDS for many biomedical applications (Kikic and Vecchione [2003], Subramaniam et al. [1997], Braga et al. [2008], Kazarian [2000]).

SSI allows the drug impregnation of most polymeric articles and, when properly employed, without altering and/or damaging their physical, chemical, and mechanical properties and without degrading their constituent drugs, additives and polymers. Furthermore, drug loading and depth penetration can be easily controlled and drugs will be homogeneously dispersed, in short treatment times and leaving no harmful solvent residues. Finally, SSI also permits to have previously prepared polymeric articles and, later, impregnate them with the desired drugs, according to the specific needs of the envisaged therapeutic application, and without interfering with the established conventional method/procedure to produce/process the original polymeric articles. This particular feature can lead to very attractive and useful medical and commercial applications (de Sousa et al. [2006a,b]).

Although carbon dioxide is the most frequently employed supercritical fluid (SCF), it also presents several limitations mainly due to its inability to dissolve high molecular weight compounds and to its non-polarity and lack of several specific solvent-solute and solvent-polymer interactions that would lead to high polymeric drug loading. A frequent strategy to increase drug solubility in supercritical carbon dioxide ($scCO_2$) is the addition of small amounts of specific cosolvents which can produce dramatic effects on its solvent power, sometimes up to several hundred percent in terms of solubility enhancement (Knox [2005], Duarte et al. [2005]).

Our long-term goal is to prepare an implantable (subconjunctival) system for sustained drug delivery, with controlled release and degradation that could deliver timolol maleate for up to 4-6 months, in an attempt to overcome the problems of low drug bioavailability and the potential occurrence of systemic toxicity. The system would deliver only the therapeutic drug amount (Ahmed and Patton [1985]) and would eliminate the problem of frequent administration (timolol eye drops are

applied twice daily), improving patient compliance.

For the present study, poly(ε-caprolactone) (PCL) was selected as the main blend homopolymer for the preparation of the biodegradable CDDS due to its good biocompatibility (Serrano et al. [2004], Tan and Teoh [2007], Pena et al. [2006]) and its known swelling ability in $scCO_2$ (Leeke et al. [2006]). Poly(ethylene-co-vinyl acetate) and poly(oxyethylene-b-oxypropylene) are copolymers which have numerous applications and recognised applications in the development of CDDSs mainly because of biocompatibility, processability (e.g. extrusion) and proved long-term release properties (Kumar et al. [2001], Scherlund et al. [2000], Chutimaworapan et al. [2000], van Laarhoven et al. [2002], Costantini et al. [2004]).

The aim of this work is to evaluate the effects of operational pressure, of blend chemical nature and composition, as well as of cosolvent effects, on the supercritical solvent impregnation process of different poly(ε-caprolactone) blends, in order to determine the best operating conditions to achieve maximum drug loading and optimal drug release profiles.

2.2 Experimental section

2.2.1 Materials

Timolol maleate, (99,6 % purity) was purchased from Cambrex Profarmaco Cork Ltd., Ireland. Poly(ε-caprolactone) pellets (PCL, average M_w 65000 g/mol) were obtained from Sigma-Aldrich. Poly(ethylene-co-vinyl acetate), Luwax EVA 3 (Lw, 13-15 % vinylacetate content) and poly(oxyethylene-b-oxypropylene-b-oxyethylene), Lutrol F 127 (Lu, 9000-14000 g/mol, 70 % by weight of polyoxyethylene) were bought from BASF. It was not possible to obtain (from supplier) the average molecular weight of Luwax EVA 3. The chemical formulae of the employed copolymers are shown in Fig. 2.1. Tetrahydrofurane (THF, HPLC grade) was obtained from Sigma-Aldrich. Phosphate buffer saline (PBS) tablets (pH 7.4, 10 mM phosphate, 137 mM sodium, 2.7 mM potassium) were used to prepare the drug release medium and were bought from Sigma-Aldrich. Carbon dioxide (99.998 % purity) was obtained from Praxair. All products were used without further purification.

2.2.2 Blends preparation

Several PCL-based blends were prepared by solvent casting and according to the procedure described below. The blends (Lutrol F 127/PCL: 25/75, 50/50 and Luwax EVA 3/PCL: 25/75, 50/50, 75/25, % w/w) were prepared by dissolution in

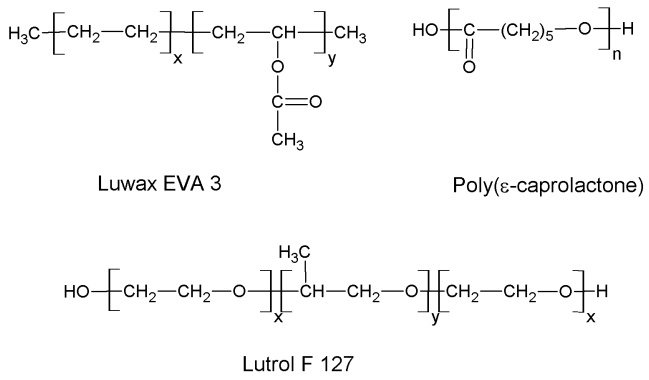

Figure 2.1: Chemical structures of the employed polymers and copolymers

THF (10 % w/v total polymer solutions) at 40 °C and 60 °C, respectively. Blends films were obtained by solvent casting at room temperature in glass Petri dishes. Then, the films were vacuum-dried at 37 °C, for 24 h, to ensure the complete removal of the solvent. After drying, the films were removed from the Petri dishes and cut in rectangular pieces of approximately 0.5 cm×0.5 cm and used as such subsequent impregnation and characterization experiments.

2.2.3 Supercritical fluid impregnation process

The supercritical impregnation equipment is schematically presented in Fig. 2.2. The equipment consists of a cylindrical high-pressure stainless steel cell (21.57 cm^3) placed in a water bath that maintains the temperature within ± 1 °C. The water bath temperature was measured by means of a thermocouple. A magnetic stirring plate (750-800 rpm) was used to homogenise cell-containing high pressure mixtures (CO_2, timolol maleate and cosolvent). Carbon dioxide was liquefied through a cooling unit and compressed to the operating pressure with a high-pressure liquid pump. A one-way high-pressure valve (3) was introduced in the system. System pressure was measured with a pressure transducer in-line with the impregnation cell.

The drug or drug solution (in the cases when cosolvents were used), was loaded in the bottom of the cell and the polymer films (with masses between 0.01-0.02 g) were separated in a metallic grid, placed in the centre of the cell. The amount of drug was established in order to obtain a saturated environment at the operational conditions. A cosolvent concentration of 10 % (v/v), at NTP conditions, was used in order to increase drug solubility in $scCO_2$ (Coimbra [2004]). Then, carbon dioxide was allowed to flow through the cell to remove all the air from the system. Then, valves 11 and 12 were closed and the cell was loaded with CO_2 until the desired pressure and temperature conditions were attained. After this, valve 6 was

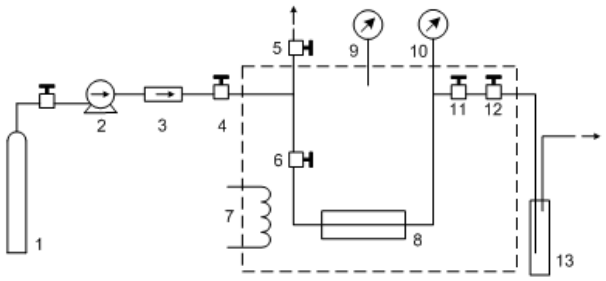

Figure 2.2: Schematic diagram of the experimental supercritical solvent impregnation apparatus: (1) CO_2 reservoir, (2) high-pressure CO_2 pump, (3) one-way valve, (4, 5, 6, 11, 12) valves, (7) water bath heater/controller, (8) high-pressure stainless steel impregnation cell, (9) digital thermometer, (10) pressure transducer, and (13) glass trap

closed and the system was maintained static and under constant pressure during the 2 h of impregnation experiments.

At the end of the impregnation period, the system was depressurized (depressurization rate was 5 bar/min) in order not to alter or damage the polymeric samples. For this, two consecutive valves (11 and 12) were used in order to have a greater control over the depressurization rate. Impregnated samples were then recovered in a dry or soaked state (when cosolvent was used). Wet samples were dried in a vacuum oven at 37 °C for 2 h. Then, sample masses were registered in order to calculate the impregnation efficiency (Section 2.2.4).

A pressure of 200 bar and a temperature of 40 °C were chosen because $scCO_2$ has the highest solubility (3.2 g CO_2/g of PCL) in poly(ε-caprolactone) at these operating conditions (Leeke et al. [2006]). At these conditions, PCL presents a maximum swelling degree which, supposedly, may help diffusion and increase drug loading yields. A second operational pressure (110 bar) was chosen in order to study the possible pressure effects on the resulting polymer blends on which we did not have any previous data regarding the solubility of $scCO_2$ in these polymeric matrices. The operational parameters for each of the performed experiments are summarised in Table 2.1.

2.2.4 Impregnation efficiency

The impregnated timolol maleate mass (m_d) was determined spectrophotometrically by UV-vis analysis (Jasco V-530 Spectrophotometer), at 299.5 nm, after dissolving the impregnated blends in tetrahydrofuran. The impregnation yield was

Exp.	P (bar)	T (°C)	Time (h)	Cosolvent concentration (v/v), NTP	Depressurisation rate (bar/min)
1	200	40	2	None	5
2	200	40	2	Water(10%)	5
3	200	40	2	Ethanol(10%)	5
4	110	40	2	None	5
5	110	40	2	Water(10%)	5
6	110	40	2	Ethanol(10%)	5

Table 2.1: Employed impregnation experiments operational conditions

calculated using Eq. 2.1. Triplicate assays were performed in order to obtain the experimental standard deviation.

$$Impregnation\ efficiency\ (g\ drug/g\ blend)\ =\ \frac{m_d}{m_p} \tag{2.1}$$

In this equation, m_p is the polymer mass after the impregnation process. For each different blend composition, the operating conditions leading to the highest impregnation were selected and only these impregnated samples were tested for the in vitro kinetics drug release experiments.

2.2.5 Contact angle measurements

The contact angle formed between a water droplet placed on the surface of a material and the kinetics of spreading is related to the hydrophilicity/hydrophobicity of the material. Water contact angles of the prepared polymer blend films were evaluated by static contact angle measurements using an OCA 20 from Dataphysics. The tests were performed on the air-facing surfaces of the samples, using water and employing the sessile drop method. Nine measurements on different sample points were performed to calculate the mean static contact angle and its standard deviation.

2.2.6 DSC - Crystallinity determination

Differential scanning calorimetry (DSC) was carried out using a SDT Q 600 calorimeter, from TA Instruments. Films were heated under a nitrogen gas flow at a heating rate of 10 °C/min. DSC results were calibrated using indium as the calibration standard. The melting temperature of the blends was considered as the temperature at which the endothermic peak occurred. The fusion enthalpy, for each blend, was determined integrating the peaks from the melting endotherm using

TA Analysis software. The relative crystallinity, X_{rel} of the blends was calculated using Eq. 2.2 (Kong and Hay [2002, 2003]):

$$X_{rel}\,(\%) \;=\; \frac{\Delta H_f}{\Delta H_{f,100\%}} \times 100 \tag{2.2}$$

In Eq. 2.2, ΔH_f is the experimental fusion enthalpy of the blends. The value of $\Delta H_{f,100\%}$ was used considering the reported fusion enthalpy of 100 % crystalline polycaprolactone (Tsuji and Ikada [1998]).

2.2.7 In vitro kinetics of drug release studies

The kinetics of timolol maleate release from the prepared materials was studied in PBS medium at 37 °C. The impregnated blend samples were compressed in a mould, using a press, into discs of 6 mm diameter and 1 mm thickness. These discs were weighed and introduced in vials containing 4 ml of PBS and maintained at 37 °C. At scheduled time intervals (every 15 min during the first hour, then every hour during 6 h, twice a day during 2 days and finally once a day for the remaining time), half of the the PBS/drug solution was removed from the vial and a fresh PBS solution of identical volume was added to maintain sink conditions. The timolol maleate concentration in each of the collected samples was measured at 299.5 nm using a Jasco V-530 Spectrophotometer. The amount of timolol maleate released at time t (m_t), was determined from a pre-determined standard curve (with an absorption coefficient $\varepsilon_{299.5} = 20.97 \pm 1.51$ ml/mg cm). The total amount (m_{total}) of impregnated timolol maleate was determined after the release test ended, by dissolving the blends in THF and adding this residual mass to the accumulated released mass. The percentage of released drug was calculated using Eq. 2.3. Calculations of the amount of released drug took into account the drug removal and the replacement with fresh medium at each sampling point:

$$\textit{Released drug}\;(\%) \;=\; \frac{m_t}{m_{total}} \times 100 \tag{2.3}$$

In order to study the drug release mechanism, the Korsmeyer-Peppas equation (Eq. 2.4) was used (Korsmeyer et al. [1983]):

$$\frac{m_t}{m_{total}} \;=\; k \cdot t^n \tag{2.4}$$

In this equation, m_t/m_{total} is the fractional release of the drug, k is the kinetic constant and n is the release exponent, which gives an indication of drug release type of mechanism. Following the Korsmeyer-Peppas equation, only the experimental drug release data that satisfied the relation $m_t/m_{total} \leq 0.6$ were employed for the

determination of the release exponent. Release exponents, n, were calculated as the slopes of the straight lines fitted to the release data using a least squares method.

2.3 Results and discussion

2.3.1 Contact angle measurements

Contact angles are characteristic constants of liquid-solid systems and, when water or aqueous solutions are used as the liquids, may provide valuable information on the solid surface hydrophilicity or hydrophobicity. This information is of great importance for the development of polymeric CDDS since water-promoted polymeric swelling will strongly influence drug diffusion through the polymeric network as well as polymeric erosion/dissolution and degradation (Heller [1996]). The obtained water-polymeric blends contact angles are presented in Table 2.2. These results show that all the prepared blends, as well as the individual polymers and copolymers, are mainly hydrophilic (contact angles $\leq 90°$). But, and for the investigated individual samples, we can assume that Lu is the more hydrophilic sample, PCL has an intermediate hydrophilic character and Lw is the less hydrophilic sample. Moreover, and as expected, obtained blend contact angles are intermediate values of the constitutive polymers and copolymers. Thus, as PCL content is increased in Lu/PCL blends, the resulting blend samples become less hydrophilic. The same behaviour is observed when Lw content is increased in Lw/PCL blends: contact angle increased because the overall hydrophobic content of the blend was also increased. These results were confirmed by water swelling experiments, which will be reported in due time, together with other blend characterization data. Due to the specific interactions that may occur between polymers/copolymers, resulting blends and the involved solvents, these different relative hydrophobicity/hydrophilicity characters may have a strong influence on the obtained kinetics of drug release results and on the impregnation efficiency results, as it will be discussed later.

2.3.2 DSC - Crystallinity determination

Polymer and copolymer crystallinity is known to play an important role in determining degradability, erosion, water and drug permeability because the bulk crystalline phases that may be present become more inaccessible to water diffusion. Moreover, $scCO_2$ induced crystallization of polymeric substrates can also influence the overall supercritical solvent impregnation process as well as the final relative crystallinity of the processed polymeric materials (Kikic and Vecchione [2003],

Samples	Contact angle (deg)
Lu	48.3 (0.8)
50/50 Lu/PCL	50.1 (1.2)
25/75 Lu/PCL	55.9 (1.3)
PCL	61.8 (1.8)
25/75 Lw/PCL	63.6 (1.0)
50/50 Lw/PCL	66.1 (0.9)
75/25 Lw/PCL	70.9 (1.3)
Lw	72.5 (1.4)

Table 2.2: Obtained contact angle for the employed homo- and copolymers and for prepared blends

Kazarian [2000], Zhou et al. [2003], Berens et al. [1992], Xu and Chang [2004], Condo et al. [1996]).

PCL, Lu and Lw are semi-crystalline polymers and copolymers and, in their blends, the overall final crystallinity degree may be strongly influenced by blend composition, by the relative crystallinity of each component in the blend and by the specific interactions that may occur between blend components or between specific blocks of the involved copolymers in the blend. As shown in Table 2.3, the relative crystallinity, X_{rel} (%), calculated using Eq. 2.2 increases with the PCL ratio in Lw/PCL blends and decreases with the PCL ratio in Lu/PCL blends.

We did not find any previously reported values for the fusion enthalpy of 100% crystalline Lu and Lw, $\Delta H_{f,100\%}$, and thus it was not possible to calculate the relative crystallinities for these pure copolymers. However, the measured fusion enthalpies for both pure Lu and Lw are higher than the corresponding value for PCL. Usually this is an indication that their relative crystallinity values should also be higher than the corresponding value for PCL.

Therefore, it should be expected that blends with higher Lu and Lw contents should also present higher relative crystallinities. This happens for Lu/PCL blends and this behaviour was already found and discussed in other works involving, for example, polyethylene oxide/PCL blends (Qiu et al. [2003]).

Despite this rule, some exceptions may occur especially when the co-crystallization of blend components can take place with some crystallization restrictions of one component due to the presence of the second one. For example, in the case of Lw/PCL blends, as the proportion of Lw in the blend is increased, the expected higher crystallization ability of Lw can be restricted and, as a consequence, the final relative crystallinity decreases. Furthermore, and again in the case of Lw/PCL blends, it has been proposed that the carbonyl groups from polyesters can interact favourably with the α-hydrogens of the poly(vinylacetate)

Samples	Δ H_f (J/g)	X_{rel} (%)
Lu	109.6	-
50/50 Lu/PCL	85.7	60.4
25/75 Lu/PCL	80.9	57.0
PCL	72.8	51.3
25/75 Lw/PCL	70.4	49.6
50/50 Lw/PCL	62.1	43.7
75/25 Lw/PCL	57.4	40.4
Lw	116.8	-

Table 2.3: Fusion enthalpies and relative crystallinities

(PVAc) block due to their proton accepting and proton donating properties, respectively. Such favourable interactions between PCL and the PVAc block can be responsible for the commonly found miscibility of PCL/PVAc blends (Sivalingam et al. [2004]). It is also accepted that the favourable interactions that are often established between two constituents in miscible blends can contribute to slowing down of the formation rate of crystallising species being drawn into (or diffusing to) the crystals (Ajili and Ebrahimi [2007]). Therefore, these are other possible explanations of why, in the Lw/PCL series, the addition of Lw causes a decrease in relative crystallinity in comparison with pure PCL. The obtained fusion enthalpies of these blends are also smaller than that obtained for PCL alone, further sustaining these hypotheses.

2.3.3 Supercritical drug impregnation process

The 75/25 Lu/PCL blend was not studied because it was found that it dissolves in PBS at 37 °C, and thus it is not a good material for the intended CDDs application. The 25/75 Lu/PCL, 50/50 Lu/PCL blends, as well as PCL samples, were not impregnated using 10% of ethanol as cosolvent because the samples would dissolve completely at these operational conditions.

It is important to notice that the employed cosolvent compositions are expressed in terms of volume fractions (v/v) and are referred to NTP conditions. In the case of ethanol, at the experimental conditions (40 °C/110 bar and 40 °C/200 bar), these compositions are slightly different from this value but all ethanol was dissolved and the experiments were performed employing a homogeneous supercritical fluid phase mixture (CO_2+ethanol). However, in the case of water, and because an excess of cosolvent was added to the cell, there are always two immiscible phases inside the cell, with compositions determined by the high pressure vapour-liquid equilibria of CO_2+water mixtures, at those pressure and temperature conditions:

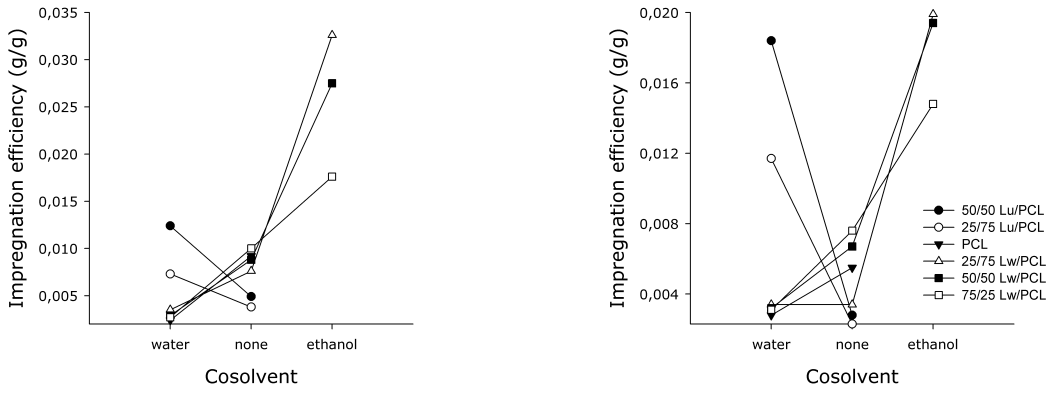

(a) (b)

Figure 2.3: Cosolvent (water and ethanol) effects on the impregnated samples: (a) 110 bar and (b) 200 bar

a high pressure fluid mixture (CO_2+water), in contact with the polymeric samples, and a high pressure liquid phase (water+CO_2), at the bottom of the cell.

In general terms, the obtained results indicate that not just timolol maleate solubility (which is highly dependent on the presence or absence of the cosolvent) in $scCO_2$ plays an important role in the overall impregnation process efficiency, but also all the other specific and complex interactions that may occur between all the involved components of the system: $scCO_2$-polymeric matrices-cosolvent interactions (which determine cosolvent and $scCO_2$ solubility in the polymeric matrix and, consequently, swelling and plasticization effects) and drug-polymeric matrices-cosolvent interactions (which control the entrapment/deposition of the drug in the polymeric network).

In Fig. 2.3(a) and Fig. 2.3(b), the effect of cosolvent on impregnation efficiency is illustrated for both employed impregnation pressures. It is clear that, for the Lw/PCL blends, the highest impregnation yields (0.018-0.033 g/g) were obtained when using ethanol (at both operational pressures) while for Lu/PCL blends, highest impregnation yields (0.012-0.018 g/g) occurred in the presence of water as cosolvent (also at both employed pressures). For pure PCL samples, best results (0.009 g/g) were achieved when no cosolvent was used and, as observed, water addition decreased the amount of impregnated drug. As already referred, ethanol was not employed with pure PCL.

Therefore, the presence of the cosolvent and its inherent nature radically changed the impregnation results for these blends: ethanol visibly promoted Lw/PCL blends impregnation while water promoted Lu/PCL blends impregnation.

These results can be explained by the favourable specific interactions drug-CO_2-cosolvent that may occur, i.e., by the timolol maleate (a water-soluble polar drug) solubility enhancement in the high pressure fluid phase, which was caused by the polarity increase of the mobile phase when the polar cosolvents (ethanol and water) were added (Li et al. [2003]). As more drug can be dissolved, more drug can be carried out into the polymeric network by the mobile high pressure phase. In the case of timolol maleate, this ethanol induced solubility enhancement was already measured in our group (Coimbra [2004]).

For water, and to the best of our knowledge, there is not any high pressure timolol maleate-CO_2-water solubility data in the literature. However, and because timolol is a water soluble molecule and water is much more polar than ethanol, we should expect the same (or even higher) solubility enhancement as the one observed for ethanol. However, when water was employed as cosolvent, the impregnation efficiencies increased for Lu/PCL blends but for Lw/PCL blends were drastically reduced. This suggests that other different phenomena should also be involved in the impregnation process. A possible explanation can be the occurrence of favourable specific timolol-maleate-polymeric matrix-ethanol interactions for Lw/PCL blends and of specific timolol-maleate-polymeric matrix-water interactions for Lu/PCL blends. Ethanol/blends contact angle measurements were not performed but water/blends contact angle experiments indicated that Lu/PCL blends were more hydrophilic than pure PCL and than Lw/PCL blends. Therefore, a high pressure mobile phase containing water may interact more efficiently with Lu/PCL blends than with pure PCL and with Lw/PCL blends, thus promoting a higher swelling degree and consequently favouring diffusion. This effect seems to be increased at higher pressures (200 bar). Furthermore, and if there is some water absorption in the hydrophilic portions of Lu/PCL blends (as expected), this will also create the conditions for a water-soluble molecule, like timolol maleate, to be deposited in these blends, instead of being removed with the mobile phase during depressurization.

A recognized advantage of SCF polymeric processing is that SCF can enhance the diffusion of drugs+SCF mixtures into some polymeric matrices because, in most cases, they can increase the polymeric free volume and the side groups chain mobility. Furthermore, this diffusion enhancement can be controlled ("tuned") just by changing the operational pressure and temperature. When polymer-SCF phase interactions are present and are favourable, high pressures usually facilitate the diffusion process mostly because they will allow more fluid absorption which will generate a higher swelling degree. This is the case when higher operational pressure determines higher drug loading in the polymeric matrix. On the other hand, when drug-SCF phase interactions are stronger than drug-polymer interactions, pressure

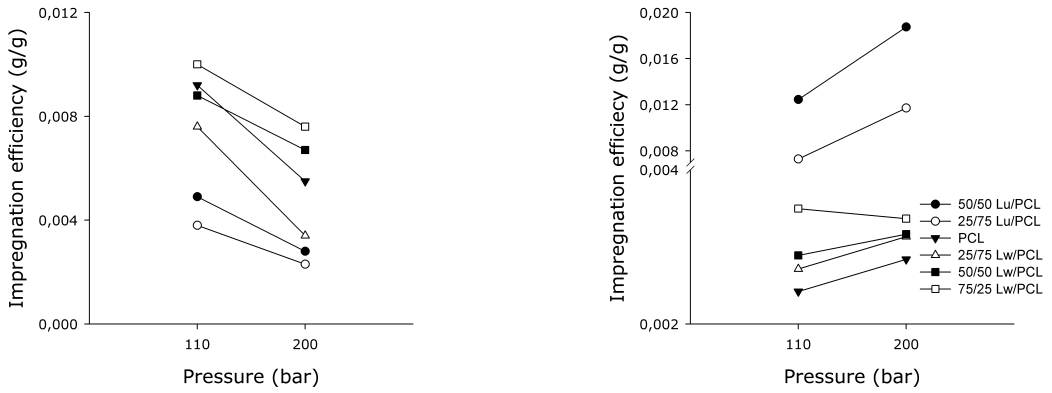

(a) (b)

Figure 2.4: Pressure effect on impregnated samples: a) no cosolvent and b) 10% water

usually will be an unfavourable factor because higher pressures will originate an increase in SCF phase density, thus leading to an increased solvating power of the mobile phase. At the same time, and if the polymer-SCF phase interactions are still appreciable, this increased density will also originate an increase in polymer swelling. As a result of these two combined factors, more drug will "choose" to diffuse out the polymeric matrix and stay in the mobile phase, originating a low polymeric loading (Kazarian et al. [1998]).

In Fig. 2.4(a), Fig. 2.4(b) and Fig. 2.5, we present the explicit effect of pressure on the impregnation efficiencies. Pressure effects complement the previous discussion about the cosolvent effects on impregnation efficiencies and can also help to explain why impregnation efficiencies are higher at 200 bar for Lu/PCL blends, while Lw/PCL blends and PCL have higher impregnation efficiencies at 110 bar. More effective drug-polymer interactions are expected to take place for Lu/PCL blends because of Lu/PCL blends higher hydrophilicities. Thus, higher pressures will favour drug deposition. For Lw/PCL blends and for PCL samples, drug diffusion into the polymeric samples also takes place but, during depressurization, more drug comes out with the mobile phase, due to the weaker drug-polymer interactions (when compared to the drug-SCF phase interactions). This is also in agreement with other works in which the efficiency of the impregnation decreases at higher pressures (Duarte et al. [2007]).

As already referred, copolymer/polymer chemical structures can strongly affect drug-polymer and polymer-SCF phase interactions, thus controlling the overall impregnation process. These complex interactions can be understood, for example, through the supercritical surfactants theory. Generally, surfactants for use with

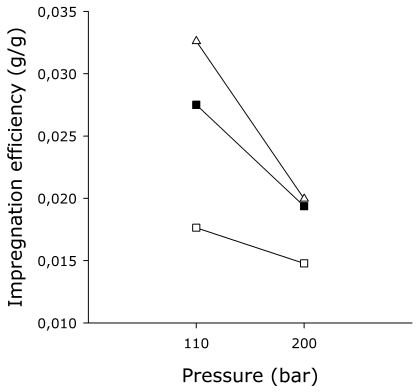

Figure 2.5: Pressure effect on impregnated samples with 10% ethanol

carbon dioxide are amphiphilic molecules containing both a CO_2-phobic and a CO_2-philic portion (Woods et al. [2004]). For Lutrol F 127 (which is a non-ionic surfactant), the ethylene oxide segment is the hydrophilic portion of the block copolymer but it also is less CO_2-philic than the polypropylene oxide segment. However, it still interacts with CO_2 thus still having some swelling degree in scCO2 media. The polypropylene oxide segment has superior CO_2-philicity (when compared to the polyethylene oxide block) mainly because of the pending methyl groups along its backbone). Luwax is a copolymer containing a hydrophobic part (polyethylene) and a slightly hydrophilic one (polyvinylacetate). In terms of CO_2 interactions, we can assume than the polyethylene block will interact in a stronger way with CO_2 than the polyvinylacetate block, thus being more CO_2-philic than the PVAc segment. Finally, PCL is a homopolymer that is known to interact strongly with CO_2 (Leeke et al. [2006]). This happens because of the methylene groups present on its backbone as well of the specific interactions that can occur between CO_2 and carbonyl groups.

Therefore, a hydrophilic drug (like timolol maleate) when is transported by a SCF, or by a SCF-cosolvent mixture, will have a tendency to specifically interact and deposit on the hydrophilic portions of the employed polymeric matrices. However, and because CO_2 is also interacting in a strong way with the hydrophobic (CO_2-philic) portions of the polymeric matrix, a hydrophilic drug can also be deposited (in a lower extent) in these hydrophobic portions. The use of a hydrophilic cosolvent (like water and ethanol, as already discussed), will yet increase these interactions with the more hydrophilic parts of the polymeric matrices thus increasing impregnation efficiency. If a hydrophobic drug is used, we should expect that these effects will influence impregnation efficiency in an opposite way.

Consequently, we should expect that more timolol maleate would be impregnated

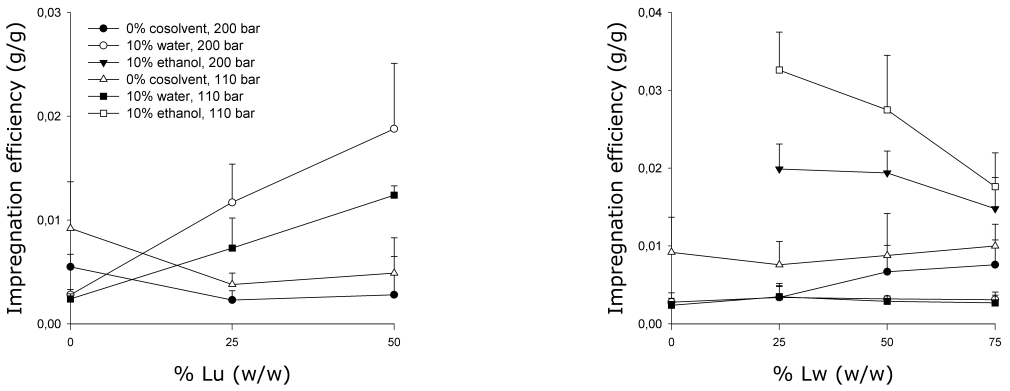

(a) (b)

Figure 2.6: Effects of blends compositions: a) Lu/PCL blends and b) Lw/PCL blends

in Lu/PCL blends as the composition, in terms of the more hydrophilic blend compound (Lu), is increased. In Fig. 2.6(a), this is verified but only when water is used as the cosolvent. For Lw/PCL blends, Fig. 2.6(b), the same effect is observed and as the Lw content is increased (the more hydrophobic component), the impregnation efficiency decreases, but only in the case when ethanol is employed. In the case of Lw/PCL blends, and as already discussed in terms of water-samples contact angles and relative hydrophilicity, water seems not to affect greatly the impregnation efficiency.

Finally and as already mentioned, the $scCO_2$ induced crystallization of some polymeric substrates can occur during the impregnation experiments, decreasing the overall chain mobility of the involved polymeric materials. This effect is contrary to the favourable plasticization effect and can increase the final relative crystallinity of the processed polymeric materials, thus influencing negatively the overall impregnation efficiency (Kikic and Vecchione [2003], Kazarian [2000], Zhou et al. [2003], Berens et al. [1992], Xu and Chang [2004], Condo et al. [1996]). However, we did not measure the relative crystallinity of the employed materials after $scCO_2$ and $scCO_2$+cosolvent processing and therefore we did not know if crystallinity increased or decreased. This work is still being performed and results will be presented in due time.

2.3.4 In vitro kinetics of drug release studies

In vitro kinetics of drug release studies were performed for selected impregnated samples. This selection was made taking in consideration the best impregnation

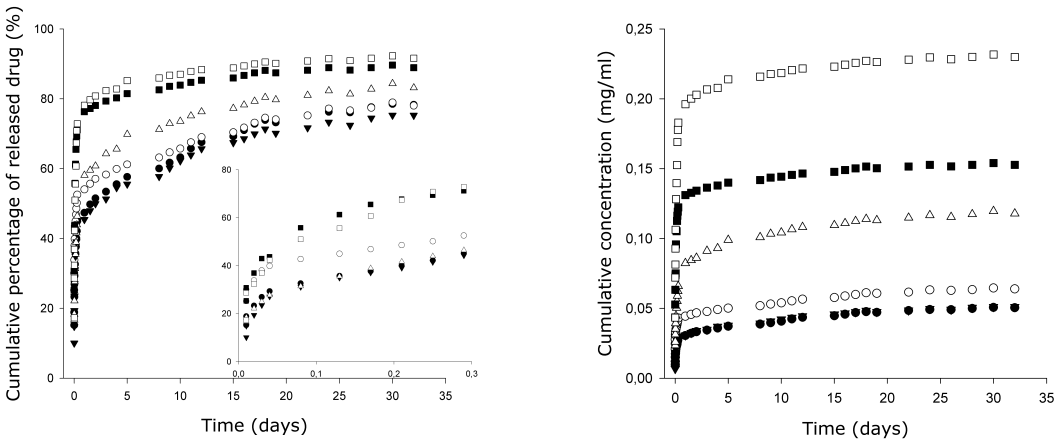

(a) (b)

Figure 2.7: Kinetics of drug release studies: a) cumulative percentages of released timolol maleate and b) cumulative concentrations of released timolol maleate and (c) linear regressions to calculate kinetic constants and release exponents

conditions, in terms of impregnation efficiency, for each set of blends or sample: 200 bar/ 10 % water for Lu/PCL blends, 110 bar/ 10 % ethanol for Lw/PCL blends and 110 bar/ 0 % cosolvent for PCL samples. Results are presented in Fig. 2.7(a) and 2.7(b). The cumulative percentages of released timolol maleate are shown in Fig. 2.7(a). A magnification of the initial 8 hour release period is also shown. After 32 days of release studies, the cumulative released percentages were found to be higher for the Lw/PCL blends, followed by the Lu/PCL blends and, finally, by PCL (84.6-92.3 %, 79.2-79.9 % and 77.2 %, respectively). All the impregnated samples presented almost the same drug release profile, i.e., a biphasic release pattern: an initial burst period exhibiting a very rapid release rate (probably caused by the drug deposited on/near the polymeric surface), followed by a polymeric swelling and/or erosion period, exhibiting an almost constant release rate (3-10 μg/day after the first day). We must remember that Lutrol F 127 is soluble in water and poly(ε-caprolactone) undergoes hydrolytic degradation.

The obtained results seem to indicate that the initial drug loading of the supercritical impregnated samples somehow influenced drug release kinetics results: the higher cumulative percentages of released drug were obtained for the samples which were impregnated with higher drug amounts (Lw/PCL blends impregnated with 10% ethanol). However this could not be the true reason for these observations and a possible explanation may be that timolol maleate was released faster in Lw/PCL blends because most part of impregnated drug was probably deposited very close to the surface. This will be confirmed further on when the kinetics modelling results will be discussed.

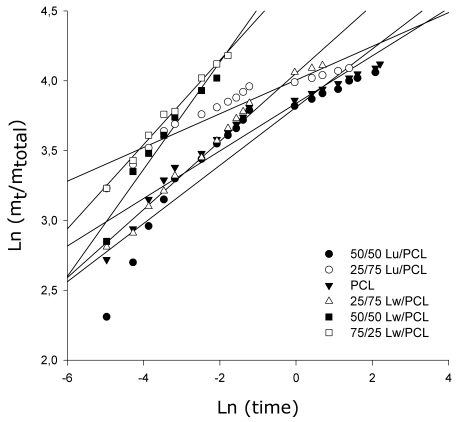

Figure 2.8: Linear regressions to calculate kinetic constants and release exponents

Lu/PCL blends and PCL were impregnated in a lesser extent but show more sustained drug release profiles. These results are probably due to the fact that these lower impregnated amounts of drug (when compared to Lw/PCL blends) were deposited more deeply in the polymeric structure (thus more homogeneously dispersed throughout all the polymeric samples). And, this was the result of the favourable specific interactions that were established between timolol maleate, water (cosolvent) and the highly hydrophilic segments of the Lu/PCL blends (as discussed in section 2.3.3). In addition, sample crystallinity may also control the drug release rates (higher crystallinity degrees usually lead to slower release rates) and Lu/PCL blends and PCL present the highest percentage of crystalline phases (see Table 2.3).

Cumulative released drug concentration results are presented in Fig. 2.7(b). It can be seen that, after the initial first day burst release, timolol maleate concentration becomes almost constant (1.2-4 μg/ml/day corresponding to a mass of 3-10 μg/day), which is located above the therapeutic limit of timolol maleate (5 μg/day) (Bartels [1988]) and below the maximum recommended human ophthalmic dose (0.42 mg/day, considering a patient weight of 60 kg) (Ophthalmic dose). The burst dose, released by the systems during the first day is below the maximum recommended human ophthalmic dose, with two formulations surpassing this value (0.53 mg for 50/50 Lw/PCL and 0.78 mg for 75/25 Lw/PCL). Even these values are well below the maximum recommended daily oral dose, which is 60 mg/day (considering a patient weight of 60 kg) (Oral dose). The knowledge of these values is essential for the development of efficient and safe controlled drug release systems because the released drug concentrations must always be kept between the therapeutic and toxic levels.

The Korsmeyer-Peppas model (Eq. 2.4) is usually employed to analyse kinetics

Sample	k (days^{-n})	n	R^2
50/50 Lu/PCL	45.22	0.21	0.88
25/75 Lu/PCL	54.93	0.12	0.91
PCL	46.48	0.17	0.94
25/75 Lw/PCL	57.65	0.24	0.96
50/50 Lw/PCL	134.71	0.38	0.96
75/25 Lw/PCL	115.97	0.30	0.99

Table 2.4: Obtained kinetic parameters for kinetic drug release studies: release exponents (n) and kinetic constants (k)

of drug release from systems where the release mechanism is not well-known or when more than one type of release phenomena (diffusion-, swelling- or erosion-controlled) are involved. For cylindrical systems, release profiles having a release exponent, n, around 0.45, exhibit a drug release mechanism controlled by classical/Fickian diffusion. When $n \sim 0.89$, the drug release rate is controlled by a polymer relaxation mechanism (or Case II transport). Systems having release exponents, $n < 0.45$, account for pseudo-Fickian behaviour, while when $0.54 < n < 0.89$ are an indication of the superposition of both the above referred phenomena. In this case, the release mechanism is termed anomalous transport (Peppas and Brannon-Peppas [1994], Neogi [1996]).

The value of the release exponent, n, was calculated as the slope of the straight lines fitted to the release data using the least squares method (Fig. 2.8). The obtained values are presented in Table 2.4 and, for all systems, $n < 0.45$, accounting for pseudo-Fickian release behaviour. Steeper slopes were obtained for Lw/PCL blends which confirmed the already discussed higher initial burst release behaviour observed for these systems. As expected, and in general terms, results suggest that the release mechanism is quite complex, as drug diffusion, polymeric swelling, crystallinity and polymer erosion are all likely to contribute to the overall release phenomenon.

2.4 Conclusions

Lu/PCL, Lw/PCL blends and PCL samples were successfully impregnated with timolol maleate, an anti-glaucoma drug, in order to, as a final objective, prepare polymeric implantable (subconjunctival) systems for long-term timolol delivery, with controlled release and degradation.

Different blends (with distinct blend components and compositions) were prepared and characterized in terms of water-sample contact angle measurements and

sample relative crystallinity. Several SSI experimental conditions were tested: blend composition, impregnation pressure and different cosolvents (water and ethanol).

Impregnation efficiency was determined and the obtained showed indicated that, and in general terms, the overall impregnation process and its efficiency is the result of the relative specific interactions that may be established between all the involved components of this complex system: $scCO_2$-cosolvent-drug interactions (which control drug solubility in the high pressure mobile phase and its overall polar character), $scCO_2$-polymeric matrices-cosolvent interactions (which determine cosolvent and $scCO_2$ solubility in the polymeric matrix and, consequently, swelling and plasticization effects) and drug-polymeric matrices-cosolvent interactions (which control the entrapment/deposition of the drug in the polymeric network). In addition, the employed polymeric samples, with the exception of PCL, are copolymer blends and each one of these copolymers has blocks/segments with different hydrophobic/hydrophilic characters, thus increasing even more the system complexity.

However, in specific impregnation conditions, the addition of a cosolvent (water and ethanol for Lu/PCL and Lw/PCL, respectively) promotes higher drug loading. This happened because, in these conditions, drug solubility is increased and higher drug amounts can be transported by the mobile phase. Moreover, the relative hydrophilicity/hydrophobicity of prepared blends, together with the cosolvent addition, also seemed to affect favourably the impregnation process (because of the specific favourable interactions that are formed between the drug, cosolvent and the more hydrophilic blend segments). Higher pressures were either a favourable factor (for Lu/PCL blends) or an unfavourable factor (for Lw/PCL blends and for PCL samples).

Selected impregnated samples (the ones that presented higher impregnation efficiencies) were employed in kinetics of drug release studies and the obtained results indicated that the higher cumulative percentages of released drug were obtained for the samples which were impregnated with higher drug amounts (Lw/PCL blends impregnated with 10% ethanol). However, these systems presented high initial drug burst release profiles. Lu/PCL blends and PCL were impregnated in a lesser extent but they showed more sustained/controlled drug release profiles. These results are probably due to the fact that timolol maleate was more homogeneously dispersed throughout all the polymeric samples, as the result of the favourable specific interactions that were established between timolol maleate, water (cosolvent) and the highly hydrophilic segments of Lu/PCL blends. In addition, and for these blends, sample crystallinity may have also influenced drug release rates because of the Lu/PCL blends and PCL higher percentages of crystalline phases. These results

were confirmed by the application of Korsmeyer-Peppas model, that accounted for pseudo-Fickian release behaviour for all the tested samples, which indicates that the release mechanism is quite complex, as drug diffusion, polymeric swelling, crystallinity and polymer erosion are all expected to contribute to the global release phenomenon.

After the first release day, all samples showed a sustained release of 1.2-4 μg/ml/day, corresponding to a mass of 3-10 μg/day, during a period of 1 month. These values are between the therapeutic and toxic levels of timolol maleate. The obtained impregnation efficiencies and drug release results suggested that a desired final sustained drug release rate can be achieved by changing several operational impregnation conditions and by modulating blend compositions, i.e., as a way to control crystallinity, hydrophilicity and drug affinity for the polymer matrix.

As final conclusions, the prepared timolol maleate-loaded polymeric matrices can be a feasible and promising alternative to the conventional repeated daily administration of timolol maleate eye drops for glaucoma treatment. Moreover, the SSI method proved to be a good choice and a "tunable" method for the preparation of these long-term controlled release systems.

Bibliography

I. Ahmed and T.F. Patton. Importance of the noncorneal absorption route in topical ophthalmic drug delivery. *Invest. Ophthalmol. Vis. Sci.*, 26:584–587, 1985. [PubMed:3884542].

S.H. Ajili and N.G. Ebrahimi. Miscibility of TPU(PCL diol)/PCL blend and its effect on PCL crystallinity. *Macromol. Symp.*, 249-250:623–627, 2007. [DOI:10.1002/masy.200750446].

S.P. Bartels. Aqueous humor flow measured with fluorophotometry in timolol-treated primates. *Invest. Ophthalmol. Vis. Sci.*, 29:1498–1504, 1988. [PubMed:3170122].

A.R. Berens, G.S. Huvard, R.W. Korsmeyer, and F.W. Kunig. Application of compressed carbon dioxide in the incorporation of additives into polymers. *J. Appl. Polym. Sci.*, 46:231–237, 1992. [DOI:10.1002/app.1992.070460204].

J.L. Bourges, C. Bloquel, A. Thomas, F. Froussart, A. Bochot, F. Azan, R. Gurny, D. BenEzra, and F. Behar-Cohen. Intraocular implants for extended drug delivery: therapeutic applications. *Adv. Drug Deliv. Rev.*, 58:1182–1202, 2006. [DOI:10.1016/j.addr.2006.07.026].

C.L. Bourlais, L. Acar, H. Zia, P.A. Sado, T. Needham, and R. Leverge. Ophthalmic drug delivery systems–Recent advances. *Prog. Retin. Eye Res.*, 17:33–58, 1998. [PubMed:9537794].

M.E.M. Braga, M.T. Vaz Pato, H.S.R. Costa Silva, E.I. Ferreira, M.H. Gil, C.M.M. Duarte, and H.C. de Sousa. Supercritical solvent impregnation of ophthalmic drugs on chitosan derivatives. *J. Supercrit. Fluid*, 44:245–257, 2008. [DOI:10.1016/j.supflu.2007.10.002].

S. Chutimaworapan, G. C. Ritthidej, E. Yonemochi, T. Oguchi, and K. Yamamoto. Effect of water-soluble carriers on dissolution characteristics of nifedipine solid dispersions. *Drug Dev. Ind. Pharm.*, 26:1141–1150, 2000. [DOI:10.1081/DDC-100100985].

P. Coimbra. Solubilidade de fármacos oftalmológicos em díoxido de carbono supercrítico. Master's thesis, University of Coimbra, 2004.

P.D. Condo, S.R. Sumpter, M.L. Lee, and K.P. Johnston. Partition coefficients and polymer-solute interaction parameters by inverse supercritical fluid chromatography. *Ind. Eng. Chem. Res.*, 35(4):1115–1123, 1996. [DOI:10.1021/ie950356x].

L.C. Costantini, S.R. Kleppner, J. McDonough, M.R. Azar, and R. Patel. Implantable technology for long-term delivery of nalmefene for treatment of alcoholism. *Int. J. Pharm.*, 283:35–44, 2004. [DOI:10.1016/j.ijpharm.2004.05.034].

H.C. de Sousa, M.H.M. Gil, EO. B. Leite, C.M.M. Duarte, and A.R.C. Duarte. Method for preparing sustained-release therapeutic ophthalmic articles using compressed fluids for impregnation of drugs, 2006a. EP1611877A1.

H.C. de Sousa, M.H.M. Gil, E.O.B. Leite, C.M.M. Duarte, and A.R.C. Duarte. Method for preparing therapeutic ophthalmic articles using compressed fluids, 2006b. US20060008506A1.

S. Ding. Recent developments in ophthalmic drug delivery. *Pharm. Sci. Technol. Today*, 1:328–335, 1998. [DOI:10.1016/S1461-5347(98)00087-X].

A.R.C. Duarte, S. Santiago, H.C. de Sousa, and C.M.M. Duarte. Solubility of acetazolamide in supercritical carbon dioxide in the presence of ethanol as a cosolvent. *J. Chem. Eng. Data*, 50:216–220, 2005. [DOI:10.1021/je049722m].

A.R.C. Duarte, A.L. Simplicio, A. Vega-González, P. Subra-Paternault, P. Coimbra, M.H. Gil, H.C. de Sousa, and C.M.M. Duarte. Supercritical fluid impregnation

of a biocompatible polymer for ophthalmic drug delivery. *J. Supercrit. Fluids*, 42:373–377, 2007. [DOI:10.1016/j.supflu.2007.01.007].

J. Heller. *Biomaterials Science. An Introduction to Materials in Medicine*, chapter Drug Delivery Systems, pages 346–356. Academic Press, 1996.

S. G. Kazarian. Polymer processing with supercritical fluids. *Polym. Sci. Ser. C*, pages 78–101, 2000.

S.G. Kazarian, M.F. Vincent, B.L. West, and C.A. Eckert. Partitioning of solutes and cosolvents between supercritical CO2 and polymer phases. *J. Supercrit. Fluids*, 13:107–112, 1998. [DOI:10.1016/S0896-8446(98)00041-2].

I. Kikic and F. Vecchione. Supercritical impregnation of polymers. *Curr. Opin. Solid St. M.*, 7:399–405, 2003. [DOI:10.1016/j.cossms.2003.09.001].

D.E. Knox. Solubilities in supercritical fluids. *Pure Appl. Chem.*, 77:513 – 530, 2005. [DOI:10.1351/pac200577030513].

I. Kocur and S. Resnikoff. Visual impairment and blindness in Europe and their prevention. *Br. J. Ophthalmol.*, 86:716–722, 2002. [PubMed:12084735].

Y. Kong and J.N. Hay. The measurement of the crystallinity of polymers by DSC. *Polymer*, 43:3873–3878, 2002. [DOI:10.1016/S0032-3861(02)00235-5].

Y. Kong and J.N. Hay. The enthalpy of fusion and degree of crystallinity of polymers as measured by DSC. *Europ. Polym. J.*, 39:1721–1727, 2003. [DOI:10.1016/S0014-3057(03)00054-5].

R.W. Korsmeyer, R. Gurny, E. Doelker, P. Buri, and N.A. Peppas. Mechanisms of solute release from porous hydrophilic polymers. *Int. J. Pharm.*, 15:25–35, 1983. [DOI:10.1016/0378-5173(83)90064-9].

N. Kumar, M.N. Ravikumar, and A.J. Domb. Biodegradable block copolymers. *Adv. Drug Deliv. Rev.*, 53:23–44, 2001. [PubMed:11733116].

G.A. Leeke, J. Cai, and M. Jenkins. Solubility of supercritical carbon dioxide in polycaprolactone (CAPA 6800) at 313 and 333 K. *J. Chem. Eng. Data*, 51: 1877–1879, 2006. [DOI:10.1021/je060230e].

P.R. Lewis, T.G. Phillips, and J.W. Sassani. Topical therapies for glaucoma: what family physicians need to know. *Am. Fam. Physician*, 59:1871–1879, 1999. [PubMed:10208706].

Q. Li, Z. Zhang, C. Zhong , Y. Liu, and Q. Zhou. Solubility of solid solutes in supercritical carbon dioxide with and without cosolvents. *Fluid Phase Equilib.*, 207:183–192, 2003.

A. Ludwig. The use of mucoadhesive polymers in ocular drug delivery. *Adv. Drug Deliv. Rev.*, 57:1595–1639, 2005. [DOI:10.1016/j.addr.2005.07.005].

P. Neogi. *Diffusion in Polymers*, chapter Transport Phenomena in Polymer Membranes, pages 173–209. Marcel Dekker, 1996.

Ophthalmic dose. Timoptic safety information. `http://www.accessdata.fda.gov/drugsatfda_docs/label/2006/018086s070s072lbl.pdf."`, 2005.

Oral dose. Timolol, maximum recommended therapeutic dose (MRTD) database. `http://www.fda.gov/aboutfda/centersoffices/cder/ucm092199.htm#T"`, 2009.

J. Pena, T. Corrales, I. Izquierdo-Barba, M.C. Serrano, M.T. Portoles, R. Pagani, and M. Vallet-Regi. Alkaline-treated poly(ε-caprolactone) films: degradation in the presence or absence of fibroblasts. *J. Biomed. Mater. Res. A*, 76:788–797, 2006. [DOI:10.1002/jbm.a.30547].

N.A. Peppas and L. Brannon-Peppas. Water diffusion and sorption in amorphous macromolecular systems and foods. *J. Food Eng.*, 22:189–210, 1994. [DOI:10.1016/0260-8774(94)90030-2].

Z. Qiu, T. Ikehara, and T. Nishi. Miscibility and crystallization of poly(ethylene oxide) and poly(ε-caprolactone) blends. *Polymer*, 44:3101–3106, 2003. [DOI:10.1016/S0032-3861(03)00167-8].

M. Scherlund, A. Brodin, and M. Malmsten. Micellization and gelation in block copolymer systems containing local anesthetics. *Int. J. Pharm.*, 211:37–49, 2000. [PubMed:11137337].

M.C. Serrano, R. Pagani, M. Vallet-Regi, J. Pena, A. Ramila, I. Izquierdo, and M.T. Portoles. In vitro biocompatibility assessment of poly(ε-caprolactone) films using L929 mouse fibroblasts. *Biomaterials*, 25:5603–5611, 2004. [DOI:10.1016/j.biomaterials.2004.01.037].

G. Sivalingam, R. Karthik, and G. Madras. Blends of poly(ε-caprolactone) and poly(vinyl acetate): mechanical properties and thermal degradation. *Polym. Degrad. Stab.*, 84:345–351, 2004. [DOI:10.1016/j.polymdegradstab.2004.01.011].

B. Subramaniam, R.A. Rajewski, and K. Snavely. Pharmaceutical processing with supercritical carbon dioxide. *J. Pharm. Sci.*, 86:885–890, 1997. [DOI:10.1021/js9700661].

P.S. Tan and S.H. Teoh. Effect of stiffness of polycaprolactone (PCL) membrane on cell proliferation. *Mater. Sci. Eng. C*, 27:304–308, 2007. [DOI:10.1016/j.msec.2006.03.010].

H. Tsuji and Y. Ikada. Blends of aliphatic polyesters. II. Hydrolysis of solution-cast blends from poly(D,L-lactide) and poly(ε-caprolactone) in phosphate-buffered solution. *J. Appl. Polym. Sci.*, 67:405–415, 1998. [DOI:10.1002/(SICI)1097-4628(19980118)67:3¡405::AID-APP3¿3.0.CO;2-Q].

A. Urtti. Challenges and obstacles of ocular pharmacokinetics and drug delivery. *Adv. Drug Deliv. Rev.*, 58:1131–1135, 2006. [DOI:10.1016/j.addr.2006.07.027].

J. A. van Laarhoven, M. A. Kruft, and H. Vromans. In vitro release properties of etonogestrel and ethinyl estradiol from a contraceptive vaginal ring. *Int. J. Pharm.*, 232:163–173, 2002. [PubMed:11790500].

H.M. Woods, M.M.C.G. Silva, C. Nouvel, K.M. Shakesheff, and S.M. Howdle. Materials processing in supercritical carbon dioxide: surfactants, polymers and biomaterials. *J. Mater. Chem.*, 14:1663–1678, 2004. [DOI:10.1039/B315262F].

Q. Xu and Y. Chang. Complex interactions among additive/supercritical CO2/polymer ternary systems and factors governing the impregnation efficiency. *J. Appl. Polym. Sci.*, 93:742–748, 2004. [DOI:10.1002/app.20539].

T. Yasukawa, Y. Ogura, Y. Tabata, H. Kimura, P. Wiedemann, and Y. Honda. Drug delivery systems for vitreoretinal diseases. *Prog. Retin. Eye Res.*, 23: 253–281, 2004. [DOI:10.1016/j.preteyeres.2004.02.003].

H. Zhou, J. Fang, J. Yang, and X. Xie. Effect of the supercritical CO2 on surface structure of PMMA/PS blend thin films. *J. Supercrit. Fluids*, 26:137–145, 2003. [DOI:10.1016/S0896-8446(02)00155-9].

Chapter 3

Drug-eluting electrospun fibers for controlled release applications

The text that comprises this Chapter was published in the journal *International Journal of Pharmaceutics* (2010), volume 397, pages 50–58.

Abstract

Bicomponent fibers of two semi-crystalline (co)polymers, poly(ε-caprolactone), PCL and poly(oxyethylene-b-oxypropylene-b-oxyethylene), Lu were obtained by electrospinning. Acetazolamide and timolol maleate were loaded in the fibers in different concentrations (below and above the drug solubility limit in polymer) in order to determine the effect of drug solubility in polymer, drug state, drug loading and fiber composition on fiber morphology, drug distribution and release kinetics. The high loadings fibers (with drug in crystalline form) showed higher burst and faster release than low drug content fibers, indicating the release was more sustained when the drug was encapsulated inside the fibers, in amorphous form. Moreover, timolol maleate was released faster than acetazolamide, indicating that drug solubility in polymer influences the partition of drug between polymer and elution medium, while fiber composition also controlled drug release. At low loadings, total release was not achieved (cumulative release percentages smaller than 100 %), suggesting that drug remained trapped in the fibers. The modeling of release data implied a three stage release mechanism: a dissolution stage, a desorption and subsequent diffusion through water filled pores, followed by polymer degradation control.

3.1 Introduction

Electrospinning is a versatile technique through which a variety of constructs can be obtained with application in biomedicine (medical prosthesis, tissue scaffolds, wound dressings, drug delivery, cosmetics), textiles, electricity and optics, sensors, filtration, catalysis, unconventional energy sources and storage cells (Hunley and Long [2008], Huang et al. [2003]). In the field of drug delivery and tissue engineering, electrospun polymer fibers have gained increasing importance because they present several advantages: relatively easy drug entrapment during the electrospinning process, obtaining of high loadings if so desired, burst control, stability and preservation of drug/growth factor activity, high surface area (which enhances drug release) and specific morphology which can be easily controlled during the electrospining process (Agarwal et al. [2008]). Multicomponent fibers have attracted special attention because new properties can be obtained through the combination of different materials. Synthetic polymers with good processability and good mechanical properties can be mixed with natural polymers producing an increase in cellular attachment and biocompatibility (McClure et al. [2009]). Multicomponent fibers can be obtained mainly by two techniques (Sawicka and Gouma [2006]): direct electrospinning of polymers solution (in a single-needle configuration, if a mixture of polymers is co-dissolved in the electrospinning solution or a multi-needle configuration in which the polymer solutions are separated in parallel or concentric syringes) and post-treatment of the single-component electrospun fibers (which can include coating with other inorganic-polymer layers (Casper et al. [2007], Lee et al. [2009]), grafting (Ma et al. [2006]), crosslinking (Lee et al. [2007], chemical vapour deposition (Zeng et al. [2005a]), functionalization with other (bio)polymers (Casper et al. [2005])). In addition to the new physico-chemical properties that arise from using various components, a variety of fiber structures can be obtained such as core-shell fibers, micro/nanotubes, interpenetrating phase morphologies (matrix dispersed or co-continuous fibers) (Bogntizki et al. [2001], Wei et al. [2006]), nanoscale morphologies (spheres, rods, micelles, lamellae, vesicle tubules, and cylinders) (Kalra et al. [2006]) and multilayered constructs (either with different composition or different fiber diameter) (Vaz et al. [2005], Pham et al. [2006]).

For drug delivery applications, several polymers (in terms of degradability and crystallinity) have been studied as well as drug/growth factor loading in crystalline or amorphous form in order to fulfill specific requirements of drug-eluting fiber mats (usually, good mechanical properties and biocompatibility are required together with control of drug release and burst effect in order to ensure physical integrity of the construct, long term delivery or immediate action at the targeted location).

There are several factors that can affect the drug release from electrospun fibers: fiber construct geometry and thickness (Okuda et al. [2010]), fiber diameter and porosity (Cui et al. [2006]), fiber composition (Buschle-Diller et al. [2007]), fiber crystallinity (Kenawy et al. [2002]), fiber swelling (Buschle-Diller and Xie [2009]), drug loading (Cui et al. [2006], Buschle-Diller and Xie [2009]), drug state (Zamani et al. [2010], Xie and Wang [2006]), drug molecular weight (Buschle-Diller et al. [2007], Taepaiboon et al. [2006]), drug solubility in the release medium (Buschle-Diller and Xie [2009]), drug-polymer-electrospinning solvent interactions (Chew et al. [2005], Zeng et al. [2005b]). The release characteristics of the fiber mat are highly influenced by the state of the drug and the structure of the polymer that forms the fiber. For example, the crystallinity of the polymer controls the rate of drug release as semi-crystalline polymers showed in general a higher extent of burst because of two reasons: on one hand, the instantaneous release of the drug deposited at the fiber surface, and on the other hand, the hindered release of the drug from the fiber bulk due to limited water uptake in the semi-crsytalline regions (Kenawy et al. [2002]). The drug state in the fibers is also an important factor since it was shown that a drug that is incorporated in crystalline form will mainly be deposited outside the fibers and trigger burst release, while drug in amorphous state will be loaded inside the fibers and be released in a sustained manner (Zamani et al. [2010], Xie and Wang [2006], Thakur et al. [2008]). Drug loading is another factor that can affect the drug release: higher loadings will produce faster release (Cui et al. [2006], Buschle-Diller and Xie [2009], Zamani et al. [2010]); on one hand, at high loadings, there is more surface segregated drug that dissolves fast and on the other hand, there is an increase in porosity during drug elution proportional to the initial amount of drug (Cui et al. [2006]). Drug compatibility with polymer solution was also shown to be an important factor in controlling release, as lipophilic drugs should be incorporated in lipophilic polymers and hydrophilic drugs in hydrophilic polymers in order to avoid drug deposition outside fibers and subsequent burst (Zeng et al. [2005b]). Moreover, the interaction between drug and the polymer can block the crystallization of the drug in the fibers, if so desired (Yu et al. [2009]) and can even determine sustained release of drugs in crystalline state because of chemical interaction with the polymer (Taepaiboon et al. [2006]).

In our study, bicomponent fibers were prepared using poly(ε-caprolactone), a semi-crystalline, more hydrophobic polymer and Lutrol F127 (poly(oxyethylene-b-oxypropylene-b-oxyethylene)), also semi-crystalline, hydrophilic block copolymer. Poly(ε-caprolactone) was selected because it has been used in a variety of electrospun fibers applications (Agarwal et al. [2008]), while Lutrol F127 was added as hydrophilicity enhancer and release modulator (Natu et al. [2008]). The prop-

erties of the bicomponent fibers were studied in order to determine the effect of processing on crystallinity, water contact angle and mass loss. As both polymers are semi-crystalline, we could test the influence of such organization on the loading and release of drugs. Two drugs were selected for incorporation in the fibers in different concentrations (below and above the drug solubility limit in polymers), acetazolamide, a hydrophobic drug and timolol maleate, a hydrophilic drug in order to determine the effect of drug solubility in polymer, drug state, drug loading and fiber composition on fiber morphology, drug distribution and release kinetics. Moreover, modeling of the release data using a semi-empirical model (power law (Peppas and Brannon-Peppas [1994])) and a mechanistic model (desorption model (Srikar et al. [2008])) was performed, determining the release mechanism, while the models were compared in terms of goodness of fit.

3.2 Materials and methods

3.2.1 Materials

Timolol maleate, (lot no. 90191189, 99,6 % purity) was purchased from Cambrex Profarmaco Cork Ltd., while acetazolamide was obtained from Sigma-Aldrich. Poly(ε-caprolactone) pellets (PCL, average M_w 65000 g/mol) were obtained from Sigma-Aldrich. Lutrol F127 (Lu, 9000-14000 g/mol, 70 % by weight of polyoxyethylene) was bought from BASF. Acetone and methanol, both spectrophotometric grade were obtained from Sigma-Aldrich. Phosphate buffer saline (PBS) tablets (pH 7.4, 10 mM phosphate, 137 mM sodium, 2.7 mM potassium), used to prepare the release medium were bought from Sigma-Aldrich. All products were used without further purification.

3.2.2 Electrospinning

Lutrol F127 and PCL mixtures (25/75, 50/50, w/w) or PCL alone were dissolved in acetone/methanol (4/1, v/v) at 15 % (w/v) and at 40 ° C. The final volume of each polymer solution was 3 ml. Acetazolamide and timolol maleate were co-dissolved with the polymers (1 %, w/w). The electrospinning set-up consisted of a high voltage power supply (SL 10W-300W, Spellman), delivery system (syringe, teflon tubing, 30 gauge needle, syringe pump (NE-1000 Multiphaser, New Era Pump Systems)) and a rectangular copper collector. A voltage of 20 kV was applied, while the syringe pump was operated at a flow rate of 10 ml/min. Polymeric fibers were deposited on aluminium paper covering the collector placed at a distance of 8 cm from the needle tip. All electrospinning experiments were carried out under

ambient conditions (25 ° C, 50 % humidity in average). The films deposited on the aluminium paper were peeled off and cut in rectangular pieces of 1 cm×1 cm. They were used as such in drug release experiments.

3.2.3 Morphological analysis and drug mapping

The morphology of the electrospun fiber and drug distribution were examined using scanning electron microscopy (SEM, Jeol JSM 5310) coupled to an X-ray energy dispersion unit to determine the presence of elemental sulphur (present in both drugs). The drug mapping for some of the samples was done using electron probe microanalysis (Camebax SX50, Cameca) at 15 kV accelerated voltage and 40 nA probe current. SEM images were analyzed using an image analysis software (ImageJ 1.42 (ImageJ)) and the average fiber diameter was calculated by measuring the diameter of 40 fibers, selected from different areas of the samples.

3.2.4 Fiber mat crystallinity, drug solubilitity in polymer and drug state

Films containing different drug percentages were prepared by solvent casting. Differential scanning calorimetry was carried out on a DSC Q100 equipment (TA Instruments). Samples with masses of approximately 4 mg were heated until 350 °C, at a heating rate of 10 °C/min in a hermetic pan, under nitrogen atmosphere (100 mL/min). Drug concentration in the film was plotted against drug melting enthalpy (calculated using Universal Analysis 2000 software (TA Instruments)) and the drug solubility in the polymer (as percentage) was determined as the intercept of the linear regression curve. The relative crystallinity of the fibers was calculated using Eq. 3.1.

$$\mathrm{X_{rel}\,(\%)} \;=\; \frac{\Delta \mathrm{H_f}}{\mathrm{x_{Lu}}\Delta \mathrm{H_{f,100\%Lu}} + \mathrm{x_{PCL}}\Delta \mathrm{H_{f,100\%PCL}}} \times 100 \tag{3.1}$$

where ΔH_f is the melting enthalpy determined in analysis by integrating the peaks corresponding to polymer/blend melting, x_{Lu} and x_{PCL} are Lu and PCL mass fractions in the blend, while $\Delta H_{f,100\%Lu}$=181 J/g is the melting enthalpy of 100 % crystalline Lu and $\Delta H_{f,100\%PCL}$=142 J/g is the melting enthalpy of 100 % crystalline PCL (Tsuji and Ikada [1998]). The melting enthalpy of 100 % crystalline Lu was calculated using Eq. 3.2.

$$\Delta \mathrm{H_{f,100\%Lu}} = \mathrm{x_{PPO}}\Delta \mathrm{H_{f,100\%PPO}} + \mathrm{x_{PEO}}\Delta \mathrm{H_{f,100\%PEO}} \tag{3.2}$$

where x_{PPO} and x_{PEO} are polypropyleneoxide and polyethyleneoxide mass fractions in Lutrol and $\Delta H_{f,100\%PPO}$ and $\Delta H_{f,100\%PEO}$ are the corresponding melting enthalpies of 100 % crystalline polymer (ATHAS).

3.2.5 Swelling and mass loss

Fiber films were accurately weighed and immersed in 4 ml phosphate saline buffer (PBS) in sealed vials at 37 $°C$. At scheduled time intervals, samples were withdrawn from the vials, blotted with a tissue paper to remove the surface water and weighed. The water content (Δw) was calculated using the Eq. 3.3.

$$\Delta w(\%) = \frac{m_t - m_i}{m_t} \times 100 \tag{3.3}$$

where m_t denotes the mass of the wet sample at immersion time t and m_i denotes the initial mass of the sample.

For mass loss determination, at scheduled time intervals, samples were withdrawn from the vials and vacuum dried until constant weight at 37 $°C$. The percentage of mass loss (Δm) was calculated using Eq. 3.4.

$$\Delta m(\%) = \frac{m_i - m_d}{m_i} \times 100 \tag{3.4}$$

where m_i denotes the initial mass and m_d is the mass of the dried sample after a certain immersion time.

3.2.6 Drug loading and release

The drug release from the fibers was studied in PBS medium (4 ml), using a shaker (37 °C, 100 rpm). At scheduled time intervals (1, 2, 3, 4, 7, 8, 9, 10, 11, 15, 19, 36, 52 days), 2 ml of sample was taken and fresh PBS medium of identical volume was added to maintain sink conditions. The mass of timolol maleate and acetazolamide released at time t, m_t, as well as the total drug amount (m_{tot}) were determined by UV spectroscopy (Jasco V-650 Spectrophotometer) at 299.5 nm and 265 nm, in PBS and 4/1 (v/v) THF/methanol solution, respectively. The drug loading was determined using Eq. 3.5. The percentage of released drug was calculated using Eq. 3.6. Calculations of the amount of released drug took into account replacement with fresh medium at each sampling point. Controls (fibers without drug) were also tested and their contribution to the absorbance was substracted.

$$\text{Loading}\,(\%) \;=\; \frac{\mathrm{m_{tot}}}{\mathrm{m_{fiber}}} \times 100 \tag{3.5}$$

in which m_{fiber} is the mass of the fiber mat.

$$\text{Released drug}\,(\%) \;=\; \frac{\mathrm{m_t}}{\mathrm{m_{tot}}} \times 100 \tag{3.6}$$

In order to study the drug release mechanism, different equations (Eq.3.7, 3.8) were used to model the release data. The equations were fitted to the data using non-linear regression and the results were compared in terms of goodness of the fit. The power law equation (Eq.3.7) is one of them and was chosen because it is the most widely used equation in works concerning drug release (Peppas and Brannon-Peppas [1994]):

$$\frac{\mathrm{m_t}}{\mathrm{m_{tot}}} \;=\; \mathrm{a_0} + \mathrm{k\,t^n} \tag{3.7}$$

where m_t/m_{tot} is the fractional release of the drug at time t, a_0 is a constant, representing the percentage of burst release, k is the kinetic constant and n is the release exponent, indicating the mechanism of drug release.

In most models, the release mechanism has been attributed to diffusion of the drug from the polymers and under this assumption, a 100 % release of the drug is expected in a certain time. In the desorption model, the authors suggest that release is not controlled by solid-state diffusion, but by the desorption of the drug from pores of the fibers or from the outer surface of the fibers. Thus, only the drug on the fiber and pore surfaces can be released, whereas the drug from the bulk can not be released within the time scales characteristic of the release experiments. The Eq.3.8 is based on a pore model, in which the effective drug diffusion coefficient, D_{eff} is considered and not the actual diffusion coefficient in water, D (with $D_{eff}/D \ll 1$) because desorption from the pore is the rate limiting step and not drug diffusion in water, which is relatively fast.

$$\frac{\mathrm{m_t}}{\mathrm{m_{tot}}} \;=\; \alpha \left[1 - \exp\left(-\frac{\pi^2}{8}\,\frac{\mathrm{t}}{\tau_\mathrm{r}}\right)\right] \tag{3.8}$$

where the porosity factor $\alpha = m_{s0}/(m_{s0} + m_{b0}) < 1$, with $\mathrm{m_{s0}}$ and $\mathrm{m_{b0}}$ being the initial amount of drug at the fiber surface and the initial amount of drug in the fiber bulk, respectively; m_t is the drug amount released at time t, while the total initial amount of drug in the fiber is $m_{tot} = m_{s0} + m_{b0}$ and τ_r is the characteristic time of the release process (Srikar et al. [2008]).

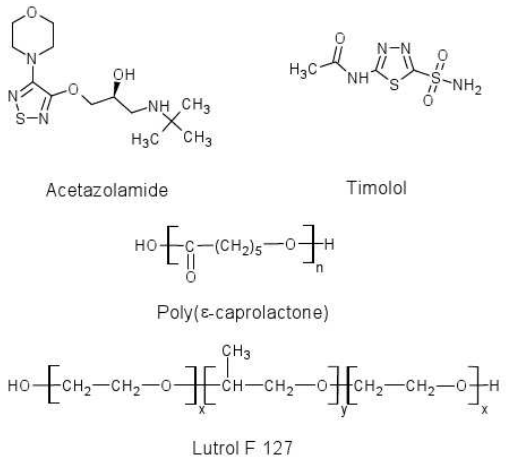

Figure 3.1: Chemical structures

3.2.7 Statistics

All values are presented as mean (n=3) and standard error of the mean (SEM). Linear regression analysis was performed using OpenOffice.org Calc 3.1 (Openoffice), while non-linear regression was done using the regression module of SigmaPlot 10 (SigmaPlot). Adjusted R^2 ($AdjR^2$) was calculated instead of R^2 to evaluate goodness of fit for the two equations that have different number of model parameters.

3.3 Results and discussion

3.3.1 Fiber mat crystallinity, drug solubilitity in polymer and drug state

In this work, two drugs, timolol maleate (pk_a= 3.9, experimental logP= 1.2, experimental water solubility= 2.74 mg/ml (Timolol)) and acetazolamide (pk_a=7.2, experimental logP= -0.26, experimental water solubility= 0.98 mg/ml (Acetazolamide)) with the chemical structures shown in Fig. 3.1 were chosen because of different hydrophilic/hydrophobic character that would allow us to understand how the interactions between the drug and polymers contribute to drug release. Thus, as a measure of interaction, the drug solubility in polymers was determined and the obtained results are presented in Table 3.1. Moreover, the drug solubility is expected to influence the loading and the state of the drug in the fibers. Thus, fibers with low and high drug loadings (see Table 3.4) were prepared corresponding to drug percentages below and above the drug solubility limit, respectively.

Sample	Drug solubility (%)		Rel. degree of crystallinity (%)	
	Timolol maleate	Acetazolamide	Timolol maleate	Acetazolamide
PCL	4.48 (1.11)	16.53 (2.1)	54.39	54.59
25/75 Lu/PCL	5.14 (0.94)	15.94 (4.81)	54.71	59.55
50/50 Lu/PCL	6.97 (1.86)	14.81 (0.8)	64.01	59.89
Lu	8.34 (1.54)	11.25 (3.92)		

Table 3.1: Drug solubility in polymer

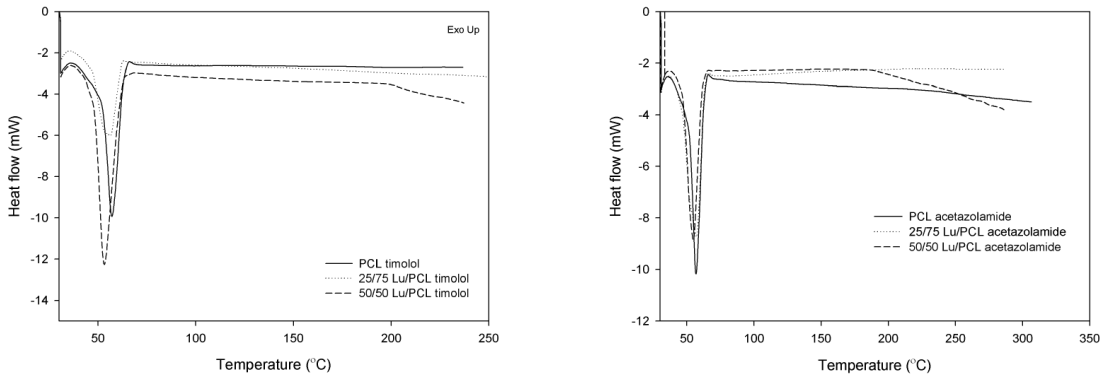

(a) (b)

Figure 3.2: DSC curves of fiber mats. a) low timolol loading and b) low acetazolamide loading

It was observed that acetazolamide had higher solubility in all fibers when compared to timolol maleate probably because of enhanced interaction with the hydroxyl/carboxyl groups of the polymers (the chemical structures are shown in Fig. 3.1). Furthermore, a tendency of increase in solubility was noticed when PCL ratio is increased. On the other hand, timolol is more hydrophilic, therefore a higher solubility is expected in the fibers that contain more Lu and are more hydrophilic, which is the case of 50/50 Lu/PCL (Natu et al. [2008]). An opposite trend was observed for timolol maleate when an increase in solubility was obtained with decrease in PCL content. We will discuss in section 3.3.4 how the solubility affects the drug release.

Polymer crystallinity is known to play an important role in determining degradability, water and drug release because the bulk crystalline phases are more inaccessible to water. The polymers used in this work are semi-crystalline and the obtained fibers are expected to be semi-crystalline too. DSC analysis confirmed this hypothesis showing a clear melting peak in all fibers (PCL melts at 65.1 °C and Lu melts at 59.4 °C). The relative degree of crystallinity of drug loaded fibers is presented in Table 3.1, where it can be seen that the fibers showed similar crystallinity values regardless the type of loaded drug. Another important fact was

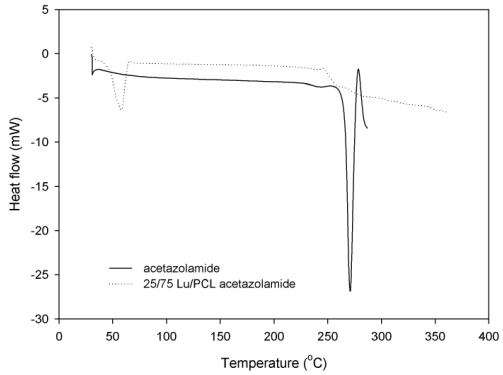

Figure 3.3: DSC curves of fiber mats with high acetazolamide loading and pure drug

that the drug appeared to be in amorphous state in fibers with low drug loadings as proven by the absence of drug melting peak in Fig. 3.2(a) and Fig. 3.2(b) (acetazolamide melts at 271.0 °C, while timolol maleate melts at 205.6 °C). In fibers with high loadings, part of the drug was in crystalline form as confirmed by morphological analysis (in the DSC scans of these sample (Fig. 3.3), there is a broad peak possibly corresponding to drug melting, that is unfortunately masked by fiber degradation process that starts at around 250 °C).

3.3.2 Morphological analysis and drug mapping

The morphology of the fibers with low drug loadings as function of composition is presented in Fig. 3.4, while the calculated fiber diameters are shown in Table 3.2. There was a slight variation in fiber diameter as a function of loaded drug and a more significant one with respect to fiber composition. Morphological differences between samples loaded with the two drugs above or below the solubility limit were also assesed by SEM analysis. In Fig.3.5(a) and Fig. 3.5(c) surface and cross-section images of fibers that contain acetazolamide above solubility limit are shown. As the loaded mass of drug was above the solubility limit in the polymer, the drug was expected to be in crystalline form as confirmed by the images where drug crystals were visible outside or inside the fibers. On the other hand, no crystals were observed in the fibers that contain drug in low loadings (Fig.3.4) suggesting that the drug was in amorphous state in the fibers in agreement with DSC analysis results.

SEM coupled with elemental analysis was performed in order to assess the drug distribution inside the fiber mats. It was seen that both surface and cross-section showed relatively homogeneous drug distribution regardless of composition or type of loaded drug (Fig. 3.5(b) to Fig. 3.6(d)).

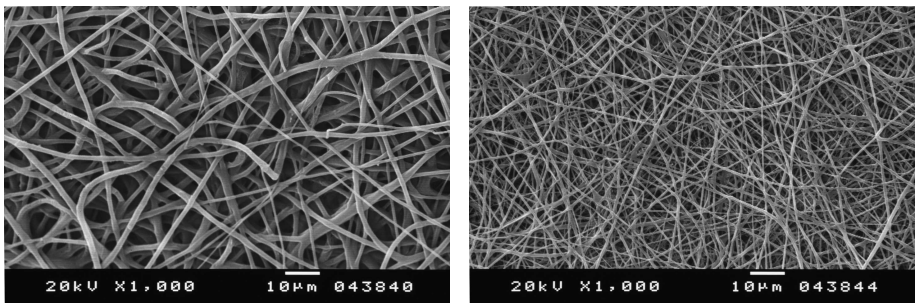

(a) (b)

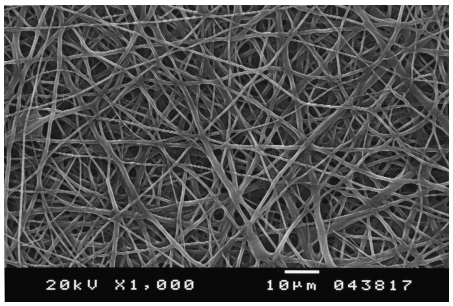

(c)

Figure 3.4: SEM images of fibers with low drug loadings. a) PCL with timolol; b) 50/50 Lu/PCL with timolol; c) 25/75 Lu/PCL with acetazolamide

Sample	Drug	d (μm)
PCL	timolol	1.59 (0.36)
PCL	acetazolamide	0.71 (0.45)
25/75 Lu/PCL	timolol	1.01 (0.20)
25/75 Lu/PCL	acetazolamide	0.87 (0.45)
50/50 Lu/PCL	timolol	0.56 (0.11)
50/50 Lu/PCL	acetazolamide	0.55 (0.12)

Table 3.2: Fiber diameters

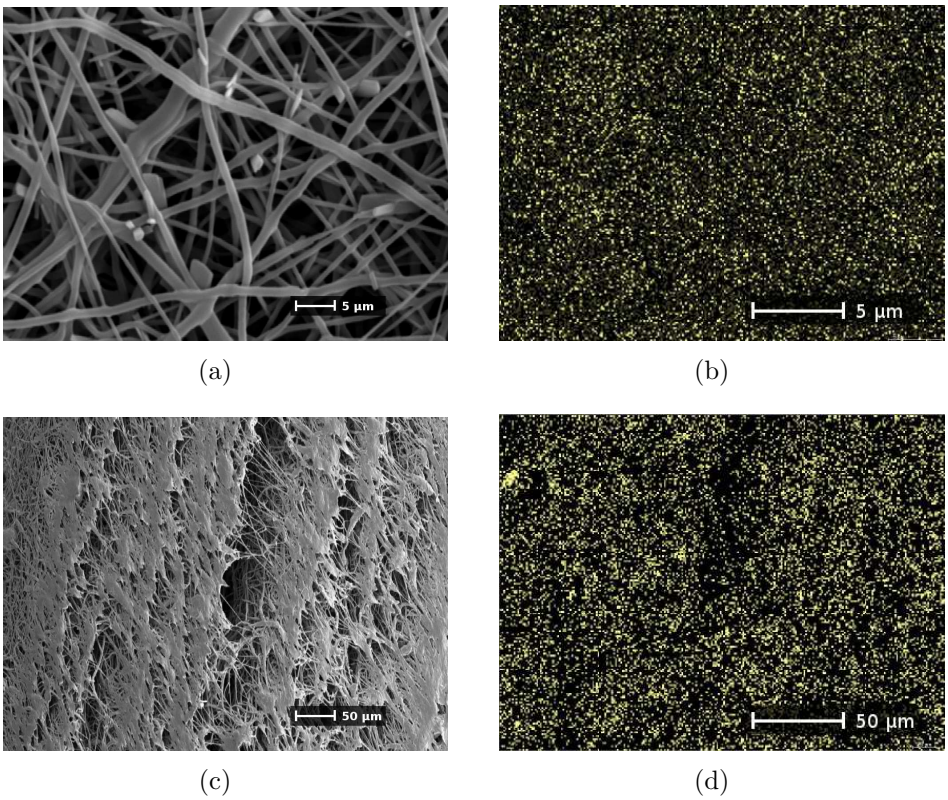

(a) (b)

(c) (d)

Figure 3.5: SEM of high acetazolamide content 25/75 Lu/PCL fibers and sulphur mapping. a) Surface view; b) Surface mapping; c) Cross-section view; d) Cross-section mapping

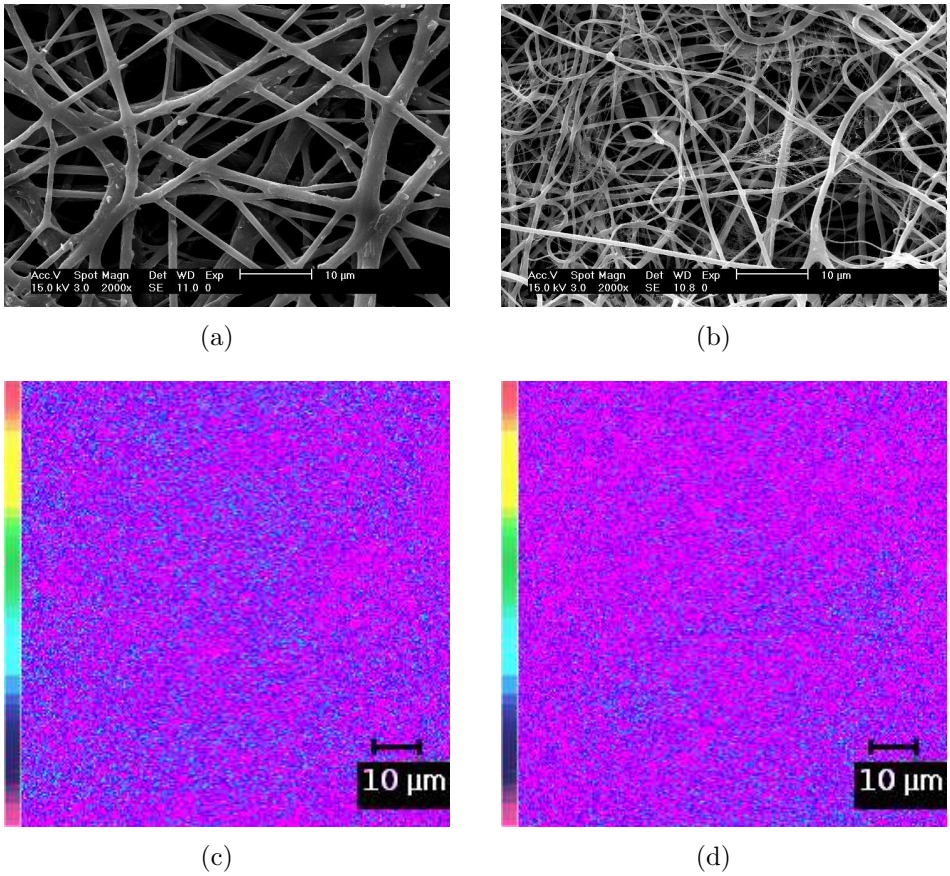

(a) (b)

(c) (d)

Figure 3.6: SEM of high timolol content fibers and sulphur mapping. a) PCL, surface view; b) 25/75 Lu/PCL, surface view; c) PCL, surface mapping; d) 25/75 Lu/PCL, surface mapping

Sample	Contact angle (deg)
PCL	123.18 (0.98)
25/75 Lu/PCL	18.28 (4.07)
50/50 Lu/PCL	16.25 (2.16)

Table 3.3: Static contact angle with water

3.3.3 Swelling and mass loss

The fiber mats are supposed to function in an aqueous environment, so their properties in the presence of water have to be known. In Table 3.3, the values of the water contact angles are given for the different fibers. PCL fibers were highly hydrophobic, while the bicomponent fibers were highly hydrophilic. These results were surprising since in a previous work films with the same compositions presented contact angles in the range 50-62 degrees (Natu et al. [2008]). Water contact angle is determined by both chemical structure and surface morphology. In general, fiber mats have a rougher surface morphology when compared to films and as a result they present higher contact angle than the films made of the same polymers (Kang et al. [2008]). It seems this is the case of PCL that showed an increase in water contact angle from 62 for films to 123 for fibers. In contrast, the bicomponent fibers presented much lower contact angles probably because of a preferential arrangement of Lu (that is very hydrophilic) towards the margin of the fibers. Lu has a lower molecular weight than PCL and higher molecular mobility and consequently it migrates to the regions of highest shear rate (at the walls of the needle). The higher viscosity component (PCL) occupies mostly the center of the fiber (Wei et al. [2006]).

Consequently, PCL fibers absorbed water gradually (see Fig. 3.7(a)) because the fibers were hydrophobic and semi-crystalline, hindering the water penetration inside the fiber mat, while the bicomponent fibers presented a sudden increase in water content during the first day (79.0 % for 50/50 Lu/PCL and 68.5 % for 25/75 Lu/PCL), followed by a constant value thereafter as Lu content in the fiber was diminished due to dissolution.

As observed in the mass loss plot (Fig. 3.7(b)), there was an initial increase in mass loss for bicomponent fibers (42.5 % for 50/50 Lu/PCL and 16.6 % for 25/75 Lu/PCL), while PCL fibers did not show almost any mass loss (0.45 %). Mass loss of PCL is detectable only after the molecular weight reaches a value of 10000 g/mol (Hglund et al. [2007]) and thus the initial high mass loss of the bicomponent fibers can only be attributed to the dissolution of Lu as the sample with higher Lu content had the highest mass loss.

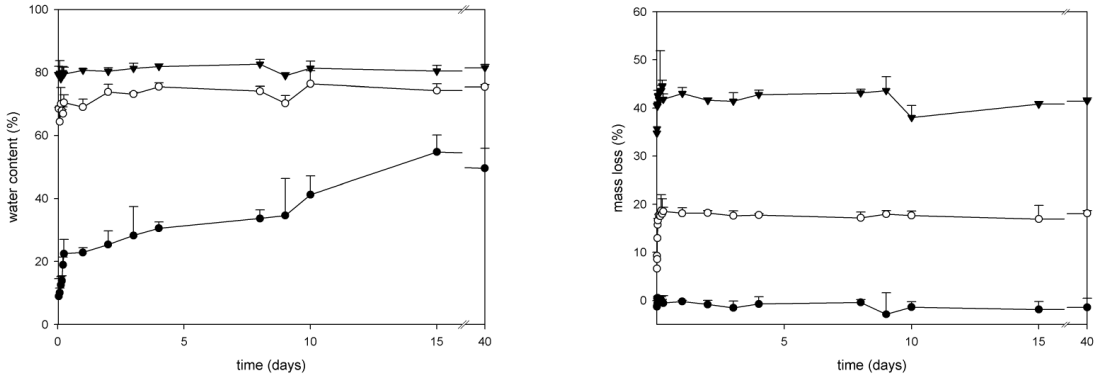

(a) (b)

Figure 3.7: a) Fibers water uptake and b) mass loss, (•) PCL, (○) 25/75 Lu/PCL, (▼) 50/50 Lu/PCL

The morphology of aged fibers (immersed in PBS during 3 days) was also investigated in order to determine the change in fiber structure. In Fig. 3.8(a), it can be noticed the smooth surface of the fibers, while in Fig. 3.8(b) pores were observed that were formed due to the dissolution and leaching of Lu. A different appearance was shown by 25/75 Lu/PCL fiber mat (Fig. 3.8(d)), where the fibers appeared more wrinkled in comparison with the initial ones and no pores were visible, probably because of lower Lu content.

3.3.4 Drug release

We previously showed how the fiber morphology and drug deposition were affected by the drug state in the fibers: when drug was in amorphous state, it was incorporated inside the fibers, while the drug present in amounts above the solubility limit crystallized inside and on the fiber surface (as shown in Fig. 3.5(a)). In Fig. 3.9(a) and Fig. 3.9(b), the cumulative percentage of released acetazolamide and timolol maleate from fibers with low drug content is presented, while in Fig. 3.10, the released drug for fibers with high loadings is shown. It was noticed that fibers with high drug loading presented burst release in contrast with low drug content fibers that showed a more sustained release. The former contained drug crystals at the fiber surface or inside the fibers that were not totally encapsulated and were instantaneously "released", implying that the predominant mechanism of release was drug dissolution. On the other hand, in the low loadings fibers, the drug was amorphous and dissolved in the fiber, decreasing burst. These findings were in agreement with another study where bicomponent fibers loaded with 25% drug (by weight) showed burst release as opposed to 5% drug fibers (Kenawy et al. [2002]) that did not, suggesting that the drug state can control the burst extent.

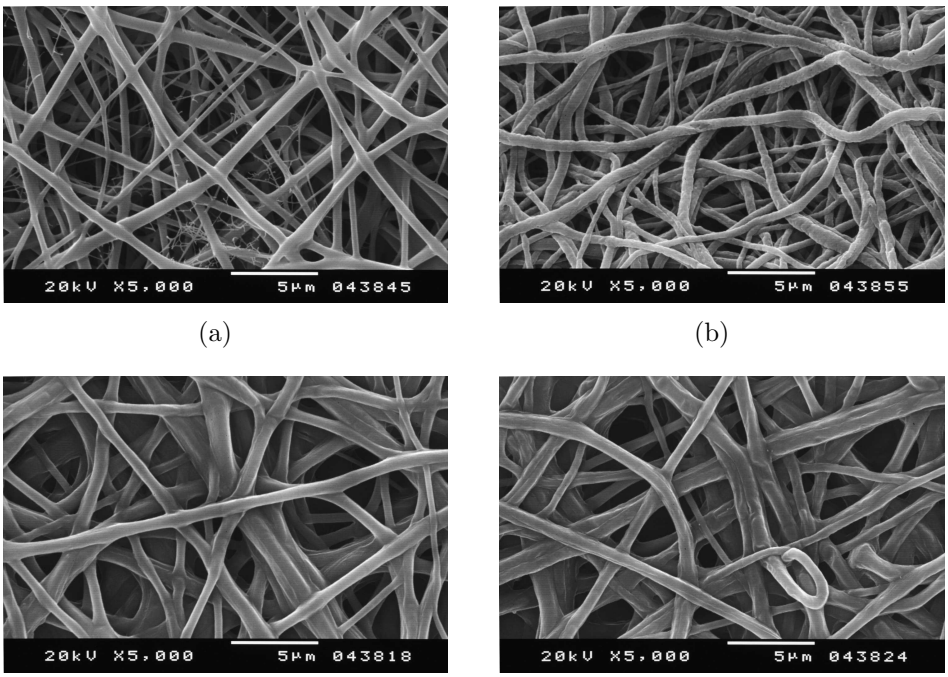

(a) (b)

(c) (d)

Figure 3.8: SEM images of fibers. a) initial 50/50 Lu/PCL, b) 50/50 Lu/PCL aged, c) initial 25/75 Lu/PCL, d) 25/75 Lu/PCL aged

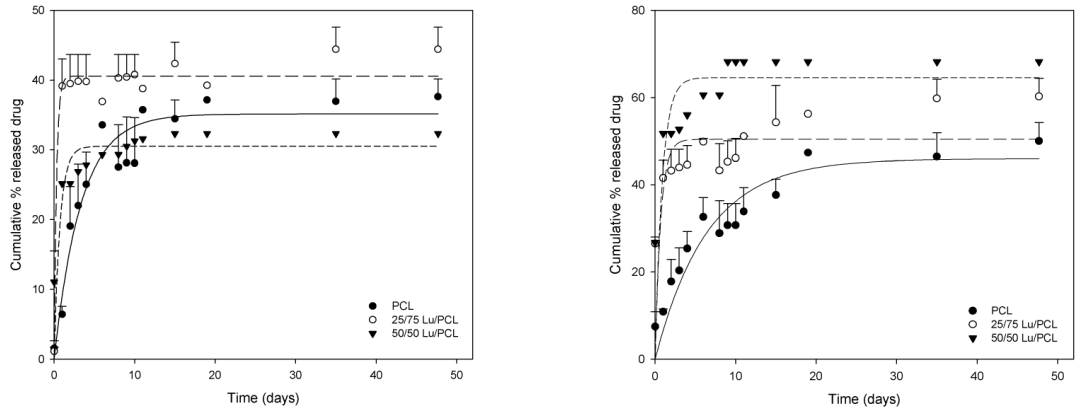

(a) (b)

Figure 3.9: Drug release a) low loadings fibers with acetazolamide, b) low loadings fibers with timolol maleate (solid and dashed lines corresponding to non-linear fit of Eq.3.8)

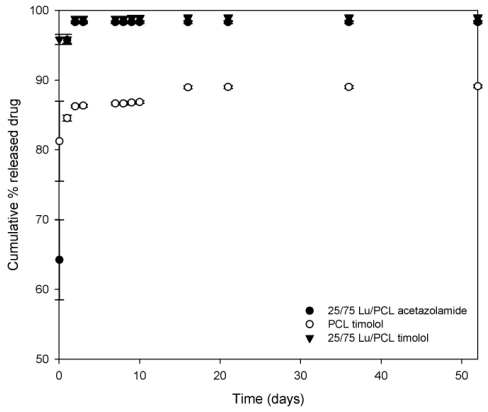

Figure 3.10: Drug release from high loadings fibers

In Table 3.4, the results of non-linear regression are presented. The objective behind fitting these equations to the release data was to understand the underlying phenomena involved in the drug release mechanism. The parameters a_0, α and k define the burst stage and the bigger values they have, the higher extent of burst. On the other hand, τ and n indicate the magnitude of the drug desorption/diffusion stage and the higher values they have, more sustained is the release.

Drug solubility in polymer as well as drug solubility in solution are important as they control the partitioning of the drug from the polymer toward the elution medium. For the same type of fibers, higher percentages of timolol maleate were released in comparison with acetazolamide (for example, in the case of PCL fibers, α=45.96 (2.92) for timolol and α=35.14 (1.43) for acetazolamide). This can be explained by the combined effect of lower polymer solubility and higher water solubility of timolol maleate in contrast with acetazolamide that has higher polymer solubility and lower water solubility. The compatibility between drug and polymer is indeed important as it ensures sustained release during drug diffusion from the polymer (Zeng et al. [2005b]), when the drug is completely encapsulated and dissolved in the fiber.

Fiber composition influenced the release kinetics as drug was released in a more sustained manner from PCL fibers (α=45.96 (2.92) and k=11.51 (3.23) for timolol) than from bicomponent fibers regardless of the drug type (α=50.41 (2.95) and k=12.58 (2.72) for 25/75 Lu/PCL with timolol, while α=64.60 (2.99) and k=25.97 (4.09) for 50/70 Lu/PCL with timolol). Certainly, as erosion was very fast (see section 3.3.3), the drug was released faster from bicomponent fibers than from the hydrophobic PCL fibers that released the drug at the pace dictated by water uptake.

It was observed that a steady state was attained (after approximately 10 days for

bicomponent fibers and after 20 days for PCL fibers) without total release of loaded drug (cumulative release percentages significantly smaller than 100 %). There is a fraction of the drug that is desorbed from the fiber and then diffuses out through the water filled pores, while another portion of the drug encapsulated probably in crystalline areas (and inaccessible to water) can only be released by polymer degradation (which is insignificant during the time scale of release experiment) (Srikar et al. [2008], Tzafriri [2000]). This was not the case for the high drug loading fibers where release was almost complete in the time frame of the experiment. At high loadings, when a significant amount of drug was in crystalline form, only a small portion of drug was trapped (approximately 10 % in the case of PCL, see Fig. 3.10). As drug was in crystalline state (with crystal dimensions between 1 to 6 μm), additional regions of macroporosity were created after drug dissolution besides those created by water uptake and polymer erosion, increasing surface area and enhancing drug release. Thus, the state of the drug in the fiber has an important part in further controlling release kinetics.

Sample, drug	Loading (%, w/w)	Desorption model			Power law			
		α	τ (days)	Adj R^2	a_0	k (day^{-n})	n	Adj R^2
PCL, timolol	0.88 (0.01)	45.96	7.94	0.86	5.08	11.51	0.37	0.92
		(2.92)	(0.03)		(3.63)	(3.23)	(0.06)	
25/75 Lu/PCL, timolol	0.86 (0.02)	50.41	0.87	0.00	26.93	12.58	0.26	0.90
		(2.95)	(0.76)		(2.71)	(2.72)	(0.05)	
50/50 Lu/PCL, timolol	0.88 (0.04)	64.60	1.10	0.33	26.34	25.97	0.15	0.90
		(2.99)	(0.40)		(3.74)	(4.09)	(0.03)	
PCL, timolol	7.60 (0.32)	87.29	0.02	0.55				
		(0.46)	(6.51)					
25/75 Lu/PCL, timolol	6.99 (0.19)	98.55	0.01	0.40				
		(0.27)	(8.66)					
PCL, acetazolamide	1.24 (0.28)	35.14	4.11	0.92	0.00	17.09	0.24	0.82
		(1.43)	(0.05)		(4.76)	(4.88)	(0.06)	
25/75 Lu/PCL, acetazolamide	1.55 (0.60)	40.59	0.37	0.96	1.16	36.60	0.03	0.98
		(0.62)	(1.48)		(1.66)	(1.92)	(0.01)	
50/50 Lu/PCL, acetazolamide	1.16 (0.20)	30.50	0.91	0.54	10.99	14.49	0.12	0.96
		(1.16)	(0.46)		(1.06)	(1.18)	(0.02)	
25/75 Lu/PCL, acetazolamide	12.67 (0.35)	98.08	0.05	0.99				
		(0.24)	(0.59)					

Table 3.4: Drug loading and model parameters determined by non-linear regression

The release kinetics and regression analysis results implied a three stage release mechanism, with different stages depending on fiber composition: the first stage was drug dissolution (mainly because of crystalline drug that is not totally encapsulated in the fibers), the second was drug desorption and subsequent diffusion through water-filled pores (Miyajima et al. [1997]) (created either due to Lu leaching or water uptake in the amorphous regions of PCL), while the last stage was controlled by polymer degradation.

3.4 Conclusions

Fibers were obtained by electrospinning of two semi-crystalline (co)polymers, PCL and Lu, and were loaded with two drugs, acetazolamide and timolol maleate, in concentrations below and above the drug solubility limit in polymer. The PCL fibers were semi-crystalline and hydrophobic, while the bicomponent fibers were semi-crystalline and hydrophilic. Thus, the bicomponent fibers showed high water uptake and extensive erosion during the first day, whereas PCL fibers swelled gradually, without any significant erosion during the time frame of the release experiment. Morphological examination showed that fibers with high drug loadings (above solubility limit) had drug crystals inside and outside the fibers, while fibers with low drug content (below solubility limit) had drug encapsulated in amorphous form. These results were further supported by DSC analysis, where thermograms of low drug loading fibers didn't show the peak corresponding to drug melting.

The high loadings fibers showed higher extent of burst and shorter periods of release (almost 90 % of drug released after 2 days) than low drug content fibers (around 50 % of drug released after 52 days), suggesting that loading and drug encapsulation in either crystalline or amorphous form are interrelated and control the release rate, especially in the burst stage. Thus, in long term release applications where high amounts of loaded drug are desirable, a compromise must be found in order to balance the loading and release rate that seem to vary in opposite directions according to the present study.

Total release was not attained at low loadings, suggesting that the last stage of the release kinetics was polymer degradation limited. Moreover, it was observed that timolol maleate was released faster than acetazolamide in the same type of fibers and similar loadings, indicating that drug solubility in polymer influenced the partition of drug between polymer and elution medium. This could offer a mean to control the total percentage of released drug by choosing the best pair of polymer and drug, although some applications require very specific material properties that may not match in terms of compatibility the drugs used in the

treatment of the targeted diseases. Finally, the modelling of release data implied a three stage release mechanism: a dissolution stage (mainly produced by crystalline drug that was not properly encapsulated), a drug desorption coupled to diffusion stage, followed by polymer degradation control stage. The fiber composition also controlled drug release, since release was slower from PCL fibers than from bicomponent fibers regardless of the drug type. By choosing the polymers making up the bicomponent fibers and their ratio, the magnitude of the dissolution or diffusion stage can be controlled, attaining the targeted short or long term release application, respectively.

Bibliography

Acetazolamide. Drug card for acetazolamide (DB00819), drugbank database. `http://www.drugbank.ca/drugs/DB00819`, 2010.

S. Agarwal, J.H. Wendorff, and A. Greiner. Use of electrospinning technique for biomedical applications. *Polymer*, 49:5603–5621, 2008. [DOI:10.1016/j.polymer.2008.09.014].

ATHAS. The Advanced THermal Analysis System (ATHAS) data bank. `http://athas.prz.edu.pl/Default.aspx?op=db`, 2010.

M. Bogntizki, T. Frese, M. Steinhart, A. Greiner, and J.H. Wendorff. Preparation of fibers with nanoscaled morphologies: Electrospinning of polymer blends. *Polym. Eng. Sci.*, 41:982–989, 2001. [DOI:10.1002/pen.10799].

G. Buschle-Diller and Z. Xie. Electrospun poly(D,L-lactide) fibers for drug delivery: The influence of cosolvent and the mechanism of drug release. *J. Appl. Polym. Sci.*, 115:1–8, 2009. [DOI:10.1002/app.31026].

G. Buschle-Diller, J. Cooper, Z. Xie, Y. Wu, J. Waldrup, and X. Ren. Release of antibiotics from electrospun bicomponent fibers. *Cellulose*, 14:553–562, 2007. [DOI:10.1007/s10570-007-9183-3].

C.L. Casper, N. Yamaguchi, K.L. Kiick, and J.F. Rabolt. Functionalizing electrospun fibers with biologically relevant macromolecules. *Biomacromolecules*, 6: 1998–2007, 2005. [DOI:10.1021/bm050007e].

C.L. Casper, W. Yang, M.C. Farach-Carson, and J.F. Rabolt. Coating electrospun collagen and gelatin fibers with perlecan domain I for increased growth factor binding. *Biomacromolecules*, 8:1116–1123, 2007. [DOI:10.1021/bm061003s].

S.Y. Chew, J. Wen, E.K. Yim, and K W. Leong. Sustained release of proteins from electrospun biodegradable fibers. *Biomacromolecules*, 6:2017–2024, 2005. [DOI:10.1021/bm0501149].

W. Cui, X. Li, X. Zhu, G. Yu, S. Zhou, and J. Weng. Investigation of drug release and matrix degradation of electrospun poly(D,L-lactide) fibers with paracetanol inoculation. *Biomacromolecules*, 7:1623–1629, 2006. [DOI:10.1021/bm060057z].

A. Hglund, M. Hakkarainen, and A.-C. Albertsson. Degradation profile of poly(ε-caprolactone)-the influence of macroscopic and macromolecular biomaterial design. *J. Macromolecular Sci. Part A*, 44:1041–1046, 2007. [DOI:10.1080/10601320701424487].

Z.-M. Huang, Y.-Z. Zhang, M. Kotaki, and S. Ramakrishna. A review on polymer nanofibers by electrospinning and their applications in nanocomposites. *Comp. Sci. Tech.*, 63:2223 – 2253, 2003. [DOI:10.1016/S0266-3538(03)00178-7].

M.T. Hunley and T.E. Long. Electrospinning functional nanoscale fibers: a perspective for the future. *Polym. Int.*, 57:385–389, 2008. [DOI:10.1002/pi.2320].

ImageJ. ImageJ, image processing and analysis in java. `http://rsbweb.nih.gov/ij/"`, 2010.

V. Kalra, P.A. Kakad, S. Mendez, T. Ivannikov, M. Kamperman, and Y.L. Joo. Self-assembled structures in electrospun poly(styrene-block-isoprene) fibers. *Macromolecules*, 39:5453–5457, 2006. [DOI:10.1021/ma052643a].

M. Kang, R. Jung, H.-S. Kim, and H.-J. Jin. Preparation of superhydrophobic polystyrene membranes by electrospinning. *Colloids and Surfaces A: Physicochemical and Engineering Aspects*, 313-314:411–414, 2008. [DOI:10.1016/j.colsurfa.2007.04.122].

E.-R. Kenawy, G.L. Bowlin, K. Mansfield, J. Layman, D.G. Simpson, E H. Sanders, and G.E. Wnek. Release of tetracycline hydrochloride from electrospun poly(ethylene-co-vinylacetate), poly(lactic acid), and a blend. *J. Control. Release*, 81:57–64, 2002. [PubMed:11992678].

J.A. Lee, K.C. Krogman, M. Ma, R.M. Hill, P.T. Hammond, and G.C. Rutledge. Highly reactive multilayer-assembled TiO2 coating on electrospun polymer nanofibers. *Adv. Mater.*, 21:1252–1256, 2009. [DOI:10.1002/adma.200802458].

S.J. Lee, J.J. Yoo, G.J. Lim, A. Atala, and J. Stitzel. In vitro evaluation of electrospun nanofiber scaffolds for vascular graft application. *J. Biomed. Mater. Res. A*, 83:999–1008, 2007. [DOI:10.1002/jbm.a.31287].

Z. Ma, M. Kotaki, and S. Ramakrishna. Surface modified nonwoven polysulphone (psu) fiber mesh by electrospinning: A novel affinity membrane. *J. Membr. Sci.*, 272:179 – 187, 2006. [DOI:10.1016/j.memsci.2005.07.038].

M.J. McClure, S.A. Sell, C.E. Ayres, D.G. Simpson, and G.L. Bowlin. Electrospinning-aligned and random polydioxanone-polycaprolactone-silk fibroin-blended scaffolds: geometry for a vascular matrix. *Biomed. Mater.*, 4:055010, 2009. [DOI:10.1088/1748-6041/4/5/055010].

M. Miyajima, A. Koshika, J. Okada, M. Ikeda, and K. Nishimura. Effect of polymer crystallinity on papaverine release from poly(L-lactic acid) matrix. *J. Control. Release*, 49:207–215, 1997. [DOI:10.1016/S0168-3659(97)00081-3].

M.V. Natu, M.H. Gil, and H.C. de Sousa. Supercritical solvent impregnation of poly(ε-caprolactone)/poly(oxyethylene-b-oxypropylene-b-oxyethylene) and poly(ε-caprolactone)/poly(ethylene-vinyl acetate) blends for controlled release applications. *J. Supercrit. Fluids*, 47:93–102, 2008. [DOI:10.1016/j.supflu.2008.05.006].

T. Okuda, K. Tominaga, and S. Kidoaki. Time-programmed dual release formulation by multilayered drug-loaded nanofiber meshes. *J. Control. Release*, 143:258–264, 2010. [DOI:10.1016/j.jconrel.2009.12.029].

Openoffice. Openoffice.org, the free and open productivity suite. `http://www.openoffice.org/`, 2010.

N.A. Peppas and L. Brannon-Peppas. Water diffusion and sorption in amorphous macromolecular systems and foods. *J. Food Eng.*, 22:189–210, 1994. [DOI:10.1016/0260-8774(94)90030-2].

Q.P. Pham, U. Sharma, and A.G. Mikos. Electrospun poly(ε-caprolactone) microfiber and multilayer nanofiber/microfiber scaffolds: characterization of scaffolds and measurement of cellular infiltration. *Biomacromolecules*, 7:2796–2805, 2006. [DOI:10.1021/bm060680j].

K. Sawicka and P. Gouma. Electrospun composite nanofibers for functional applications. *J. Nanopart. Res.*, 8:769–781, 2006. [DOI:10.1007/s11051-005-9026-9].

SigmaPlot. Sigmaplot graphing software. `http://www.sigmaplot.com/products/sigmaplot/sigmaplot-details.php`, 2010.

R. Srikar, A. L. Yarin, C.M. Megaridis, A.V. Bazilevsky, and E. Kelley. Desorption-limited mechanism of release from polymer nanofibers. *Langmuir*, 24:965–974, 2008. [DOI:10.1021/la702449k].

P. Taepaiboon, U. Rungsardthong, and P. Supaphol. Drug-loaded electrospun mats of poly(vinyl alcohol) fibres and their release characteristics of four model drugs. *Nanotechnology*, 17:2317, 2006. [DOI:10.1016/j.polymer.2007.11.019].

R.A. Thakur, C.A. Florek, J. Kohn, and B.B. Michniak. Electrospun nanofibrous polymeric scaffold with targeted drug release profiles for potential application as wound dressing. *Int. J. Pharm.*, 364:87–93, 2008. [DOI:10.1016/j.ijpharm.2008.07.033].

Timolol. Drug card for timolol (DB00373), drugbank database. `http://www.drugbank.ca/drugs/DB00373`, 2010.

H. Tsuji and Y. Ikada. Blends of aliphatic polyesters. II. Hydrolysis of solution-cast blends from poly(D,L-lactide) and poly(ε-caprolactone) in phosphate-buffered solution. *J. Appl. Polym. Sci.*, 67:405–415, 1998. [DOI:10.1002/(SICI)1097-4628(19980118)67:3¡405::AID-APP3¿3.0.CO;2-Q].

A. R. Tzafriri. Mathematical modeling of diffusion-mediated release from bulk degrading matrices. *J. Control. Release*, 63:69–79, 2000. [PubMed:10640581].

C.M. Vaz, S. van Tuijl, C.V. Bouten, and F.P. Baaijens. Design of scaffolds for blood vessel tissue engineering using a multi-layering electrospinning technique. *Acta Biomater.*, 1:575–582, 2005. [DOI:10.1016/j.actbio.2005.06.006].

M. Wei, B. Kang, C. Sung, and J. Mead. Core-sheath structure in electrospun nanofibers from polymer blends. *Macromol. Mater. Eng.*, 291:1307–1314, 2006. [DOI:10.1002/mame.200600284].

J. Xie and C.H. Wang. Electrospun micro- and nanofibers for sustained delivery of paclitaxel to treat C6 glioma in vitro. *Pharm. Res.*, 23:1817–1826, 2006. [DOI:10.1007/s11095-006-9036-z].

D.-G. Yu, X.-X. Shen, C. Branford-White, K. White, L.-M. Zhu, and S.W.A. Bligh. Oral fast-dissolving drug delivery membranes prepared from electrospun polyvinylpyrrolidone ultrafine fibers. *Nanotechnology*, 20:055104, 2009. [DOI:10.1088/0957-4484/20/5/055104].

M. Zamani, M. Morshed, J. Varshosaz, and M. Jannesari. Controlled release of metronidazole benzoate from poly(ε-caprolactone) electrospun nanofibers for periodontal diseases. *Eur. J. Pharm. Biopharm.*, 75:179–185, 2010. [DOI:10.1016/j.ejpb.2010.02.002].

J. Zeng, A. Aigner, F. Czubayko, T. Kissel, J.H. Wendorff, and A. Greiner. Poly(vinyl alcohol) nanofibers by electrospinning as a protein delivery system and the retardation of enzyme release by additional polymer coatings. *Biomacromolecules*, 6:1484–1488, 2005a. [DOI:10.1021/bm0492576].

J. Zeng, L. Yang, Q. Liang, X. Zhang, H. Guan, X. Xu, X. Chen, and X. Jing. Influence of the drug compatibility with polymer solution on the release kinetics of electrospun fiber formulation. *J. Control. Release*, 105:43–51, 2005b. [DOI:10.1016/j.jconrel.2005.02.024].

Chapter 4

A poly(ε-caprolactone) device for sustained release of an anti-glaucoma drug

The text that comprises this Chapter was published in the journal *Biomedical Materials* (2011), volume 6, pages 025003 (in press).

Abstract

Implantable dorzolamide loaded disks were prepared by blending poly(ε-caprolactone), PCL with poly(ethylene oxide)-b-poly(propylene oxide)-b-poly(ethylene oxide), Lu. By blending, crystallinity, water uptake and mass loss were modified relative to the pure polymers. Burst was diminished by coating the disks with a PCL shell. All samples presented burst release except PCL-coated samples that showed controlled release during 18 days. For PCL-coated samples, barrier-control of diffusion coupled with partition control from the core slowed down the release, while for 50/50 Lu/PCL-coated samples, the enhancement in porosity of the core diminished partition-control of drug release. Non-linear regression analysis suggested that a degradation model fully describes the release curve considering a triphasic release mechanism: the instantaneous diffusion (burst), diffusion and polymer degradation stages. MTT test indicated that the materials are not cytotoxic for corneal endothelial cells. A good in vitro-in vivo correlation was obtained, with similar amounts of drug released in vitro and in vivo. The disks decreased intraocular pressure (IOP) in normotensive rabbit eyes by 13.0 % during 10 days for PCL-coated and by 13.0 % during 4 days for 50/50 Lu/PCL-coated. The percentages of IOP decrease are similar to those obtained by dorzolamide eyedrop instillation (11.0 %).

4.1 Introduction

Glaucoma is a condition affecting the posterior segment of the eye and major cause of irreversible blindness (Quigley [2005]). Progressive visual loss is associated with elevated intraocular pressure, IOP which damages the optic nerve. Current treatments for glaucoma can be divided into three main modalities: pharmaceutical, laser and surgical. Despite continued advances in laser and filtration surgery, medical therapy still appears to be the primary means by which IOP is controlled (Schwartz and Budenz [2004]). These studies have focused on the role of lowering IOP in the prevention of field loss and optic nerve damage. It was shown that reducing IOP is effective in preventing disease progression in ocular hypertension, primary open angle glaucoma, and even in normal tension glaucoma (Khaw et al. [2004]).

In most glaucoma patients, medical therapy consists of topical eyedrops and oral tablets. Eyedrops present low ocular bioavailability and produce undesired side effects (Amo and Urtti [2008]). A large portion of the drop can be lost due to overflow from the cojunctival sac, while the drop remaining on the ocular surface can be washed away through the nasolacrimal duct, thereby decreasing the amount of the drug that reaches the targeted ocular structures. High systemic bioavailability of ophthalmic drugs can occur due to systemic drug loss, which can be highly dangerous to patients suffering from cardiovascular and/or respiratory diseases (Korte et al. [2002]). Moreover, patients do not use their eyedrops as prescribed. The poor compliance can be due to uncomfortable sensations (Noecker et al. [2004]), as well as difficulty of instillation or forgetfulness (Kulkarni et al. [2008]).

Controlled drug release devices were shown to produce continuous release of drug at predetermined rates which allows the elimination of frequent dosing by the patient, ensures night time medication and provides better patient compliance (Bourges et al. [2006]). Furthermore, therapeutic drug levels are achieved without exposure of ocular tissues to toxic level of drugs. The devices are more economic because smaller amounts of drugs are required to achieve the same effect as eyedrops since these systems release the drugs over extended periods of time.

For topical ocular use, gel forming solutions (Timoptic-XE®, Pilogel®, Azasite®) are already in clinical use. These formulations enhance the drug retention relative to eyedrops and produce increased drug absorption into the eye and reduce dosing frequency (Nanjawade et al. [2007]). However, the duration of drug activity can be increased by hours, not by days or weeks. Other sustained release systems include contact lenses (Costa et al. [2010], Hiratani et al. [2005]), mucoadhesive formulations (Ludwig [2005]), hydrogels (Natu et al. [2007], Anumolu et al. [2009]),

hybrid systems (Barbu et al. [2009]), particulates (Marchal-Heussler et al. [1993], Kaur et al. [2004], Zimmer and Kreuter [1995]), fiber composites (Kashanian et al. [2010]) and ocular inserts (Macoul and Pavan-Langston [1975], Baeyens et al. [2002], Pijls et al. [2007], Sasaki et al. [2003]). Only the latter category is capable of sustained release of drugs during several days. Unfortunately, such ocular inserts generally require patient self-administration and a sufficient degree of manual dexterity. In addition, inadvertent loss of the ocular device due insert movement can occur (Macoul and Pavan-Langston [1975]).

Implantable devices with prolonged action exist on the market or undergoing clinical trials: non-biodegradable implants such as Medidur®, Retisert®, Vitrasert®or biodegradable implants such as Posurdex®. Unfortunately, they were developed for the treatment of diseases that affect the posterior segment of the eye such as diabetic macular edema, uveitis or cytomegalovirus retinitis (Amo and Urtti [2008]) and not glaucoma.

Our long-term goal is to prepare a drug loaded biodegradable implant designed to provide a localized, sustained release of dorzolamide hydrochloride (a carbonic anhydrase inhibitor used to lower IOP) that can be used in the treatment of open-angle glaucoma. The implant will degrade within the site of implantation thereby slowly releasing the drug at the site to be treated until the entire implant will degrade without the need for further surgery. A subconjunctival placement of the implant is simple to perform because of easy access to the implantation area and low vascularization. By delivering controlled amounts of drug, the implant would be highly efficient, increase patient compliance and cost effectiveness.

Polymer blending is a simple process in which specific properties from different polymers can be combined in order to tailor the degradability and the drug release properties (Shen et al. [2000], Lyu et al. [2005]). For the present study, poly(ε-caprolactone), PCL and Lutrol F 127, Lu were selected because they are both biocompatible, biodegradable and they can be easily processed by conventional polymer processing techniques. Moreover, they are commercially available, inexpensive and well characterised polymers. PCL is a slowly degradable polymer, while Lu can be used as a release modulator (Natu et al. [2008, 2010]). Unfortunately, some controlled drug release systems present a burst stage due to surface deposited drug (Natu et al. [2010]), which can be pharmacologically dangerous and economically inefficient. One strategy to diminish/remove burst is through additional polymer coating which can provide a layer/shell that separates the drug in the core of the device and acts as an extra diffusional barrier to drug transport. Moreover, this device is capable of achieving a zero-order drug delivery due to the fact that the drug diffuses through the membrane at a finite, controllable rate (Huang and Brazel

[2001]).

In this work, we studied how crystallinity, water uptake and mass loss are changed by blending and how these new properties influence the drug release and release mechanism. Disks were prepared and coated or used as such in in vitro and in vivo drug release experiments. Non-linear regression analysis using a degradation model and diffusion model was done in order to understand the underlying phenomena involved in the drug release. The implantable drug loaded disks were further evaluated in vivo by measuring the capacity to decrease IOP in normotensive rabbit eyes and compared in terms of performance with available eyedrop treatment (Trusopt®, dorzolamide eydrops).

4.2 Materials and methods

4.2.1 Device preparation

Poly(ε-caprolactone) (PCL, average M_w 65000 g/mol, Sigma-Aldrich) and Lutrol F 127 (Lu, poly(ethylene oxide)-b-poly(propylene oxide)-b-poly(ethylene oxide), 9000-14000 g/mol, 70 % by weight of polyoxyethylene, BASF) films were prepared by solvent casting from acetone (UV grade, Sigma-Aldrich) at 40 °C, using a 15 % w/v total polymer concentration. Films (Lu/PCL: 25/75, 50/50 % w/w) were vacuum dried (37 °C until constant weight) and cut in rectangular pieces and used as such in different characterization tests. The blend 75/25 Lu/PCL was not studied since it dissolves in PBS at 37 °C and thus it is not a good material for the intended application.

Disks with a diameter of 6 mm and a thickness of 1 mm were punched out from dorzolamide hydrochloride (Chemos GmbH) loaded films (2/1 (w/w) polymer/drug, approximately 1 mg of drug in each disc) and then coated by dip-coating in 0.15 g/ml PCL solution or used as such in drug release experiments.

4.2.2 Characterization tests

Dynamic mechanical analysis (DMA) was performed on polymer films (10 mm×5 mm×0.1 mm, lwt) using a Tritec 2000 DMA (Triton Technology) equipment in tension mode in multifrequency, with a heating rate of 2 °C/min from -150 to 100 °C, using liquid nitrogen. The glass transition temperature (T_g) was determined at the frequency-dependent peak in $tan\ \delta$ plot (with $tan\ \delta = E''/E'$, where E'' and E' are the loss and storage modulus, respectively) and accompanied by a decrease in the loss modulus value.

Differential scanning calorimetry (DSC) and thermogravimetric analysis (TGA) were carried out using a SDT Q 600 equipment (TA Instruments). Nitrogen at a rate of 100 mL/min was used as purge gas. Samples with masses between 5 and 10 mg were heated until 600 °C, at a heating rate of 10 °C/min. The degradation temperature (T_d) was determined at the onset point of the TGA plot. The relative crystallinity of the films was calculated as previously described considering the melting enthalpy of 100 % crystalline PCL (ATHAS) and 100 % crystalline Lu (Natu et al. [2010]).

X-ray diffraction was performed using Philips X'Pert diffractometer employing Co radiation. A scan range between 10° and 50° and a step of 0.04°/s was used to obtain the diffraction patterns. Samples were analysed as films or as powders in the case of constitutive polymers. The degree of crystallinity was calculated as the percentage of the scattered intensity of the crystalline phase over the scattered intensity of the crystalline and amorphous phases. The decomposition of crystalline and amorphous intensity profiles from the total intensity profile was accomplished by a curve fitting technique using a Voigt function (Peak fitting module, Origin v.6 software) (Cao and Billows [1999]).

4.2.3 Water uptake and degradation

Water uptake and mass loss experiments were performed as previously reported (Natu et al. [2010]). The water uptake was calculated using Eq.4.1.

$$Water\ content\,(\%) = \frac{M_t - M_i}{M_t} \times 100 \tag{4.1}$$

where M_t denotes the mass of the wet sample at immersion time t and M_i denotes the initial mass of the sample.

The percentage of mass loss was calculated using Eq.4.2.

$$Mass\ loss\,(\%) = \frac{M_i - M_d}{M_i} \times 100 \tag{4.2}$$

where M_i denotes the initial mass and M_d is the mass of the dried sample after a certain immersion time.

4.2.4 Dorzolamide hydrochloride release

Dorzolamide hydrochloride release was performed as previously reported (Natu et al. [2010]) in 10 ml PBS, with the drug concentration determined by UV spectroscopy at 254 nm (Jasco V-650 Spectrophotometer). The percentage of

released drug was calculated using Eq.4.3.

$$Released\,drug\,(\%) \;=\; \frac{M_t}{M_{total}} \times 100 \tag{4.3}$$

In Eq. 4.3, M_t is mass of dorzolamide hydrochloride released at time t and M_{total} is the total mass of loaded drug (that was determined by dissolving the discs in 4/1 (v/v) THF/methanol solution and adding this residual drug mass to the released mass of drug).

The power law equation (Eq.4.4) was fit to the release data in order to determine the release mechanism (Natu et al. [2010]).

$$\frac{M_t}{M_{total}} \;=\; k\,t^n \tag{4.4}$$

In Eq. 4.4, M_t/M_{total} is the fractional release of the drug, k is the kinetic constant and n is the release exponent, indicating the mechanism of drug release.

An alternative model (Eq.4.5) based on polymer degradation control of drug release was used to fit the release data. In this model, two pools of drug are considered: a pool of mobile drug which readily diffuses out of the matrix upon immersion in an aqueous medium and a pool of immobilized drug which can diffuse only after matrix degradation (Tzafriri [2000]). This model can be applied to slow-degrading polymers such as PCL due to the fact that polymer degradation is much slower than drug diffusion and as such it is the rate limiting step for immobilized drug transport.

$$M(\tau) \;=\; A_0 + |\Omega|\,S_0\,(1 - \exp\,(-\tau)),\; \bar{\alpha}_{lmn}^{-1} \to 0 \tag{4.5}$$

In Eq. 4.5, A_0 is the load of the mobile active agent, S_0 is the initial concentration of immobilized active agent, τ is the dimensionless time and is defined by $\tau = \mu\,t$ (μ is the degradation rate constant) and Ω is the geometrical factor. The model parameters were determined by non-linear regression and the goodness of the fit was assessed.

4.2.5 Biocompatibility evaluation

Corneal endothelial cells were obtained and cultured as previously reported (Natu et al. [2007]). For all the experiments, the samples were sterilised using UV radiation for 30 minutes and preconditioned in culture media for 24 hours prior to seeding. Second passage endothelial corneal cells were seeded, at a density of 200000 cells per well, into a 96 well glass-bottom plate (P96G-0-5-F, MatTek Corp.

USA) containing the biomaterials. The plate was incubated at 37°C, under carbon dioxide (5 %) atmosphere, for 24 hours. After the incubation, the mitochondrial redox activity was assessed through the reduction of the MTT reagent (3-[4,5-dimethyl-thiazol-2-yl]-2,5-diphenyltetrazolium bromide, MTT colorimetric assay kit, ATCC). 50 μl of MTT (5 mg/ml PBS) were added to each sample and incubated for 4 h at 37°C, under carbon dioxide (5 %) atmosphere. Medium was aspirated and the culture cells were treated with 50 μl of isopropanol/HCl (0.04 N) for 90 minutes. The absorbance at 570 nm was measured using a Biorad Microplate Reader Benchmark. Wells containing cells in culture medium without biomaterials were used as negative control.

4.2.6 In vivo performance - Intraocular pressure measurement

New Zealand white rabbits, males and females, with an age of 10 weeks and a weight 2.6± 0.3 kg were used in animal experiments in agreement with European Union Council Directive 86/609/EEC regarding the protection of animals used for experimental and other scientific purposes (86/609/EEC, 2007/526/EC). Animal experimentation was approved by the Ethics Committee of the University of Coimbra (document reference: 078-CE-10). Corneal thickness (349.2±15.4 μm) was determined with a pachymeter (PachPen, Accutome). Animals were housed under a 12-hour light, 12-hour dark cycle with free access to food and water. Prior to the beginning of the experiments, the rabbits were accustomed to the laboratory environment, handling and measurement procedure in order to reduce stress and encourage cooperation during measurement routine.

Animals were anesthetized with intramuscular ketamine (50 mg/kg, Ketalar injectable solution 50 mg/ml, Pfizer) and topical oxybuprocaine hydrochloride (Anestocil eyedrops 4 mg/ml, Edol). A small incision was made under the conjunctiva, forming a pocket in the upper part of the eyeball at 5 mm from the limbus region. The disks were introduced in the subconjunctival pocket and carefully covered by the conjunctiva, without any sutures. Azithromycin eyedrops (Azyter, 15 mg/g, Théa) were instilled during some days in order to treat eyes that presented symptoms of conjunctivitis. The animals were divided in two groups: group 1 received drug loaded polymer disks (the right eye contained the drug loaded disk, while the left had the control disk) and group 2 was submitted to Trusopt®eyedrops (dorzolamide hydrochloride 2 %, Chibret) treatment (1 drop three times a day in the right eye, while the left eye received a drop of balanced salt solution, BSS sterile solution, Alcon).

The IOP measurement was performed using a Schiotz tonometer, every 3 hours during the first 10 hours, followed by once or twice a day (morning and evening) measurements thereafter. During the measurement, the animal was kept in prone position, one to two drops of oxybuprocaine hydrocholoride was applied on the surface of the eye, the tonometer was placed perpendicularly on the cornea and the scale was read.

4.2.7 Statistics

All values are presented as mean and standard error of the mean (SEM). Experiments were performed in triplicates. Statistical analysis (paired T-test, two-tailed, for the IOP results and independent T-test, two-tailed, for the rest of the results) was done using OpenOffice.org Calc 3.1 (Openoffice).

4.3 Results and discussion

4.3.1 Characterization tests

Blend miscibility can influence blend crystallinity, since either co-crystallization of the components takes place or crystallization restriction of one component occurs due to the presence of the second (Ajili and Ebrahimi [2007]). In Table 4.1, the T_g values of the blends are presented. It can be seen that the blends are immiscible and present two T_g probably because as Lu is an amphiphilic copolymer, there is a phase segregation on addition of PCL. PCL will interact more with the polypropylene oxide segment and not with the more hydrophilic polyethylene oxide block. This will cause the appearance of two T_g in the $tan\ \delta$ curve corresponding to a two phase system that replaces the initial one phase system (Chen et al. [2003]).

Sample	T_g (°C)	T_d (°C)	T_m (°C)	X_{rel} (%)	
				XRD	DSC
PCL	-47.5	389.5	65.5	53.6	54.2
25/75 Lu/PCL	-53.2, 49.3	367.8	65.6	54.8	51.4
50/50 Lu/PCL	-54.0, 44.1	341.3	62.8	56.2	57.7
100/0 Lu/PCL	-58.2	358.8	59.4	56.8	60.5

Table 4.1: Thermo-mechanical properties

Polymer crystallinity is known to play an important role in determining degradability, water and drug permeability because the bulk crystalline phases are more inaccessible to water (Tsuji and Ikada [1998]). PCL and Lu are semi-crystalline

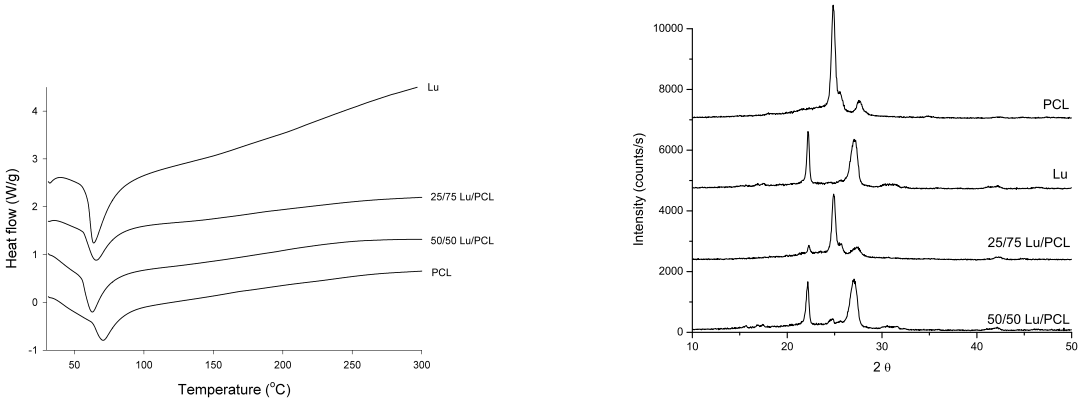

(a) (b)

Figure 4.1: a) DSC comparative scans and b) X-ray diffraction patterns (plots were shifted vertically for the sake of clarity)

(co)polymers and their blends are expected to be semi-crystalline also. The relative degree of crystallinity (X_{rel}) was determined by DSC and XRD analysis. The melting endotherms are presented in Fig.4.1(a), while Fig.4.1(b) shows the diffraction patterns. Two diffraction peaks were identified for Lu at 2θ=22.2, 27.1, whereas two characteristic peaks at 2θ=24.9, 27.5 are noted for PCL in agreement with the literature (Ha et al. [1999]). The blends have three characteristic peaks: for sample 50/50 Lu/PCL, the sharp crystalline peak of PCL at 2θ=24.9 was relatively reduced, whereas characteristic peaks of Lu appeared as a result of the blending. Sample 25/75 Lu/PCL also shows three peaks with a higher intensity for the peak corresponding to PCL as it has a higher fraction of PCL.

The melting temperatures and crystallinity values (X_{rel}) are presented in Table 4.1, where it can be seen that the relative crystallinity of the blends decreases when PCL ratio is increased. On addition of PCL, phase seggregation occurs so that crystallization capacity of Lu is restricted and crystallinity decreased (Qiu et al. [2003]). There is agreement between the values obtained by XRD with those determined using DSC. The results suggest that the crystallinity of the blends can be controlled by the composition with possible effects on drug release (as discussed in section 4.3.3).

4.3.2 Water uptake and degradation

Since these blends are designed to perform and degrade in biological environments, their water uptake behaviour plays an important role. Fig. 4.2(b) shows the change of water content percentage with time, and similar trends can be observed for the blends. Water absorption increased steadily with time, reached a

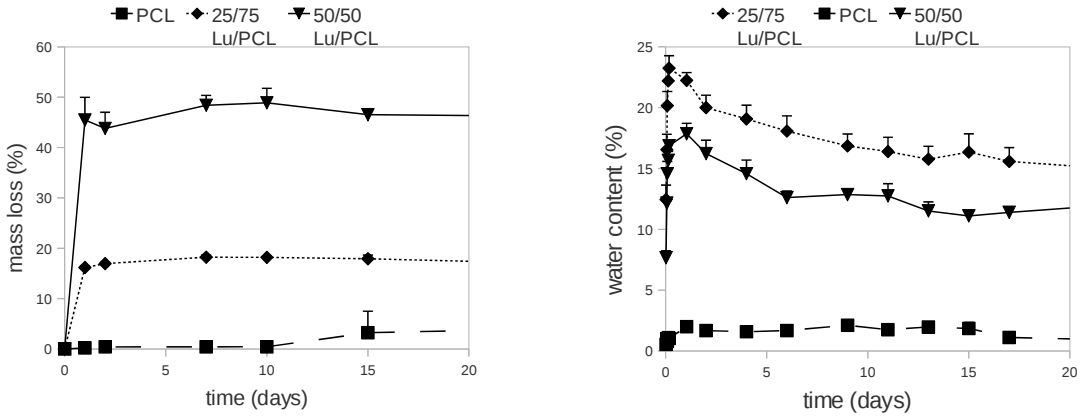

(a) (b)

Figure 4.2: a) Mass loss and b) water uptake (all differences between PCL and blend mass loss and water uptake values are statistically significant at p = 0.05 level)

maximum and then decreased. This pattern is the result of the superposition of two phenomena: the dissolution of water-soluble Lu and the water uptake of the residual material. After the ascending portion of the curve, corresponding to water uptake, there is a maximum and then the descending part, corresponding to water and polymer loss. As more polymer is dissolved due to water uptake, there is mass loss and less water is kept in the blend. The blends absorbed higher amounts of water since they are more hydrophilic (lowest contact angle) than PCL, while PCL had very low water content (Natu et al. [2008]).

Poly(ε-caprolactone) is known to undergo hydrolytic degradation, catalysed by the carboxylic acid residues formed in the reaction. Water access to the ester bonds is determined by the combined effect of the polymer hydrophobicity/hydrophilicity, the crystallinity of the sample, the molecular weight and the bulk sample dimensions (Tsuji and Ikada [1996], Grizzi et al. [1995]). When the polymers undergo hydrolysis of the main chain of the polymers, the mass loss of the films will take place, in addition to a change in the molecular weight. In Fig. 4.2(a), it can be observed that mass loss of PCL increased very slowly, while Lu/PCL samples lost mass very rapidly during the first day of test (45.5 % for sample 50/50 Lu/PCL and 16.2 % for 25/75 Lu/PCL), followed by small variations in mass loss thereafter. Mass loss of PCL is detectable only after the molecular weight reaches a value of 10000 g/mol (Hglund et al. [2007]) and thus the initial high mass loss of Lu/PCL samples can only be attributed to the dissolution of Lu as the sample with higher Lu content had the highest mass loss. We are going to discuss how this behaviour affect drug release in section 4.3.3.

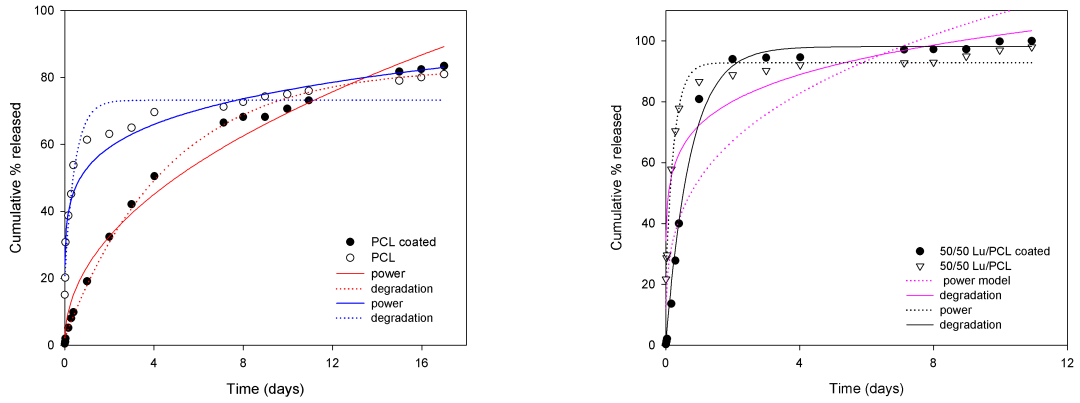

(a) (b)

Figure 4.3: Release kinetics and regression curves for a) PCL and b) 50/50 Lu/PCL

4.3.3 Dorzolamide hydrochloride release

As already mentioned, some of the blends were loaded with dorzolamide hydrochoride and used as such in drug release experiments or coated in order to diminish burst effect and better control the release. PCL and 50/50 Lu/PCL were selected so that a higher difference existed between the samples in terms of hydrophilicity and erodability. Table 4.2 presents the disk masses and the corresponding drug mass used in drug release experiments and in vivo tests.

The cumulative percentage of released drug is presented in Fig. 4.3(a) and Fig. 4.3(b). It can be observed that all samples except PCL-coated samples showed a certain degree of burst release. Burst is expected for the uncoated samples due to the high drug loadings (average drug loading 24.1±3.7 %, by weight) as high amounts of drug are deposited at the surface of the disk. The coating is efficient in the case of PCL (where no burst is shown) and makes only a small difference for 50/50 Lu/PCL. For reservoir systems, we can consider two controlling phenomena: diffusion through the polymer shell (barrier diffusion) or partition of the drug from the core to the shell. Shell porosity must be carefully controlled since the drug from the core will be released through water-filled channels rather than through the barrier/shell polymer (Tiwari et al. [2010]). In the case of 50/50 Lu/PCL, there is effectively no partitioning because of the porosity created by Lu dissolution (this blend is highly erodible (see Fig. 4.2(a)). Thus, the release is mostly a burst release. On the other hand, PCL-coated sample shows controlled release during 18 days (it should be noted that in this case, there is barrier-control of diffusion coupled with partition control from the core). In the case of 50/50 Lu/PCL, the added porosity of the core to the membrane porosity diminishes both partition and diffusion-control of drug release.

Sample	Drug mass (mg)	Disk mass (mg)	Released (%)	
			in vitro	in vivo
PCL-coated	1.29	6.38	83.46	81.29
PCL	0.82	4.43	81.20	-
50/50 Lu/PCL-coated	0.81	5.20	100.00	95.93
50/50 Lu/PCL	0.80	3.81	96.25	-

Table 4.2: Comparison between the amounts of released drug in vitro and in vivo from the disks

In Table 4.3, the non-linear regression results are presented (in spite of the fact that Eq. 4.4 and Eq. 4.5 were not developed taking into account polymer erosion phenomenon contribution to drug release, regression analysis results for 50/50 Lu/PCL samples are presented for comparative purposes). The objective behind fitting these equations to the release data was to understand the underlying phenomena involved in the drug release mechanism. If A_0 (or the load of the mobile drug) has higher values, then the instantaneous diffusion (or burst) contributes more to the release as it is shown by the uncoated samples (19.20 for PCL and 20.75 for 50/50 Lu/PCL). Smaller values for S_0 suggest higher amounts of immobilized drug that will not be released (46.78 for PCL-uncoated and 27.89 for 50/50 Lu/PCL-uncoated). The percentage of immobilized drug is higher for PCL than for 50/50 Lu/PCL because in the latter case erosion creates more surface area and exposes more drug to dissolution that otherwise would be trapped. It is important to note that in the case of the studied polymers, physical immobilization of the drug occurs due to the presence of crystalline regions where the drug is trapped. Diffusion from these regions is hindered because water enters initially only in the amorphous parts (Loo et al. [2005]). This fraction of the drug (that is immobilized in the crystalline regions) will be released only with polymer degradation (due to the time scale of the release experiment that is much shorter than the time required for polymer degradation, the steady state value of released drug percentage is smaller than 100 %, which would correspond to total release).

The regression results obtained using power law equation reinforce the previous observations. The high value of k indicates the extent of burst, much higher for uncoated than for coated samples (72.27 versus 54.48 for 50/50 Lu/PCL). The smaller value of n, the faster the release (0.47 for PCL and 0.30 for 50/50 Lu/PCL). The range of values for the release exponent is indicative of a diffusion mechanism for drug release (Peppas and Brannon-Peppas [1994]). This model fails to explain the last stage of the release ("the plateau" that appears at less than 100 % released drug) as it does not consider the effect of polymer degradation (better fit is obtained

Sample	Degradation model				Power law		
	A_0	S_0	μ (day^{-1})	R^2_{adj}	k (day^{-n})	n	R^2_{adj}
PCL-coated	2.14 (0.82)	80.96 (1.41)	0.22 (0.01)	0.9965	23.41 (1.60)	0.47 (0.03)	0.9821
PCL	19.20 (3.47)	53.22 (3.74)	2.19 (0.46)	0.9319	52.92 (1.34)	0.16 (0.01)	0.9504
50/50 Lu/PCL-coated	0.00 (1.53)	98.16 (1.39)	1.37 (0.09)	0.9924	54.48 (5.68)	0.30 (0.05)	0.8548
50/50 Lu/PCL	20.75 (2.11)	72.11 (2.28)	4.01 (0.34)	0.9876	72.27 (2.87)	0.15 (0.02)	0.8618

Table 4.3: Model parameters determined by non-linear regression for in vitro tested disks

with Eq.4.5 than with Eq.4.4 as inferred from R^2_{adj} values). In conclusion, the release takes place in three stages: the instantaneous diffusion (or burst), followed by the diffusion-controlled stage, succeeded by the polymer degradation-controlled stage. Some samples, like 50/50 Lu/PCL samples show only the burst stage, while PCL samples present all three stages, with total release expected to occur only when water penetration and degradation extends to the crystalline regions. By selecting the proper ratio between the components, the prevalence of a certain stage during drug release can be changed, obtaining an overall effect in drug release that fits the intended application.

A good in vitro-in vivo correlation was obtained, with similar amounts of drug released in vitro and in vivo (83.46 % released in vitro versus 81.29 % released in vivo for PCL-coated sample, see Table 4.2).

4.3.4 Biocompatibility evaluation

Before testing the materials in vivo, we performed cytotoxicity assessment using MTT test. Fig.4.4 shows the corneal endothelial cell viability test (the cells were chosen considering the application as materials for controlled release in ophthalmology). The results indicated that PCL effect on the cell viability is similar (p value = 0.65) to that of the negative control (glass-bottom multiwell culture plate, see section 4.2.5), while the blends presented slightly lower cell viability (approximately 80%, p value $\leq$ 0.05) than the negative control.

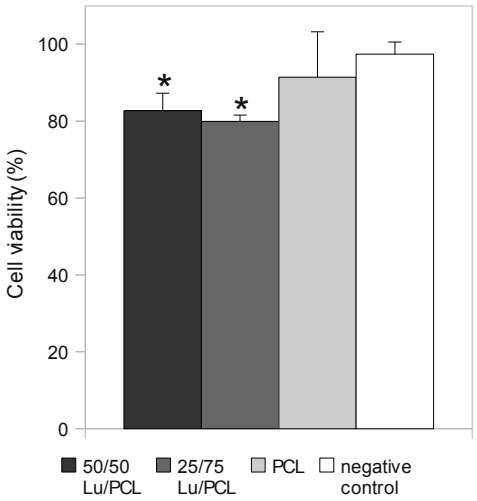

Figure 4.4: MTT assay results (∗, p≤ 0.05 with respect to negative control)

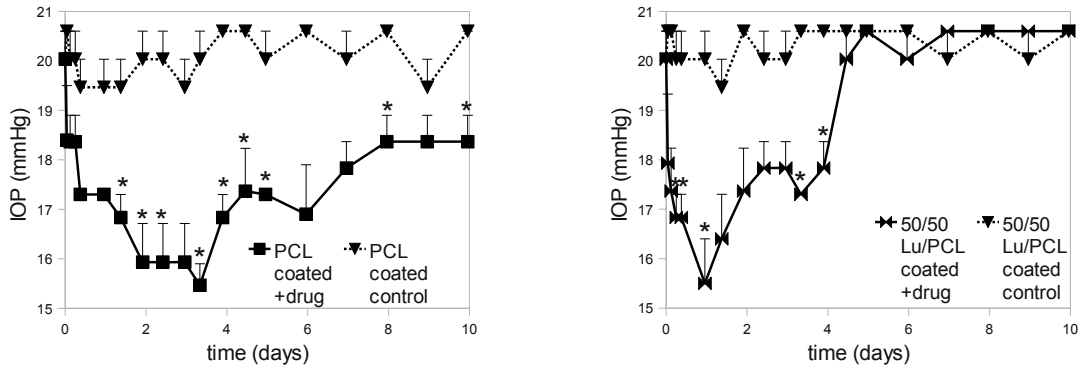

(a) (b)

Figure 4.5: IOP values in eyes treated with a) PCL-coated implants and b) 50/50 Lu/PCL-coated implants (∗, p≤ 0.05 with respect to control eye)

4.3.5 In vivo performance - Intraocular pressure measurement

The surgical procedure to insert the disks is relatively easy to perform because of easy access to the implantation area and low vascularization. Moreover, the wound does not need to be sutured because a pocket is created that keeps the disk in place. The fixation of the disk is further enhanced by fast wound healing (the disk is completely encapsulated by the conjunctiva after approximately 1 week). Ocular adverse events included conjunctivitis, that resolved clinically in less than 1 week (with antibiotic eyedrops). No other events were observed.

Disks were tested in rabbit normotensive eyes that presented an average IOP value of 20.1±0.8 mmHg. Dorzolamide is known to decrease IOP in normotensive

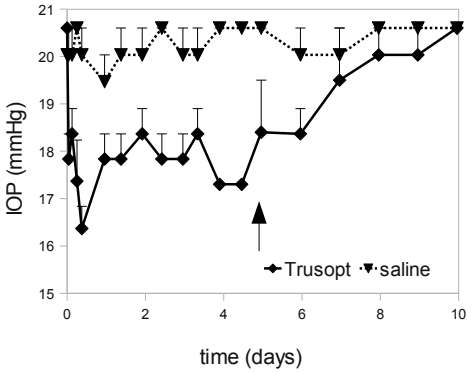

(a)

Figure 4.6: IOP values in eyes treated with Trusopt eyedrops ($*$, $p \leq 0.05$ with respect to control eye; the arrow indicates the moment when the last drop of Trusopt was instilled)

eyes (Harris et al. [2000]). In Fig. 4.5(a) and Fig. 4.5(b), it can be seen that sample PCL decreased in average IOP by 13.0 % getting closer to the baseline value after 10 days, while sample 50/50 Lu/PCL decreased IOP in average by 13.0 % during 4.5 days. The decrease in IOP obtained with the disks was comparable with the one obtained by applying Trusopt eyedrops (11.0 % in average). A decrease of around 20% is desired in order to reduce the rate of open angle glaucoma-related damage (Yudcovitch [2010]). The obtained values for IOP decrease with Trusopt are in agreement with literature values for normotensive eyes (Harris et al. [2000], Scozzafava et al. [1999]), while those obtained with the drug delivery systems are similar with the decrease in IOP with Ocusert ocular insert (Macoul and Pavan-Langston [1975]).

Peak IOP decrease (22.6 %) occurred for 50/50 Lu/PCL after the first day, while peak IOP decrease (22.6 %) occurred for PCL after 3 days. This behaviour is in agreement with the release kinetics and mass loss tests. Most of the polymer erosion takes place during the first day and the highest amount of released drug with direct effect on IOP is expected in the same period. For Trusopt peak IOP decrease (18.2 %) happened after 9 hours from instillation, faster than from the implanted disks. Drug release is insignificant in the absence of water and as such a lag time is expected between implantation time and actual release from the disks. In contrast, drug release from the eyedrop formulations is faster as there is no carrier involved and the drug can diffuse across the ocular tissues the moment is applied on the ocular surface.

4.4 Conclusions

Implantable dorzolamide loaded disks were prepared by blending poly(ε-caprolactone), PCL with poly(ethylene oxide)-b-poly(propylene oxide)-b-poly(ethylene oxide), Lu. By blending, crystallinity, water uptake and mass loss were modified relative to the pure polymers. PCL and 50/50 Lu/PCL disks were coated with a PCL shell in order to diminish burst effect and better control the release. All samples presented burst release except PCL-coated samples that showed controlled release during 18 days. The uncoated samples showed burst due to the high drug loading as high amounts of drug are deposited at the surface of the disk. For PCL-coated, barrier-control of diffusion coupled with partition control from the core, slowed down the release, while for 50/50 Lu/PCL-coated, the added porosity of the core (created by Lu dissolution) diminished partition-control of drug release.

The release data was modeled with a degradation model, which considers that the immobilized drug in the crystalline regions can only be released with polymer degradation. This model produced a better fit than the diffusional model that failed to explain the last stage of the release. The curve fitting to the release data suggested a triphasic release mechanism: the instantaneous diffusion (or burst), the diffusion-controlled stage, followed by the polymer degradation-controlled stage. Some samples, like 50/50 Lu/PCL samples showed only the burst stage, while PCL samples presented all three stages, with total release expected to occur only when water penetration and degradation extends to the crystalline regions.

MTT test showed that the materials are not cytotoxic for corneal endothelial cells and they were further evaluated in vivo. A good in vitro-in vivo correlation was obtained, with similar amounts of drug released in vitro and in vivo. Ocular adverse events included conjunctivitis, that resolved clinically in less than 1 week. No other events were observed. The disks decreased IOP in normotensive rabbit eyes by 13.0 % during 10 days for PCL-coated sample and by 13.0 % during 4 days for 50/50 Lu/PCL-coated. The percentages of IOP decrease are similar to those obtained by dorzolamide eyedrop instillation (11.0 %). This drug delivery system offers promise in the treatment of open-angle glaucoma, providing an alternative to eyedrops.

Bibliography

2007/526/EC. Commission recommendation of 18 june 2007 on guidelines for the accommodation and care of animals used for experimental and other scientific

purposes. http://eur-lex.europa.eu/LexUriServ/LexUriServ.do?uri=OJ:L:2007:197:0001:0089:EN:PDF, 2010.

86/609/EEC. Council directive 86/609/EEC of 24 november 1986 on the approximation of laws, regulations and administrative provisions of the member states regarding the protection of animals used for experimental and other scientific purposes. http://eur-lex.europa.eu/LexUriServ/LexUriServ.do?uri=CELEX:31986L0609:en:HTML, 2010.

S.H. Ajili and N.G. Ebrahimi. Miscibility of TPU(PCL diol)/PCL blend and its effect on PCL crystallinity. *Macromol. Symp.*, 249-250:623–627, 2007. [DOI:10.1002/masy.200750446].

E.M. Del Amo and A. Urtti. Current and future ophthalmic drug delivery systems. A shift to the posterior segment. *Drug Discov. Today*, 13:135–143, 2008. [DOI:10.1016/j.drudis.2007.11.002].

S.S. Anumolu, Y. Singh, D. Gao, S. Stein, and P.J. Sinko. Design and evaluation of novel fast forming pilocarpine-loaded ocular hydrogels for sustained pharmacological response. *J. Control. Release*, 137:152–159, 2009. [DOI:10.1016/j.jconrel.2009.03.016].

ATHAS. The Advanced THermal Analysis System (ATHAS) data bank. http://athas.prz.edu.pl/Default.aspx?op=db, 2010.

V. Baeyens, O. Felt-Baeyens, S. Rougier, S. Pheulpin, B. Boisrame, and R. Gurny. Clinical evaluation of bioadhesive ophthalmic drug inserts (BODI) for the treatment of external ocular infections in dogs. *J. Control. Release*, 85:163–168, 2002. [PubMed:12480321].

E. Barbu, L. Verestiuc, M. Iancu, A. Jatariu, A. Lungu, and J. Tsibouklis. Hybrid polymeric hydrogels for ocular drug delivery: nanoparticulate systems from copolymers of acrylic acid-functionalized chitosan and N-isopropylacrylamide or 2-hydroxyethyl methacrylate. *Nanotechnology*, 20:225108, 2009. [DOI:10.1088/0957-4484/20/22/225108].

J.L. Bourges, C. Bloquel, A. Thomas, F. Froussart, A. Bochot, F. Azan, R. Gurny, D. BenEzra, and F. Behar-Cohen. Intraocular implants for extended drug delivery: therapeutic applications. *Adv. Drug Deliv. Rev.*, 58:1182–1202, 2006. [DOI:10.1016/j.addr.2006.07.026].

J. Cao and C.A. Billows. Crystallinity determination of native and stretched wool by X-ray diffraction. *Polym. Int.*, 48:1027–1033, 1999. [DOI:110.1002/(SICI)1097-0126(199910)48:10¡1027::AID-PI264¿3.0.CO;2-9].

C.C. Chen, J.Y. Chueh, H. Tseng, H.M. Huang, and S.Y. Lee. Preparation and characterization of biodegradable PLA polymeric blends. *Biomaterials*, 24: 1167–1173, 2003. [PubMed:12527257].

V.P. Costa, M.E.M. Braga, C.M.M. Duarte, C. Alvarez-Lorenzo, A. Concheiro, M.H. Gil, and H.C. de Sousa. Anti-glaucoma drug-loaded contact lenses prepared using supercritical solvent impregnation. *J. Supercrit. Fluids*, 53:165–173, 2010. [DOI:10.1016/j.supflu.2010.02.007].

I. Grizzi, H. Garreau, S. Li, and M. Vert. Hydrolytic degradation of devices based on poly(D,L-lactic acid) size-dependence. *Biomaterials*, 16:305–311, 1995. [PubMed:7772670].

J.C. Ha, S.Y. Kim, and Y.M. Lee. Poly(ethylene oxide)-poly(propylene oxide)-poly(ethylene oxide) (Pluronic)/poly(ε-caprolactone) (PCL) amphiphilic block copolymeric nanospheres. I. Preparation and characterization. *J. Control. Release*, 62:381–392, 1999. [PubMed:10528075].

A. Harris, O. Arend, H.S. Chung, L. Kagemann, L. Cantor, and B. Martin. A comparative study of betaxolol and dorzolamide effect on ocular circulation in normal-tension glaucoma patients. *Ophthalmology*, 107:430–434, 2000. [PubMed:10711877].

A. Hglund, M. Hakkarainen, and A.-C. Albertsson. Degradation profile of poly(ε-caprolactone)-the influence of macroscopic and macromolecular biomaterial design. *J. Macromolecular Sci. Part A*, 44:1041–1046, 2007. [DOI:10.1080/10601320701424487].

H. Hiratani, A. Fujiwara, Y. Tamiya, Y. Mizutani, and C. Alvarez-Lorenzo. Ocular release of timolol from molecularly imprinted soft contact lenses. *Biomaterials*, 26:1293–1298, 2005. [DOI:10.1016/j.biomaterials.2004.04.030].

X. Huang and C.S. Brazel. On the importance and mechanisms of burst release in matrix-controlled drug delivery systems. *J. Control. Release*, 73:121–136, 2001. [PubMed:11516493].

S. Kashanian, F. Harding, Y. Irani, S. Klebe, K. Marshall, A. Loni, L. Canham, D. Fan, K.A. Williams, N.H. Voelcker, and J.L. Coffer. Evaluation of mesoporous

silicon/polycaprolactone composites as ophthalmic implants. *Acta Biomater.*, 6: 3566–3572, 2010. [DOI:10.1016/j.actbio.2010.03.031].

I.P. Kaur, A. Garg, A.K. Singla, and D. Aggarwal. Vesicular systems in ocular drug delivery: an overview. *Int. J. Pharm.*, 269:1–14, 2004. [PubMed:14698571].

P.T. Khaw, P. Shah, and A.R. Elkington. Glaucoma–2: treatment. *BMJ*, 328: 156–158, 2004. [DOI:10.1136/bmj.328.7432.156].

J.M. Korte, T. Kaila, and K.M. Saari. Systemic bioavailability and cardiopulmonary effects of 0.5% timolol eyedrops. *Graefes Arch. Clin. Exp. Ophthalmol.*, 240: 430–435, 2002. [DOI:10.1007/s00417-002-0462-2].

S.V. Kulkarni, K.F. Damji, and Y.M. Buys. Medical management of primary open-angle glaucoma: Best practices associated with enhanced patient compliance and persistency. *Patient Prefer. Adherence*, 2:303–314, 2008. [PubMed:19920977].

S.C. Loo, C.P. Ooi, S.H. Wee, and Y.C. Boey. Effect of isothermal annealing on the hydrolytic degradation rate of poly(lactide-co-glycolide) (PLGA). *Biomaterials*, 26:2827–2833, 2005. [DOI:10.1016/j.biomaterials.2004.08.031].

A. Ludwig. The use of mucoadhesive polymers in ocular drug delivery. *Adv. Drug Deliv. Rev.*, 57:1595–1639, 2005. [DOI:10.1016/j.addr.2005.07.005].

S.P. Lyu, R.Sparer, C. Hobot, and K. Dang. Adjusting drug diffusivity using miscible polymer blends. *J. Control. Release*, 102:679–687, 2005. [DOI:10.1016/j.jconrel.2004.11.007].

K.L. Macoul and D. Pavan-Langston. Pilocarpine ocusert system for sustained control of ocular hypertension. *Arch. Ophthalmol.*, 93:587–590, 1975. [PubMed:1164218].

L. Marchal-Heussler, D. Sirbat, M. Hoffman, and P. Maincent. Poly(ε-caprolactone) nanocapsules in carteolol ophthalmic delivery. *Pharm. Res.*, 10:386–390, 1993. [PubMed:8464811].

B.K. Nanjawade, F.V. Manvi, and A.S. Manjappa. In situ-forming hydrogels for sustained ophthalmic drug delivery. *J. Con. Rel.*, 122:119–134, 2007. [DOI:10.1016/j.jconrel.2007.07.009].

M.V. Natu, J.P. Sardinha, I.J. Correia, and M.H. Gil. Controlled release gelatin hydrogels and lyophilisates with potential application as ocular inserts. *Biomed. Mater.*, 2:241–249, 2007. [DOI:10.1088/1748-6041/2/4/006].

M.V. Natu, M.H. Gil, and H.C. de Sousa. Supercritical solvent impregnation of poly(ε-caprolactone)/poly(oxyethylene-b-oxypropylene-b-oxyethylene) and poly(ε-caprolactone)/poly(ethylene-vinyl acetate) blends for controlled release applications. *J. Supercrit. Fluids*, 47:93–102, 2008. [DOI:10.1016/j.supflu.2008.05.006].

M.V. Natu, H.C. de Sousa, and M.H. Gil. Effects of drug solubility, state and loading on controlled release in bicomponent electrospun fibers. *Int. J. Pharm.*, 397:50–58, 2010. [DOI:10.1016/j.ijpharm.2010.06.045].

R.S. Noecker, M.S. Dirks, and N. Choplin. Comparison of latanoprost, bimatoprost, and travoprost in patients with elevated intraocular pressure: a 12-week, randomized, masked-evaluator multicenter study. *Am. J. Ophthalmol.*, 137:210–211, 2004. [PubMed:14700685].

Openoffice. Openoffice.org, the free and open productivity suite. `http://www.openoffice.org/`, 2010.

N.A. Peppas and L. Brannon-Peppas. Water diffusion and sorption in amorphous macromolecular systems and foods. *J. Food Eng.*, 22:189–210, 1994. [DOI:10.1016/0260-8774(94)90030-2].

R.T. Pijls, L.P. Cruysberg, R.M. Nuijts, A.A. Dias, and L.H. Koole. Capacity and tolerance of a new device for ocular drug delivery. *Int. J. Pharm.*, 341:152–161, 2007. [DOI:10.1016/j.ijpharm.2007.04.007].

Z. Qiu, T. Ikehara, and T. Nishi. Miscibility and crystallization of poly(ethylene oxide) and poly(ε-caprolactone) blends. *Polymer*, 44:3101–3106, 2003. [DOI:10.1016/S0032-3861(03)00167-8].

H.A. Quigley. Glaucoma: macrocosm to microcosm the Friedenwald lecture. *Invest. Ophthalmol. Vis. Sci.*, 46:2662–2670, 2005. [DOI:10.1167/iovs.04-1070].

H. Sasaki, T. Nagano, K. Sakanaka, S. Kawakami, K. Nishida, J. Nakamura, N. Ichikawa, J. Iwashita, T. Nakamura, and M. Nakashima. One-side-coated insert as a unique ophthalmic drug delivery system. *J. Control. Release*, 92: 241–247, 2003. [PubMed:14568405].

K. Schwartz and D. Budenz. Current management of glaucoma. *Curr. Opin. Ophthalmol.*, 15:119–126, 2004. [PubMed:15021223].

A. Scozzafava, L. Menabuoni, F. Mincione, F. Briganti, G. Mincione, and C.T. Supuran. Carbonic anhydrase inhibitors. Synthesis of water-soluble, topically

effective, intraocular pressure-lowering aromatic/heterocyclic sulfonamides containing cationic or anionic moieties: is the tail more important than the ring? *J. Med. Chem.*, 42:2641–2650, 1999. [DOI:10.1021/jm9900523].

Y. Shen, W. Sun, K.J. Zhu, and Z. Shen. Regulation of biodegradability and drug release behavior of aliphatic polyesters by blending. *J. Biomed. Mater. Res.*, 50: 528–535, 2000. [PubMed:10756311].

S.K. Tiwari, R. Tzezana, E. Zussman, and S.S. Venkatraman. Optimizing partition-controlled drug release from electrospun core-shell fibers. *Int. J. Pharm.*, 392: 209–217, 2010. [DOI:10.1016/j.ijpharm.2010.03.021].

H. Tsuji and Y. Ikada. Blends of aliphatic polyesters. II. Hydrolysis of solution-cast blends from poly(D,L-lactide) and poly(ε-caprolactone) in phosphate-buffered solution. *J. Appl. Polym. Sci.*, 67:405–415, 1998. [DOI:10.1002/(SICI)1097-4628(19980118)67:3¡405::AID-APP3¿3.0.CO;2-Q].

H. Tsuji and Y. Ikada. Blends of aliphatic polyesters. I. Physical properties and morphologies of solution-cast blends from poly(D,L-lactide) and poly(ε-caprolactone). *J. Appl. Polym. Sci.*, 60:2367–2375, 1996.

A. R. Tzafriri. Mathematical modeling of diffusion-mediated release from bulk degrading matrices. *J. Control. Release*, 63:69–79, 2000. [PubMed:10640581].

L. Yudcovitch. Pharmaceutical, Laser and Surgical Treatments for Glaucoma: An Update. `http://www.pacificu.edu/optometry/ce/courses/15166/pharglapg1.cfm#Introduction`, 2010.

A. Zimmer and J. Kreuter. Microspheres and nanoparticles used in ocular delivery systems. *Adv. Drug Deliv. Rev.*, 16:61–73, 1995. [DOI:10.1016/0169-409X(95)00017-2].

Chapter 5

In vitro and in vivo evaluation of an intraocular implant for glaucoma treatment

The text that comprises this Chapter was submitted to the journal *European Journal of Pharmaceutics and Biopharmaceutics* (2011).

Abstract

Implantable disks for glaucoma treatment were prepared by blending poly(ε-caprolactone), PCL, poly(ethylene oxide)-b-poly(propylene oxide)-b-poly(ethylene oxide) and dorzolamide. Their in vivo performance was assessed by their capacity to decrease intraocular pressure (IOP) in normotensive and hypertensive eyes. Drug mapping showed that release was complete from blend disks and the low molecular weight (MW) PCL after 1 month in vivo. The high MW PCL showed non-cumulative release rates above the therapeutic level during 3 months in vitro. In vivo, the fibrous capsule formation around the implant controls the drug release, working as a barrier membrane. Histologic analysis showed normal foreign body reaction response to the implants. In normotensive eyes, a 20 % decrease in IOP obtained with the disks during 1 month was similar to Trusopt®eyedrops treatment. In hypertensive eyes, the most sustained decrease was shown by the high MW PCL (40 % after 1 month, 30 % after 2 months). It was shown that the implants can lower IOP in sustained manner in a rabbit glaucoma model.

5.1 Introduction

Glaucoma is a chronic condition that requires long-term treatment in order to stop progressive and irreversible blindness (Quigley [2005]). Treatment of glaucoma focuses on preserving vision by slowing down damage to the optic nerve. Therapy aims at preventing further damage by lowering IOP (or ocular hypertension) and it usually consists of pharmaceutical treatment and laser or surgical procedures (Schwartz and Budenz [2004]). It was shown that reducing IOP is effective in preventing disease progression in ocular hypertension, primary open angle glaucoma, and even in normal tension glaucoma (Khaw et al. [2004]).

In most glaucoma patients, medical therapy consists of topical eyedrops and oral tablets. However, administration and compliance are often problematic. Eyedrops produce low ocular bioavailability (Amo and Urtti [2008]), unnecessary systemic exposure (Korte et al. [2002]) and have low patient compliance due to uncomfortable sensations (Noecker et al. [2004]), as well as difficulty of instillation or forgetfulness (Kulkarni et al. [2008]). Two main strategies have already been used clinically to diminish such effects, namely gel forming (viscous) solutions (Nanjawade et al. [2007]) and controlled drug delivery systems (CDDS).

CDDS in the form of intraocular implants can deliver therapeutically effective amounts of drugs to targeted ocular tissues over sustained period of time without significant ocular/systemic side effects (Bourges et al. [2006]). Thus, CDDS can extremely suitable for chronic diseases, which require a constant level of medication to be maintained in the body over a long period of time. The major motivation for development and use of these devices is that they eliminate the need to take multiple doses of a drug during the day or week, thereby improving patient compliance and therapy outcomes (Amo and Urtti [2008]).

In a previous work, implants based on poly(ε-caprolactone), PCL were prepared by solvent-casting, followed by dip-coating (Natu et al. [2011]). Unfortunately, this preparation method is not reproducible and low drug loadings were achieved. High drug loads are needed for long term treatment of chronic diseases such as glaucoma. Moreover, the volume of such devices should be as small as possible in order to be easily introduced at the implantation site. Melt compression is a reproducible, easily scalable method of producing implants of different shapes and sizes (Yasukawa et al. [2005], Kuno and Fujii [2010]). In addition, compact implants can be obtained with small polymer-to-drug ratio, which enables high drug loads in a relatively small implant volume.

The objective of the present work was to prepare a drug loaded biodegradable implant designed to provide a localized, long-term (6 months to 2 years) sustained

release of the drug, that can be used in the treatment of glaucoma. A subconjunctival placement of the implant is simple to perform because of easy access to the implantation area and low vascularization. PCL and Lutrol F 127, Lu were selected because they are both biocompatible, biodegradable and they can be easily processed by conventional polymer processing techniques (Breitenbach [2002]). Moreover, they are commercially available, inexpensive and well characterised polymers. PCL is a slowly degradable polymer, while Lu can be used as a release modulator (Natu et al. [2008, 2010]). Two molecular weights of PCL were used because it was shown that molecular weight determines the time lag before erosion and the rate of bioerosion in vivo (Pitt et al. [1981]). The implantable drug loaded disks were prepared by melt compression and their performance in vivo was evaluated by assessing the capacity to lower IOP in normotensive and hypertensive rabbit eyes.

5.2 Materials and methods

5.2.1 Preparation of polymer disks

Poly(ε-caprolactone) (PCL40, average M_w 65000 g/mol and PCL10, average M_w 15000 g/mol, Sigma-Aldrich) and Lutrol F 127 (Lu, poly(ethylene oxide)-b-poly(propylene oxide)-b-poly(ethylene oxide), 9000-14000 g/mol, 70 % by weight of polyoxyethylene, BASF) films and dorzolamide hydrochloride (Chemos GmbH) loaded films (Lu/PCL: 13/87, 6/94, 0/100 % w/w) were prepared by solvent casting from acetone (UV grade, Sigma-Aldrich) at 40 °C, using a 15 % w/v total polymer concentration and 33.3 % w/w theoretical drug loading. Polymer sheets were fabricated by compression moulding of the polymer films in a stainless steel mould by applying a pressure of 201.5 kg/m^2 for 20 minutes at 100°C. The mould was subsequently cooled under a jet of cold water (20°C) during 2 minutes. Discs of 4 mm diameter (1 mm thickness, 4-5 mg drug mass, 13-16 mg total mass) were punched from the polymer sheets. They were used as such in characterization tests. Prior to in vivo implantation, the disks were sterilized using UV radiation during 20 minutes (at 254 nm) in a UV chamber (Camag UV cabinet).

5.2.2 Disk characterization

Differential scanning calorimetry (DSC) was carried out using a DSC Q100 equipment (TA Instruments) under nitrogen atmosphere (100 mL/min). Samples with masses of approximately 5 mg were heated until 100°C, at a heating rate of 10°C/min. The relative crystallinity of the disks was calculated as previously

described considering the melting enthalpy of 100 % crystalline PCL and 100 % crystalline Lu (Natu et al. [2010]). Thermogravimetric analysis (TGA) was carried out using a SDT Q 600 equipment (TA Instruments). Samples with masses of approximately 10 mg were heated until 600°C, at a heating rate of 10°C/min. The degradation temperature (T_d) was determined at the onset point of the TGA plot.

Water contact angle was evaluated by static contact angle measurements using an OCA 20 Video-Based Contact Angle Meter (Dataphysics) and employing the sessile drop method.

Drug loading of the disks was assessed by elemental analysis (quantification of sulphur, present only in the drug molecule).

5.2.3 Morphology and drug distribution

The morphology of the disks (before and after implantation) was examined using scanning electron microscopy, SEM (JSM 5310, Jeol). The drug mapping (elemental sulphur) of the disks surface and cross-section (showing the center of the disk) was done using electron probe microanalysis, EPMA (Camebax SX50, Cameca) at 15 kV accelerated voltage and 40 nA probe current.

5.2.4 In vitro and in vivo degradation

The extent of hydrolytic degradation of the disks (as prepared, in vitro degraded and in vivo degraded) was evaluated by determining the change of MW in time. Polymer disks were placed in 4 mL PBS with 0.001 % sodium azide, at 37°C. The changes in the MW were measured by size exclusion chromatography (SEC), using chloroform as mobile phase (1 ml/min, 30 °C) and a PLgel MIXED-C column (300 mm×7.5 mm, 5 μm, Varian). PL-EMD 960 (Polymer Laboratories) evaporative light scattering detector was used to acquire the data. Universal calibration was performed using polystyrene (PS) standards and Mark-Houwink parameters k_{PCL}=1.09 $\times 10^{-3}$ dl/g, α_{PCL}=0.60, k_{PS}=1.25 $\times 10^{-4}$ dl/g, α_{PS}=0.71. Peak integration was performed using Clarity chromatography software (DataApex).

5.2.5 In vitro drug release and release modelling

Dorzolamide hydrochloride release was studied in 10 ml phosphate saline buffer medium (PBS tablets, pH 7.4, 10 mM phosphate, 137 mM sodium, 2.7 mM potassium, Sigma-Aldrich) at 37°C. At scheduled time intervals, samples were taken and the entire medium volume was replaced with fresh medium to maintain sink conditions. The mass of dorzolamide hydrochloride released at time t was

determined by UV spectroscopy at 254 nm (Jasco V-650 Spectrophotometer). The percentage of in vitro released drug was calculated using Eq.5.1.

$$Released\,drug\,in\,vitro\,(\%) \;=\; \frac{M_{dt}}{M_{d0}} \times 100 \tag{5.1}$$

In Eq. 5.1, M_{dt} is the drug mass released at time t and M_{d0} is the initial drug mass.

In order to study the drug release mechanism, the power law equation, which is based on diffusional model of drug transport, was used (Natu et al. [2010]). An alternative model (Eq.5.2) based on polymer degradation control of drug release was also used to fit the release data. In this model, two pools of drug are considered: a pool of mobile drug which readily diffuses out of the matrix upon immersion in an aqueous medium and a pool of immobilized drug which can diffuse only after matrix degradation (Natu et al. [2010]). This model can be applied to slow-degrading polymers such as PCL due to the fact that polymer degradation is much slower than drug diffusion and as such it is the rate limiting step for drug transport. In Eq. 5.2, A_0 is the load of the mobile drug, S_0 is the load of immobilized drug, τ is the dimensionless time and is defined by $\tau = \mu\, t$ (μ is the degradation rate constant) and Ω is the geometrical factor. The model parameters were determined by non-linear regression and the goodness of the fit was assessed.

$$M(\tau) \;=\; A_0 + |\Omega|\, S_0\,(1 - \exp\,(-\tau)),\; \bar{\alpha}_{lmn}^{-1} \to 0 \tag{5.2}$$

5.2.6 Disk implantation, glaucoma model, intraocular pressure measurement and in vivo drug release

New Zealand white rabbits were used in animal experiments in agreement with European Union Council Directive 86/609/EEC regarding the protection of animals used for experimental and other scientific purposes as described before (Natu et al. [2011]). The disk implantation procedure and the IOP measurement by tonometry were already described (Natu et al. [2011]). In order to produce high IOP, we used a low temperature ophthalmic cautery (Bovie, Aaron Medical) to produce 30 to 50 burns that were directed at the limbal plexus and at the episcleral veins (Levkovitch-Verbin et al. [2002], Ruiz-Ederra and Verkman [2006]).

The animals were divided in three groups: group 1 (n=26) received drug loaded polymer disks (the right eye contained the drug loaded disk–PCL40, PCL10, 6%Lu,PCL40 and 13%Lu,PCL40, while the left had the control disk–polymers without drug), group 2 (n=3) was submitted to Trusopt®eyedrops (dorzolamide hydrochloride 2 %, Chibret) treatment (1 drop twice a day in the right eye, while

the left eye received a drop of balanced salt solution, BSS sterile solution, Alcon), while group 3 (n=3) was the glaucoma model reference.

For in vivo release tests, previously weighed polymer disks were implanted as described before for predetermined periods of time and subsequently removed, cleaned of ocular tissues, rinsed with distilled water and vacuum-dried to constant weight. The in vivo released mass of drug was determined gravimetrically using Eq. 5.3. In Eq. 5.3, M_i is the initial disk mass, M_t is the disk mass after implantation time t, M_c is the mass loss of the control disk and M_{d0} is the initial drug mass.

$$Released\,drug\,in\,vivo\,(\%) = \frac{M_i - M_t - M_c}{M_{d0}} \times 100 \tag{5.3}$$

In vivo drug released percentages were also determined by elemental analysis (the residual drug was determined after in vivo implantation).

5.2.7 Histologic evaluation

The local implant site and important organs were excised for histological evaluation. The collected organs included kidneys, spleen, liver, lung (only after 2 months implantation). The organs and tissue samples were fixed in 10 % neutral buffered formaldehyde. The samples were then embedded in paraffin and dehydrated by isopropanol processing. Thin layers were cut from the samples with a microtome and stained with hematoxylin and eosin for optical microscopy.

5.2.8 Statistics

All values are presented as mean and standard error of the mean (SEM). Experiments were performed in triplicates. Statistical analysis (Student's T-test, independent, two-tailed) was done using OpenOffice.org Calc 3.1.

5.3 Results and discussion

5.3.1 Disk characterization

In Table 5.1, melting (T_m) and degradation temperatures (T_d) are presented for drug loaded and control disks because their knowledge is required when dealing with polymer processing methods for the manufacture of drug-eluting implants. Blend disks are more hydrophilic than PCL disks due to the incorporation of hydrophilic Lu (Natu et al. [2008, 2010]) as shown by the lower contact angle values. The low T_m enables processing at temperatures much lower than the degradation temperature of dorzolamide (T_d=251.26°C). The PCL samples show a two step

Sample	T_d (°C)	T_m (°C)	Contact angle (deg)
PCL40+drug	279.38, 420.20	61.53 (0.03)	80.23 (2.63)
PCL40	375.51	61.26 (0.31)	73.88 (3.31)
PCL10+drug	275.00, 420.33	60.67 (0.19)	78.26 (1.24)
PCL10	269.62, 421.88	61.23 (0.61)	70.24 (1.86)
6%Lu,PCL40+drug	-	61.45 (0.42)	46.87 (2.78)
6%Lu,PCL40	-	62.07 (0.17)	32.52 (2.12)
13%Lu,PCL40+drug	-	58.22 (0.26)	39.88 (0.80)
13%Lu,PCL40	-	58.86 (0.45)	40.20 (2.53)
Lu	358.80	55.57 (0.65)	59.33 (0.35)

Table 5.1: Water contact angle, melting and degradation temperatures of the disks

degradation process, the first step corresponding to drug degradation, while the second corresponds to polymer degradation.

All disks presented an average content of sulphur of 33.6 %, which corresponds to approximately 5 mg of loaded drug in each disk.

5.3.2 General considerations about implantation surgical procedure and animal wellbeing

The surgical procedure to insert the disks is relatively easy to perform because of easy access to the implantation area and low vascularization. Moreover, the wound does not need to be sutured because a pocket is created that keeps the disk in place. The fixation of the disk is further enhanced by fast wound healing as the disk is completely encapsulated by the conjunctiva. Ocular adverse events included conjunctivitis (6 eyes in 64 eyes), that resolved clinically in less than 1 week (with antibiotic eyedrops). No other events were observed. It should be mentioned that such ocular adverse events (conjunctival hyperemia, stinging, burning, foreign body sensation, tearing, vision blurring) are quite frequent in topical treatment with eyedrops (Noecker et al. [2004]).

5.3.3 In vitro and in vivo drug release

Each disk was loaded with approximately 5 mg of drug in order to achieve a release rate of 18 μg/day (similar with the one obtained with Trusopt 2% instillation three times a day (Schmitz et al. [1999])) for at least 4.5 months (we considered 50 % drug losses during the transport from conjunctiva to cilliary body).

The release kinetics shown in Fig. 5.1(b) presents similar released drug percentages regardless of the PCL molecular weight. Fig. 5.1(a) presents the release from

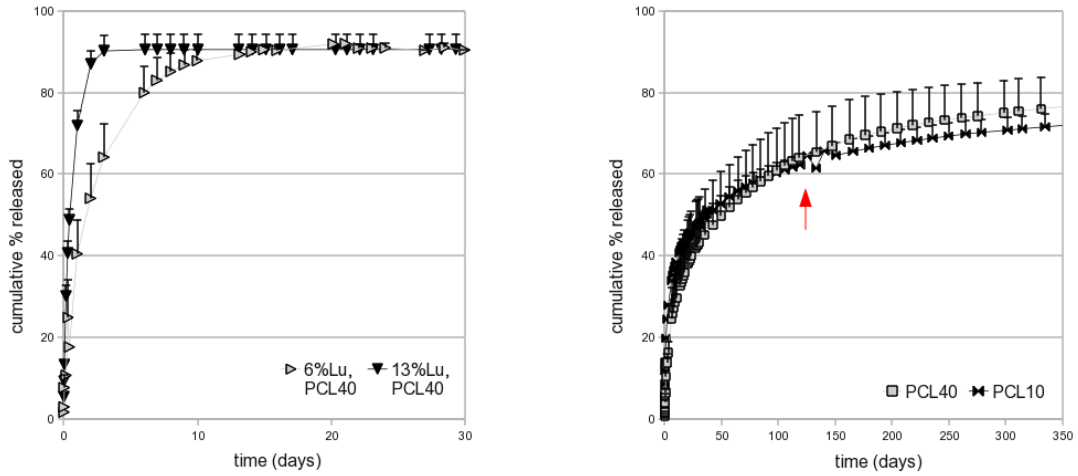

(a) (b)

Figure 5.1: In vitro drug release for a) PCL40 and PCL10 samples and b) 6%Lu,PCL40 and 13%Lu,PCL40 (the red arrow indicates the point on the kinetics curve when the released dose is smaller than the effective dose)

blends: release is almost complete after 10 days for 13%Lu,PCL40 and after 20 days for 6%Lu,PCL40.

A comparison between released drug percentages in vitro and in vivo is shown in Table 5.2. It can be noted that there are significant differences between released percentages in vitro and in vivo for PCL40 and PCL10 samples, while the released drug percentages of 6%Lu,PCL40 and 13%Lu,PCL40 are similar in vitro and in vivo. In vivo drug released percentages (calculated by mass balance) for PCL40 implant were confirmed by elemental analysis (the residual drug was determined after in vivo implantation): after 8 days, 22.69 (5.82) % released drug, after 14 days, 24.09 (2.93) % released drug and after 22 days 35.74 (11.54) % released drug.

In vivo release kinetics (Fig. 5.2) seems to approach a zero-order kinetics, while the in vitro kinetics curves (Fig. 5.1(b)) appear to have a $t^{0.5}$ profile. This may be due to different release controlling phenomena: in vitro, diffusion controls drug release (from here the classic, Fickian $t^{0.5}$ profile), while in vivo, the fibrous capsule formation around the implant (see section 5.3.7) controls the drug release, functioning as a barrier membrane that slows down release. Thus, there should be significant differences between drug released in vitro and in vivo (see Table 5.2) for PCL40 and PCL10 samples. For blend samples, due to polymer erosion that takes place mostly in the first day of release (Natu et al. [2010]), the fibrous capsule/barrier control is absent (only after 1 week, the disks were fully encapsulated) and as such the released drug percentages are similar both in vitro and in vivo.

In Table 5.3, the non-linear regression results are presented. The objective

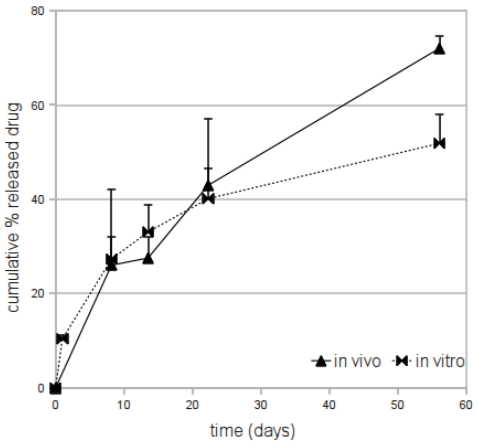

Figure 5.2: Comparison between in vivo and in vitro drug release for sample PCL40

Sample	In vitro		In vivo			
	Rel. drug (%)		Rel. drug mass (mg)		Rel. drug (%)	
	1 month	2 months	1 month	2 months	1 month	2 months
PCL40	40.14 (6.48)	51.88 (6.07)	2.22 (0.72)	3.72 (0.13)	42.99 (14.06)	72.02 (2.49)
PCL10	47.29 (0.96)	-	4.47 (0.18)	-	83.30 (4.01)	-
6%Lu,PCL40	90.98 (1.06)	-	4.74 (0.20)	-	96.80 (1.62)	-
13%Lu,PCL40	90.57 (3.79)	-	4.95	-	94.56	-

Table 5.2: Released drug percentages for in vitro tested disks and disks implanted during 1 month or 2 months

Sample	Power law			Degradation model			
	k (day^{-n})	n	R^2_{adj}	A_0	S_0	μ (day^{-1})	R^2_{adj}
PCL40	17.05	0.26	0.98	10.75	62.21	0.02	0.96
	(0.65)	(0.01)		(1.42)	(1.64)	(0.00)	
PCL10	24.11	0.19	0.97	15.86	51.45	0.04	0.92
	(0.60)	(0.01)		(1.67)	(1.86)	(0.00)	
6%Lu,PCL40	41.31	0.27	0.92	5.90	84.12	0.42	0.99
	(3.14)	(0.03)		(1.33)	(1.46)	(0.03)	
13%Lu,PCL40	56.23	0.17	0.83	7.01	83.41	1.66	1.00
	(3.53)	(0.02)		(0.66)	(0.69)	(0.04)	

Table 5.3: Model parameters determined by non-linear regression

behind fitting these equations to the release data was to understand the underlying phenomena involved in the drug release mechanism. Smaller values for S_0 suggest higher amounts of immobilized drug that will not be released (37.8 % for PCL40 and 16.6 % for 13%Lu,PCL40). The percentage of immobilized drug is higher for PCL40 than for blend samples because in the latter case erosion creates more surface area and exposes more drug to dissolution that otherwise would be trapped. In the case of the studied polymers, physical immobilization of the drug occurs due to drug entrapment in crystalline regions. Drug diffusion from these regions is hindered because water enters initially only in the amorphous parts. The immobilized fraction of the drug will be released only with polymer degradation (this explains why the steady state value of released drug percentage is smaller than 100 %, which would correspond to total release).

The regression results obtained using power law equation reinforce the previous observations. The high value of k indicates the extent of burst, higher for blend samples. The range of values for the release exponent is indicative of a diffusion mechanism for drug release. This model fails to explain the last stage of the release (steady-state at less than 100 % released drug) as it does not consider the effect of polymer degradation.

The release kinetics suggested a three stage release mechanism, with different steps depending on disk composition. Dissolution of the surface loaded drug and subsequent diffusion, followed by diffusion of the mobile drug through water-filled pores (created either due to Lu leaching or polymer recrystallization (Natu et al. [2010], Miyajima et al. [1997])), while the last stage was controlled by polymer degradation and subsequent diffusion of the immobilized drug. In blends, most of the drug is released due to polymer erosion, while the residual drug was released by diffusion through water-filled pores. The mechanism from PCL40/PCL10 disks

and blend disks are essentially the same, except for the initial stage when drug diffusion is coupled with polymer erosion in the case of blends. By selecting the proper ratio between the components, the preponderance of a certain stage during drug release can be changed, obtaining an overall effect in drug release that fits the intended application.

5.3.4 Intraocular pressure measurement

In order to simulate ocular hypertension, we developed a rabbit glaucoma model by increasing the IOP values (Fig. 5.3(d)) from an average of 20.9 mmHg (normotensive eyes) to an average of 30.1 mmHg (hypertensive eyes). A second procedure was performed after 1 month because IOP values returned to baseline after this period (in Fig. 5.3(a), Fig. 5.3(c) and Fig. 5.3(d), the red arrow indicated the point when a second cauterization was performed) (Levkovitch-Verbin et al. [2002], Ruiz-Ederra and Verkman [2006]). Disks were first tested in normotensive eyes in order to select the best performing systems. In Fig. 5.3(e) and Fig. 5.3(f), it can be seen that sample 13%Lu,PCL40 decreased IOP by 16.59 % (see also Table 5.4) reaching the baseline value after 15 days, while sample 6%Lu,PCL40 decreased IOP by 23.85 % during 25 days. More sustained decrease in IOP was shown by sample PCL40 (16.91 %) and PCL10 (23.73 %) during the 30 days of test. The decrease in IOP obtained with the disks was comparable with the one obtained by applying Trusopt eyedrops (16.55 %). A decrease of at least 20% is desired in order to reduce the rate of open angle glaucoma-related damage (Yudcovitch [2010]).

Fig.5.3(a) and Fig.5.3(b) present IOP change in hypertensive eyes with implanted disks and in eyes treated with Trusopt®(Fig. 5.3(c)). PCL40 presented a decrease of 42.78 % after 1 month and a decrease of 33.21 % after 2 months, which is particularly suitable for patients with moderate to severe glaucoma (Yudcovitch [2010]). IOP values in eyes with PCL40 implants are expected to approach the baseline values after approximately 3 months (see Fig. 5.1(b)). Samples PCL10 and 6%Lu,PCL40 showed similar IOP decrease percentages and peak IOP percentage in hypertensive eyes, while peak IOP was attained faster for sample 6%Lu,PCL40 due to faster drug release (see section 5.3.3). Thus, the release rate from the disks can be manipulated by blending in order to achieve the desired decrease in IOP.

Table 5.4 presents the average IOP decrease percentages achieved by the implanted disks in normotensive and hypertensive eyes, while Table 5.5 shows the peak IOP decrease and the time interval from instillation/implantation to peak IOP. It can be noted that there was a higher IOP decrease in hypertensive eyes than in normotensive eyes for eyedrops and disks. Sample PCL40 showed the best performance in vivo (constant decrease in IOP for longer time) due to more

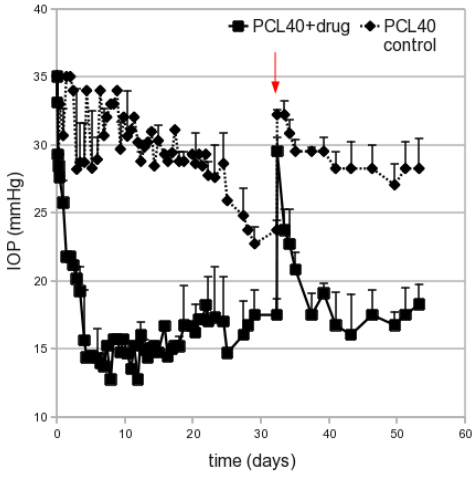

(a)

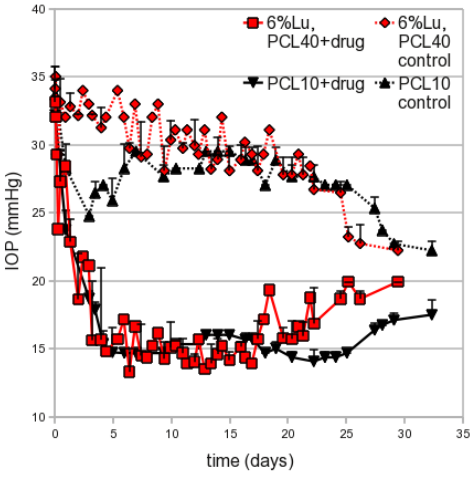

(b)

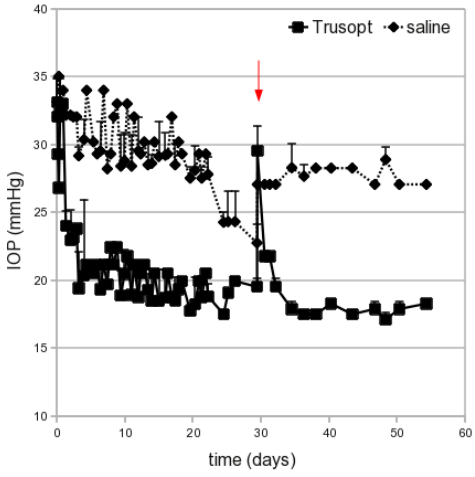

(c)

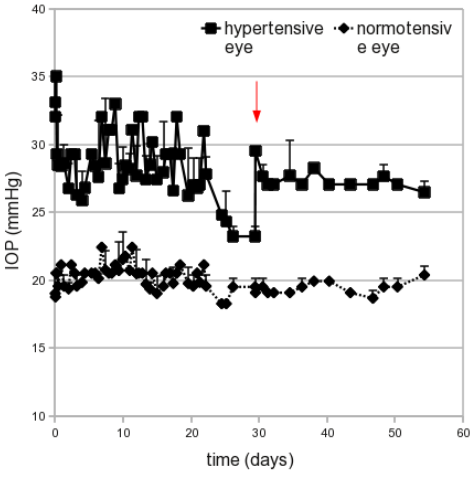

(d)

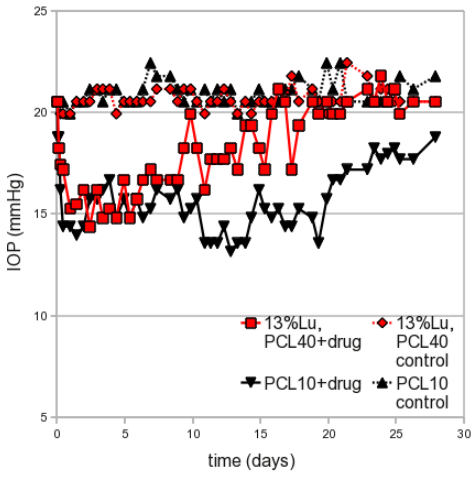

(e)

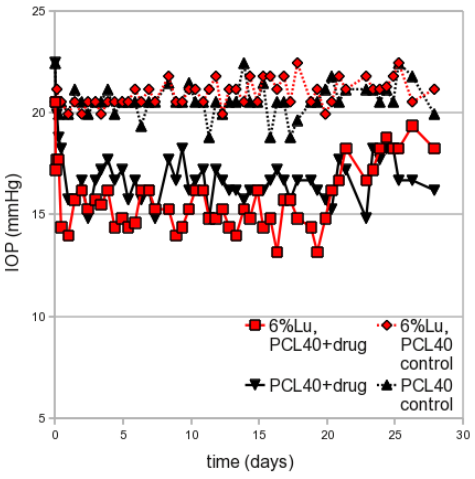

(f)

Figure 5.3: a), b) IOP in hypertensive eyes undergoing implant treatment, c) IOP in hypertensive eyes undergoing Trusopt treatment, d) IOP in glaucoma model group, e), f) IOP in normotensive eyes undergoing implant treatment

Sample	Average IOP reduction (%)		
	Normotensive eyes	Hypertensive eyes	
	1 month	1 month	2 months
Trusopt	23.89 (7.53)	28.46 (9.99)	29.52 (13.41)
PCL40	16.91 (6.43)	40.30 (12.23)	33.33 (9.64)
PCL10	23.73 (8.15)	39.61 (11.90)	-
6%Lu,PCL40	23.85 (7.24)	39.24 (15.21)	-
13%Lu,PCL40	13.35 (9.31)	-	-

Table 5.4: Average IOP reduction

sustained drug release. The obtained values for IOP decrease with Trusopt®are in agreement with literature values for normotensive (Harris et al. [2000], Scozzafava et al. [1999]) and hypertensive eyes (Konstas et al. [2008], Seki et al. [2005]). There was a higher decrease in IOP for eyes treated with disks than in those treated with eyedrops probably because of higher amounts of drug released by the disks (average in vitro release rate of 0.43 (0.04) mg/day for PCL40 or 1.34 (0.12) mg/day for PCL10 during 1 month versus 0.02 mg/day delivered by eyedrops (Schmitz et al. [1999])). The changes in IOP obtained in the eyes with implanted disk are similar to those obtained with the Ocusert drug delivery system (Macoul and Pavan-Langston [1975]). Trusopt®eyedrops produced the fastest decrease in IOP in normotensive eyes with peak IOP attained after 0.96 days, followed by blend disks in agreement with in vitro release results (peak IOP was reached fastest for blend disks with higher content of Lu). In hypertensive eyes, the same trend in IOP decrease was maintained, but the average IOP and peak IOP values were higher than those obtained in normotensive eyes. Peak IOP occured at similar times in hypertensive eyes, except for Trusopt®. Probably, dorzolamide administered by eyedrops might require multiple doses to build up to steady state levels of concentration in the cilliary processes that are required for IOP decrease in hypertensive eyes.

5.3.5 Morphology and drug distribution, SEM and EPMA

SEM and EMPA were performed in order to determine the morphology of the disks and the drug distribution inside the disks before and after the in vivo implantation.

Fig. 5.4(a) to Fig. 5.4(f) show the surface morphology of the prepared disks and in vivo degraded disks. There are significant signs of degradation on the implanted disk surface such as pores (Fig. 5.4(b)), cracks (Fig. 5.4(d)) and scales (Fig. 5.4(f)). The in vitro degraded samples showed fewer signs of material cracking (images not

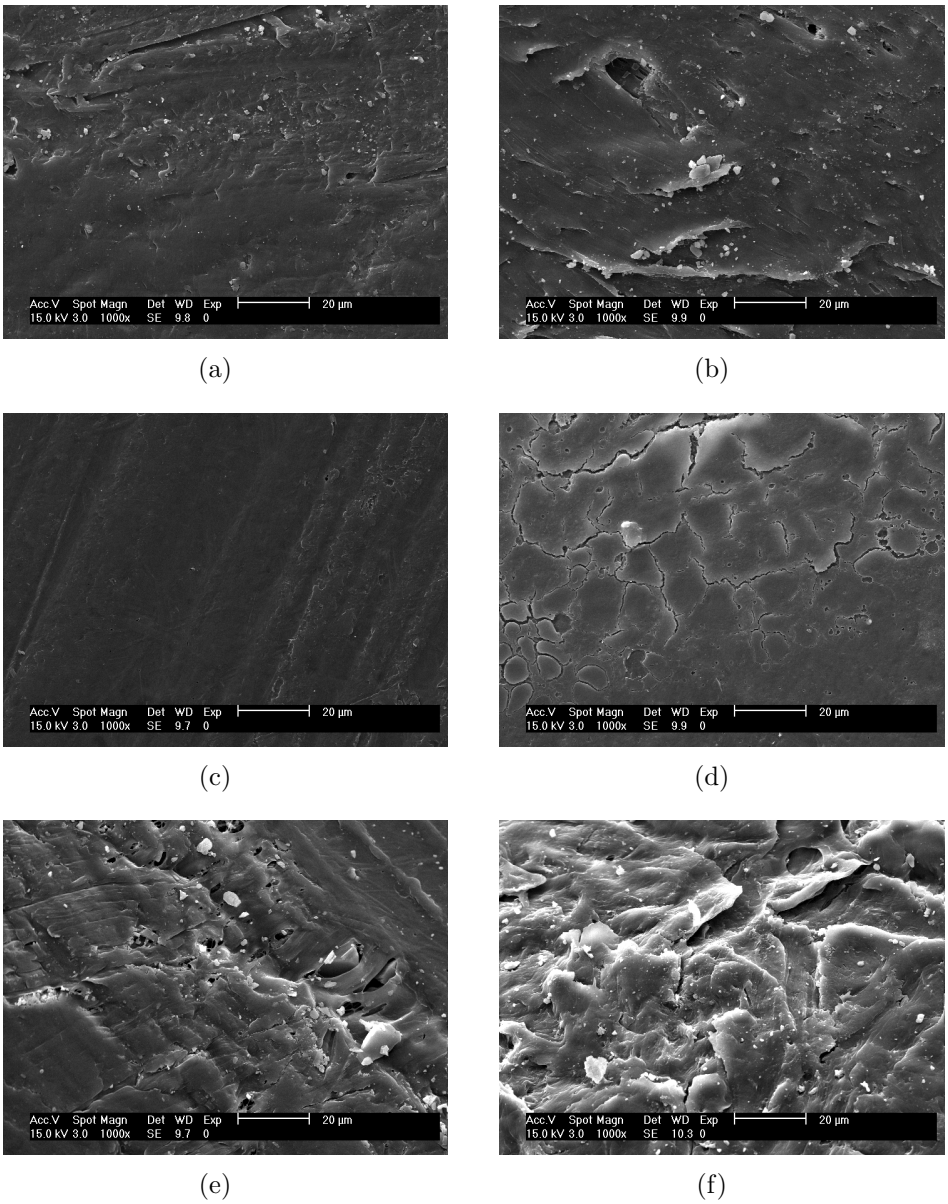

Figure 5.4: SEM of disks (with drug) surface. a) PCL40 as prepared, b) PCL40 in vivo, c) PCL10 as prepared, d) PCL10 in vivo, e) 6%Lu,PCL40 as prepared, f) 6%Lu,PCL40 in vivo

Sample	Peak IOP reduction (%)/time (days)		
	Normotensive eyes	Hypertensive eyes	
	1 month	1 month	2 months
Trusopt	27.85/0.96	36.59 (2.37)/3.38	40.73 (3.65)/34.56
PCL40	25.67/7.35	55.26 (0.98)/6.90	43.24 (2.55)/25.06
PCL10	35.92/6.90	50.21 (0.00)/6.94	-
6%Lu,PCL40	32.00/4.38	55.23 (5.03)/3.18	-
13%Lu,PCL40	29.96/2.42	-	-

Table 5.5: Peak IOP and the time interval from instillation/implantation to peak IOP

shown). This suggested enhanced degradation in vivo in comparison with in vitro conditions (see section 5.3.7).

After preparation, the disks presented a heterogeneous drug distribution (Fig. 5.5(a)) probably because of phase separation between drug and polymers due to the high drug loading. After in vivo testing, there was almost no drug at the surface (Fig. 5.5(b)), while in the disk cross-section there were still significant amounts of drug present in sample PCL40 after 1 month in vivo (Fig. 5.5(c)). The mapping of the other disks sections show that the release was complete after 1 month of implantation.

5.3.6 In vitro and in vivo degradation

To differentiate between a physical or a chemical degradation mechanism, the crystallinity and MW was determined for initial, in vitro and in vivo degraded samples, the table 5.6 presents the change of disk crystallinity and MW due to in vitro and in vivo degradation). There was MW decrease due to chemical hydrolysis for PCL40+drug sample both after 1 month and 2 months and for 6%Lu,PCL40+drug after 1 month. Sample PCL10+drug did not degrade in vivo probably due to higher initial crystallinity as crystalline regions are more inaccessible to water uptake. The MW of the in vitro degraded samples was also determined, but the obtained differences were not statistically significant ($p \geq 0.17$). The samples presented lower crystallinity than the pure polymers (50.26 (0.33) % for PCL40 and 68.51 (2.12) % for Lu) and the drug loaded samples showed lower crystallinity than the control samples probably due to co-crystallization of dorzolamide (that is above the solubility limit in the polymer). In general, there was an increase in crystallinity for in vitro and in vivo degraded samples because the amorphous regions are degraded first and because during drug elution, the mobile polymer chains rearrange themselves and crystallize (Natu et al. [2010],

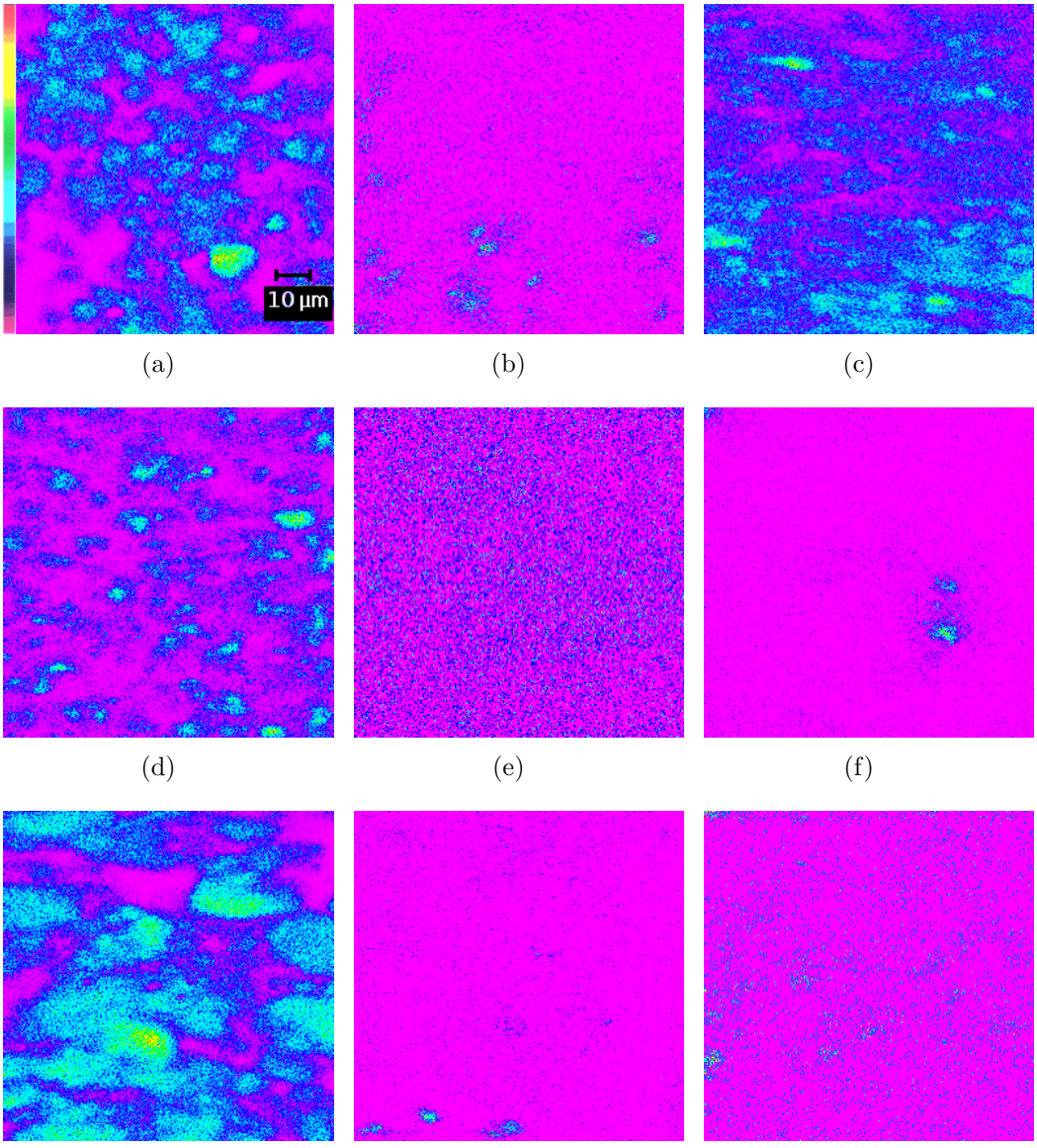

Figure 5.5: Sulphur drug mapping after 1 month in vivo. a) PCL40 surface as prepared, b) PCL40 surface in vivo, c) PCL40 section in vivo, d) PCL10 surface as prepared, e) PCL10 surface in vivo, f) PCL10 section in vivo, g) 6%Lu,PCL40 surface as prepared, h) 6%Lu,PCL40 surface in vivo, i) 6%Lu,PCL40 section in vivo (in the scale bar, the colour gradient represents 0% drug (pink) and 100% drug (red))

Miyajima et al. [1997]). Crystallinity was higher only for some in vivo degraded samples with respect to the in vitro degraded samples, suggesting that there is crystallinity increase and enhanced mechanical breakdown in vivo (see section 5.3.7).

Sample	As prepared	In vitro		In vivo					
	X_{rel} (%)	X_{rel} (%)	mass loss (%)	X_{rel} (%)	mass loss (%)	M_w (g/mole)		ΔM_w (%)	
		1 month		1 month		1 month	2 months	1 month	2 months
PCL40+drug	36.97 (1.93)	29.13 (0.97)	13.46 (1.14)	38.89 (0.03)†	15.07 (4.93)	62377.5 (725.5)	60274.5 (112.4)	4.9∗	8.1∗
PCL40	50.26 (0.33)	43.62 (1.27)	0.74 (0.11)	46.13 (1.62)	0.90 (0.07)	62727.3 (3555.6)	57653.5 (210.0)	4.4	12.1∗
PCL10+drug	40.06 (0.15)	42.26 (4.36)	22.68 (1.76)	50.66 (1.48)	30.75 (1.19)	16906.5 (2556.2)	-	10.8	
PCL10	56.41 (0.34)	-	1.73 (0.42)	60.85 (1.51)	2.98 (0.21)	15152.5 (55.9)	-	0.7	-
6%Lu,PCL40+drug	32.12 (0.17)	38.51 (0.72)	36.77 (0.01)	47.18 (0.70)†	33.37 (0.48)	60625.5 (102.5)	-	7.6∗	-
6%Lu,PCL40	43.41 (0.19)	-	1.30 (0.10)	45.15 (1.79)	1.51 (0.14)	58144.5 (748.8)	-	11.4∗	-
13%Lu,PCL40+drug	30.32 (0.52)	41.43 (0.56)	41.12 (0.45)	44.07 (2.69)	37.36	61636.5 (2686.3)	-	6.0	-
13%Lu,PCL40	38.40 (1.13)	-	7.71 (0.56)	44.43 (2.96)	5.84	61606	-	6.1	-

Table 5.6: Crystallinity, mass loss and molecular weight evolution for in vitro and in vivo degraded samples ($p \leq 0.05$, $*$, relative to initial MW, †, relative to in vitro crystallinity)

5.3.7 Histologic evaluation

The tissue samples collected from various organs showed normal cell morphology. The histological analysis of the tissues from the implantation site showed rapid resolution of the acute and chronic inflammatory stages and the development of normal foreign body reaction, consisting of adherent macrophages (Fig. 5.6(b)), fibroblasts, lymphocytes and foreign body giant cells (Fig. 5.6(c)) on the surface of the disk and fibrous capsule formation (Fig. 5.6(d)). Blood vessels (Fig. 5.6(a)) that formed in the fibrous capsule were also observed. There was a higher density of cells on the drug loaded disk with respect to control disks. No acute and/or chronic inflammation was seen after 2 months, indicating that the disks were biocompatible and did not produce inflammatory reactions characteristic to toxic materials.

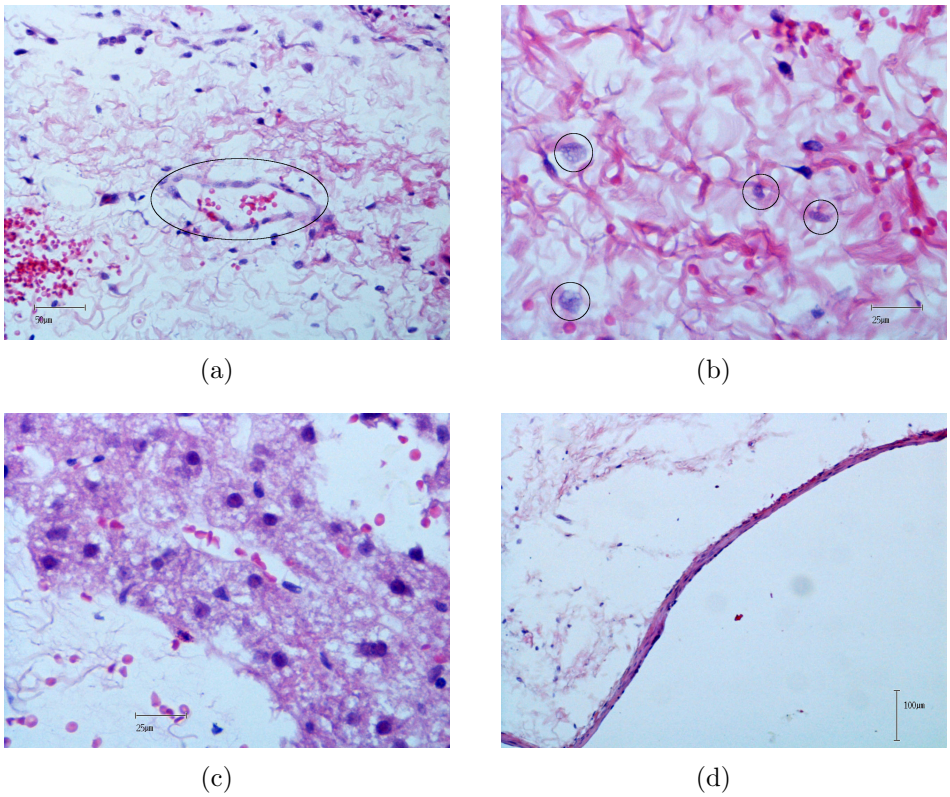

(a) (b)

(c) (d)

Figure 5.6: Light microscopy images of implanted disk showing a) cells and blood vessel (shown in the ellipse); b) macrophage cells (highlighted by circles); c) foreign-body giant cell; d) fibrous capsule

5.4 Conclusions

Subconjunctival disks based on PCL and loaded with dorzolamide hydrochloride were implanted in rabbit eyes and their in vivo performance was assessed by their

capacity to lower IOP in normotensive and hypertensive eyes. The high MW PCL showed non-cumulative release rates above the therapeutic level during 3 months. Histologic analysis showed normal foreign body reaction response consisting of adherent macrophages, fibroblasts, lymphocytes, foreign body giant cells and fibrous capsule formation. The release kinetics suggested a three stage release mechanism based on drug diffusion, polymer erosion and polymer degradation, with different steps depending on disk composition. In vivo, the fibrous capsule formation around the PCL implant controls the drug release, working as a barrier membrane. For blend disks, due to polymer erosion that takes place mostly in the first day of release, the fibrous capsule/barrier control is absent.

In normotensive eyes, a 20 % decrease in IOP obtained with the disks during 1 month was comparable with the one obtained by applying Trusopt®eyedrops. In hypertensive eyes, higher decrease percentages (around 40 %) were obtained for all samples, with the most sustained decrease from the high MW PCL (40 % after 1 month, 30 % after 2 months). Peak IOP occured earlier for blend disks due to enhanced drug release triggered by polymer erosion. It was proven that the devices can lower IOP in sustained manner in a rabbit glaucoma model. The blending offers the possibility to manipulate release rate and the amount of released drug in order to prepare devices tailored to the needs of patients (target IOP decrease percentages should take into account risk factors and disease progression).

Bibliography

E.M. Del Amo and A. Urtti. Current and future ophthalmic drug delivery systems. A shift to the posterior segment. *Drug Discov. Today*, 13:135–143, 2008. [DOI:10.1016/j.drudis.2007.11.002].

J.L. Bourges, C. Bloquel, A. Thomas, F. Froussart, A. Bochot, F. Azan, R. Gurny, D. BenEzra, and F. Behar-Cohen. Intraocular implants for extended drug delivery: therapeutic applications. *Adv. Drug Deliv. Rev.*, 58:1182–1202, 2006. [DOI:10.1016/j.addr.2006.07.026].

J. Breitenbach. Melt extrusion: from process to drug delivery technology. *Eur. J. Pharm. Biopharm.*, 54:107–117, 2002. [PubMed:12191680].

A. Harris, O. Arend, H.S. Chung, L. Kagemann, L. Cantor, and B. Martin. A comparative study of betaxolol and dorzolamide effect on ocular circulation in normal-tension glaucoma patients. *Ophthalmology*, 107:430–434, 2000. [PubMed:10711877].

P.T. Khaw, P. Shah, and A.R. Elkington. Glaucoma–2: treatment. *BMJ*, 328: 156–158, 2004. [DOI:10.1136/bmj.328.7432.156].

A.G. Konstas, V.P. Kozobolis, S. Tsironi, I. Makridaki, R. Efremova, and W.C. Stewart. Comparison of the 24-hour intraocular pressure-lowering effects of latanoprost and dorzolamide/timolol fixed combination after 2 and 6 months of treatment. *Ophthalmology*, 115:99–103, 2008. [DOI:10.1016/j.ophtha.2007.03.007].

J.M. Korte, T. Kaila, and K.M. Saari. Systemic bioavailability and cardiopulmonary effects of 0.5% timolol eyedrops. *Graefes Arch. Clin. Exp. Ophthalmol.*, 240: 430–435, 2002. [DOI:10.1007/s00417-002-0462-2].

S.V. Kulkarni, K.F. Damji, and Y.M. Buys. Medical management of primary open-angle glaucoma: Best practices associated with enhanced patient compliance and persistency. *Patient Prefer. Adherence*, 2:303–314, 2008. [PubMed:19920977].

N. Kuno and S. Fujii. Biodegradable intraocular therapies for retinal disorders: progress to date. *Drugs Aging*, 27:117–134, 2010. [DOI:10.2165/11530970-000000000-00000].

H. Levkovitch-Verbin, H.A. Quigley, K.R. Martin, D. Valenta, L.A. Baumrind, and M.E. Pease. Translimbal laser photocoagulation to the trabecular meshwork as a model of glaucoma in rats. *Invest. Ophthalmol. Vis. Sci.*, 43:402–410, 2002. [PubMed:11818384].

K.L. Macoul and D. Pavan-Langston. Pilocarpine ocusert system for sustained control of ocular hypertension. *Arch. Ophthalmol.*, 93:587–590, 1975. [PubMed:1164218].

M. Miyajima, A. Koshika, J. Okada, M. Ikeda, and K. Nishimura. Effect of polymer crystallinity on papaverine release from poly(L-lactic acid) matrix. *J. Control. Release*, 49:207–215, 1997. [DOI:10.1016/S0168-3659(97)00081-3].

B.K. Nanjawade, F.V. Manvi, and A.S. Manjappa. In situ-forming hydrogels for sustained ophthalmic drug delivery. *J. Con. Rel.*, 122:119–134, 2007. [DOI:10.1016/j.jconrel.2007.07.009].

M.V. Natu, M.H. Gil, and H.C. de Sousa. Supercritical solvent impregnation of poly(ε-caprolactone)/poly(oxyethylene-b-oxypropylene-b-oxyethylene) and poly(ε-caprolactone)/poly(ethylene-vinyl acetate) blends for controlled release applications. *J. Supercrit. Fluids*, 47:93–102, 2008. [DOI:10.1016/j.supflu.2008.05.006].

M.V. Natu, H.C. de Sousa, and M.H. Gil. Effects of drug solubility, state and loading on controlled release in bicomponent electrospun fibers. *Int. J. Pharm.*, 397:50–58, 2010. [DOI:10.1016/j.ijpharm.2010.06.045].

M.V. Natu, M.N. Gaspar, C.A.F. Ribeiro, I.J. Correia, D. Silva, H.C. de Sousa, and M.H. Gil. A poly(ε-caprolactone) device for sustained release of an anti-glaucoma drug. *Biomed. Mater.*, 6:025003, 2011. [DOI:10.1088/1748-6041/6/2/025003].

R.S. Noecker, M.S. Dirks, and N. Choplin. Comparison of latanoprost, bimatoprost, and travoprost in patients with elevated intraocular pressure: a 12-week, randomized, masked-evaluator multicenter study. *Am. J. Ophthalmol.*, 137:210–211, 2004. [PubMed:14700685].

C.G. Pitt, F.I. Chasalow, Y.M. Hibionada, D.M. Klimas, and A. Schindler. Aliphatic polyesters. I. The degradation of poly(ε-caprolactone) in vivo. *J. Appl. Polym. Sci.*, 26:3779–3787, 1981. [DOI:10.1002/app.1981.070261124].

H.A. Quigley. Glaucoma: macrocosm to microcosm the Friedenwald lecture. *Invest. Ophthalmol. Vis. Sci.*, 46:2662–2670, 2005. [DOI:10.1167/iovs.04-1070].

J. Ruiz-Ederra and A.S. Verkman. Mouse model of sustained elevation in intraocular pressure produced by episcleral vein occlusion. *Exp. Eye Res.*, 82:879–884, 2006. [DOI:10.1016/j.exer.2005.10.019].

K. Schmitz, P. Banditt, M. Motschmann, F.P. Meyer, and W. Behrens-Baumann. Population pharmacokinetics of 2% topical dorzolamide in the aqueous humor of humans. *Invest. Ophthalmol. Vis. Sci.*, 40:1621–1624, 1999. [PubMed:10359348].

K. Schwartz and D. Budenz. Current management of glaucoma. *Curr. Opin. Ophthalmol.*, 15:119–126, 2004. [PubMed:15021223].

A. Scozzafava, L. Menabuoni, F. Mincione, F. Briganti, G. Mincione, and C.T. Supuran. Carbonic anhydrase inhibitors. Synthesis of water-soluble, topically effective, intraocular pressure-lowering aromatic/heterocyclic sulfonamides containing cationic or anionic moieties: is the tail more important than the ring? *J. Med. Chem.*, 42:2641–2650, 1999. [DOI:10.1021/jm9900523].

M. Seki, T. Tanaka, H. Matsuda, T. Togano, K. Hashimoto, J. Ueda, T. Fukuchi, and H. Abe. Topically administered timolol and dorzolamide reduce intraocular pressure and protect retinal ganglion cells in a rat experimental glaucoma model. *Br. J. Ophthalmol.*, 89:504–507, 2005. [DOI:10.1136/bjo.2004.052860].

T. Yasukawa, Y. Ogura, E. Sakurai, Y. Tabata, and H. Kimura. Intraocular sustained drug delivery using implantable polymeric devices. *Adv. Drug Deliv. Rev.*, 57:2033–2046, 2005. [DOI:10.1016/j.addr.2005.09.005].

L. Yudcovitch. Pharmaceutical, Laser and Surgical Treatments for Glaucoma: An Update. `http://www.pacificu.edu/optometry/ce/courses/15166/pharglapg1.cfm#Introduction`, 2010.

Chapter 6

Long term degradation of poly(ε-caprolactone) constructs obtained through different polymer processing techniques

The text that comprises this Chapter was submitted to the journal *Polymer Degradation and Stability* (2011).

Abstract

Films, fibers, sponges and disks, based on poly(ε-caprolactone), PCL were prepared using solvent-casting, electrospinning, supercritical fluid processing and melt-compression, respectively. The influence on degradation rate of several factors (construct type, crystallinity, MW, drug presence, blending) was assessed through water uptake, mass loss, crystallinity and molecular weight (MW) evaluation. The degradation rate was higher for blends than for PCL and it was similar between the two type of blends. The low MW disks had a degradation rate that was lower by one order of magnitude than high MW constructs. Porosity was shown to be a very important factor because at initial stage (or initial porosity) will enhance water uptake and degradation, while at a later stage (or developed porosity) will decrease degradation rate because of diminished autocatalytic effects. High initial porosity produced an acceleration of degradation for sponges, fibers and films when compared to disks, while developed porosity reduced degradation for drug-loaded disks when compared to disks without drug. Modelling of the experimental data suggested that the contribution of surface effects was as significant as autocatalytic effects in overall bulk degradation.

6.1 Introduction

Solvent-casting, compression, supercritical fluid (SCF) processing and electrospinning are well known techniques to produce materials for tissue engineering and controlled drug delivery (CDDS) applications (Morales and McConville [2010], Kuno and Fujii [2010], Davies et al. [2008], Liang et al. [2007]). Poly(ε-caprolactone), PCL and other polyesters are usually the materials of choice for the preparation of scaffolds for tissue engineering applications and of implants/matrices for CDDS applications (Woodruff and Hutmacher [2010]). These polymers are commercially available, inexpensive, biocompatible and biodegradable (which ensures scaffold/implant integration at the site of implantation). Moreover, they can be easily processed using diverse techniques, that allow control of scaffold/implant morphology and/or control of drug loading and distribution and subsequently release profile.

Degradation profile has to be carefully controlled because it will directly influence the in vivo performance of the scaffold or CDDS. Usually, during degradation several simultaneous physical (water uptake, dissolution) and chemical phenomena (thermolysis, oxidation, hydrolysis) take place that will lead to a change in material properties and induce a certain in vivo response. For a scaffold, the degradation period of the polymer has to be manipulated in a such a way that the scaffold ensures the support to three-dimensional tissue formation and then it gradually disappears in order to integrate the new tissue with the surrounding one. For a CDDS, the degradation period can determine the drug release period and/or the release profile (Woodruff and Hutmacher [2010]).

Several factors that influence the degradation process of polyesters were studied such as polymer chemical stability, polymer molecular weight (MW), sample size and geometry, surface-to-volume ratio, degradation medium (type, temperature and pH), blending, end-group chemistry, hydrophilicity, crystallinity, drug presence, drug loading, polymer processing, sterilization (Alexis [2005]).

Blending or copolymerization of hydrophlic compounds/polymers/blocks was shown to produce an increase in degradation rate due to an enhancement in water uptake (Lam et al. [2008]). Other authors have not found such a correlation between hydrophilicity and degradation (Li et al. [1998]). The shape or the size of the samples was shown to influence degradation, with larger particles degrading faster than smaller ones due to an enhancement in autocatalytic effect (Dunne et al. [2000]), while in other works no evidence was found for internal catalysis (Lam et al. [2009]).

Degradation kinetics was also shown to be highly dependent upon the MW of

the polymer. An increase in MW resulted in a decrease in the degradation rate (Jenkins and Harrison [2008]), while other authors found an opposite relationship between degradation and MW, with higher degradation rate for high MW polymer (Wu and Wang [2001]). A higher crystallinity was indicated as a reason for the decrease in degradation, because degradation rate of amorphous regions is higher than that of crystalline regions. Nevertheless, other works found that samples with initial higher crystallinity degraded faster due to the formation of a highly microporous structure (Alexis [2005]). Careful consideration of processing method is necessary when comparing results from various works, because there can be differences in degradation kinetics even between semi-crystalline samples that have crystallites of different sizes (Hou et al. [2007]). Moreover, during degradation, several material properties change simultaneously, which makes the assessment of factor influence on degradation difficult.

Porosity is another factor that was found to influence enzymatic degradation, with more porous sponges degrading faster than less porous films, due to a higher surface area in the former case (Vidaurre et al. [2008]). In many degradation studies, no attempts were made to determine the degradation kinetics. Thus, it is not surprising to find differences between degradation profiles: in vivo, MW variation was found to follow an exponential decay (Pitt et al. [1981]), while other authors presented a linear variation (Sun et al. [2006]).

In this work, various constructs based on PCL and Lutrol F127 (poly(oxyethylene-b-oxypropylene-b-oxyethylene), Lu were prepared using different processing techniques (solvent-casting, compression, SCF processing and electrospinning) so that samples of certain morphology and composition were obtained. Lu was shown to work as a hydrophilicity enhancer and release modulator (Natu et al. [2008]). Moreover, two MW of PCL were used as well as drug incorporation in some of the constructs. This allowed the assessment of different factors (such as construct type, crystallinity, MW, drug presence, composition) influence on degradation profile. Additionally, degradation rates were determined by regression to MW data using a zero-order and a first-order model (autocatalytic equation) of hydrolytic degradation (Tsuji and Ikada [1998], Levenspiel [1999a]).

6.2 Materials and methods

6.2.1 Construct preparation

Poly(ε-caprolactone) (PCL, average M_w 65000 g/mol and PCL10, average M_w 15000 g/mol, Sigma-Aldrich) and Lutrol F 127 (Lu, poly(ethylene oxide)-b-poly(propylene oxide)-b-poly(ethylene oxide), 9000-14000 g/mol, 70 % by weight of polyoxyethylene, BASF) and dorzolamide hydrochloride (Chemos GmbH) were used to prepare drug-loaded disks (33.3 % w/w theoretical dorzolamide loading) and control disks (no drug) by melt compression as already described. The ratio of polymers in the blends was : 0/100, 25/75, 50/50 % (w/w) Lu/PCL. The same polymer and the same ratios were used to prepare disks (by melt-compression), films (by solvent-casting), fibers (by electrospinning) and sponges (by supercritical fluid processing, SCF) as previously reported (Natu et al. [2011b, 2008, 2010]). The dimensions of the constructs were the following: 4 mm × 1 mm, diameter × thickness (for disk), 10 mm × 10 mm × 0.5 mm, length × width × thickness (for films and fibers) and 4 mm × 4 mm × 4 mm, length × width × thickness (for sponges). The samples were used as such in degradation experiments.

6.2.2 Construct characterization

The relative crystallinity of the constructs was determined by differential scanning calorimetry (DSC) and calculated as previously described, considering the melting enthalpy of 100 % crystalline PCL and 100 % crystalline Lu (Natu et al. [2010]). Water contact angle was evaluated using the sessile drop method as previously reported (Natu et al. [2010]).

6.2.3 Morphology

The morphology of the disks was examined using scanning electron microscopy, SEM.

6.2.4 Mass loss

Mass loss experiments were performed as previously reported (Natu et al. [2010]). The percentage of mass loss was calculated using Eq.6.1.

$$Mass\ loss\,(\%) = \frac{M_i - M_t}{M_i} \times 100 \tag{6.1}$$

where M_i is the initial mass and M_t is the dried sample mass after immersion time, t.

6.2.5 Molecular weight evolution

The changes in the MW and polydispersity index, PI (due to hydrolytic degradation) were measured by size exclusion chromatography (SEC) as described previously (Section 5.2.4). The degradation rate constant was determined by regression using Eq. 6.4 and Eq. 6.6.

Eq. 6.4 is obtained by assuming that hydrolysis is autocatalysed by the carboxylic groups of the polyester chains, with reaction rate (r) proportional to water (c_{water}) and polyester (c_{ester}) concentrations.

$$-r = -\frac{dc_{acid}}{dt} = k \cdot c_{acid} \cdot c_{ester} \cdot c_{water} \tag{6.2}$$

If the concentration of water and polyester is assumed constant because the chain cleavage is small, a pseudo-first order equation (Eq. 6.3) is obtained, which, by integration leads to Eq. 6.4:

$$-r = -\frac{dc_{acid}}{dt} = k \cdot c_{acid} \tag{6.3}$$

$$M_{n,t} = M_{n,0} \cdot exp(-kt) \tag{6.4}$$

where $M_{n,0}$ and $M_{n,t}$ are the number-average MW of the undegraded sample and of the degraded sample after hydrolysis time t, respectively, while k is the degradation rate constant (Tsuji and Ikada [1998].

Polyester hydrolysis is a diffusion-reaction phenomenon, involving mass transport and chemical reaction simultaneously. Thus, a shrinking core model for particles of unchanging size might be used (Levenspiel [1999a]). In the case of semi-crystalline polymers, the "particles" can be interpreted as micro-regions, where the polymer chains are grouped either in amorphous or crystalline state inside the polymer bulk. For slow degrading polymers, like PCL, the controlling step is chemical reaction, while for fast degrading polymers (like PLGA) the controlling step is water diffusion. Since the progress of the reaction is not affected by any diffusion resistance, the rate is proportional to the available non-reacted surface (Levenspiel [1999b]). Thus, an equation based on a zero-order model can be used to fit the MW data.

$$-r = -\frac{dc_{acid}}{dt} = k \tag{6.5}$$

$$M_{n,t} = M_{n,0} - kt \tag{6.6}$$

6.2.6 Statistics

All values are presented as mean and standard error of the mean (SEM). Experiments were performed in triplicates. Statistical analysis (linear regression, independent two-tailed T test, one-way ANOVA and Tukey HSD test) was done using OpenOffice.org Calc 3.2 and OOoStat Statistics Macro 0.5. The results were considered statistically significant when $p \leq 0.05$.

6.3 Results and discussion

6.3.1 Construct characterization

In Table 6.1, an overview of the methods used to load the drug and process the samples is presented. In general, there was an increase in hydrophilicity with Lu and drug addition. The disks (either with or without drug) showed a similar hydrophilic-hydrophobic character regardless of MW. The most significant differences were exhibited by blend samples processed by electrospinning and SCF that did not contain any drug and still presented very low values of the water contact angle. This behaviour can be correlated to the porosity of these samples, which present two different regions of porosity (macroporosity region with pores on the μm scale and a porosity region with pores on the nm scale) (Natu et al. [2011a, 2010]). In a fiber mat or sponge, there are regions of macroporosity where water can easily penetrate, while in films or disks these regions are smaller (see for comparison Fig. 6.1(c), Fig. 6.2(c), Fig. 6.3(c) and Fig. 6.4(e)).

Processing	Construct	Drug	Composition	Contact angle (deg)	T_m ($^\circ C$)	Relative degree of crystallinity (%)
Solvent-casting	Films	no	PCL	61.80 (1.80)	57.09 (0.19)	41.95 (0.60)
		no	25/75 Lu/PCL	55.90 (1.30)	56.17 (0.38)	37.80 (2.87)
		no	50/50 Lu/PCL	50.10 (1.20)	56.69 (0.00)	46.89 (0.23)
Melt compression	Disks	no	PCL	73.88 (3.31)	61.26 (0.31)	50.26 (0.33)
		no	25/75 Lu/PCL	48.32 (1.79)	60.47 (0.70)	47.88 (0.57)
		no	50/50 Lu/PCL	55.83 (2.70)	58.70 (0.31)	39.32 (1.12)
		yes	PCL	80.23 (2.63)	61.54 (0.02)	33.55 (0.85)
		yes	25/75 Lu/PCL	30.10 (0.52)	60.11 (0.42)	35.43 (2.84)
		yes	50/50 Lu/PCL	23.94 (0.63)	60.14 (0.48)	31.42 (0.72)
Electrospinning	Fibers	no	PCL	124.49 (6.37)	59.99 (0.15)	49.76 (2.87)
		no	25/75 Lu/PCL	14.15 (2.50)	58.15 (2.93)	55.04 (0.29)
		no	50/50 Lu/PCL	13.63 (1.48)	56.44 (2.75)	58.94 (0.06)
Supercritical fluids	Sponges	no	PCL	73.52 (5.22)	63.25 (0.13)	52.28 (1.28)
		no	25/75 Lu/PCL	46.21 (3.79)	61.70 (0.20)	48.15 (3.06)
		no	50/50 Lu/PCL	27.00 (3.79)	61.66 (0.29)	49.70 (0.35)
Melt compression	Disks	no	PCL10	70.24 (1.86)	61.23 (0.61)	56.41 (0.34)
		no	25/75 Lu/PCL10	57.23 (1.50)	59.67	56.30 (0.22)
		no	50/50 Lu/PCL10	59.58 (2.17)	59.20	55.45 (0.16)
		yes	PCL10	78.26 (1.24)	60.67 (0.19)	40.06 (0.15)
		yes	25/75 Lu/PCL10	35.11 (0.20)	61.35 (0.64)	38.17 (2.33)
		yes	50/50 Lu/PCL10	29.23 (0.85)	60.55 (0.42)	38.77 (1.53)

Table 6.1: Sample description, water contact angle and relative degree of crystallinity

Overall, there was a decrease in crystallinity with Lu and drug addition, the presence of an additional component (either drug or another polymer) in the mixture producing crystallization restriction of the other component, as evident from the decrease in melting temperature (T_m) in blends when compared to the single-component samples (only T_m corresponding to PCL is presented in Table 6.1, but the same observation is valid for T_m corresponding to Lu). This trend, which was observed for disks, was not observed for films and fibers in terms of crystallinity values. Nevertheless, a decrease of T_m with blending was registered for all samples.

PCL films presented the lowest crystallinity, while blend fibers showed the highest crystallinity values from all the constructs. In electrospinning, polymer chain alignment takes place during the stretching of the polymer solution jet in a similar fashion to crystallinity increase after fiber drawing. The sponges presented higher crystallinity values than films and disks and the highest T_m. This can be explained by the SCF-solvent induced crystallization during processing, since SCF swells and plasticizes polymers (López-Periago et al. [2009]). Regarding the effect of MW, PCL10 disks showed higher crystallinity than PCL disks as shorter PCL chains are expected to crystallize in a higher proportion than longer PCL chains. We will discuss how the crystallinity will influence degradation in section 6.3.5.

6.3.2 Morphology

In this section, images showing the morphology of the non-degraded and degraded constructs are presented. Initially, the films present large pores (Fig. 6.1(a)) or fine grooves (Fig. 6.1(c)) due to solvent evaporation. Fine grooves are formed for blends instead of pores probably because of phase separation after solvent casting. PCL chains can not aggregate intra-molecularly because of the presence of Lu and as such the solvent can easily exit the polymer phase without producing large pores. With aging, spherulites (that are composed of lamellae spreading from nuclei) separated by large pores (≥ 10 μm) are formed due to polymer re-crystallization in PCL films (Fig. 6.1(b)) or pores (~ 1 μm) obtained due to Lu leaching are formed in blend films (Fig. 6.1(d)).

With aging, the fibers lost their structural integrity: large diameters fibers collapsed and small diameter fibers "glued" on the larger ones in PCL samples (Fig. 6.2(b)), while for blend samples, the fiber mat was almost transformed into a film, with fine grooves showing the position of the initial fibers (Fig. 6.2(d)).

With SCF processing (supercritical carbon dioxide), in the depressurization step, carbon dioxide passes from the supercritical to the gas state and exits the polymer matrix, creating pores (Fig. 6.3(c)). Due to the fact that the SCF decreases the

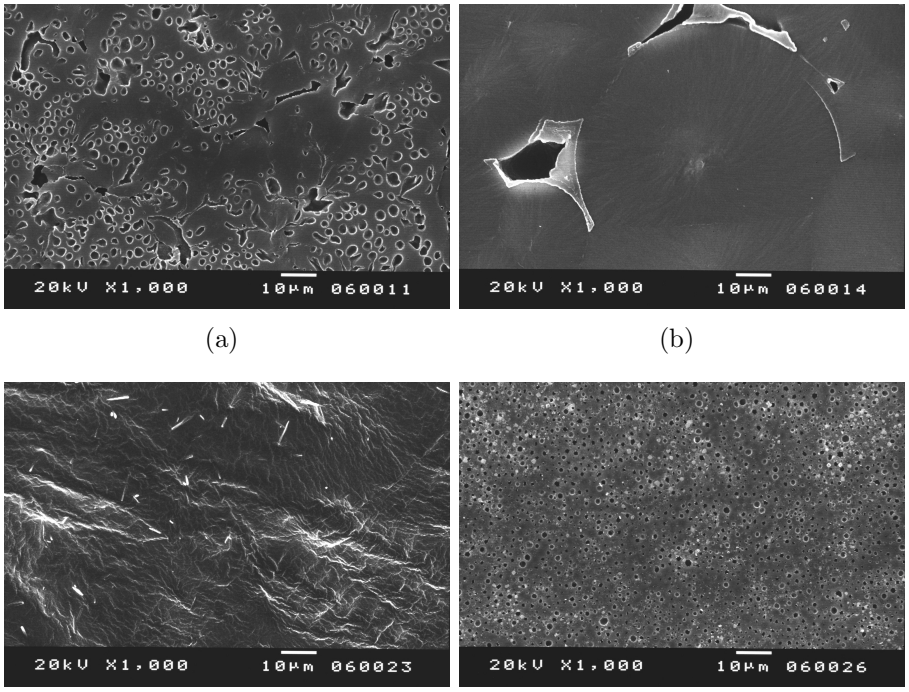

(a) (b)

(c) (d)

Figure 6.1: Films a) PCL as prepared, b) PCL degraded during 12 months, c) 50/50 Lu/PCL as prepared, d) 50/50 Lu/PCL degraded during 12 months

melting temperature of PCL, this sample melts during SCF processing and solidifies at depressurization. Thus, PCL sample shows a slightly different morphology than blend samples, with smaller pores (Fig. 6.3(a)). During degradation, all the samples preserve their initial morphology (Fig. 6.3(b) and fig. 6.3(d)).

In Fig. 6.4(a), circular structures can be observed probably corresponding to spherulites (as we have seen in section 6.3.1, the disks without drug have higher crystallinity than drug-loaded disks). The drug-loaded disks present a rougher morphology due to drug crystallization and phase separation from the polymer phase (Fig. 6.4(c) and Fig. 6.4(e)). With aging, the morphology of PCL disk without drug does not change much with the exception of the appearance of some pores (Fig. 6.4(b)). On the other hand, the surface of drug-loaded shows significant modification: a filament-like structure composed of "channels" created by drug elution and Lu leaching is shown by PCL (Fig. 6.4(d)) and blend disks (Fig. 6.4(f)), while PCL10 disks present various pores, cracks and spherulitic structures (Fig. 6.4(h)).

6.3.3 Mass loss

The hydrolytic degradation mechanisms of PCL is a random chain scission process. Polymer degradation is a complex process composed of several simultaneous

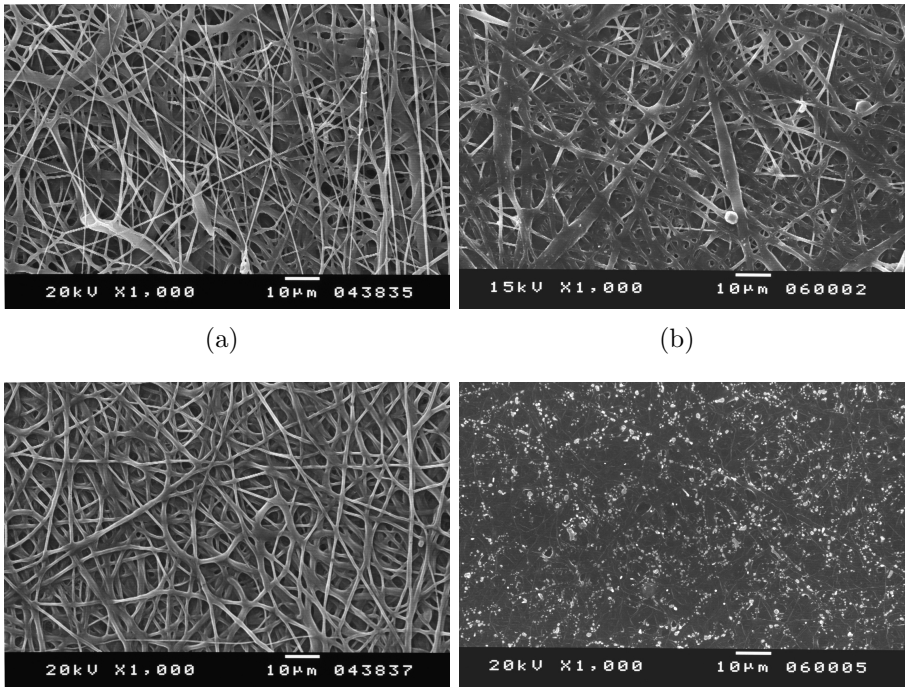

Figure 6.2: Fibers a) PCL as prepared, b) PCL degraded during 12 months, c) 50/50 Lu/PCL as prepared, d) 50/50 Lu/PCL degraded during 12 months

physical (water uptake, swelling, dissolution, crystallization, stress cracking) and chemical phenomena (thermolysis, oxidation, hydrolysis, photolysis). Nevertheless, for polyesters, the most important steps are water uptake/diffusion and hydrolysis (Woodruff and Hutmacher [2010]). Polyesters can present surface or bulk degradation mechanisms depending on the rate limiting step, which is water diffusion in the first case and hydrolysis in the second case. Mass loss or erosion occurs when water-soluble fragments that form due to hydrolysis, are able to leach out from the polymer matrix. As hydrolysis is a random chain cleavage process, the probability to obtain a water-soluble fragment that is small enough to diffuse from the bulk increases as MW decreases. This explains the relatively low mass loss shown by PCL before reaching a low MW.

The profile of mass loss curves for films and fibers is shown in Fig. 6.5(a) and Fig. 6.5(b), respectively. Mass loss is constant after the first days for all the constructs that did not contain drug because PCL is a bulk degrading polymer and Lu is a water-soluble polymer (most of it being leached out in the first week). Thus, even after 30 months, mass loss of 25/75 Lu/PCL fibers is approximately 20%, while mass loss of 50/50 Lu/PCL fibers is around 45%. The curves shown in Fig. 6.7 present similar profiles (one-step mass loss for PCL and two-step mass for blends) to fibers mass loss. Mass loss shown by films is slightly higher than

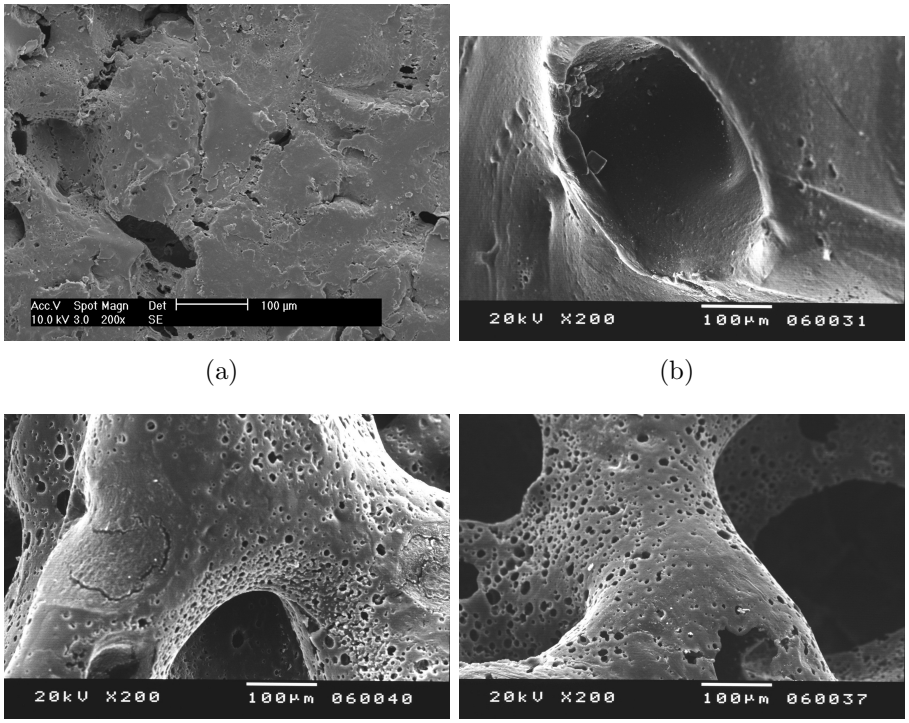

(a) (b)

(c) (d)

Figure 6.3: Sponges a) PCL as prepared, b) PCL degraded during 12 months, c) 50/50 Lu/PCL as prepared, d) 50/50 Lu/PCL degraded during 12 months

mass loss of fibers during the same period of time: around 50% for 25/75 Lu/PCL and approximately 60% for 50/50 Lu/PCL. Besides this, the films also show a gradual increase in mass loss over time, uncharacteristic to the other constructs. Mass loss can occur either due to erosion (as discussed above) or due to mechanical breakdown during sample handling. Small parts of non-degraded material are lost during handling procedure because of sample fragility. We believe that this is what happened in the case of degraded blend films (that are highly porous and very thin, see also Fig. 6.1(d)).

The mass loss of drug-loaded disks is shown in Fig. 6.6(a) and Fig. 6.6(b). The curves present a different profile than the rest of the constructs: there is a gradual increase in mass loss during 18 months due to the leaching of the drug. A high amount of drug is released during the first 3 months of the study (the so-called mobile drug), while the rest (the immobilized drug) is released only with polymer degradation (Natu et al. [2010]). PCL10 disks show slightly higher mass loss than PCL disks probably because of higher crystallinity and porosity (cracks and spherulites are visible in Fig. 6.4(h)), which enhances drug elution.

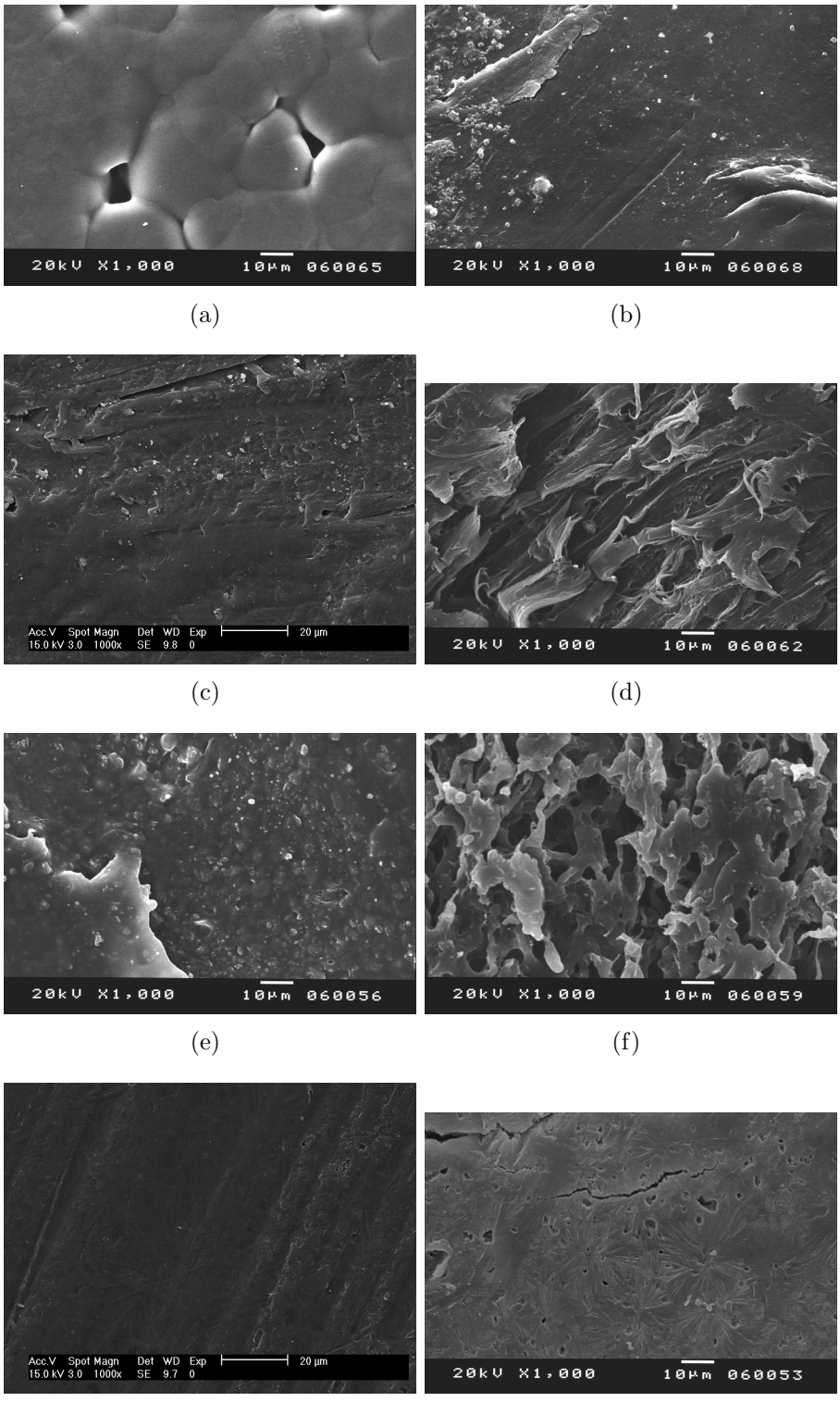

Figure 6.4: Disks a) PCL as prepared, b) PCL degraded during 12 months, c) PCL+drug as prepared, d) PCL+drug degraded during 12 months, e) 50/50 Lu/PCL+drug as prepared, f) 50/50 Lu/PCL+drug degraded during 12 months, g) PCL10+drug as prepared, h) PCL10+drug degraded during 12 months

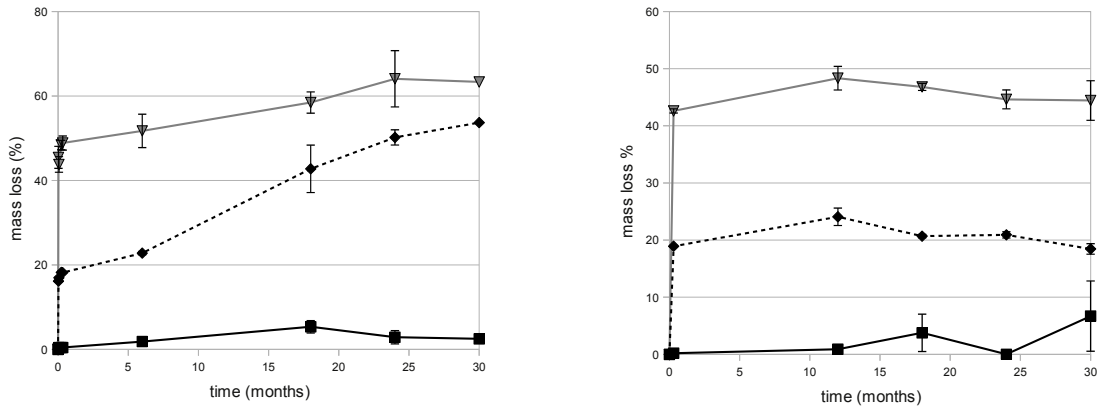

(a) (b)

Figure 6.5: Mass loss of a) films and b) fibers

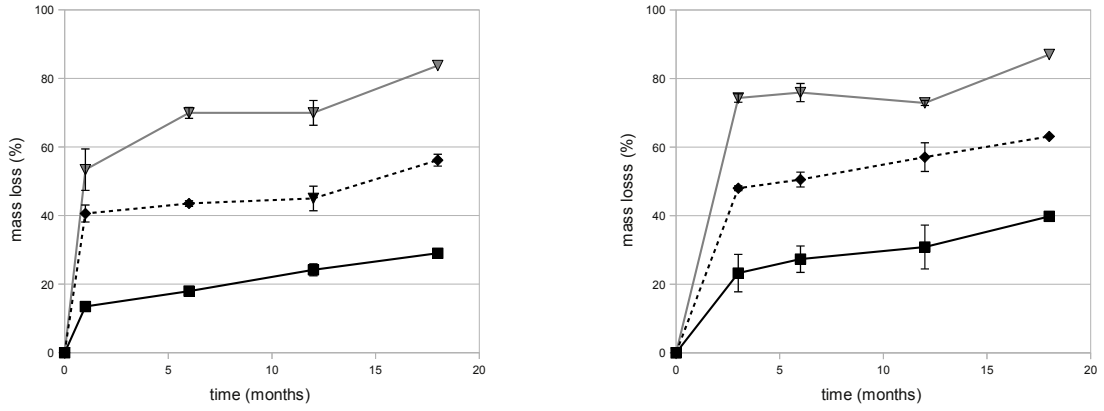

(a) (b)

Figure 6.6: Mass loss of a) PCL disks with drug and b) PCL10 disks with drug

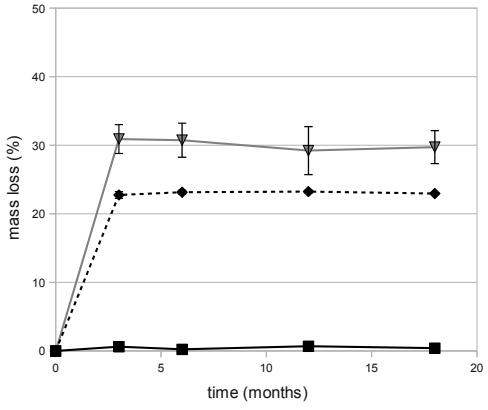

Figure 6.7: Mass loss of sponges

6.3.4 Evolution of crystallinity degree during degradation

Table 6.2 presents the evolution of crystallinity degree and of T_m during degradation. For semi-crystalline polymers, crystallinity can change during processing (as discussed in section 6.3.1) and/or during degradation. Usually, during degradation, there is an increase in crystallinity due to mainly two mechanisms: on one hand, solvent-induced crystallization of non-degraded polymer (water uptake allows polymer chain rearrangement and subsequent crystallization) and, on the other hand, crystallization of degraded fragments (oligomers) trapped in the non-degraded polymer bulk. Thus, an increase in crystallinity is expected during degradation. This trend is, in general, observed for disks, films and sponges, but it is not observed for fibers that show only a slight increase in crystallinity for PCL and a high decrease in crystallinity with degradation. Additionally, in some cases (film and sponges), 50/50 Lu/PCL blend presents lower crystallinity after 6 months of test. This behaviour might be related with the presence in the blend of a water-soluble polymer. Lu dissolution produces a decrease in crystallinity because it can cause the fragmentation and erosion of non-degraded crystalline regions (Lam et al. [2008]). Thus, there is a higher decrease in crystallinity for the blend that contains more Lu (20% decrease in crystallinity for 25/75 Lu/PCL fiber and 28% decrease in crystallinity for 50/50 Lu/PCL fiber only after 7 days). When dissolution is complete, there is a slight increase in crystallinity of the remaining PCL phase due to re-crystallization.

For drug-loaded disks, an increase in crystallinity was observed at 6 months regardless the composition or MW. In this case, the more compact structure and hydrophobicity produce slower water uptake and more gradual mass loss (see also Fig. 6.6(a) and Fig. 6.6(b)). Only after 1 day, water content is very high for fibers (81% for 50/50 Lu/PCL and 70% for 25/75 Lu/PCL) and sponges (69% for 50/50 Lu/PCL and 32% for 25/75 Lu/PCL), while lower for disks (23% for 50/50 Lu/PCL and 17% for 25/75 Lu/PCL). This will have high impact on Lu and drug dissolution and subsequent erosion of crystalline regions. Moreover, due to the less porous structure, it is more probable that oligomers will be trapped in the polymer bulk and crystallize, contributing to an increase in the overall crystallinity (see section 6.3.5).

T_m increased during the period of study for all samples in spite of a decrease or increase in the degree of crystallinity. The increase in T_m is a proof of crystallite growth and preferential hydrolysis of the amorphous regions. Usually, when hydrolysis occurs in crystalline regions, T_m decreases because the crystallites are

being destroyed. Only after 25 months, T_m does not increase anymore or starts decreasing, suggesting that only now hydrolysis extends to crystalline regions in agreement to previous works (Tsuji and Ikada [1998]).

	Disks							Films			Fibers			Sponges		
Lu/PCL	0/100	25/75	50/50	0/100	0/100	25/75	50/50	0/100	25/75	50/50	0/100	25/75	50/50	0/100	25/75	50/50
M_n (g/mol)	40				10			40			40			40		
Drug	yes	yes	yes	no	yes	yes	yes	no	no	no	no	no	no	no	no	no
Time (months)	Relative degree of crystallinity (%)															
0	33.55 (0.85)	35.43 (2.84)	31.42 (0.72)	50.26 (0.33)	40.06 (0.15)	38.17 (2.33)	38.77 (1.53)	41.95 (0.60)	37.80 (2.87)	46.89 (0.23)	49.76 (2.87)	55.04 (0.29)	58.94 (0.06)	52.28 (1.28)	48.15 (3.06)	49.70 (0.35)
6	39.81	46.77	45.69	47.5 (0.35)	55.16 (1.52)	54.44 (1.13)	50.61 (0.94)	54.79	50.78	44.83	50.58 (2.23)	49.87 (0.15)	44.1	51.88	48.45	45.38
18	44.96 (0.01)	48.73 (1.26)	47.05 (0.91)	53.2	50.32	52.7 (0.63)	50.35	52.11 (2.69)	52.01	48.20	51.77 (0.54)	46.47 (0.06)	45.43 (2.87)	56.08	51.5	48.51
30	na	na	na	na	na	na	na	58.51	55.46	50.34	52.76 (1.57)	47.56 (0.91)	45.40 (3.53)	na	na	na
Time (months)	Melting temperature (°C)															
0	61.54 (0.02)	60.11 (0.42)	60.14 (0.48)	61.26 (0.31)	60.67 (0.19)	61.35 (0.64)	60.55 (0.42)	57.09 (0.19)	56.17 (0.38)	56.69 (0.00)	60.06 (0.29)	59.38 (0.20)	59.50 (0.17)	63.25 (0.13)	61.70 (0.20)	61.66 (0.29)
6	63.82	62.95	63.77	63.79 (0.00)	62.8 (0.16)	61.67 (0.05)	61.80 (0.22)	63.73	61.83	63.08	62.27 (0.12)	63.00 (0.48)	62.01	65.45	65.41	65.53
18	66.67 (1.52)	65.15 (0.33)	65.52 (0.07)	65.77	66.41 (2.01)	63.77 (0.25)	63.03	66.41 (0.63)	65.51	65.26	63.05 (0.24)	62.98 (0.06)	62.90 (1.13)	66.59	65.81	65.99
30	na	na	na	na	na	na	na	65.87	65.78	66.10	63.77 (0.11)	63.33 (0.55)	64.10 (0.45)	na	na	na

Table 6.2: Relative degree of crystallinity and melting temperature evolution with degradation

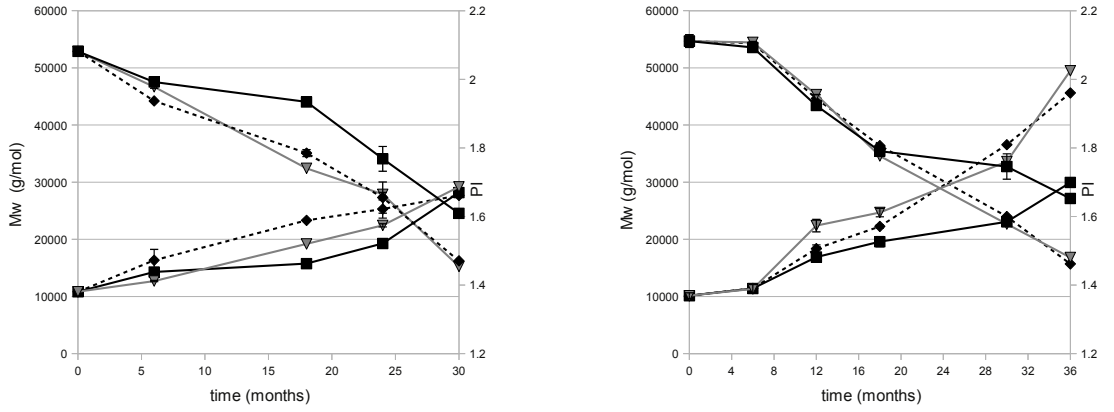

(a) (b)

Figure 6.8: Weight average molecular weight and polydispersity index evolution of a) films and b) disks

6.3.5 Evolution of molecular weight during degradation

In Fig. 6.8(a), Fig. 6.8(b) and Fig. 6.9(a) the change in weight-average MW (M_w) and PI is presented for films, disks and fibers, respectively. It can be noted, that in terms of M_w, there is a higher decrease in M_w at 6 months for PCL films (10%) and fibers (8%) than for disks (1%), while the trend is reversed at 12 (21% for disk, 16% for fiber, 17% for film) and 18 months (37% for disk, 28% for fiber, 17% for film). The slower degradation after 6 months for the PCL disks might be related to their lower uptake (1% for disk, 23% for fiber, 17% for sponge after 1 day) in relation to the other constructs. The water uptake is slower at the beginning for the disks, but water will eventually penetrate the entire disk given enough time. This observation is further supported by the fact that the blend disks show statistically significant differences in M_w when compared to sponges, films or fibers only at 6 ($p \leq 0.01$ for 50/50 Lu/PCL, $p \leq 0.01$ for 25/75 Lu/PCL) and 12 months ($p=0.03$ for 50/50 Lu/PCL, $p=0.03$ for 25/75 Lu/PCL), but not at 18 months ($p=0.11$ for 50/50 Lu/PCL, $p=0.14$ for 25/75 Lu/PCL). Thus, at 18 months water content of the various constructs is expected to be similar. At 30 months, there is again higher decrease in M_w for films (54% for PCL, 69% for 25/75 Lu/PCL) and fibers (58% for PCL, 63% for 25/75 Lu/PCL) than for disks (40% for PCL, 56% for 25/75 Lu/PCL).

The decrease in M_w is generally accompanied by an increase in PI (thus, higher values for PI at 30 months for fibers and films in comparison with disks). A relatively low scattering of PI values is shown by films, disks and sponges, while fibers presented a much larger scattering of the values starting from 18 months. This scattering might be explained by the occurrence of heterogeneous degradation.

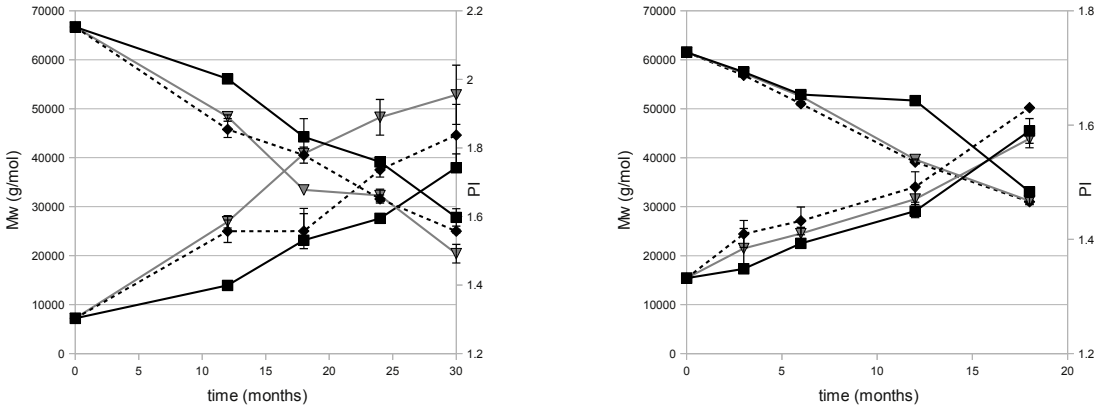

(a) (b)

Figure 6.9: Weight average molecular weight and polydispersity index evolution of a) fibers and b) sponges

A heterogeneous distribution of pores might result in regions with different degrees of degradation. The fibers and PCL films showed a more heterogeneous morphology than blend films or sponges (see also section 6.3.2) and thus present higher PI for similar decrease in M_w (1.9 as fiber versus 1.6 as sponge for 50/50 Lu/PCL at 18 months). Also, PCL film has a similar PI to blend films at 30 months in spite of lower decrease in M_w.

When comparing the degradation curves for different compositions of the same construct, the blends degrade faster than PCL as films and fibers for the entire period of study. When in disks, PCL degrades faster than the blends until 18 months. This behaviour might be explained by the autocatalytic effect as the lower porosity of the PCL disk might promote entrapment of oligomers that can catalyse the hydrolysis. After this time, pores and cracks will eventually develop due an increase in crystallinity and degradation would slow down (at 30 months, 40% decrease for PCL, ∼57% decrease for blends). When the chromatograms were analysed, peaks corresponding to oligomers (∼580, ∼320 g/mol) and monomers (∼110 g/mol) were detected in the PCL disks after 3, 6, 12 and even after 18 months. Usually, the area of these peaks, which is proportional to the concentration, decreased in time, being higher at 3 and 6 months. In contrast, the blends showed only monomer peaks until 12 months in small concentrations because degradation products could easily escape from the polymer bulk (see also section 6.3.2).

Degradation curves of the drug-loaded disks are shown in Fig. 6.10(a) and Fig. 6.10(b). It can be observed that the drug-loaded disks, in spite of lower initial crystallinity and smaller increase in crystallinity during aging, present lower M_w than disks without drug at similar time intervals. Additionally, there seems to be no difference in degradation behaviour with respect to composition. This is

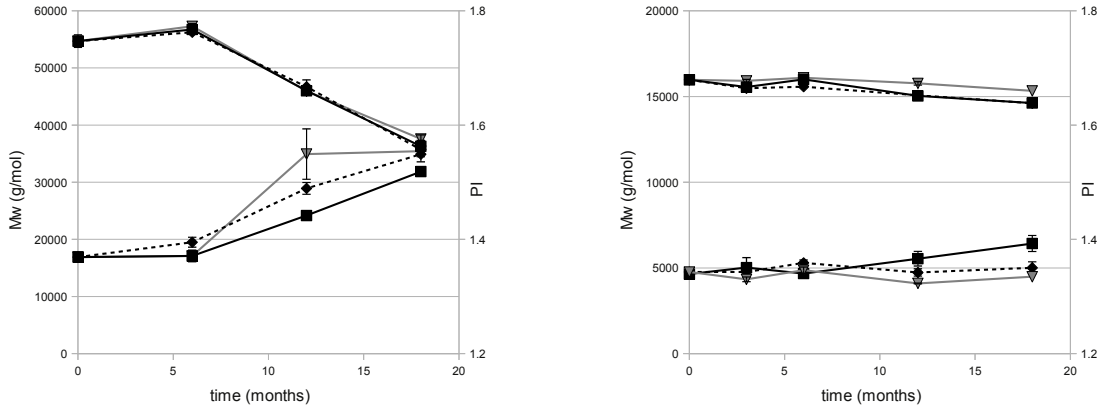

(a) (b)

Figure 6.10: Weight average molecular weight and polydispersity index evolution of a) PCL disks with drug and b) PCL10 disks with drug

expected because of the porous structure created due to Lu and/or drug leaching that will diminish autocatalytic effects.

Low MW disks degrade only slightly during 18 months, with no differences (in terms of M_w and PI) due to drug addition or composition (10% for drug-loaded PCL10, 9% for PCL10, 9% for 25/75 Lu/PCL10, 4% for 50/50 Lu/PCL10). First, these disks have higher initial crystallinity than PCL disks (see Table 6.2). Secondly, they have a compact structure that slows down water penetration (1% water content after 1 month) and thirdly, crystallization during aging produces polymer cracking (see Fig. 6.4(h)). Additionally, for a short chain polymer, there is a higher probability to obtain short water soluble fragments at hydrolysis, that leach out, especially through a porous structure (this was observed in the mass loss curves, when PCL10 disks presented higher mass loss than PCL disks in spite of similar drug loading, see Fig. 6.6(b)). Oligomers and monomers (∼340, ∼110 g/mol) in small concentrations were only detected at 3 and 6 months, while some monomer (∼105 g/mol) was detected at 12 months. All these factors contributed synergistically to the observed degradation delay.

In Fig. 6.9(b), M_w and PI evolution are presented for sponges obtained by SCF processing. Sponges showed highest decrease in M_w from all constructs at 18 months (46% for PCL, 50% for 25/75 Lu/PCL, 49% for 50/50 Lu/PCL), but similar decrease in M_w with films or fibers at 6 (17% as sponge and 16% as film, for 25/75 Lu/PCL, p=0.46 and 15% as sponge, 12% as film, for 50/50 Lu/PCL, p=0.37) and at 12 months (36% as sponge, 31% as fiber, for 25/75 Lu/PCL, p=0.17). These results suggest that again porosity and hydrophilicity have a great impact on water uptake and consequently on degradation. As we have seen in the degradation of drug-loaded disks, porosity that develops at a later stage (due to drug elution,

Construct	Drug	Composition	Autocatalytic eq.		Zero-order eq.	
			k ($month^{-1}$)	R^2	k (g/mol·month)	R^2
Films	no	PCL	0.023 (0.005)	0.85	865.8 (159.7)	0.91
	no	25/75 Lu/PCL	0.035 (0.007)	0.91	1134.1 (103.7)	0.98
	no	50/50 Lu/PCL	0.038 (0.007)	0.91	1198.0 (91.9)	0.98
Disks	no	PCL	0.020 (0.002)	0.95	786.0 (108.3)	0.93
	no	25/75 Lu/PCL	0.034 (0.004)	0.95	1142.8 (77.6)	0.98
	no	50/50 Lu/PCL	0.034 (0.003)	0.98	1145.2 (89.3)	0.98
	yes	PCL	0.024 (0.008)	0.83	1098.4 (349.7)	0.83
	yes	25/75 Lu/PCL	0.024 (0.008)	0.82	1107.6 (349.6)	0.83
	yes	50/50 Lu/PCL	0.022 (0.007)	0.82	1045.2 (351.1)	0.82
Disks	yes	PCL10	0.005 (0.001)	0.83	75.4 (20.1)	0.82
	yes	25/75 Lu/PCL10	0.005 (0.001)	0.95	70.1 (9.5)	0.95
	yes	50/50 Lu/PCL10	0.002 (0.001)	0.74	35.3 (12.1)	0.74
Fibers	no	PCL	0.028 (0.004)	0.93	1289.9 (122.8)	0.98
	no	25/75 Lu/PCL	0.032 (0.002)	0.98	1377.6 (86.6)	0.99
	no	50/50 Lu/PCL	0.038 (0.005)	0.95	1520.8 (149.0)	0.97
Sponges	no	PCL	0.031 (0.008)	0.84	1423.3 (299.4)	0.88
	no	25/75 Lu/PCL	0.039 (0.001)	0.99	1744.1 (72.3)	0.99
	no	50/50 Lu/PCL	0.039 (0.002)	0.99	1746.7 (78.8)	0.99

Table 6.3: Degradation rate constant

for example) will decrease hydrolysis rate relative to disks without drug, due to a decrease in autocatalytic effects. But, initial porosity will have a opposite effect on degradation, because on one hand, there is a higher surface for reaction and on the other hand, it enhances water uptake. Thus, sponges, films and fibers have high initial porosity and high water uptake relative to disks and show fast degradation at 6 months.

This effect is even more pronounced for blends than for PCL (fibers: 8% decrease for PCL, 15% for 50/50 Lu/PCL). In this case, both samples are very porous, but PCL fiber is much more hydrophobic and it inhibits water uptake (Natu et al. [2010]). Thus, initial porosity is important only if it promotes water uptake. Porosity and subsequently the surface available for reaction, that changes during aging, has important consequences. Sponges maintain their high initial porosity during aging (Fig. 6.3(c) and Fig. 6.3(d)), while PCL films and PCL/blend fibers do not (Fig. 6.1(a) and Fig. 6.1(b)). This might be the reason why PCL fibers (20% decrease in M_w) and films (17% decrease in M_w) are degraded less at 18

months than sponges (46% decrease in M_w). Additionally, scattering of PI values for sponges is very low, which suggests the occurrence of homogeneous degradation due to homogeneous porosity.

Table 6.3 presents the degradation rate constant values obtained by regression. It can be seen that, in general, the degradation rate is higher for blends than for PCL and it is similar between the two type of blends. The highest difference in degradation rate in terms of composition is shown by the disks without drug (p=0.0014). The presence of the drug in the disks produces a decrease in hydrolysis rate. The low MW disks have a degradation rate that is lower by one order of magnitude than high MW constructs. It should also be noted that the zero-order equation provides a better fit to the experimental data for all the samples, with one exception: PCL disk without drug. For this sample, the autocatalytic equation provides a slightly better fit for the reasons that were discussed above.

The contribution of surface reactions in the degradation of PCL was already suggested in other works (Pitt et al. [1981]). As we have seen in section 6.3.4, there is preferential degradation of amorphous regions until 24 months. Porosity will have a significant influence on the degradation of these regions. On one hand, it controls water transport in the polymer bulk and on the other hand, it increases surface-to-volume ratio that will increase the number of ester groups that are available for hydrolysis.

6.4 Conclusions

Various constructs were prepared based on PCL and Lu, such as films, fibers, sponges and disks using different techniques such as solvent-casting, electrospinning, supercritical fluid processing and melt-compression, respectively. The influence on degradation rate of several factors (construct type, crystallinity, MW, drug presence, composition) were tested. Overall, there was an increase in crystallinity with degradation, although some constructs showed lower crystallinty after 6 months due to the erosion of non-degraded crystalline regions during Lu or drug leaching. Nevertheless, melting temperature increased steadily until 24 months, suggesting preferential degradation of amorphous regions. The degradation rate was higher for blends than for PCL and it was similar between the two type of blends. The blends were more hydrophilic and had higher water content, which enhanced degradation. The low MW disks had a degradation rate that is lower by one order of magnitude than high MW constructs. These disks had high initial crystallinity, low initial porosity (and consequently low water uptake) and high developed porosity, which decreased degradation. Porosity was shown to be a very important factor because

at initial stage (or initial porosity) will enhance water uptake and degradation, while at a later stage (or developed porosity) will decrease degradation rate because of diminished autocatalytic effects. Initial porosity that was high for sponges, fibers and films produced an acceleration of degradation of these samples when compared to disks, while developed porosity, like for drug loaded disks and blend disks reduced degradation when compared to disks without drug. Thus, the presence of the drug in the disks produced a decrease in hydrolysis rate. A zero-order equation provided a better fit than a first-order equation to the experimental data for all the samples, suggesting that the contribution of surface effects was as significant as autocatalytic effects in overall bulk degradation.

Bibliography

F. Alexis. Factors affecting the degradation and drug-release mechanism of poly(lactic acid) and poly[(lactic acid)-co-(glycolic acid)]. *Polym. Int.*, 54:36–46, 2005.

O.R. Davies, A.L. Lewis, M.J. Whitaker, H. Tai, K.M. Shakesheff, and S.M. Howdle. Applications of supercritical CO2 in the fabrication of polymer systems for drug delivery and tissue engineering. *Adv. Drug Deliv. Rev.*, 60:373–387, 2008. [DOI:10.1016/j.addr.2006.12.001].

M. Dunne, I. Corrigan, and Z. Ramtoola. Influence of particle size and dissolution conditions on the degradation properties of polylactide-co-glycolide particles. *Biomaterials*, 21:1659–1668, 2000.

Y. Hou, J. Chen, P. Sun, Z. Gan, and G. Zhang. In situ investigations on enzymatic degradation of poly(ε-caprolactone). *Polymer*, 48:6348 – 6353, 2007. [DOI:10.1016/j.polymer.2007.08.054].

M.J. Jenkins and K.L. Harrison. The effect of crystalline morphology on the degradation of polycaprolactone in a solution of phosphate buffer and lipase. *Polym. Adv. Technol.*, 19:1901–1906, 2008.

N. Kuno and S. Fujii. Biodegradable intraocular therapies for retinal disorders: progress to date. *Drugs Aging*, 27:117–134, 2010. [DOI:10.2165/11530970-000000000-00000].

C.X. Lam, M.M. Savalani, S.H. Teoh, and D.W. Hutmacher. Dynamics of in vitro polymer degradation of polycaprolactone-based scaffolds: accelerated versus simulated physiological conditions. *Biomed. Mater.*, 3:034108, 2008.

C.X. Lam, D.W. Hutmacher, J.T. Schantz, M.A. Woodruff, and S.H. Teoh. Evaluation of polycaprolactone scaffold degradation for 6 months in vitro and in vivo. *J. Biomed. Mater. Res. A*, 90:906–919, 2009.

O. Levenspiel. *Chemical Reaction Engineering*, chapter Fluid-Particle Reaction: Kinetics, pages 566–586. John Wiley & Sons, 1999a.

O. Levenspiel. *Chemical Reaction Engineering*, chapter Interpretation of Batch Reactor Data, pages 38–77. John Wiley & Sons, 1999b.

S. Li, H. Garreau, M. Vert, T. Petrova, N. Manolova, and I. Rashkov. Hydrolytic degradation of poly(oxyethylene)–poly-(ε-caprolactone) multiblock copolymers. *J. Appl. Polym. Sci.*, 68:989–998, 1998.

D. Liang, B.S. Hsiao, and B. Chu. Functional electrospun nanofibrous scaffolds for biomedical applications. *Adv. Drug Deliv. Rev.*, 59:1392–1412, 2007. [DOI:10.1016/j.addr.2007.04.021].

A. López-Periago, C.A. García-González, and C. Domingo. Solvent- and thermal-induced crystallization of poly-L-lactic acid in supercritical CO_2 medium. *J. Appl. Polym. Sci.*, 11:291–300, 2009.

J.O. Morales and J.T. McConville. Manufacture and characterization of mucoadhesive buccal films. *Eur. J. Pharm. Biopharm.*, 2010. [DOI:10.1016/j.ejpb.2010.11.023].

M.V. Natu, M.H. Gil, and H.C. de Sousa. Supercritical solvent impregnation of poly(ε-caprolactone)/poly(oxyethylene-b-oxypropylene-b-oxyethylene) and poly(ε-caprolactone)/poly(ethylene-vinyl acetate) blends for controlled release applications. *J. Supercrit. Fluids*, 47:93–102, 2008. [DOI:10.1016/j.supflu.2008.05.006].

M.V. Natu, H.C. de Sousa, and M.H. Gil. Effects of drug solubility, state and loading on controlled release in bicomponent electrospun fibers. *Int. J. Pharm.*, 397:50–58, 2010. [DOI:10.1016/j.ijpharm.2010.06.045].

M.V. Natu, H.C. de Sousa, and M.H. Gil. *Active Implants and Scaffolds for Tissue Regeneration*, chapter Electrospun Drug-Eluting Fibers for Biomedical Applications. Studies of Mechanobiology, Tissue Engineering and Biomaterials. Springer, 2011a. [DOI:10.1007/8415_2010_56].

M.V. Natu, M.N. Gaspar, C.A.F. Ribeiro, I.J. Correia, D. Silva, H.C. de Sousa, and M.H. Gil. A poly(ε-caprolactone) device for sustained release of an anti-glaucoma drug. *Biomed. Mater.*, 6:025003, 2011b. [DOI:10.1088/1748-6041/6/2/025003].

C.G. Pitt, F.I. Chasalow, Y.M. Hibionada, D.M. Klimas, and A. Schindler. Aliphatic polyesters. I. The degradation of poly(ε-caprolactone) in vivo. *J. Appl. Polym. Sci.*, 26:3779–3787, 1981. [DOI:10.1002/app.1981.070261124].

H. Sun, L. Mei, C. Song, X. Cui, and P. Wang. The in vivo degradation, absorption and excretion of PCL-based implant. *Biomaterials*, 27:1735–1740, 2006.

H. Tsuji and Y. Ikada. Blends of aliphatic polyesters. II. Hydrolysis of solution-cast blends from poly(D,L-lactide) and poly(ε-caprolactone) in phosphate-buffered solution. *J. Appl. Polym. Sci.*, 67:405–415, 1998. [DOI:10.1002/(SICI)1097-4628(19980118)67:3¡405::AID-APP3¿3.0.CO;2-Q].

A. Vidaurre, J.M.M. Due nas, J.M. Estellés, and I.C. Cortázar. Influence of enzymatic degradation on physical properties of poly(ε-caprolactone) films and sponges. *Macromol. Symp.*, 269:38–46, 2008.

M.A. Woodruff and D.W. Hutmacher. The return of a forgotten polymer–polycaprolactone in the 21st century. *Prog. Polym. Sci.*, 35:1217 – 1256, 2010. [DOI:10.1016/j.progpolymsci.2010.04.002].

X.S. Wu and N. Wang. Synthesis, characterization, biodegradation, and drug delivery application of biodegradable lactic/glycolic acid polymers. Part II: Biodegradation. *J. Biomater. Sci. Polym. Ed.*, 12:21–34, 2001.

Chapter 7

Conclusions and outlook

In this work, in order to prepare CDDS for intraocular application, several polymer processing and drug loading techniques were used.

Polymer blends can be easily impregnated with drugs using SCF technology as long as the polymer swells under the action of SCF and/or the drug is soluble in SCF. Better drug loading was achieved when a cosolvent was used and when specific drug-polymer interactions occurred as a consequence of different chemical structures due to polymer blending. Some process parameters, such as pressure can also be manipulated in order to improve drug impregnation in the polymer matrix. Moreover, besides control of drug impregnation, SCF processing will affect polymer matrix morphology (porosity), crystallinity and consequently, water uptake, drug release and degradation.

Electrospinning is another technique through which drug loaded polymer constructs can be obtained. This processing method allows control over construct microstructure, which will produce special properties in comparison with other polymer processing techniques. For example, crystallinity and hydrophilicity will be very different when compared to other constructs obtained from the same polymer. Selection of the drug and the polymer carrier has to be carefully considered since drug solubility in polymer and drug loading will determine fiber morphology, drug distribution and release kinetics. Loading and drug encapsulation in either crystalline or amorphous form are interrelated and can control the release rate, especially in the burst stage. Thus, in long term release applications where high amounts of loaded drug are desirable, a compromise must be found in order to balance the loading and release rate that seem to vary in opposite directions.

SCF and electrospinning techniques offer great flexibility in terms of drug loading and polymer processing. We have seen in Chapter 2 and Chapter 3 that various polymer morphologies can be easily obtained. Nevertheless, they are limited in one aspect: the extent of drug loading. With SCF, maximum timolol loading

of 1.8% and with electrospinning, maximum acetazolamide loading of 12.7% were attained. Through SCF, the drug loaded amount will always be limited by the drug solubility in the SCF. The same observation is valid for electrospinning. The maximum amount of drug that can be loaded in the fibers can not be higher than the drug solubility in the polymer, otherwise as we have seen in Section 3.3.4, burst release will be produced.

Therapy with drug-eluting implants only makes sense if the benefits (such as therapeutic efficiency, local delivery, patient compliance) are higher than the risks (invasive method of introduction, complicated in vivo response). Sustained delivery of drugs is feasible only if long term release (usually higher than 1 year) is achieved in order to overcome the risks always involved with the surgical procedure of insertion. For long term release, high amounts of drug are required which restrains the use of SCF or electrospinning for the preparation of CDDS for the treatment of chronic diseases such as glaucoma. Physical mixture of drugs and polymers and subsequent processing into implants is a simple technique through which high loadings can be achieved in a relatively small volume device.

The understanding of drug release mechanism is essential since control of drug release can only be achieved when the effect of several factors (device morphology, crystallinity, drug loading, drug distribution, just to name a few) is thoroughly known. In this work, two types of CDDS were prepared and studied: monolithic (Chapter 2, Chapter 3 and Chapter 5) and hybrid (Chapter 4).

Basically, in a monolithic device, drug diffusion through the polymer matrix should be the controlling-phenomena. Nevertheless, when using a bulk degrading polymer such as PCL, the system is more complicated and polymer degradation is also an important step in the release process (as we have seen in Chapter 3 and Chapter 5). This will have an important effect on the in vivo performance of the device as total release will be achieved only after a prolonged time. Additionally, the non-cumulative release rate will drop to zero in spite of significant amounts of drug still present in the device. Thus, there is the need for constant drug release rate device such as a reservoir system.

For a reservoir system, two controlling phenomena contribute to drug release: partition of the drug from the core to the polymer membrane and drug diffusion through the membrane. As long as membrane porosity is carefully controlled, drug release will present a zero-order profile during the entire life time of the implant. When reaching a low MW, the polymer membrane is expected to suddenly and completely disintegrate. Nevertheless, this disintegration will not produce any toxic effects, since by then, the drug load of the implant is expected to be almost insignificant. That is why the polymer degradation period has to accurately match

the intended release period of the implant. Thus, the degradation profile (MW decrease, degradation rate) and the change in materials properties (such as porosity, crystallinity) have to be completely understood (Chapter 6).

Unfortunately, a reservoir system presents a clear disadvantage with respect to the monolithic one: the accidental release of the entire drug load in a very short period of time due to defects in the polymer membrane. This could have a highly dangerous effect in vivo. Thus, there is the need of a hybrid device (Chapter 4) that combines the relatively safe release profile of the monolithic device with the constant release rate of the reservoir device. In this system, release is controlled by the diffusion through the polymer matrix, the partition of the drug from the polymer matrix to the membrane and finally, by the diffusion through the membrane.

There is a long way from the in vitro tests to the actual in vivo performance of the implant. Thus, in vivo experimentation is necessary if the implant is ever to be arrive on the market. Animal experimentation is currently in dispute regarding its usefulness and ethics, but all the phenomena involved in the foreign body reaction triggered by the implant are so complex that it is very hard to simulate such a system in the laboratory. For implants, the wound healing in and around the device can determine how well the host can heal and accept the implanted material. Moreover, the fibrous capsule formation can often have a direct effect on the device performance. Thus, as long as the animal tests are carefully planned, the smallest number of animals can be used, the benefits obtained from understanding the changes in implant properties and in tissue response and subsequently in vivo drug release can largely overcome the mentioned issues.

We have seen that there is no direct way to forecast in vivo drug release from in vitro drug release data (Chapter 5). In vivo, the fibrous capsule formation around the implant controlled the drug release, working as a barrier membrane. Thus, the release kinetics changed from a $t^{0.5}$ profile to a t^0 profile. Nevertheless, all the prepared devices had an effect on the decrease of IOP, which proves the feasibility of the subconjunctival transport route to the cilliary body. Still, without pharmacokinetic data it is difficult to understand exactly how this transport occurs.

In vivo, the drug-eluting implants were able to reduce IOP in an animal model of glaucoma. Unfortunately, the maximum duration of the in vivo tests was 2 months. More prolonged in vivo tests are necessary in order to determine the performance of the CDDS during periods of time closer to the real situation. We have seen in Chapter 5 that small amounts of drug are sufficient to produce a pharmacologic response in vivo. Thus, small devices will be able to decrease IOP during long periods of time (and only limited by polymer degradation) as necessary in the treatment of glaucoma, a life long condition.

This work has revealed some insights in possible polymer processing and drug loading techniques for the preparation of CDDS for intraocular delivery. It also presented some results regarding the preliminary pre-clinical evaluation of PCL-based implants. Nevertheless, two other extremely important issues have to be addressed: cost estimation of implant manufacturing and patient compliance. Patience compliance is of extreme importance especially in the therapy of chronic diseases because patients have to keep up constantly with their pharmacological regimen. The superiority of CDDS relative to conventional therapy has to be proven in long term compliance studies because this is one of the main reasons of developing CDDS therapy in the first place. Most of the studies present in the literature fail to present compliance data, including this work.

Sensible cost evaluation of implant production is necessary in order to estimate the final product price. CDDS are expected to present higher costs than conventional therapy (eyedrops, in the case of glaucoma). Anyway, due to their improved performance, a higher price can be justified. But how much higher? This is an important question to be answered and can make the difference between another purely academical study and actual commercialization of the product and usefulness for the society.

Finally, efforts have to be made to the miniaturization of the device or the development of simple insertion surgical procedures. If an implant requires a complicated procedure to be placed in the eye, ophthalmologists may look to simpler therapies. A simple office-based procedure offers advantages to implantations that must be performed in the operating room.